THE TREATMENT OF BENZENE, TOLUENE, ETHYLBENZENE AND O-XYLENE USING TWO-PHASE PARTITIONING BIOSCRUBBERS

by

Jennifer V. Littlejohns

A thesis submitted to the Department of Chemical Engineering

In conformity with the requirements for

the degree of Doctor of Philosophy

Queen's University

Kingston, Ontario, Canada

August, 2009

Abstract

This thesis examined the biological treatment of gas streams containing benzene, toluene, ethylbenzene and o-xylene (BTEX) using solid-liquid two-phase partitioning bioscrubbers (SL-TPPBs). SL-TPPBs consist of a cell containing aqueous phase and a polymeric solid phase that sequesters poorly water soluble and/or toxic substrates, mitigating substrate toxicity in the aqueous phase and improving the gas mass transfer during treatment of VOC contaminated gases.

An initial investigation of oxygen transport determined that the polymers in a stirred-tank SL-TPPB enhance gas-liquid mass transfer. In addition, a study on biodegradation kinetics of BTEX by a bacterial consortium identified and quantified substrate interactions such as inhibition, enhancement and cometabolism. The stirred-tank SL-TPPB was then experimentally investigated for treatment of BTEX gas streams during steady-state and dynamic step-change operation to determine performance of the system relative to other biotreatment methods. A mathematical model was developed to predict system performance, which included the microbial kinetic model structure and parameters estimated during kinetic and oxygen mass transfer studies.

As a less energy intensive alternative, an airlift SL-TPPB was operated and characterized. The airlift SL-TPPB was compared to an airlift liquid-liquid TPPB (silicone oil as sequestering phase) and a single phase airlift over dynamic step-change loadings, which showed that the airlift SL-TPPB outperformed the single phase airlift by >30% and had similar performance to the liquid-liquid airlift. However, the airlift SL-TPPB performance was lower relative to the stirred-tank SL-TPPB by >15%. Steady-state operation of the airlift SL-TPPB identified a range of operating conditions that provided maximum performance and conditions that were not oxygen limited. This prompted a study of oxygen mass transfer and hydrodynamics in the airlift system, which identified that the addition of polymers to an airlift does not cause physical enhancement of the gas-liquid mass transfer coefficient, but improves aqueous phase mixing and enhances overall oxygen transfer rate. A tanks-in-series mathematical model was formulated to predict performance of the airlift SL-TPPB, wherein the number of tanks-in-series to

describe mixing in the airlift was obtained from a residence time distribution analysis of the airlift system completed during the hydrodynamic investigation. This thesis contributes a low-energy solution for the effective treatment of gases contaminated with BTEX.

Co-Authorship

Chapters 2, 3, 4, 5, 6, 7 and 8 have been accepted or submitted to refereed journals and were co-authored by Dr. Andrew J. Daugulis, who provided editorial and technical advice. Chapters 5 and 8 were co-authored by Dr. Kim McAuley, who provided editorial and technical modeling advice.

Acknowledgements

First and foremost, I would like to thank my supervisor Andrew Daugulis for his continual commitment and strong mentorship. Your passion for research and talent for educating has truly inspired me and I am indebted to you for my experience over the last four years. Also, thanks for the trips to North Campus, painful tube rides, and boat loans! In addition, many thanks to Kim McAuley for enthusiastically sharing her vast expertise.

I would also like to thank my amazing original labmates / friends; Dave, George, Lars, McMuffin and Krista with whom who I have shared many scientific discussions, personal conversations, and pints. You have all given me endless advice. In addition, I would like to thank my more recent labmates; Fang, Pedro (lab king) and Tanya for advice on my research (and emails!), swims, taking my "mama bird" advice, and providing me with lots of laughs.

I would like to thank my Mother for her continued support and friendship and my sister Heather for being a rock. I'm lucky to have incredible people like both of you in my life. Finally, my brother and Heidi have been there to take me on vacation when needed. In addition, I would like to thank the rest of the people in my family, including Nick's side, who have been very supportive and provided me with lots of advice. I would also like to thank my amazing friends that I made in Kingston, Guelph and Ridgetown for all the incredibly fun times and helping me cut polymers (you know who you are).

I would finally like to thank a million times over my partner Nick who has adjusted his life to support and accompany me on this experience. You have listened to my presentations repetitively, fixed my bioreactors when I'm in desperation and taken me fishing and hiking when I needed a break. I hope I can return the favour someday.

Statement of Originality

I hereby certify that all of the work described within this thesis is the original work of the author. Any published (or unpublished) ideas and/or techniques from the work of others are fully acknowledged in accordance with the standard referencing practices.

Jennifer Littlejohns

August, 2009

Table of Contents

List of Figures

List of Tables

List of Symbols

Symbol	Unit	Definition
A	m^2	Cross-sectional area
C	mg L^{-1}	Concentration
C^*	mg L^{-1}	Aqueous phase equilibrium concentration
D	m^2 s^{-1}	Diffusion coefficient
D_{ax}	m^2 s^{-1}	Axial dispersion coefficient
E_P		Physical enhancement coefficient
EC	mg L^{-1} h^{-1}	Elimination capacity
F	L s^{-1}	Volumetric flow rate
g	m s^{-1}	Acceleration due to gravity
H	mg L^{-1} mg^{-1} L	Henry's constant
$I_{I,i}$		Interaction parameter for effect of interacting substrate on substrate i
k	m s^{-1}	Mass transfer coefficient
k_d	s^{-1}	Endogenous respiration coefficient
$k_L a$	s^{-1}	Volumetric mass transfer coefficient
k_m	s^{-1}	Specific rate of substrate consumption for maintenance
k_O	m s^{-1}	Overall mass transfer coefficient between liquid and polymer
K	mg L^{-1} mg^{-1} L	Partition coefficient between liquid and polymer
K_c	mg L^{-1}	Half saturation constant of oxygen
K_I	mg L^{-1}	Inhibition constant
K_S	mg L^{-1}	Half saturation constant
LR	mg s^{-1}	Loading rate
M	g mol^{-1}	Molecular weight of the carbon source
n		Number of substrates in an experimental run
N		Number of tanks-in-series
OTR	mg L^{-1} h^{-1}	Oxygen transfer rate
P_g	W	Power input
Pe		Peclet number
Q		In a single molecule of carbon source, number of atoms of subscript
Q'	%	In a single cell, percentage of subscript
r	mg L^{-1} h^{-1}	Rate of depletion of substrate or oxygen
R_P	m	Radius of polymer
RE	%	Removal efficiency
S_θ		Uncertainty scaling factors
SR	mg s^{-1}	Stripping rate
t_c	s	Circulation time
t_m	s	Mixing time
T_i^X	mg mg^{-1}	Growth substrate transformation capacity = mg xylene mg growth substrate^{-1}
U_c	m s^{-1}	Mean circulation velocity
$\bar{U}$	m s^{-1}	Average velocity
V	L	Volume
x_c	m	Distance traveled by an element of fluid during one circulation

X	mg L^{-1}	Biomass concentration
$Y_{X/i}$	mg L^{-1} mg^{-1} L	Yield coefficient (or oxygen growth yield for if $i = O$)
$z*$		Dimensionless geometrical distance between injection and detection
Greek Letters		
ε		Gas holdup
θ		Dimensionless time
μ	s^{-1}	Specific growth rate
μ_{max}	s^{-1}	Maximum specific growth rate
ρ	kg L^{-1}	Density
τ_P	s	Time constant of probe
υ_S	m s^{-1}	Superficial gas velocity
ψ		Proportionality factor
Subscripts		
1		First species present in mixed substrate experiments
2		Second species present in mixed substrate experiments
3		Third species present in mixed substrate experiments
4		Fourth species present in mixed substrate experiments
aq		Sample containing aqueous phase
b		Bottom section in airlift
B		Benzene
C		Carbon
d		Downcomer section in airlift (1 to 8)
eff		Effective (system contains particles with oxygen affinity)
E		Ethylbenzene
$FR\#$		One of flow rates 2, 3 or 4 L min^{-1}
$FR3$		Flow rate 2 L min^{-1}
$FR3$		Flow rate 3 L min^{-1}
$FR4$		Flow rate 4 L min^{-1}
g		Gas phase
G		Growth substrate
gl		Between gas and liquid phases
H		Hydrogen
HS		In the headspace of the sample
i		Species B,T,E, X or O
I		Interacting species for mixed substrate experiments
in		At the inlet
$INERT$		Inert (system contains particles with negligible oxygen sorption)
INH		Inhibitory concentration
l		Liquid phase
lp		Between liquid and polymer phases
$L20$		Loading of 20 mg L^{-1} h^{-1}
$L60$		Loading of 60 mg L^{-1} h^{-1}
$L100$		Loading of 100 mg L^{-1} h^{-1}
n		Number of interacting species
N		Non-growth substrate
Nit		Nitrogen

O	Oxygen
out	At the outlet
overall	Overall transient period
P	Polymer phase
poly	Sampling containing polymer and aqueous phases
PRO	Read by the dissolved oxygen probe
r	Riser section in airlift
sec	Section in airlift (*b, t, r, d1, d2, d3, d4, d5, d6, d7* or *d8*)
sys	Polymer + aqueous phase
t	Top section in airlift
T	Toluene
X	Xylene
∞	At equilibrium
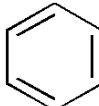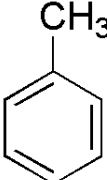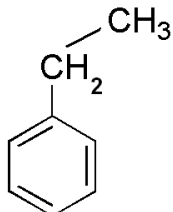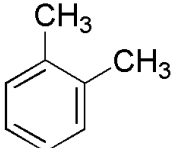
Chapter 1

Introduction

1.1 BTEX

Benzene, toluene, ethylbenzene and o-xylene, collectively known as BTEX, are toxic volatile organic compounds (VOCs) that are present in crude oil, and are therefore present in many industries that utilize crude oil for processing or manufacturing. The physical properties of BTEX components, which can be seen in Table 1-1, include high water solubility and vapour pressure in comparison to other petroleum components. This causes BTEX to be a health and ecological concern, as these toxic compounds have rapid transport pathways into the environment including both water and air. This thesis examined the treatment of gaseous BTEX using solid-liquid two-phase partitioning bioscrubbers (SL-TPPBs).

Table 1-1: Properties of BTEX

Property	Benzene	Toluene	Ethylbenzene	o-Xylene
Structure				
Molecular Weight[1]	78.11	92.13	106.16	106.16
Specific gravity[1]	0.879	0.866	0.867	0.881
Melting Point [1] (C°)	5.5	-95	-94.4	-25
Boiling Point[1] (C°)	80.1	110.8	136.2	144
Water Solubility[2] (mg L^{-1}) at 30°C	1780	515	152	198
Henry's Constant[3] (mg L^{-1} mg^{-1} L) at 30°C	0.279	0.343	0.419	0.279
Vapour Pressure[2] (mmHg) at 30°C	95.2	22	7	10
Log K_{ow}[2] at 30°C	2.13	2.73	3.15	3

[1](Perry and Green, 1997) [2](Kuo, 1999) [3](EPA, 2006a)

1.1.1 BTEX Contaminated Gas Streams

Due to the physical properties of BTEX and the wide-spread use of petroleum for manufacturing and processing, BTEX are possibly the most common industrially emitted VOCs. One natural gas refining plant can emit up to 25 tons of BTEX per year (Clean Air Act Amendments, 1990). During oil and gas refining, BTEX is released via breathing and loading losses from storage tanks, venting of process vessels, leaks from piping and equipment, wastewater streams, and heat exchange systems (Khan and Kr. Ghoshal, 2000). These types of releases are relatively recurrent and have the potential to release BTEX to the atmosphere in very high concentrations (Jutras et al., 1997). Solvent laden waste remediation also frequently releases gases contaminated with high concentrations of BTEX, as it involves the treatment of solvent-laden solids, such as rags used in cleaning operations, which are classified as hazardous waste until the solvents are volatilized and treated. Glycol dehydrator vent gas emissions in natural gas processing also emit high and fluctuating concentrations of gaseous BTEX during regeneration of glycol for reuse (Stewart et al., 2001).

Intentional or unintentional gasoline and oil spills that require site remediation are also a common source of BTEX emissions. The spills can occur during underground storage, gasoline and oil transportation, or leaks from processing equipment. To treat such contaminated sites the BTEX components are volatilized to remove them from the contaminated media, but gas streams containing relatively high concentrations of gaseous BTEX can be discharged (Jutras et al., 1997). Such a remediation technique is soil vapour extraction, which involves applying a vacuum to the subsurface of a contaminated site in order to induce controlled air flow that removes volatile compounds, such as BTEX. The contaminated off-gas must then be treated before it is released into the atmosphere. This thesis developed and characterized a technology that could be applied to the treatment of BTEX contaminated gases that are created in the various aforementioned industrial practices.

1.1.2 Environmental and Health Concerns

As mentioned previously in Section 1.1, in comparison to other components present in petroleum, BTEX compounds are relatively water soluble and volatile, making them a concern for contaminating surface water, drinking water and the atmosphere. This contamination is a significant problem, as benzene is a known carcinogen, causes reproductive/developmental effects and has numerous other chronic and acute effects on humans (EPA, 2006b). Toluene, ethylbenzene and xylenes have not been identified as carcinogens, however, exposure to toluene has been reported to have chronic and acute effects on the central nervous system (EPA, 2006c), exposure to ethylbenzene has been reported to cause reproductive/developmental effects on animals (EPA, 2006d) and occupational exposure to xylenes has been reported to cause reproductive/developmental effects in humans (EPA, 2006e). Due to their toxicity and relatively high water solubility, BTEX also pose a threat to fish and wildlife. For these reasons, BTEX compounds have been heavily studied and were the compounds targeted for treatment in this thesis.

1.1.3 BTEX Biodegradation

There are a number of aerobic bacteria that are able to degrade one or a combination of BTEX compounds. For example, strains of *Pseudomonas sp.* can degrade benzene, toluene and p-xylene (Bielefeldt and Stensel, 1999; Collins and Daugulis, 1999), strains of *Klebsiella sp.* can degrade benzene and toluene (Yeom and Daugulis, 2001) and strains of *Rhodococcus rh.* can biotransform a mixture of BTEX, although not all components are completely mineralized (Deeb and Alvarez-Cohen, 1999). Despite the wide array of bacteria that can degrade select components of BTEX, there is no single bacterium that has been successful in the complete mineralization of all BTEX components simultaneously (Bielefeldt and Stensel, 1999). An alternative to bacteria for BTEX biodegradation is the white rot fungus *Phanerochaete chrysosporium,* however, removal rates for aerobic bacterial degradation are significantly larger, making aerobic bacteria more promising microorganisms than fungi for practical

use (Oh et al., 1998). As well, aerobic bacteria have been shown to be substantially more efficient at the degradation of BTEX than anaerobic bacteria (Johnson et al., 2003).

In gram negative bacteria, there have been five primary aerobic metabolic pathways identified for BTEX degradation, which include toluene *o*-monooxygenation (*tom*) (Newman and Wackett, 1995), toluene *m*-monooxygenation (*tbu*) (Olsen et al., 1994), toluene *p*-monooxygenation (*tmo*) (Yen et al., 1991), xylene monooxygenase (*xyl*) (Williams and Murray, 1974) and toluene dioxygenation (*tod*) (Zylstra and Gibson, 1989). Each individual pathway may be able to mineralize several components of BTEX while other components may be biotransformed to an intermediate or possibly left unaltered. For example, toluene and m- and p-xylenes are fully mineralized by the *xyl* pathway, however, o-xylene, benzene and ethylbenzene are not affected (Attaway and Schmidt, 2002; Yu et al., 2001). Toluene, ethylbenzene and benzene are fully degraded via *tod* type degradation activity, however, xylenes cannot be fully degraded (Attaway and Schmidt, 2002; Yu et al., 2001). As well, it has been shown that the degradation of o-xylene has a mutually exclusive degradation pathway relative to p- and m-xylene (Kim et al., 2002). Genetically modifying a single bacterium to accomplish complete mineralization of BTEX has been attempted. However, maintaining sterile conditions for a pure culture may not be feasible in many applications, and therefore, a reasonable approach, which was undertaken in this thesis, is to use a consortium of aerobic bacteria.

The simultaneous aerobic degradation of a BTEX mixture is not straightforward, as several interactions between substrates and microorganisms have been observed. Bielefeldt and Stensel (1999) utilized an aerobic bacterial consortium for the treatment of benzene, toluene, ethylbenzene, o-xylene and p-xylene and found the rates of degradation for each compound were slower when in a mixture relative to each component being metabolized individually by an identical consortium. This was attributed to competitive inhibition occurring among the microorganisms, as BTEX loadings were not high enough for the degradation rates to be decreased due to toxicity. Similar results were obtained by Deeb and Alvarez-Cohen (1999) who found that the consumption rates of BTEX were reduced when the components were

present in mixtures, which was attributed to a combination of competitive and non-competitive inhibition within the bacterial consortium, as multiple species are present and, therefore, multiple metabolic pathways are used. To understand performance of the degrading culture, it is important to determine the interactions between BTEX substrates during their consumption by a bacterial consortium, which is investigated in this thesis prior to utilization of a bacterial consortium in a biotreatment system.

1.1.4 Biotreatment Methods

In order to utilize a microbial population for the degradation of BTEX components within gas streams, several treatment methods have been developed. The most commonly studied biotreatment method is biofiltration, which is a process in which polluted air is directed through a filter bed, often composed of peat or compost, containing immobilized biomass. However, there are many limitations associated with biofilter use including ineffectiveness at treating gas streams with high concentrations, as substrate toxicity can occur near the gas inlet due to the plug flow nature of the system, and the inability to treat gas streams with very low concentrations, as threshold concentrations may not be met (Mason et al., 2000). In addition, transfer of the contaminants out of the gas phase to reach the microbial population is challenging due to the relatively high Henry's constants of BTEX (Khan and Kr. Ghoshal, 2000). These limitations cause a dependence on physical or chemical methods for the destruction of high or fluctuating concentrations of gaseous BTEX. Physical or chemical methods also have several limitations relative to biological methods including the production of toxic by-products, energy intensiveness and potentially elevated costs (Khan and Kr. Ghoshal, 2000).

In order to overcome several of the aforementioned limitations associated with the use of biofilters for BTEX degradation, activated carbon can be used, often within the biofilter unit. Activated carbon utilized in biodegradation processes, which is referred to as biological activated carbon (BAC), has the ability to adsorb the target contaminants, making poorly water soluble compounds bioavailable (Mason et al., 2000). As well, threshold concentrations of contaminants in the system can be maintained,

5

as microorganisms can utilize the accumulated BTEX when there is a reduction in concentration in the gaseous inflow. The system is also capable of handling higher loadings of contaminants without substrate inhibition occurring, as the contaminants will be adsorbed onto the activated carbon, separating the biomass from the toxic substances. A major limitation of BAC systems lies in the formation of biofilm on the surface of the activated carbon, as the biomass maintains close proximity to the adsorbed substrate, which can limit the mass transfer from the aqueous phase to the BAC (Mason et al., 2000). If transfer onto the BAC is limited, the purpose of the addition of BAC is defeated, as the system may still be prone to substrate inhibition, threshold substrate concentrations may not be maintained, and contaminants with low water solubility will not be sorbed. Another limitation lies in the fact that activated carbon will accumulate contaminants until all active sites are occupied (Mason et al., 2000). Therefore, the system relies on biological metabolism in order to free up adsorption sites. Due to kinetics being the rate limiting step in a well designed system, it is obvious that a waiting period for adsorption could easily occur with significant loadings. This may lead to a reduction in system performance.

The use of gas permeable membrane bioreactors is another well-studied treatment configuration for VOCs that is designed to overcome limitations of traditional biotreatment methods (England et al., 2005; Kumar et al., 2008a; Studer and Rodolf von Rohr, 2008). The extractive membrane bioreactor utilizes a biofilm on the bulk liquid side of a selective tubular membrane through which contaminated gas is continuously directed through the center of the membrane. Oxygen contained in the air stream is introduced through the membrane or is bubbled into the bulk liquid side of the reactor. VOCs that are present in the gas are highly permeable to the membrane, which increases the bioavailability of the compounds to the biofilm present on the bulk liquid side of the membrane. This overcomes the limitation associated with biofiltration of reduced bioavailability due to low water solubility of contaminants. This configuration also avoids stripping of the volatile compounds by gas bubbles because the contaminants are degraded by the biofilm before they reach the bulk liquid phase (Ferreira Jorge and Livingston, 2000).

6

The major limitation of gas permeable membrane bioreactors is the fact that performance is extremely sensitive to biofilm thickness. The transfer of oxygen/substrate is impeded by the membrane surface/bulk liquid side of biofilm as thickness increases causing degradation rates to decrease (Debus, 1995). In addition, a thick biofilm on a membrane leads to a build-up of substrate at the biofilm/membrane surface interface which reduces the concentration difference between the inner and outer membrane and reduces mass transfer out of the continuous gas stream (Dos Santos and Livingston, 1995). Another limitation of these types of systems is that the membrane surface area to gas volume can only be increased to a certain extent (Wilderer, 1995).

1.2 Stirred-Tank Two-Phase Partitioning Bioscrubbers

In response to limitations of traditional biotreatment methods for toxic VOCs with low water solubility, the stirred-tank TPPB was developed. These systems are also referred to as two-phase partitioning bioreactors and it should be noted that both terms will be used interchangeably for the remainder of the thesis. These bioscrubber systems consist of a cell-containing aqueous phase and an immiscible, biocompatible and non-bioavailable second phase that can be composed of an organic solvent (Yeom and Daugulis, 2001; Nielsen et al., 2005a) or solid polymers (Boudreau and Daugulis, 2006) with a high affinity for target VOCs. As a VOC contaminated gas stream is delivered into the system, the immiscible second phase will sequester high concentrations of the VOCs relative to the cell-containing phase, reducing toxic levels in the aqueous phase and increasing mass transfer out of the gas phase. This is particularly useful during dynamic loading periods wherein the sequestering phase will uptake and release VOCs, effectively dampening concentration fluctuations (Boudreau and Daugulis, 2006; Nielsen et al., 2005a). As excess substrate is present in the aqueous phase, or as the VOCs are metabolized in the cell-containing phase, substrate is transferred to/from the sequestering phase in order to maintain thermodynamic equilibrium according to the partition coefficient between the aqueous and immiscible phases as follows:

$$K_i = \frac{C_{i,p}}{C_{i,l}}$$

<div align="right">**1-1**</div>

Therefore, TPPBs can overcome limitations typically associated with biofiltration, including avoiding substrate toxicity and increasing bioavailability of poorly water soluble VOCs. In addition, in contrast to BAC and membrane bioreactors, the majority of TPPBs are suspended cell bioreactors and therefore mass transfer limitations due to biofilm growth are not a concern. Due to the benefits of TPPBs, this thesis focused on the use of TPPB technology for the treatment of gas streams containing BTEX.

1.2.1 Liquid-Liquid TPPBs

The most common TPPBs for the treatment of gas streams are those with a liquid sequestering phase composed of an organic solvent, which is shown in Figure 1-1. Silicone oil is a convenient choice as a sequestering phase, as it is nonbioavailable to a wide range of microorganisms and has been used in suspended cell TPPBs for the treatment of hexane (Arriaga et al., 2006; Muñoz et al., 2006), α-pinene
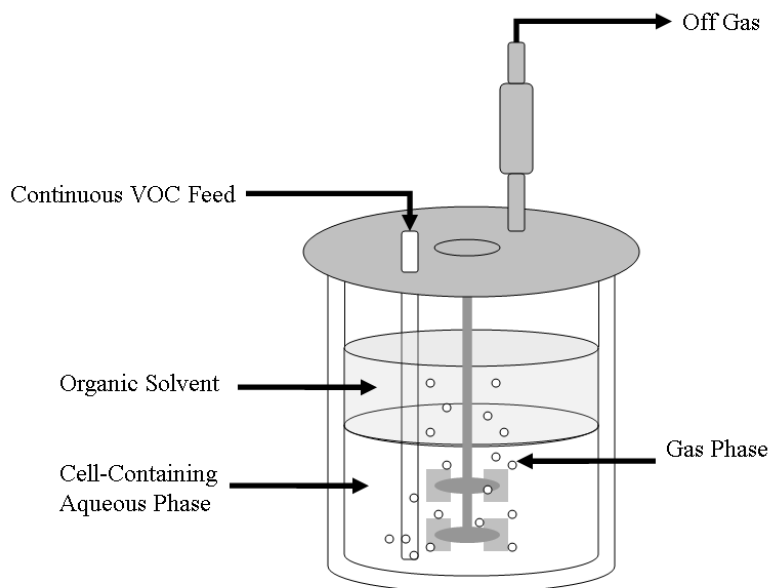
Figure 1-1: Schematic of a liquid-liquid two-phase partitioning bioscrubber

(Muñoz et al., 2008), and isopropylbenzene (Aldric et al., 2009); biotrickling filters for treatment of hexane (Van Groenestijn and Lake, 1999) and styrene (Djeribi et al., 2005) and in biofilters for the treatment of hexane (Arriga et al., 2006). However, because of its fixed chemical structure, silicone oil cannot be modified for optimal uptake and release of specific VOCs.

Other organic solvents can be selected for use in liquid-liquid TPPBs which are paired with a particular contaminant based on affinity and a single microorganism based on toxicity and bioavailability. Several other factors, such as cost and immiscibility of the solvent, are also important during solvent selection, and a strategy for rational selection of a liquid sequestering phase was previously developed by Bruce and Daugulis (1991). Examples of organic solvents used in TPPBs that were selected based on pairing with a particular contaminant include the use of n-hexadacane for the treatment of benzene (Davidson and Daugulis, 2003; Nielsen et al., 2005a) and 2,2,4,4,6,8,8-heptamethylnonane for the treatment of α-pinene (Muñoz et al., 2008). However, these systems are typically limited to the treatment of single VOCs and the use of pure strains of microorganisms due to the potential bioavailability of the organic solvent. This restricts the use of organic solvents other than silicone oil for BTEX mixtures, as treatment of waste gases containing BTEX requires the use of a bacterial consortium (Bielefeldt and Stensel, 1999). To use a bacterial consortium in a TPPB, while rationally selecting the sequestering phase for optimal uptake of BTEX, an alternative to the organic solvent second phase was used in this thesis, which is described in the following section.

1.2.2 Solid-Liquid TPPBs

The ability of polymers to extract select compounds from aqueous solutions has been studied for decades, and organic molecules that exist in aqueous solutions, such as aromatic compounds, can be strongly absorbed and readily desorbed by certain polymers (Bowen, 1970). Recently, it has been shown that the organic solvent phase in a TPPB can be replaced with solid polymer beads, which will uptake and release VOCs in a similar manner (Boudreau and Daugulis, 2006). This system is identified as the solid-
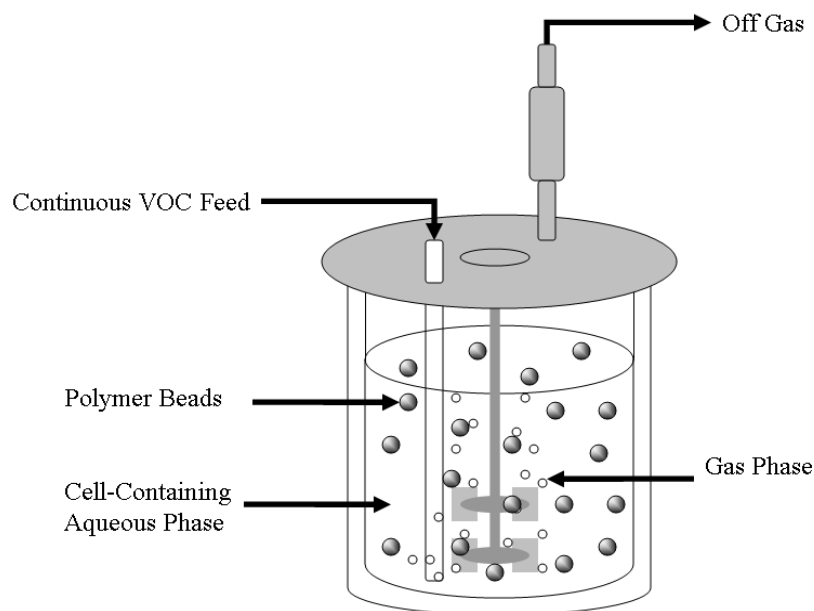
Figure 1-2: Schematic of a solid-liquid two-phase partitioning bioscrubber

liquid TPPB (SL-TPPB), which can be seen in Figure 1-2. A significant advantage of using solid

polymers for a sequestering phase in a TPPB is that polymers are generally nonbioavailable to a wide-

range of bacteria, as they are designed to be resistant to degradation. This enables the use of a bacterial

consortium, which is imperative for the treatment of BTEX.

In addition, a wide range of polymers are available that contain different functional groups. This

allows for polymers to be selected rationally, according to the target molecules for degradation. The use

of polymers for the second phase in a TPPB can be less environmentally and operationally hazardous in

comparison to organic solvents, as polymers can potentially consist of recycled polymer products and are

typically less toxic. Investigations using SL-TPPBs for the treatment of continuous gas streams have

been limited to toluene degradation prior to this thesis, where it was found that the system could handle

extremely high loadings as well as concentration step changes and spikes (Boudreau and Daugulis, 2006).

This thesis explored the application of the SL-TPPB to a more complex, and industrially realistic, mixture of compounds by investigating the treatment of a gas stream contaminated with BTEX by such a system containing a bacterial consortium.

1.2.3 Oxygen Mass Transfer

Often the sequestering phases used in TPPBs not only have a high affinity for target contaminants, but also for oxygen. An important aspect of the liquid-liquid TPPB was investigated by Nielsen et al., (2005b) who determined that the organic phase increases the oxygen transfer rate (OTR). It was found that this enhancement was due to the organic solvent having relatively high oxygen solubility in comparison to the aqueous phase, which provided an increased driving force between the gas phase and the working volume of the bioscrubber. Therefore, it was determined that the addition of an organic solvent second phase into a bioscrubber has the potential to reduce oxygen limitations relative to a system without an organic solvent. It was also observed that the measured oxygen volumetric mass transfer coefficient (k_La) was lower in the bioscrubber containing an organic solvent relative to a single phase system, which was attributed to the uptake of oxygen by the second phase during the dynamic period of measurement, causing the aqueous phase to take longer to saturate (Nielsen et al., 2005b). Other authors have also found that the addition of a second phase with a high affinity for oxygen into a bioreactor will improve oxygen bioavailability, such as the improvement in penicillin production by the addition of n-hexadecane (Ho et al., 1990) and the improvement in oxygen mass transfer by the addition of the substrate/second phase of methyl ricinoleate to enhance the biotransformation of methyl ricinoleate into γ-decalactone (Gomes et al., 2007).

More recently it was observed by Boudreau and Daugulis (2006) that oxygen limitations that were encountered during operation of a single phase bioscrubber during treatment of dynamic loadings of gaseous toluene were avoided in a SL-TPPB during operation under identical conditions. Therefore, Boudreau and Daugulis (2006) hypothesized SL-TPPB systems have the ability to alleviate oxygen

limitations that would be encountered without the presence of the second polymer phase. Furthermore, the polymers utilized in SL-TPPBs have low glass transition temperatures, which is a key parameter for oxygen permeability (Johnson and Thomas, 1999). Therefore, the characterization of oxygen transfer in a gas-liquid system containing solids with varying oxygen affinities was completed in this thesis to determine if a polymer phase with a high oxygen affinity enhances the OTR in a similar manner to organic solvents.

1.2.4 Mathematical Modeling

Mathematical modeling is common in the research area of biotreatment systems for VOC decontamination, as it serves to quantify kinetic and mass transfer mechanisms within the system, as well as to predict system performance under various operating conditions. These models are most often mechanistic, unstructured, macroscopic models that are developed based on mass balances of compounds and biomass in the system. Modeling of liquid-liquid TPPBs was completed for the treatment of a benzene contaminated gas stream which consisted of model development, sensitivity analysis and validation (Nielsen et al., 2007a; Nielsen et al., 2007b). A major assumption in the development of the liquid-liquid TPPB model is that instantaneous equilibrium of benzene between the organic solvent and the aqueous phase is achieved due to high interfacial surface area and high mass transfer rates at the agitation rates used (800 rpm). In addition, transfer in parallel from the gas phase to the aqueous and organic solvent phases was assumed.

Although these assumptions are valid for a liquid-liquid TPPB, they do not hold true for SL-TPPBs, as uptake by the polymers cannot be assumed to be instantaneous. Also, in three phase systems wherein the solids are larger than the gas-liquid boundary layer, mass is transferred from the gas phase to the aqueous phase and then subsequently to the polymer phase (Kars et al., 1997). Although solid-liquid-gas systems have been modeled for the case of immobilized biomass (Jia et al., 2009; Livingston and Chase, 1989; Toumi et al., 2008), prior to this thesis there were no models developed for suspended cell

solid-liquid-gas systems wherein the solid absorbs and desorbs the target substrate. As modeling is a useful tool for biotreatment systems, this thesis described the development of a mathematical model of a stirred-tank SL-TPPB for the treatment of a BTEX contaminated gas stream.

1.3 Airlift Bioreactors

Although stirred tanks provide a convenient configuration for preliminary investigations, scale up of mechanically agitated TPPBs is constrained by their excessive energy inputs. Airlift reactors can offer distinct advantages over stirred tank reactors, as they are more energy efficient and have the ability to transfer higher quantities of target materials out of the gas phase per unit input power (Shuler and Kargi, 2002). An internal loop airlift reactor consists of two concentric tubes, the inner tube called the riser and the outer tube called the downcomer. There are four main sections within an internal loop airlift reactor; the riser, the downcomer, the bottom section containing the gas inlet, and the top section containing the gas/liquid separator. For a concentric tube internal loop airlift reactor the gaseous phase is delivered into the vessel below the downcomer, causing the typical flow within the reactor shown in Figure 1-3.

Besides reducing energy consumption per unit volume of reactor, other advantages include reducing costs and providing a low shear environment (Chisti, 1989). Furthermore, airlift reactors can provide high fluid circulation, large mass and heat transfer, and a short mixing time (Lu et al., 1994).
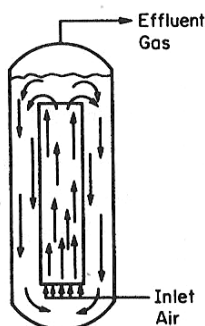
Figure 1-3: Typical flow in an internal loop airlift reactor (Shuler and Kargi, 2002)

Therefore, subsequent to investigation of a stirred-tank SL-TPPB which provided a benchmark to other TPPB systems, the SL-TPPB was applied in an airlift reactor configuration for gaseous BTEX treatment in this thesis.

1.3.1 Oxygen Mass Transfer

As described in Section 1.2.3, both liquid-liquid TPPBs and SL-TPPBs in the stirred tank configuration have the potential to avoid oxygen limiting conditions during dynamic substrate loadings. However, this result does not necessarily translate to the airlift SL-TPPB, as the airlift is a low shear environment relative to the stirred tank system. Therefore, it cannot be assumed that the addition of polymers will have the same effect on gas-liquid mass transfer in both systems. In particular, physical enhancement that can be provided by solids in a bioreactor by mixing of mass transfer boundary layers and/or reducing bubble size (Zhang et al., 2006; Ruthiya et al., 2003) may be different in a high shear environment (stirred tank) relative to a low shear environment (airlift). In addition, prior to this thesis, there was no experimental evidence to show that the addition of polymers with a high affinity for oxygen into an airlift SL-TPPB would have an effect on oxygen mass transfer.

Unlike stirred tank reactors, airlift reactors cannot be assumed to be well-mixed, as there is an axial distribution in concentration profile within the vessel, which is described in more detail in Section 3.1.2. This adds complication to quantifying oxygen mass transfer by measuring $k_L a$ using the static gassing out method, as this method assumes well-mixed conditions exist. Therefore, the utilization of the static gassing out method for an airlift system must be justified. Andre et al., (1983) compared the $k_L a$ obtained when using the static gassing out method under the assumption of well-mixed conditions to the $k_L a$ obtained when using a tanks-in-series model to account for axial variation in concentration in an airlift reactor. It was found that accurate estimates for $k_L a$ in the airlift could be obtained using the well-mixed model if Equation 1-2 is satisfied.

$$k_L a \ \ t_c \leq 2 \hspace{6cm} \textbf{1-2}$$

There are several studies that investigated oxygen transfer in solid-liquid-gas airlift bioreactors, and it was shown that the physical properties of the solid have a large impact on gas-liquid mass transfer. For example, $k_L a$ in a three phase system has been shown to increase or decrease relative to a system without solids depending on the solid density, size and hydrophobicity of the solids (Freitas and Teixeira, 2001; Schumpe et al., 1987; Özbek and Gayik, 2001). The solid phase in the airlift SL-TPPB studied in this thesis has distinctive physical properties to those systems investigated by other researchers, and therefore, this thesis characterized oxygen transfer within this system experimentally.

1.3.2 Hydrodynamics

Flow in an airlift bioreactor commonly falls somewhere between the two hydrodynamic extremes of plug flow and perfectly mixed flow (Swaine and Daugulis, 1988). The flow hydrodynamics, and, correspondingly, the extent of mixing, are often quantified for a particular airlift bioreactor by performing an analysis of the residence time distribution (RTD) within the vessel. The RTD is often obtained by injecting a detectable tracer, such as an acid or base, in a pulse or step change input to the reactor and observing the trace as the system reaches uniformity. A typical RTD trace for a pulse input into an airlift bioreactor can be seen in Figure 1-4.
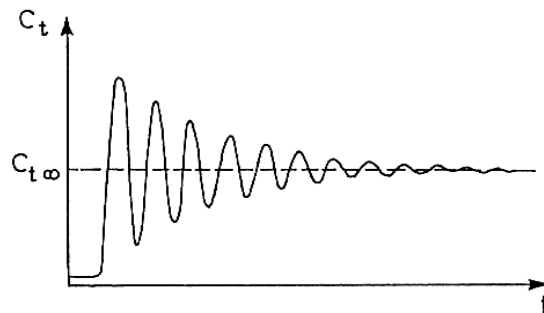
Figure 1-4: Typical response to a pulse input for an airlift loop reactor (Chisti, 1989)

The presence of a solid phase within an airlift reactor can have significant impacts on the RTD and, therefore, the hydrodynamic parameters. The effect of polystyrene and calcium alginate beads on mixing in a concentric tube airlift bioreactor was studied by Lu et al., (1994) and it was found that mixing in the riser containing polystyrene was not significantly different from the single-phase airlift, whereas mixing in a system containing calcium alginate was reduced relative to a single-phase airlift. This effect was explained to be due to the presence of styrene not reducing the liquid velocity, whereas the presence of calcium alginate did (Lu et al., 1994). This suggests that the addition of solids into an airlift bioreactor may or may not change hydrodynamic properties relative to a system without solids depending on the solid properties, and therefore must be characterized on a case-by-case basis. Therefore, to understand the impact of the solid phase on mixing in an airlift SL-TPPB, this thesis characterized hydrodynamics in such a system relative to an airlift without a polymer phase by analyzing the RTD. The information provided by the RTD analysis also provided parameter values to describe mixing within the airlift SL-TPPB, which can be used in mathematical modeling, as described in the following section.

1.3.3 Mathematical Modeling

Mathematical modeling of gas-liquid airlift bioreactors for the treatment of VOCs is a well-studied topic wherein models have been developed for both steady-state (Edwards et al., 1999; Livingston, 1991; Hecht et al., 1995) and dynamic operation (Lo and Hwang, 2004; Nikakhtari and Hill, 2005). As mentioned previously, unlike the stirred-tank SL-TPPB, the contents of the airlift SL-TPPB cannot be assumed to be well mixed. In order to model a vessel that has a level of mixing between well mixed and plug flow, there are two options; the axial dispersion model and the tanks-in-series model. Axial dispersion models consist of a set of partial differential equations to describe the axial variation in concentration using a single parameter to quantify the degree of mixing (Swaine and Daugulis, 1988). The tanks-in-series model assumes a series of perfectly mixed stages to represent the reactor and the degree of mixing is determined by the number of stages in series, N. As the number of tanks becomes

larger, the degree of mixing decreases, approaching plug flow. The model that is more often used to describe airlift bioreactors is the tanks-in-series model (Kanai et al., 2000; Sikula et al., 2006; Znad et al., 2004) as tanks-in-series modeling can provide more accurate predictions over a larger range of mixing conditions and is numerically easier to compute (Turner and Mills, 1990). Mathematical models are valuable tools for biotreatment systems, as discussed in Section 1.3.3, and therefore the airlift SL-TPPB investigated in this thesis was modeled using the tanks-in-series strategy.

1.4 Objectives

It was the overall objective of this thesis to develop and characterize a SL-TPPB for the treatment of BTEX contaminated gases; initially in a stirred tank configuration to provide a comparison to previously studied TPPB systems, and then in an airlift configuration to provide an energy efficient alternative to the stirred tank. In order to fully characterize both systems, fundamental studies in biodegradation kinetics, oxygen mass transfer, and, for the case of the airlift system, hydrodynamics, were completed. Finally, a dynamic mathematical model of the stirred tank SL-TPPB and a steady-state mathematical model of the airlift SL-TPPB were developed in order to predict performance under various operating conditions.

Chapter 2

Oxygen Transfer in a Gas-Liquid System Containing Solids of Varying Oxygen Affinity

Jennifer V. Littlejohns, Andrew J. Daugulis

2.1 Preface to Chapter 2

An advantageous feature of liquid-liquid TPPBs is the ability to enhance the oxygen transfer rate (OTR) from the gas phase, circumventing potential oxygen limitations during dynamic substrate loadings. The mechanisms of this enhancement have been investigated by Nielsen et al., (2005b), who determined that the addition of a solvent with a high affinity for oxygen (n-hexadecane) increased the overall solubility of oxygen within the system, increasing the driving force of oxygen from the gas phase and, therefore, the OTR. However, the measured volumetric mass transfer coefficients (k_Las) were found to be lower for a TPPB containing a solvent with a high affinity for oxygen, relative to a single phase system. This observation was attributed to the uptake of oxygen by the sequestering phase during the dynamic period of measurement, which caused the aqueous phase to take longer to saturate.

SL-TPPBs have been shown experimentally to have higher DO concentrations relative to single phase systems during periods of dynamic toluene loading (Boudreau and Daugulis, 2006), and therefore, it was hypothesized that the addition of polymers with a high affinity for oxygen also increases OTR in a similar manner to liquid-liquid TPPBs. This chapter shows that the polymers within a TPPB physically enhance k_La and increase the OTR, which provides an explanation for the observed higher DO concentrations in SL-TPPBs containing solids with high oxygen affinity relative to a single phase system during dynamic inlet loading periods. Furthermore, this chapter provides a method of estimating the physical enhancement of k_La in systems containing polymers with an affinity for oxygen. From the results of this chapter, it can be anticipated that a stirred-tank SL-TPPB treating BTEX may avoid oxygen limiting conditions during dynamic substrate loadings, as polymers with high affinity for oxygen (e.g. silicone rubber) will uptake and release oxygen in a similar manner to VOCs. These findings are useful for stirred tank aerobic biological systems in which oxygen limitations occur, as the addition of polymers with a high affinity for oxygen increases the OTR from the gas phase to the working volume of the reactor. The physical enhancement coefficients (E_P) and k_La determined in the present work will provide parameter estimates for the stirred-tank SL-TPPB model described in Chapter 5.

2.2 Abstract

An air sparged, mechanically agitated bioreactor containing spherical solids was studied in order to determine the effect of the solid phase on oxygen mass transfer. It was found that both nylon 6,6 and glass beads cause an enhancement of the volumetric mass transfer coefficient of up to 268%, whereas particles of silicone rubber and styrene-butadiene copolymer reduce the volumetric mass transfer coefficient by up to 63%, relative to a system without a solid phase. A simple transport in series model has been proposed to account for the observed phenomena, which includes both the physical enhancement effects of particles on gas-liquid mass transfer as well as absorption of oxygen into the polymer. Even though volumetric mass transfer coefficient reductions were observed in the system containing silicone rubber, it was demonstrated that an increased oxygen transfer rate into the working volume of a two-phase system occurs relative to a system without a solid phase. This study provides an explanation for previous results regarding the enhanced effect of the presence of a styrene-butadiene copolymer phase in reducing oxygen limitations in a solid-liquid two-phase partitioning bioreactor. Results from this study can be applied to two-phase aerobic fermentation systems that will benefit from reducing oxygen limiting conditions.

Keywords: Oxygen transfer rate; $k_L a$; Solid-liquid two-phase partitioning bioreactor

2.3 Introduction

The limiting rate in many aerobic bioreactor systems is the transport of oxygen from the gaseous phase to the liquid phase due to the low solubility of oxygen in water. As a result, the volumetric mass transfer coefficient, k_La, is often quantified in order to allow for proper system design. However, the presence of a third phase can have a large impact on k_La, which must be accounted for in order to ensure that the system is not oxygen limited, nor over designed. Liquid-liquid two-phase partitioning bioscrubbers (TPPBs), which consist of a working volume of two-phases treating a contaminated gaseous phase, have been shown to ease oxygen limitations by the presence of immiscible organic solvents such as n-hexadecane. Due to a larger oxygen concentration in the liquid-solvent phase at equilibrium with the gaseous phase, the overall mass transfer rate of oxygen into the liquid-liquid system is increased according to a larger gas-liquid driving force (Nielsen et al., 2005b). However, this causes the measured volumetric mass transfer coefficient to be lower relative to the absence of a second liquid phase due to the system taking longer to reach the higher saturation value. The measured volumetric mass transfer coefficient for a system consisting of two distinct phases in the working volume with significant oxygen affinity is defined as the effective volumetric mass transfer coefficient, k_La_{eff}. The presence of solid styrene-butadiene copolymer beads in a solid-liquid TPPB (SL-TPPB) has also been found to reduce oxygen limitations in comparison to a system without a second solid phase that encountered oxygen limitations under the same conditions as the SL-TPPB (Boudreau and Daugulis, 2006). As a result of these findings, there is an interest in quantifying the effect of polymer beads in a TPPB on oxygen mass transfer.

Many studies have been completed regarding the effect of solid particles on gas-liquid oxygen mass transfer but a simple mechanism to describe all cases does not exist. Some systems show an enhanced k_La (Guo et al., 1997; Kluytmans et al., 2003; Tinge and Drinkenburg, 1995) and some systems measure a decreased k_La (Freitas and Teixeira, 2001; Özbek and Gayik, 2001) relative to systems without particles. It is clear, however, that the effect of the particles on the system is a function of particle

properties, vessel and impellor dimensions and arrangement and operating conditions (Gogoi and Dutta, 1996; Roman and Tudose, 1997). Such particle properties include oxygen diffusivity of the solid particles (Zhang et al., 2006), particle density (Freitas and Teixeira, 2001; Öztürk and Schumpe, 1987), particle size (Beenackers and Van Swaaij, 1993; Özbek and Gayik, 2001), particle hydrophobicity (Schumpe et al., 1987), and concentration of particles (Ozkan et al., 2000; Roman and Tudose, 1997).

Enhancement of k_La was observed for small particles present in gas-liquid systems and this was originally explained to be due to a shuttling effect wherein absorptive particles enter the liquid boundary layer, absorbing dissolved gas and then desorbing the dissolved gas when back in the bulk phase (Kars et al., 1997). Shuttling has been shown to be predominant in particles with a size equal or smaller than the gas-liquid boundary layer (Kars et al., 1997; Ruthiya et al., 2003), however, this size is much smaller than that used in a SL-TPPB. It has also been shown that enhancement can occur in systems with inert particles, i.e. without absorptive properties, which indicates that there are several mechanisms acting on a gas-liquid-solid system to increase the gas-liquid mass transfer (Kluytmans et al., 2003). The possible mechanisms that can account for this phenomenon include boundary layer mixing and changes in interfacial area. Boundary layer mixing involves an increase in k_L due to turbulence at the gas-liquid interface (Ruthiya et al., 2003; Zhang et al., 2006), which causes a larger refreshment rate of liquid in the boundary layer by mixing with the bulk fluid. Changes in the gas-liquid interfacial area can be caused by particles being present at the gas-liquid interface, causing coalescence inhibition and an increase in 'a' (Ruthiya et al., 2003).

The purpose of this investigation was to determine k_La_{eff} in an abiotic solid-liquid TPPB system for various solid types. This will be compared to k_La_{INERT}, which is defined as the measured volumetric mass transfer coefficient of a system containing two distinct phases, with the solid phase having negligible oxygen affinity (inert). As well, both k_La_{eff} and k_La_{INERT} were compared to a single aqueous phase, k_La. A theoretical "transport in series" model was developed involving an estimated physical

enhancement term in order to determine the oxygen uptake by the polymer beads. Finally the increased oxygen transfer rate in a solid-liquid TPPB relative to a system without a second phase was demonstrated.

2.4 Materials and Methods

2.4.1 Volumetric Mass Transfer Coefficients

The bioreactor used was a New Brunswick Bioflo™ III with an internal diameter of 17 cm, which was agitated by a single six blade Rushton turbine impeller of diameter 7.7 cm. Four baffles were also provided to increase mixing. All experiments were operated at 30 ± 0.1 ºC, and measurements were taken in duplicate with the average value being reported.

All systems, which consisted of 500 g of each solid type in tap water to total working volume of 3L, were operated at aeration rates of 0.5, 0.75 and 1 L min^{-1}. This was repeated for agitation rates of 100, 200, 300 and 400 rpm, with the exception of glass beads, which was only stirred at 400 rpm due to the inability to suspend the glass beads at lower agitation rates. Higher operating conditions of 1, 2, and 3 L min^{-1} for each of 400, 600 and 800 rpm were also completed for each system.

Using styrene-butadiene copolymer and silicone rubber, with properties listed in Table 2-1, $k_L a_{eff}$ was determined. As well, $k_L a_{INERT}$ was determined using nylon 6,6 and glass beads, with properties also listed in Table 2-1. All solid particles used were approximately spherical in shape. Styrene-butadiene copolymer and nylon 6,6 were obtained from Scientific Polymer Products, Inc., glass beads were obtained from Fisher Scientific and silicone rubber was obtained from GE-Mastercraft® in the form of 100% silicone rubber caulking. The caulking was dried to spherically shaped beads.

The unsteady-state method was used to determine $k_L a_{eff}$, $k_L a_{INERT}$ and $k_L a$ as described by Shuler and Kargi, (2002). The system was first sparged with nitrogen in order to remove oxygen. Air was then delivered into the reactor through a 5 mm diameter single orifice sparger that was directly below the mechanical agitator and located 1.5 cm from the bottom of the tank. Oxygen concentration was measured

Table 2-1: Properties of Solids

Polymer	Oxygen diffusivity ($cm^2\ s^{-1}$)	Diameter (mm)	Density ($g\ L^{-1}$)
Nylon 6,6	1.6×10^{-9} (Jarus et al., 2002)	2.59	1140
Styrene-butadiene copolymer	1.4×10^{-6} (Roff et al., 1971)[a]	3.57	940
Silicone rubber	3.4×10^{-5} (Merkel et al., 2000)[b]	2.5	1150
Glass	$<10 \times 10^{-16}$ (Kalen et al., 1991)	6	2500

[a] Butadiene/styrene (wt:wt part %) 77:23. This is an approximation, as the styrene-butadiene used in this study was butadiene/styrene (wt:wt parts%) 72:28.
[b] Value measured at 35 °C

by an OxyProbe ® D100 Series Polarographic Dissolved Oxygen (DO) Sensor (Broadley James Corp.) until saturation was reached. For consistency, data between 30% and 80% of liquid saturation were used for the determination of $k_L a_{eff}$, $k_L a_{INERT}$ and $k_L a$. An integrated, linearized form of Equation 2-1 can then be utilized in order to determine $k_L a_{eff}$, $k_L a_{INERT}$ and $k_L a$, which is the negative slope of the log of the concentration driving force versus time.

$$\frac{dC_l}{dt} = k_L a\left(C_l^* - C_l\right) \text{ or } \frac{dC_l}{dt} = k_L a_{eff}\left(C_l^* - C_l\right) \text{ or } \frac{dC_l}{dt} = k_L a_{INERT}\left(C_l^* - C_l\right) \qquad \textbf{2-1}$$

Under circumstances in which low aeration and agitation rates were used, surface aeration for this reactor could have been significant, but it was found (data not shown) that the mass transfer coefficients due to surface aeration are negligible in comparison to those found with gas sparging and agitation.

There is a significant response time lag between the actual percent saturation of oxygen in the water and that which is read by the oxygen probe if the time constant of the probe, τ_P, is much smaller than the inverse of $k_L a_{eff}$, $k_L a_{INERT}$ and $k_L a$ (Brown, 2001). Transport through an electrode membrane can be described by Equation 2-2.

$$\frac{dC_{PRO}}{dt} = \frac{1}{\tau_P}\left(C_l - C_{PRO}\right) \qquad \textbf{2-2}$$

In order to determine τ_P, the DO probe was immersed in a bath purged with nitrogen and then quickly transferred to an oxygen saturated bath, both of which were maintained at 30 ℃ by the use of a water bath. The probe response was measured several times throughout the duration of the experiment and τ_P was found to be approximately 18.9 ± 1.01 s. This response is higher than expected from both the literature (Nielsen et al., 2003), as well as the probe manual (Broadley James Corporation, 2000), and may be due to the age of the probe. Equation 2-2 was solved simultaneously with Equation 2-1 in order to produce a second order approximation to describe the experimental data considering the probe response. From this approximation the actual k_La_{eff}, k_La_{INERT} and k_La was determined.

2.4.2 Oxygen Uptake by the Polymer Phase

Transport in series is a common model used for a gas-liquid system containing suspended solids larger than the liquid film thickness between the gas and liquid phases (Alper et al., 1980). This involves oxygen mass transfer occurring between the gas and liquid as well as between the liquid and solid, which is represented in Figure 2-1. For this model, the effects of particles on gas-liquid mass transfer must be considered. In addition, as can be seen in Figure 2-1, the absorptive effects of the particles will have an impact on the measured k_La_{eff} for particles with a considerable oxygen diffusion coefficient. For polymers with a significantly high oxygen diffusion coefficient, transport of oxygen into the liquid phase can be expressed using Equation 2-3;

$$\frac{dC_l}{dt} = E_P k_L a (C_l * - C_l) - \frac{dC_p}{dt}\left(\frac{V_p}{V_l}\right) \qquad \textbf{2-3}$$

where the physical enhancement term, E_P, is defined using Equation 2-4.

$$E_P = \frac{k_L a_{INERT}}{k_L a} \qquad \textbf{2-4}$$
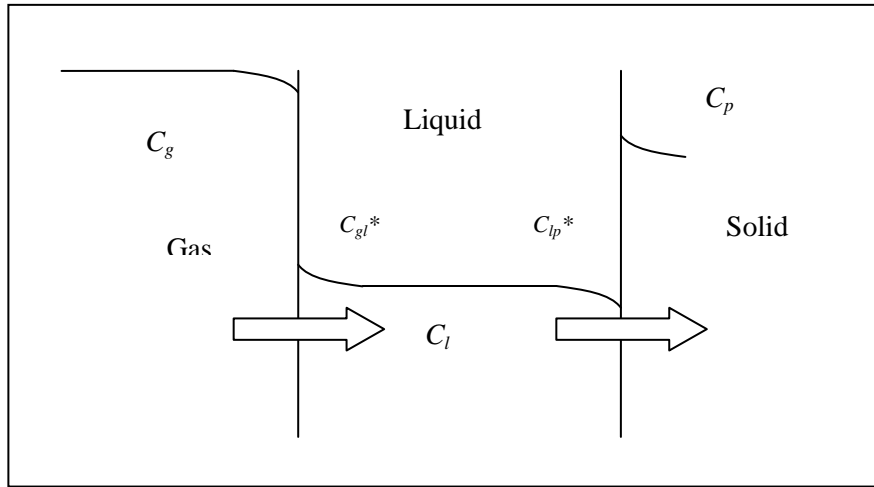
Figure 2-1: Oxygen transport in a gas-liquid-solid system

Therefore, for systems with inert polymers, oxygen transport in the liquid phase can be described using Equation 2-5.

$$\frac{dC_l}{dt} = E_P k_L a \left(C_l^* - C_l \right) = k_L a_{INERT} \left(C_l^* - C_l \right)$$

2-5

Density and radius have been identified as critical properties to physical enhancement, and it is therefore possible to choose inert and absorptive particles that will yield the same E_P. Therefore, E_P can be estimated from Equation 2-4, and used in Equation 2-3. This allows for nylon 6,6 oxygen data (virtually no oxygen absorption into the polymer) to be used in Equation 2-4 to estimate E_P to be used in Equation 2-3 for the silicone rubber system. The same could be done to estimate an E_P for the styrene-butadiene copolymer system, however this was not completed due to the inability to locate inert polymers with the proper density and radius.

In order to determine the oxygen uptake by polymers, Equation 2-3 can be rearranged to give Equation 2-6.

$$\frac{dC_p}{dt} = \frac{V_l}{V_p} \left[E_P k_L a \left(C_l^* - C_l \right) - \frac{dC_l}{dt} \right]$$

2-6

An estimation of dC_l/dt was obtained using interpolation between each data point collected for oxygen concentration in the liquid phase as a function of time. The oxygen concentration in the liquid phase that was recorded for each time can also be substituted in Equation 2-6 and an instantaneous oxygen uptake rate into the silicone rubber polymers can be calculated as a function of time. In MATLAB^{TM}, a spline was fit to the resulting plot of dC_p/dt versus time, which was integrated in MATLAB^{TM} using the trapezoidal rule in order to determine the total mass of oxygen taken up by the silicone rubber polymers. This was completed for 0.5, 0.75 and 1 L min^{-1} at an agitation rate of 400 rpm for data between 30% and 80% of liquid saturation.

2.4.3 System Oxygen Transfer Rate

The concentration of oxygen in the working volume, C_{sys}, is defined as the sum of the concentration of oxygen in the liquid phase and the concentration of oxygen in the solid phase. Oxygen transport into the working volume of the liquid-solid system can be expressed by Equation 2-7.

$$\left(V_p + V_l\right)\frac{dC_{sys}}{dt} = V_l\frac{dC_l}{dt} + V_p\frac{dC_p}{dt}$$

2-7

Substituting Equation 2-3 into Equation 2-7 yields Equation 2-8.

$$\left(V_p + V_l\right)\frac{dC_{sys}}{dt} = V_l\left(E_p k_L a\left(C_l * - C_l\right) - \frac{dC_p}{dt}\left(\frac{V_p}{V_l}\right)\right) + \frac{dC_p}{dt}V_p$$

2-8

which reduces to Equation 2-9.

$$\frac{dC_{sys}}{dt} = \frac{V_l}{\left(V_p + V_l\right)}\left(E_P k_L a\left(C_l * - C_l\right)\right)$$

2-9

This allows for the instantaneous calculation of the oxygen transfer rate into the system, dC_{sys}/dt. Again, a spline was fit and integrated in MATLAB^{TM}, in order to determine the total mass of oxygen transferred into the system. A dynamic period was used to determine the oxygen transfer rate into the system to be

consistent with the reduction in oxygen limiting conditions in a solid-liquid TPPB that was observed in previous work (Boudreau and Daugulis, 2006). The reduction occurred during transient steps in substrate concentration, which caused large oxygen uptake rates by the cellular population. Therefore, dynamic absorption rates are useful to simulate this situation.

2.5 Results and Discussion

2.5.1 Volumetric Mass Transfer Coefficients

The volumetric mass transfer coefficients for aqueous systems containing nylon 6,6, styrene-butadiene copolymer, silicone rubber, and tap water without particles are shown in, respectively, Figure 2-2a to Figure 2-2d. The k_La_{eff} values are up to 55% lower for the system with styrene-butadiene relative
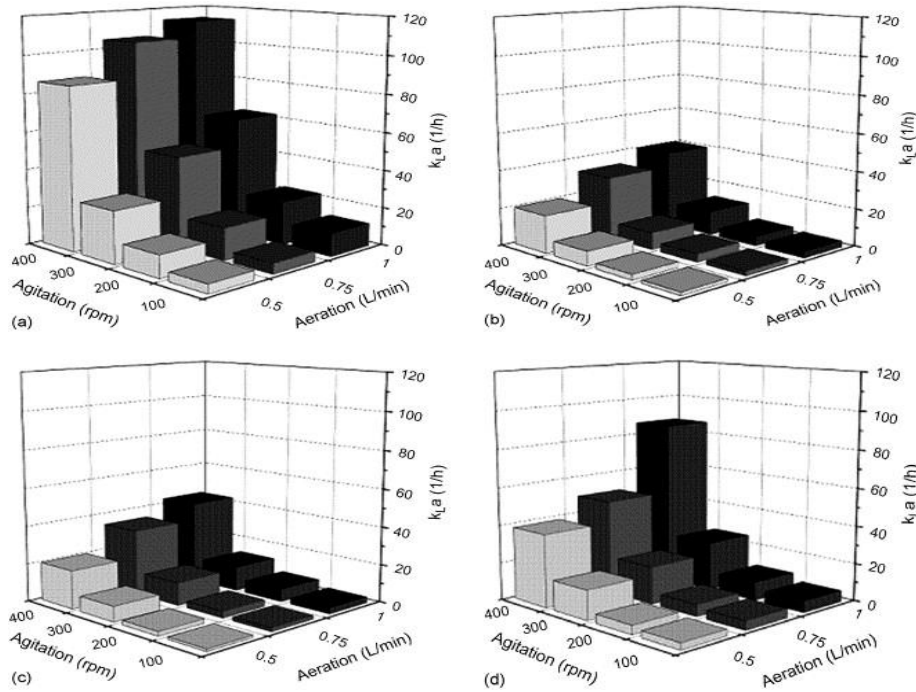
Figure 2-2: (a) Inert volumetric mass transfer coefficients for an aqueous system containing 500 g nylon 6,6. (b) Effective volumetric mass transfer coefficients for an aqueous system containing 500 g styrene-butadiene copolymer. (c) Effective volumetric mass transfer coefficients for an aqueous system containing 500 g silicone rubber. (d) Volumetric mass transfer coefficients for an aqueous system containing no polymers.

28

to the system without particles and up to 63% lower for the system containing silicone rubber. For systems containing styrene-butadiene copolymer and silicone rubber, the measurement of k_La_{eff} includes the effect of the solid polymer absorbing oxygen, as well as any effects the particles may have on gas-liquid mass transfer. The system containing nylon 6,6 shows up to a 268% increase in k_La_{eff} relative to k_La. Due to the low oxygen diffusion coefficient of nylon 6,6, the effect of the particles on the gas-liquid mass transfer coefficient is isolated, and mass transfer enhancement is clearly observed. For all systems at lower operating conditions, k_La_{eff}, k_La_{INERT} and k_La increased with both agitation and aeration rates. This increase with agitation and aeration has been documented in many other systems containing a second phase (Guo et al., 1997; Nielsen et al., 2005b; Özbek and Gayik, 2001).

Figure 2-3 clearly displays k_La_{eff}, k_La_{INERT} and k_La for different aeration rates at 400 rpm for each solid type, including glass beads, and for the water-only system. In a similar manner to nylon 6,6, glass beads are inert and enhance the gas-liquid mass transfer up to 159%. These results are in agreement with findings that describe an increase in k_La in an external loop airlift reactor containing glass beads of 2.3mm diameter (Guo et al., 1997). Figure 2-3 also shows that the enhancement of the gas-liquid mass transfer is
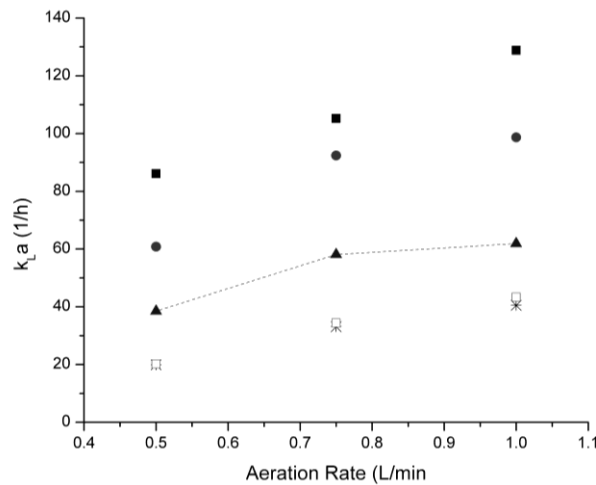
Figure 2-3: Measured volumetric mass transfer coefficients at 400 rpm for nylon 6,6 (square), glass beads (circle), water (triangle and line), silicone rubber (open square) and styrene-butadiene copolymer (star).

much larger for the system containing nylon 6,6 than for the system containing glass beads. Other authors have found that an increase in solid density results in a decrease in k_La, and this is a possible explanation for a denser solid type, glass, having a smaller k_La_{INERT} than a less dense solid type, nylon 6,6 (Freitas and Teixeira, 2001). Silicone rubber and styrene-butadiene have very similar decreases in k_La_{eff} relative to k_La. A study completed on biomass support particles made from Scotchbrite[TM] pads of volumes 0.1625, 0.65 and 1.4625 cm^3 also reported a similar decrease in k_La_{eff}. This decrease was attributed to be a result of a coalescence process, as well as occupation of the liquid volume by the biomass support particles decreasing the effective interfacial area (Özbek and Gayik, 2001).

It can be seen from Table 2-1 that both nylon 6,6 and silicone rubber have very similar dimensions and densities, which have been identified earlier as critical factors for the effect of particles of gas-liquid mass transfer. Nylon 6,6, can therefore be used to approximate the effect of silicone rubber on gas-liquid mass transfer, as both the effects of oxygen absorption by the silicone rubber and the effects on the gas-liquid mass transfer are contained within the measured k_La_{eff} for the silicone rubber system and cannot be separated. At an agitation rate of 400 rpm, nylon 6,6 resulted in enhancement factors for 0.5, 0.75 and 1 L min^{-1}, of, respectively, 2.23, 1.81 and 1.83, which should also be the approximate effects of silicone rubber on gas-liquid mass transfer. These enhancement approximations may contain error due to the assumption that particle hydrophobicity effects can be neglected. Hydrophobicity, or wettability, of the particles has been shown to be a critical property on gas-liquid mass transfer (Schumpe et al., 1987). However, due to the assumption that the system is well mixed, the interactions of the particles with the gas-liquid interface are not increased for a hydrophobic particle, but are equal for all particle types as the particles are evenly distributed throughout the system.

At larger agitation and aeration rates, k_La_{eff}, k_La_{INERT} and k_La were also measured for systems containing silicone rubber, styrene-butadiene copolymer, nylon 6,6 and water without solids (data not shown). Again, k_La_{eff}, k_La_{INERT} and k_La increased with aeration rate for each system in a similar fashion as it did at the lower operating conditions. However, all systems, with the exception of silicone rubber,

revealed an increase in k_La_{eff} and k_La_{INERT} relative to k_La at large agitation rates. This may be attributed to the oxygen uptake by the polymers not being observable, as it is possible that oxygen was transferred from the gas to the liquid at such a fast rate that the liquid was saturated before significant amounts of oxygen could be taken up by the polymer beads. The data for high agitation and aeration rates also revealed that there appears to be an optimum agitation rate of 600 rpm for the liquid-polymer systems, as the measurements at 800 rpm showed a decrease in k_La_{eff} and k_La_{INERT}. This decrease is likely due to a hydrodynamic effect that is unknown; operating zones with inconsistent behavior have been noted in other oxygen mass transfer experiments (Nielsen et al., 2005b). One author reported an increase in stirrer speed caused a plateau effect on the k_La in a gas-liquid-solid system with activated carbon at higher agitation rates (Kluytmans et al., 2003).

2.5.2 Oxygen Uptake by the Polymer Phase

The instantaneous oxygen uptake rate by silicone rubber beads was calculated using Equation 2-6. A plot of the instantaneous oxygen uptake rate versus time was then integrated in order to determine the mass taken up by the polymer between 30% and 80% of liquid saturation. The mass of oxygen taken up by silicone rubber at an agitation rate of 400 rpm is shown in Figure 2-4 for aeration rate of 0.5, 0.75 and 1 L min^{-1}. A larger amount of oxygen is taken up by the system aerated at 0.5 L min^{-1} than systems at 0.75 and 1 L min^{-1}. This result is expected, as silicone rubber has a longer time to take up oxygen if the liquid phase takes longer to saturate. It is expected that the system aerated at 0.75 L min^{-1} will take up more oxygen between 30% and 80% of liquid saturation than the 1 L min^{-1} system, however, a significant difference was not seen in the data. These results suggest that silicone rubber takes up a considerable amount of oxygen at a rate that is observable during the dynamic period of liquid saturation by gas sparging for lower operating conditions. These results shed light on previous findings in our laboratory (Boudreau and Daugulis, 2006) involving styrene-butadiene copolymer in a TPPB providing oxygen
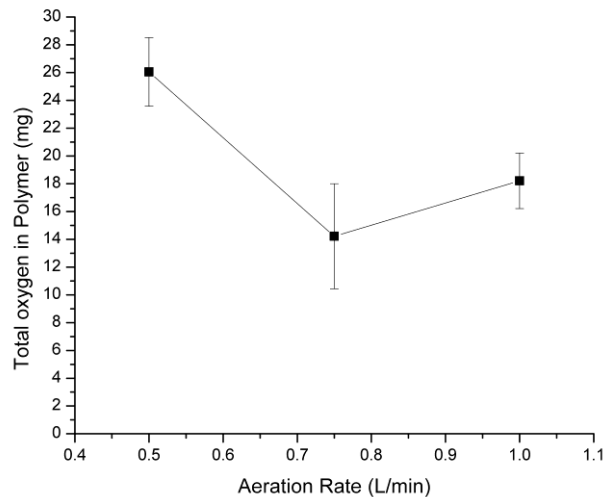
Figure 2-4: Total amount of oxygen taken up by silicone rubber during a period between 30% and 80% of saturation in the liquid phase. Error bars represent one standard deviation.

during what would otherwise be oxygen limiting conditions in the aqueous phase, as mass transfer between the polymer and aqueous phases is sufficiently fast.

2.5.3 System Oxygen Transfer Rate

In order to demonstrate a larger overall uptake of oxygen into a TPPB system relative to a system without a second phase, Equation 2-9 was utilized. The instantaneous oxygen transfer rate as a function of time at 400 rpm agitation and 1 L min^{-1} aeration for a solid-liquid system containing silicone rubber beads is shown in Figure 2-5. Also shown in Figure 2-5 is the instantaneous oxygen transfer rate as a function of time for a system without a second phase, which was calculated using Equation 2-1. This plot clearly shows that between 30% and 80% of liquid saturation the system containing silicone rubber beads has a much larger OTR during the progression to liquid saturation than the system without a second phase. As well, the system with a second phase reaches 80% liquid saturation much later than the system without a second phase. This is due to the polymers acting as an oxygen sink within the system, in turn causing the liquid oxygen concentration to be lower relative to the system without polymer, at any given

32
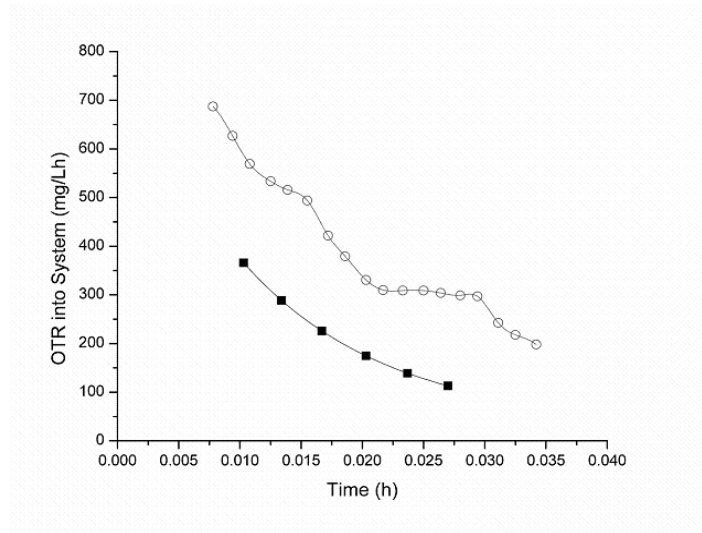
Figure 2-5: Oxygen transfer rate as a function of time between 30% and 80% of liquid saturation by a system of water with silicone beads (open circles) and water without particles (closed squares) and splines fitting both trends (lines).

time. This decrease in the liquid concentration causes an increased driving force for oxygen between the gas and liquid phases, which causes a larger oxygen transfer rate for an extended period of time. Therefore, although the $k_L a_{eff}$ is measured as lower for the reasons explained previously, the overall oxygen transfer rate into the solid-liquid system is larger. This is due to the oxygen transfer rate not only being proportional to the volumetric mass transfer coefficient, but also to the increased instantaneous concentration driving force.

The curves shown in Figure 2-5 were also obtained at 400 rpm for aeration rates of 0.5 and 0.75 L min^{-1} (data not shown). These curves were integrated in order to determine the total mass of oxygen transferred into the working volume for both a system containing absorptive polymer and a system without polymers, which can be seen in Figure 2-6. More than twice the total oxygen was transferred into the system without polymers from 30% to 80% of liquid saturation. The polymers have a large uptake of oxygen and therefore more oxygen can ultimately be contained within the system. These results are comparable to those for liquid-liquid systems that have found that oxygen is transferred at a higher rate
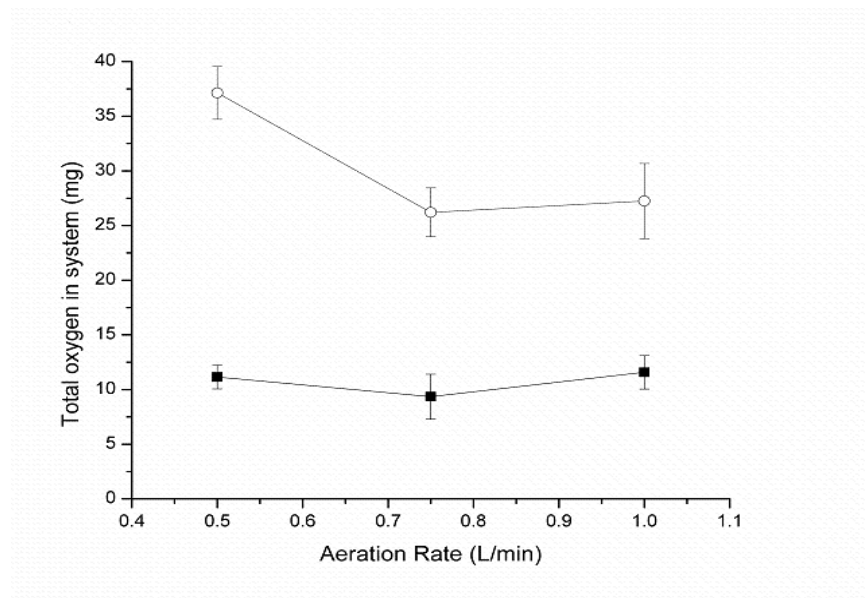
Figure 2-6: Total oxygen transferred into the system between 30% and 80% of liquid saturation for a system of silicone in water (open circles) and water without particles (squares). Error bars represent one standard deviation.

due to an increased driving force (Nielsen et al., 2005b). However, liquid-liquid systems can be viewed as increasing the working volume saturation concentration, whereas the solid-liquid system increases the driving force by decreasing the liquid concentration at any given time, as well as by possibly enhancing gas-liquid mass transfer. Nevertheless, both liquid-liquid and solid-liquid systems increase the overall amount of oxygen that can be contained within a working volume.

Also shown in Figure 2-6 is a decrease in the amount of oxygen transferred into the system containing silicone rubber as aeration rate increases. At higher aeration rates the required time for the liquid phase to saturate decreases. This may cause the polymers to have a shorter period of time to absorb oxygen and the total mass of oxygen observed to be transferred into the system between 30% and 80% of liquid saturation will decrease. It can be seen that the system without a second phase has a relatively constant total amount of oxygen transferred into the system between 30% and 80% of liquid saturation, as no oxygen sink exists.

This observed enhanced oxygen uptake into the system due to the presence of solid particles has positive implications on many aerobic fermentations. Oxygen limitations within a cell-containing liquid phase can be reduced by transfer occurring to the liquid phase from a solid phase with a large oxygen capacity in order to maintain thermodynamic equilibrium. This concept has been demonstrated for several liquid-liquid systems that contain "oxygen carriers", a liquid phase with a higher oxygen solubility than water. One study involved the use of a bioreactor containing Poly(dimethylsiloxane) (PDMS) as an oxygen carrier for the application of wood bleaching. PDMS was used to improve oxygen availability to the white rot fungus *Trametes versicolor*. This study displayed that the addition of 0.5% PDMS caused a significant improvement in the whitening of pulp, as well as the production of biomass, relative to a control with no oxygen carriers present (Ziomek et al., 1991).

2.6 Conclusions

For the solid types tested in an abiotic TPPB, relative to a system without a second phase, the k_La_{eff} was measured to be lower when containing styrene-butadiene copolymer as well as silicone rubber, and k_La_{INERT} was measured to be higher for the systems containing nylon 6,6 and glass beads. The reason for this deviation was attributed to the effect of particles on gas-liquid mass transfer for all systems, as well as an oxygen absorption effect for systems containing polymers with high oxygen diffusivity.

The proposed transport in series model, which combines the effect of gas-liquid mass transfer enhancement with oxygen absorption by the particle, allows for the calculation of the rate of oxygen transfer into the solid material. However, this calculation is reliant upon the assumption that the working volume is well mixed and particle hydrophobicity will not increase interactions with the gas-liquid interface, and therefore will not increase enhancement.

Finally, it was shown that the overall oxygen transfer rate for a system containing silicone rubber beads was more than double the oxygen transfer rate of a system without polymers during 30-80% of the liquid saturation. This clarifies our previous results regarding the presence of styrene-butadiene

copolymer particles as the second phase in a TPPB reducing oxygen limitations. As well, implications from this study can be applied to many solid-liquid aerobic fermentations with regard to their ability to avoid oxygen limiting conditions.

Chapter 3

Kinetics and Interactions of BTEX Compounds during Degradation by a Bacterial Consortium

Jennifer V. Littlejohns, Andrew J. Daugulis

3.1 Preface to Chapter 3

The ability to utilize a bacterial consortium in a SL-TPPB not only allows for the degradation of all four BTEX components simultaneously, but provides a practical advantage over systems that use pure cultures, as avoiding system contamination is no longer a concern. It is common to selectively enrich microorganisms from petroleum contaminated soil that can efficiently degrade BTEX, which often results in a diverse bacterial consortium. This chapter starts with the enrichment of such a bacterial consortium for use in the kinetic investigations described later in this chapter, and in all subsequent work in this thesis.

An understanding of the degradation abilities of a microbial consortium is essential to fully characterize SL-TPPB performance. However, biological kinetics can be challenging to quantify, particularly for the treatment of a mixture of substrates, such as BTEX, as a variety of substrate interactions can occur, including biodegradation enhancement, inhibition and cometabolism. Furthermore, the diversity of the microbial population adds complexity to quantification of the biological growth in the system, as biomass growth rates are unique for each microorganism and are a function of substrate interactions. This chapter describes a series of degradation experiments which allow for the determination of substrate interactions among BTEX components during biodegradation by the enriched bacterial consortium. The experiments result in the development of a model structure and estimation of kinetic parameters to describe substrate degradation and biomass growth. This study contributes a method to model the growth of a biological consortium of unidentified composition, which is valuable to the general area of quantification of microbial kinetics. The results of this chapter are also used in later chapters and will provide an explanation for the observed relative rates of degradation of BTEX components in the stirred-tank and airlift TPPBs, described in Chapters 4 and 6, respectively. In addition, the model structure and estimated parameters will be used to model the biological aspects in the SL-TPPB for the stirred tank configuration in Chapter 5 and the airlift configuration in Chapter 8.

3.2 Abstract

A model to describe the biodegradation of benzene, toluene, ethylbenzene and o-xylene (BTEX) and growth of a bacterial consortium was systematically developed from a series of aerobic batch degradation experiments. The bacterial consortium was enriched from petroleum contaminated soil on a mixture of BTEX components and was identified to contain 7 unique species of *Pseudomonas*. Parameter estimates are reported for both conventional Monod parameters obtained from single substrate degradation experiments and interaction parameters obtained from dual substrate experiments. Key interactions identified include both the inhibition and enhancement of biodegradation rates for mixed substrates relative to single substrate experiments. Enhancement interactions have been qualitatively observed by other authors to occur to BTEX mixtures, but have not been quantified previous to the current study. Observations include the inhibition of benzene degradation in the presence of toluene and in the presence of ethylbenzene. As well, enhanced degradation of benzene was observed in the presence of o-xylene and toluene degradation was enhanced in the presence of benzene. A sum kinetics with interaction parameters (SKIP) model was found to accurately describe these interactions. In addition, it was found that o-xylene was cometabolized in the presence of toluene and/or benzene and a mathematical model was used to describe this interaction. The SKIP and cometabolism models were combined to predict both BTEX degradation as well as biomass production for this consortium when all BTEX components are present simultaneously.

3.3 Introduction

Benzene, toluene, ethylbenzene and *o*-xylene, collectively known as BTEX, are toxic compounds commonly emitted into the environment due to their ubiquitous presence in fuel and petroleum products. Biological processes are becoming increasingly popular for the elimination of these compounds from air (Kennes and Thalasso, 1998), water (Langwaldt and Puhakka, 2000) and soil environments (Zappi et al., 1996) with the goal of achieving regulatory levels. Relative to thermochemical destruction methods, biological processes have inherent green benefits and potential cost savings. In addition, biological processes have the ability to effectively mineralize BTEX in low concentrations.

In order to properly design and model biodegradation processes it is necessary to determine the degradation kinetics of these compounds by bacterial communities. Degradation of combinations of BTEX components by pure bacterial strains has been studied, such as by bacterial cultures of *Rhodococcus rhodochrous* (Deeb and Alvarez-Cohen, 1999), several strains of *Pseudomonas putida* (Alagappan and Cowan, 2003) and *Alcaligenes xylosoxidans* (Yeom and Yoo, 2002). However, in order to efficiently degrade all BTEX components simultaneously a bacterial consortium is required, particularly for the removal of *o*-xylene, which has been found to be markedly persistent compared to other BTEX compounds (Attaway and Schmidt, 2002; Deeb and Alvarez-Cohen, 1999).

The degradation of more than one growth limiting substrate by a bacterial population is not straightforward, as many different substrate interactions have been identified for combinations of BTEX components that can alter degradation rates relative to the absence of other substrates (Deeb and Alvarez-Cohen, 1999). Such interactions can involve the enhancement or inhibition of degradation of substrates when in mixtures (Abuhamed et al., 2004; Arvin et al., 1989; Oh et al., 1994). Inhibition of BTEX degradation by a bacterial consortium has previously been modeled using purely competitive inhibition kinetics (Bielefeldt and Stensel, 1999), however enhancement interactions that have been qualitatively observed to occur during BTEX degradation by a consortium (Alvarez and Vogel, 1991; Arvin et al., 1989) have not been modeled to date. Moreover, an important stimulation interaction that has been

observed to occur to *o*-xylene in the presence of other BTEX compounds is cometabolism (Attaway and Schmidt, 2002) and models in order to describe the degradation of xylenes due to this interaction have been applied successfully (Chang et al., 1993).

Systematic approaches for determining substrate interactions during degradation by pure bacterial strains have been used for a mixture of three aromatic hydrocarbons (Reardon et al., 2000) and three PAHs (Dimitriou-Christidis and Autenrieth, 2006) and an identified and quantified bacterial consortia for a mixture of three aromatic hydrocarbons (Reardon et al., 2002). The present study successfully quantifies the kinetic parameters and substrate interactions for all four BTEX components during degradation by a bacterial consortium. As noted above, the only substrate interaction modeled for BTEX components to date has been competitive inhibition, and the current study serves to quantify additional interactions that have been observed only qualitatively. An appropriate model to describe interactions between all four BTEX components is systematically determined using dual substrate experimental data. The model structure is then verified by means of comparison to the experimental data for the degradation of all four components simultaneously. In addition, the current study investigates the use of the semi-empirical Monod model to predict biomass growth for a bacterial consortium with minimal knowledge of consortium composition. The developed model is shown to fit experimental data accurately.

3.4 Theory

For batch degradation biomass growth can be described by Equation 3-1 (Shuler and Kargi, 2002), which can describe biomass growth due to a single or multiple substrates.

$$\frac{dX}{dt} = \mu X \qquad\qquad\qquad \textbf{3-1}$$

Depletion of growth associated substrates in a batch degradation for a given substrate, *i*, can be described using Equation 3-2.

$$\frac{dC_i}{dt} = -\frac{\mu_i X}{Y_{X/i}}$$

3-2

These equations hold true when maintenance requirements are negligible, which is typically assumed during the period of kinetic measurement of rapidly growing cells, as the metabolism of substrate is primarily growth associated (Nielsen et al., 2007b). It should be noted that the yield coefficient (Equation 3-2) must consider the consumption of compounds from both gas and liquid phases due to the volatility of BTEX, assuming that transfer between gas and liquid phases is rapid.

There are several models used to describe the specific growth rate for use in Equations 3-1 and 3-2. The most common model for the biodegradation of a single growth substrate, the Monod model, is shown as Equation 3-3 (Shuler and Kargi, 2002).

$$\mu_i = \frac{\mu_{max,i} C_i}{K_{S,i} + C_i}$$

3-3

Single substrate degradation experiments can be used to estimate the kinetic parameters μ_{max} and K_S for each substrate. One method of estimating the kinetic parameters μ_{max} and K_S involves fitting Equation 3-3 to experimentally obtained specific growth rates as a function of substrate concentration for single substrate experiments.

Due to the toxic nature of BTEX and the possibility of substrate inhibition, a modified Monod model, the Andrews model, shown as Equation 3-4 (Andrews, 1968) may provide a better fit to experimental data obtained from single substrate experiments.

$$\mu_i = \frac{\mu_{max,i} C_i}{K_{S,i} + C_i + \frac{C_i^2}{K_{I,i}}}$$

3-4

Again, experimentally obtained specific growth rates can be plotted as a function of substrate concentrations and fit to Equation 3-4 to estimate the three kinetic parameters, μ_{max}, K_S and K_I.

The kinetic parameters, μ_{max}, K_S and K_I, determined from a single component degradation processes can be retained and used in specific growth rate models in which more than one growth limiting substrate is present. However, as stated previously, there is increased complexity in modeling multiple substrate degradation due to substrate interactions. Different models to describe the specific growth rate during the degradation of multiple interacting substrates have been developed in analogy to enzyme kinetics. The analogy can be made between enzyme kinetics and cellular kinetics because, if a reaction is enzyme catalyzed, then the inhibition of enzyme activity results in the inhibition of microbial growth by the same pattern (Shuler and Kargi, 2002). The models used to account for these interactions can be used in substrate degradation equations (Equation 3-2). A common interaction for BTEX compounds is competitive inhibition, which can be seen in Equation 3-5 (Segel, 1975). During competitive inhibition, substrates compete for binding sites in order to be metabolized by the bacterial population.

$$\mu_i = \frac{\mu_{max,i}C_i}{K_{S,i}\left(1+\dfrac{C_I}{K_{S,I}}\right)+C_i} \qquad \textbf{3-5}$$

Another inhibition interaction is non-competitive inhibition wherein a nonreactive complex is formed when both substrates simultaneously are bound to one enzyme. This is shown as Equation 3-6 (Segel, 1975).

$$\mu_i = \frac{\mu_{max,i}C_i}{\left(K_{S,i}+C_i\right)\left(1+\dfrac{C_I}{K_{S,I}}\right)} \qquad \textbf{3-6}$$

Uncompetitive inhibition is another interaction that can occur when multiple substrates are present, which is shown in Equation 3-7 (Segel, 1975). Uncompetitive inhibition is a situation in which one substrate can bind to only a substrate enzyme complex, not just the free enzyme.

$$\mu_i = \frac{\mu_{max,i} C_i}{K_{S,i} + C_i \left(1 + \dfrac{C_I}{K_{S,I}} \right)}$$ 3-7

Finally, a model that accounts for substrate interactions without directly specifying the type of interaction is shown as Equation 3-8 (Yoon et al., 1997). This model contains an interaction parameter that is treated as an unknown.

$$\mu_i = \frac{\mu_{max,i} C_i}{K_{S,i} + C_i + I_{I,i} C_I}$$ 3-8

Equation 3-8 is called SKIP for sum kinetics with interaction parameters (SKIP) (Reardon et al., 2000), which will become more evident as sum kinetics is described below.

In order to describe the growth rate of biomass when mixed growth substrates are present, sum kinetics, shown in Equation 3-9 (Yoon et al., 1997), can be used as an expression for specific growth rate, which can then be substituted into Equation 3-1. Sum kinetics considers the contribution of each substrate present in a system to biomass growth.

$$\mu = \mu_1 + \mu_2 + ... + \mu_n = \frac{\mu_{max,1} C_1}{K_{S,1} + C_1} + \frac{\mu_{max,2} C_2}{K_{S,2} + C_2} + ... + \frac{\mu_{max,n} C_n}{K_{S,n} + C_n}$$ 3-9

The sum kinetics equation shown in Equation 3-9 is for a situation in which there are no substrate interactions and simple Monod equations are summed. Furthermore, specific growth rate equations accounting for interactions, which have been described above, can be used in sum kinetics equations if interactions are found to occur among mixed substrates (Bielefeldt and Stensel, 1999; Reardon et al., 2000). There is a limitation in using Equation 3-9 substituted into Equation 3-1 to describe biomass growth for a bacterial consortium, as a biomass formation equation should consider the biomass concentration able to degrade each particular substrate (Okpokwasili and Nweke, 2006). However, sum kinetics equations have been used to describe biomass growth for pure strains of bacteria degrading mixtures of substrates (Reardon et al., 2000), in which the fraction of pure strain degrading each substrate

is not considered. The measured biomass concentration is multiplied by each term accounting for the biomass growth due to one substrate in the sum kinetics equation, implying that the entire biomass population will metabolize each substrate. Due to the previous success in using sum kinetics to predict biomass growth, as well as the semi-empirical nature of these kinetic equations (Shuler and Kargi, 2002), sum kinetics equations will be used to predict growth of a consortium of bacteria, with minimal knowledge of the consortium composition, in the current study.

By determining which of these models provide the most accurate fit to experimental data for a particular pair of substrates, the presence of any substrate interactions, as well as the nature of the interactions can be determined. Once the interactions between each pair of substrates is determined, a specific growth rate equation taking into account the interactions of each compound present can be determined for mixed substrates with more than two compounds present. An example of such an equation for a SKIP model with four interacting components is shown in Equation 3-10.

$$\mu_i = \frac{\mu_{\max,i} C_i}{K_{S,i} + C_i + \sum_{z=1}^{n} I_{z+1,i} C_{z+1}}$$ **3-10**

Again, models considering interactions between more than two substrates can be used in sum kinetics form to describe the growth of biomass.

For the case of cometabolism, the specific growth rate due to the degradation of a component is zero, as the substrate is not metabolized for energy purposes. However, an expression is needed to describe the disappearance of a cometabolized compound. Cometabolism has been described by Chang et al., (1993) using Equation 3-11, wherein the disappearance of the non-growth substrate is described by the disappearance of the growth substrate.

$$\frac{dC_N}{dt} = -\left(T_g^c\left(\frac{dC_G}{dt}\left(\frac{1}{X}\right)\right)\right)\left(\frac{C_N}{K_{S,N} + C_N}\right)X$$ **3-11**

Using these established interaction equations, the present study identifies and quantifies interactions that occur during the degradation of BTEX components while providing a method of estimating biomass growth for a bacterial consortium.

3.5 Materials and Methods

3.5.1 Growth Medium and Chemicals

The carbon-free medium formulation included the following components in water (Davidson, 2002); 7 g L^{-1} (NH$_4$)$_2$SO$_4$, 0.75 g L^{-1} MgSO$_4 \cdot$ 7H$_2$O, 6.6 g L^{-1} K$_2$HPO$_4$, 8.42 g L^{-1} KH$_2$PO$_4$ and 1 mL L^{-1} trace elements. Stock trace element solution was prepared as follows: 16.2 g L^{-1} FeCl$_3 \cdot$ 6H$_2$O, 9.44 g L^{-1} CaHPO$_4$, 0.15 g L^{-1} CuSO$_4 \cdot$ 5H$_2$O, and 40 g L^{-1} citric acid. All nutrients used in the growth medium were obtained from either Sigma-Aldrich (Canada) or Fisher Scientific (Canada). Carbon sources as benzene (99%, min., assay) and *o*-xylene (98%, HPLC grade) were obtained from Sigma-Aldrich and toluene and ethylbenzene were obtained from Fisher Scientific. Tryptic Soy Broth (TSB) for inoculum preparation was obtained from DIFCO (Canada).

3.5.2 Microorganisms

The bacterial consortium was previously enriched from petroleum contaminated soil obtained from a refinery in Sarnia, Ontario in a continuous reactor with BTEX as the only available carbon source. Gaseous BTEX was continuously fed into the reactor at a rate of 50 mg BTEX L^{-1} h^{-1} with approximately equal amounts of each component. The continuous addition and removal of growth medium was undertaken to achieve an aqueous dilution rate of 0.1 h^{-1} in order to effectively washout the bacteria that were not metabolizing the BTEX. This enrichment was carried out for 12 days. The consortium was then cryogenically stored at -86 ºC after preserving in 10% (v/v) dimethyl sulfoxide until inoculation. Prior to inoculation, the cryogenically preserved consortium was incubated for 24 h with sterile TSB as a carbon source in order to increase cell density. The culture was then centrifuged and the resulting biomass pellet was rinsed several times and resuspended in medium. The mixture was then used for inoculation.

In order to determine the type of bacteria present within the consortium, a denatured gradient gel electrophoresis (DGGE) was completed by Microbial Insights, TN, USA.

3.5.3 Kinetic Experiments

In total, 12 batch degradations were completed; 4 single component batch biodegradations for each of benzene, toluene, ethylbenzene and *o*-xylene, 6 dual substrate batch degradation for each combination of BTEX components, one batch degradation with all BTEX components present and one control batch degradation without the addition of biomass in order to verify there were no losses due to volatilization during sampling. Each batch degradation was carried out in a sterilized 250 ml air-sealed bottle containing 100 ml of media with a self sealing Teflon septum, which is resistant to BTEX permeation, on the cap for sampling. A sufficient amount of headspace was provided to avoid oxygen limiting conditions. The compounds for each experimental run were added in amounts to obtain an approximate total of 80 mg BTEX L^{-1} in the liquid phase, considering partitioning of the compounds between the gas and liquid phases. Each bottle, with the exception of the control, was inoculated by the same bacterial culture at approximately the same time to give a final concentration of approximately 20 mg L^{-1} biomass in the liquid phase in order to make the initial substrate to biomass ratio high to obtain intrinsic and unique parameter estimates of kinetics (Grady et al., 1996). After inoculation, each bottle was put on a rotary shaker and maintained at 30 ºC. Each bottle was periodically removed from the shaker and the headspace was sampled using a gas-tight syringe and the aqueous phase was sampled using a chemical resistant liquid sampling syringe.

3.5.4 Analytical Methods

Gas chromatography was used to measure BTEX concentrations directly in the gas phase, allowing calculation of aqueous phase concentrations using Henry's Law. This indirect method of determining the aqueous phase concentration has been shown to provide accurate kinetic measurements without being mass transfer limited (Chang et al., 1993; Oh et al., 1994). Samples were analyzed on a

Perkin-Elmer AutoSystem Gas Chromatograph, which was fitted with a flame ionizing detector and a fused silica capillary column (DB-5, 0.53 mm I.D., 30 m length, 1 μm film thickness) that was designed to be well suited for the analysis of volatile compounds, particularly BTEX compounds. Helium was used as the carrier gas, flowing at 15 mL min^{-1} and the injector and detector temperatures were set at 140 ºC and 290 ºC, respectively. The column had an initial temperature of 75 ºC, a final temperature of 140 ºC and a temperature increase rate of 25 ºC min^{-1}. Output from the gas chromatograph was recorded on a personal computer equipped with Millenium[32] (Workstation Version 3.05.01, Waters Corp., USA) software to perform peak integration and analysis.

Biomass concentrations were determined using optical density measurements, which were evaluated using a Biochrom Ultraspec 3000 UV/Visable Spectrophotometer (Biochrom, Ltd., UK) at 600 nm. A 10 ml syringe was used to extract 1 ml from each airtight bottle and serial dilutions were performed if necessary to ensure the sample was in the linear range of the instrument.

3.5.5 Parameter Estimation and Determination of Model Adequacy

In order to estimate kinetic parameters for single substrate experiments, nonlinear curve fitting was performed on Equation 3-3 fit to specific growth rate vs. substrate concentration experimental data. For each experiment, as many data points as possible were taken over the entire substrate range in order to obtain unique parameter estimates (Rehmann and Daugulis, 2006). The software performing the nonlinear curve fitting was JMP^{TM}, which uses a Gauss-Newton iteration sequence. The parameter estimates were retained based on the following criteria; residual analysis, confidence intervals for the estimated parameters and Lack of Fit (LOF) testing. Additionally, linear regression was performed in JMP^{TM} in order to estimate yield coefficients for each BTEX component. The adequacy of these parameter estimates were determined by viewing residual vs. predicted plots, mean square regression ratio tests, R^2 values and parameter significance to the 95% interval. The Andrews model (Equation 3-4)

was also fit to single substrate experimental data and the interaction constant estimated in order to see if it would provide a better fit.

Using the kinetic parameters determined from single substrate experiments, models for dual substrate degradation were determined by substituting the different possible specific growth rate equations into Equation 3-2. All possible specific growth rate equations (Equations 3-5 to 3-8) were fit to the experimental substrate degradation data in order to identify the type of substrate interaction occurring for each combination of substrates. Also, using sum kinetics, biomass growth equations (Equation 3-1) were solved for different combinations of possible substrate interactions. These equations were solved using MATLAB ® 6.1 (The MathWorks Inc. USA). ODE15S was the intrinsic ordinary differential equation solver used in MATLAB ® 6.1. The resulting model outputs were visually compared to dual substrate experimental data to determine the corresponding interaction or inhibition type that provided the most accurate fit. Visual inspection was used to estimate initial guesses for interaction parameters for the case of the SKIP model, as well as the growth substrate transformation capacity for the case of cometabolism. Finally, the kinetic parameters and substrate interactions that were determined from single and dual substrate experiments were validated by combining them to model the degradation of all four components of BTEX, which was compared to experimental data to verify model accuracy.

3.6 Results and Discussion

3.6.1 Microorganisms

It was determined that the bacterial consortium consisted of 7 distinct species of *Pseudomonas*, 5 with an excellent similarity index and 2 with a good similarity index. Each species had to constitute greater than 1-2% of the total bacterial population in order to represent a band on the DGGE. A blast search on the DGGE sequences showed that 2 of the *Pseudomonas* species present are likely *Pseudomonas putida* and *Pseudomonas fluorescens*.

49

3.6.2 Single Substrate Experiments

Substrate degradation profiles and corresponding growth as a function of time for single substrate experiments can be seen in Figure 3-1a, b, c and d for benzene, toluene, ethylbenzene and *o*-xylene, respectively. All experimental data reveal a typical saturation type shape that is characteristic of the Monod model (Okpokwasili and Nweke, 2006), with the exception of *o*-xylene in Figure 3-1d. Unlike benzene, toluene and ethylbenzene, the degradation of *o*-xylene reveals that it is not metabolized by the consortium when being the only carbon source present.

It should be noted that the lag period is not predicted by any of the unstructured kinetic models used in this study. All plots show the presence of a lag phase during these experiments, however,
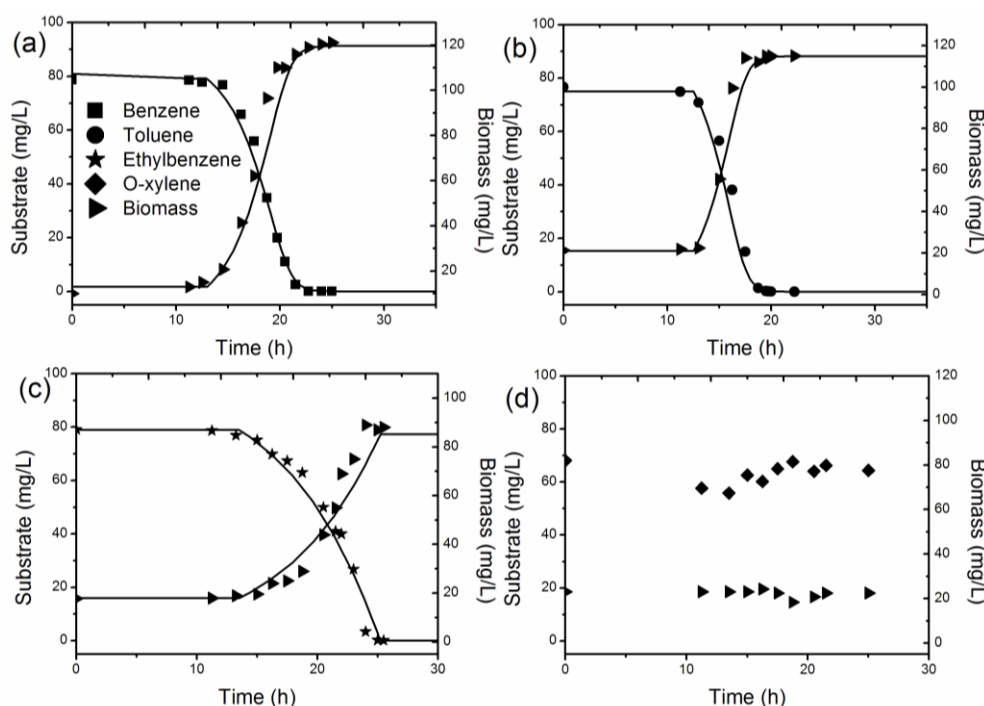
Figure 3-1: (a) Benzene and biomass concentrations in aqueous phase for single substrate experiment (shapes) and Monod model fit (lines). (b)Toluene and biomass concentrations in aqueous phase for single substrate experiment (shapes) and Monod model fit (lines). (c) Ethylbenzene and biomass concentrations in aqueous phase for single substrate experiment (shapes) and Monod model fit (lines). (d) *o*-Xylene and biomass concentrations in aqueous phase for single substrate experiment (shapes).

Table 3-1: Parameter Estimates for Single Substrate Experiments

Compound	μ_{max} (h^{-1})	μ_{max} Likelihood Interval	K_S (mg L^{-1})	K_S Likelihood Interval	$Y_{X/S}$	$Y_{X/S}$ - R^2
Benzene	0.44	0.39-0.50	27.57	19.51-38.58	1.35	0.991
Toluene	0.60	0.52-0.68	34.12	25.04-46.24	1.25	0.981
Ethylbenzene	0.13	0.11-0.16	0.36	0.11-2.12	0.85	0.879

the models were fit only to the post lag phase data. The solution to the substrate degradation equation and biomass growth equation for benzene, toluene and ethylbenzene using the Monod model can also be seen plotted with experimental data in Figure 3-1a, b and c, respectively. These results reveal that the Monod model describes the experimental data accurately and a summary of the Monod kinetic parameter estimates for single substrate biodegradation experiments is shown in Table 3-1. The likelihood intervals for the parameter estimates, also shown in Table 3-1, indicate that the estimated Monod parameters are significant for benzene, toluene and ethylbenzene, however, there were no statistically significant parameters estimated for o-xylene due to degradation not occurring. LOF tests were completed for each Monod model fit to experimental data. In order to get an estimate of the pure error, replicates completed at the beginning of each data set during the lag period were used. There was no significant lack of fit at the 95% level for the case of benzene, toluene and ethylbenzene, confirming that the Monod model adequately describes the observed trends for single substrate degradation. In addition, residual analysis was completed and no significant trend was found. These statistics show that the estimated parameters and Monod model are adequate to describe individual substrate degradation and biomass growth for benzene, toluene and ethylbenzene. The results for yield coefficients for benzene, toluene and ethylbenzene are also displayed in Table 3-1. Again, residual plots were determined to have no trend, the mean square regression ratios revealed that the variance described by the model is significant relative to inherent variance, and all yield coefficient parameter estimates were deemed to be significant.

When fitting the Andrew's model (Equation 3-4) to experimental data, the value of K_I was very large for all three cases, causing the Andrew's model to reduce to the Monod model (data not shown). Therefore, substrate inhibition was not a factor for any single substrate experiments over the range of substrate concentrations investigated and only the Monod parameters were retained.

3.6.3 Dual Substrate Experiments

Dual substrate experiments for combinations of BTEX components revealed interactions that have not been quantified previously by other authors for BTEX components. Specific growth rate models that account for competitive inhibition, noncompetitive inhibition and uncompetitive inhibition among dual substrates (Equation 3-3 to 3-7) were determined using kinetic parameters from single substrate experiments and were substituted into substrate depletion and biomass growth equations. These models did not provide an accurate fit to experimental data for any combination of BTEX components (data not shown). Therefore, the SKIP model was used in order to describe any observed substrate interactions and will be described in more detail below. Those dual substrate experiments that are combinations of substrates that can be used as sole carbon sources will be discussed first and dual experiments containing o-xylene will be discussed later in this section. Experimental data for combinations of substrates that can be used as sole carbon sources, can be seen in Figure 3-2a, b and c for benzene/toluene, benzene/ethylbenzene and toluene/ethylbenzene, respectively.

Relative to single substrate experiments (Figure 3-1a and b), the simultaneous degradation of benzene and toluene, shown in Figure 3-2a, resulted in a slightly inhibitory effect of toluene on benzene degradation as an interaction parameter, $I_{T,B}$, of 2 provided the most accurate fit to experimental data, whereas the presence of benzene had an enhancing effect on toluene degradation as an interaction parameter, $I_{B,T}$, of -0.4 provided the most accurate fit. The SKIP model using these parameters is plotted along with experimental data in Figure 3-2a. The SKIP model provides an accurate fit for benzene/toluene degradation; however, the rate of growth of biomass is slightly over predicted at lower
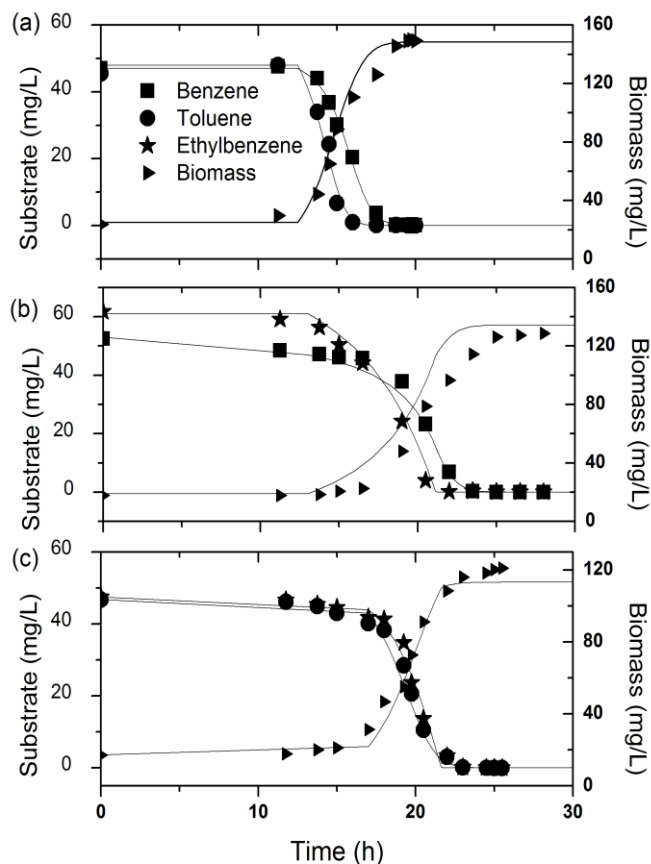
Figure 3-2: (a) Dual degradation of benzene and toluene in aqueous phase experimental data (shapes) and SKIP model (lines). (b) Dual degradation of benzene and ethylbenzene in aqueous phase experimental data (shapes) and SKIP model (lines). (c) Dual degradation of toluene and ethylbenzene in aqueous phase experimental data (shapes) and SKIP model (lines).

substrate levels. A lag of biomass growth behind the disappearance of the parent substrates has previously been noted by Chang et al., (1993) and can be attributed to the possibility of intermediate formation during the degradation of the original substrates being the rate limiting step in biomass formation, as disappearance of the parent compound is not directly proportional to biomass growth.

The dual substrate degradation of benzene and ethylbenzene, shown in Figure 3-2b, revealed that, relative to single substrate experiments (Figure 3-1a and c), the presence of ethylbenzene had an inhibitory effect on benzene degradation as an interaction parameter, $I_{E,B}$, of 4 provided the most accurate fit to experimental data and benzene had no effect on ethylbenzene degradation as an interaction

parameter, $I_{B,E}$, of 0 provided the most accurate fit. The SKIP model is plotted in Figure 3-2b along with experimental data. It should be noted that, because there was no effect of benzene on ethylbenzene degradation, the interaction parameter for ethylbenzene set to zero reduces to a simple no-interaction Monod model. Figure 3-2b also revealed that biomass growth continues after the disappearance of the parent substrate compounds. Again, this can be possibly attributed to the buildup of intermediates that result in delayed biomass growth. The model predicts a slightly higher yield than the experimental data.

The dual degradation of toluene and ethylbenzene, shown in Figure 3-2c, revealed that the degradation data for both compounds were similar to those from single degradation experiments (Figure 3-1b and c) as interaction parameters, $I_{E,T}$ and $I_{T,E}$, of 0 provided the most accurate fit to experimental data for both substrates. This is equivalent to a no-interaction Monod model, which is plotted along with experimental data in Figure 3-2c. The biomass prediction, while showing a correct growth rate, slightly under predicts the overall biomass yield.

Dual substrate experiments containing o-xylene, which cannot be used as a sole carbon source, can be seen in Figure 3-3a, b and c for o-xylene/benzene, o-xylene/toluene and o-xylene/ethylbenzene, respectively. These results show that o-xylene was cometabolized in the presence of both benzene and toluene. Therefore, Equation 3-11 was used to describe the disappearance of o-xylene in both of these cases. In addition, relative to single substrate experiments (Figure 3-1a and d), the degradation rate of benzene was enhanced in the presence of o-xylene as an interaction parameter, $I_{X,B}$, of -0.7 provided the most accurate fit to experimental data, whereas the presence of o-xylene had no effect on toluene degradation as an interaction, $I_{X,T}$, of 0 provided the most accurate fit to experimental data. The SKIP model for the degradation of benzene in the presence of o-xylene and toluene in the presence of o-xylene can be seen plotted with experimental data in Figure 3-3a and b, respectively. Again, it should be noted that the interaction parameter for toluene in the presence of o-xylene was set to zero, which reduces to a no-interaction Monod model. The cometabolism and SKIP models fit experimental substrate degradation data accurately; however, the biomass growth model slightly under predicts the overall biomass yield.
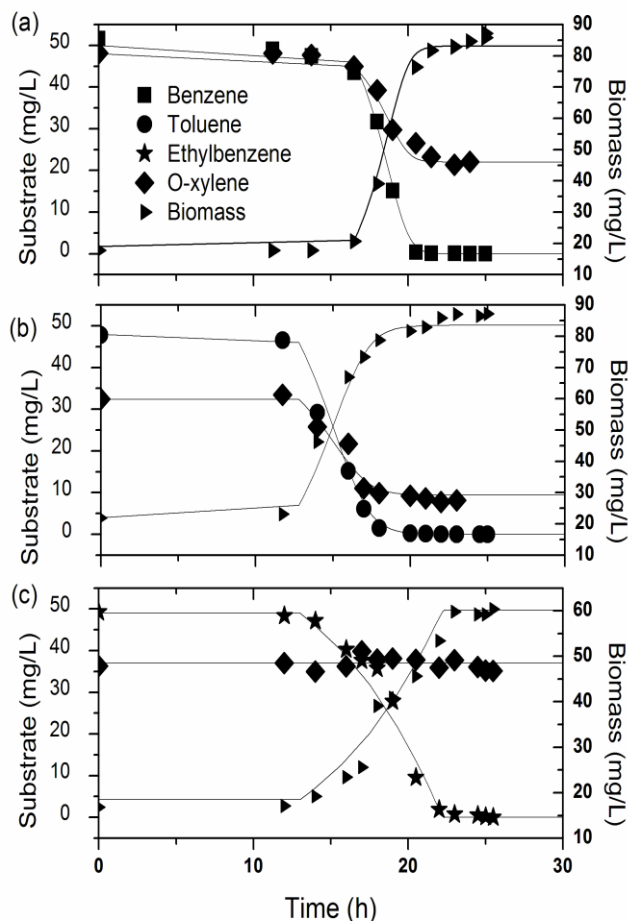
Figure 3-3: (a) Dual degradation of benzene and o-xylene in aqueous phase experimental data (shapes) and SKIP/cometabolism model (lines). (b) Dual degradation of toluene and o-xylene in aqueous phase experimental data (shapes) and SKIP/cometabolism model (lines). (c) Dual degradation of ethylbenzene and o-xylene in aqueous phase experimental data (shapes) and Monod model (lines).

The degradation of ethylbenzene with *o*-xylene revealed that *o*-xylene was not cometabolized in the presence of ethylbenzene as a growth substrate. As expected, a simple, no-interaction Monod model described ethylbenzene degradation in the presence of *o*-xylene as an interaction parameter, $I_{X,E}$, of 0 provided the most accurate fit to experimental data, and results are shown in Figure 3-3c.

It was found that the SKIP model proved to be the most accurate model type in order to describe interactions found in dual substrate experimental data and Equation 3-11 was successful at describing

Table 3-2: Parameter Estimates for Dual Substrate Experiments

Substrates	Model type	Interaction/Inhibition Parameters	
Benzene/Toluene	SKIP	$I_{T,B} = 2$	$I_{B,T} = -0.4$
Benzene/Ethylbenzene	SKIP	$I_{E,B} = 4$	
Benzene/Xylene	Cometabolism, SKIP	$I_{X,B} = -0.7$	$T_g^c = 0.5$
Toluene/Ethylbenzene	Monod	-	
Toluene/Xylene	Cometabolism, Monod	$T_g^c = 0.5$	
Ethylbenzene/Xylene	Monod	-	

cometabolism of *o*-xylene in the presence of both benzene and toluene. The estimated interaction parameters for each substrate combination are summarized in Table 3-2.

3.6.4 Quaternary Substrate Experiments

The determined kinetic parameters and substrate interactions from single and dual substrate experiments were validated by combining them in order to model the degradation of all four BTEX components simultaneously. Accounting for each interaction in a substrate mixture has been completed for purely competitive kinetics (Bielefeldt and Stensel, 1999; Yoon et al., 1997), as well as for SKIP kinetics (Reardon et al., 2000). However, the range of interactions observed in the present study has not previously been modeled for BTEX compounds. As stated previously, the specific growth rate during the degradation of mixed components can be described using Equation 3-10 for SKIP kinetics, which was the model found to best describe substrate interactions between BTEX components during dual substrate experiments. For those substrates that were found not to have an impact on the degradation of a second substrate the interaction term for the later substrate is simply set to zero, which is the equivalent of using a no-interaction Monod model. For *o*-xylene, which was shown to be cometabolized by both benzene and toluene, degradation due to the presence of both growth substrates was summed.

Both the experimental data and corresponding SKIP/cometabolism models are shown for the simultaneous degradation of all four BTEX components in Figure 3-4a, b, c and d for benzene, toluene,
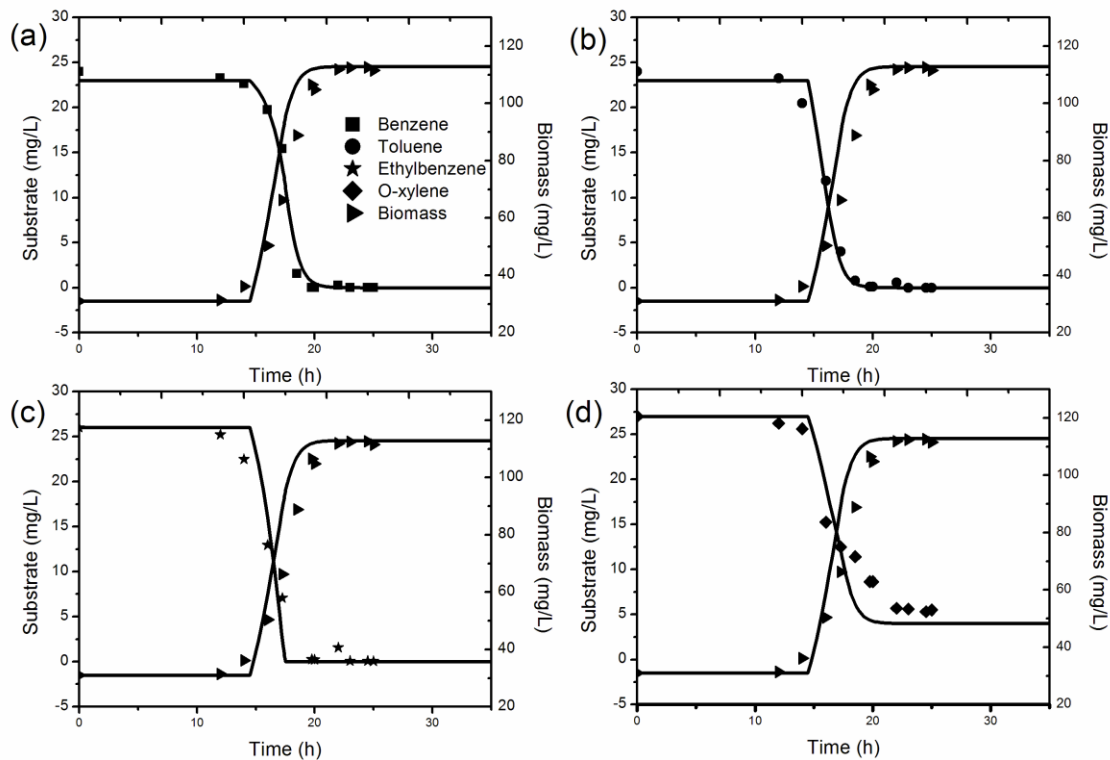
Figure 3-4: (a) Benzene and biomass concentrations in the aqueous phase in the presence of TEX compounds (shapes) and model (lines). (b) Toluene and biomass concentrations in the aqueous phase in the presence of BEX compounds (shapes) and model (lines). (c) Ethylbenzene and biomass concentrations in the aqueous phase in the presence of BTX compounds (shapes) and model (lines). (d) O-xylene and biomass concentrations in the aqueous phase in the presence of BTE compounds (shapes) and model (lines).

ethylbenzene and *o*-xylene, respectively. It can be seen that the resulting kinetics parameters, substrate interactions and interaction parameters determined from single and dual substrate experiments combine to provide an adequate prediction of the experimental data for the degradation of all four BTEX components, however, the total amount of o-xylene degraded is slightly over predicted. The control experiment confirmed that BTEX losses from the experimental runs were negligible as substrate concentrations did not decrease over the period of time during which degradation tests were performed (data not shown).

As mentioned previously, several studies have investigated the degradation of combinations of BTEX components. A summary of a number of these findings, along with kinetic parameter estimates and inhibition constants or interaction parameters, can be seen in Table 3-3. Comparing the kinetic parameters found in this study to the parameters found by other authors, it can be seen that yield coefficients and specific growth rates are of similar magnitude. The half saturation constants found in this study are much larger than those found in other studies, although a large range of values have been reported in the literature For dual substrate experiments, interaction parameters for the SKIP model are similar in this study to other reports, yet the amount of substrate cometabolized relative to growth substrate degraded was slightly higher in the current study. This can be attributed to the difference in diversity and type of bacterial populations between studies.

With the exception of cometabolism, competitive inhibition interactions between BTEX components are common and are inclusive of those that have been quantified by other authors (Bielefeldt and Stensel, 1999; Chang et al., 1993; Oh et al., 1994). The enhancement interactions observed during the present study have not been quantified previously by other authors, although, enhancement interactions occurring among BTEX components have been qualitatively observed, including the enhancement of benzene degradation in the presence of *o*-xylene and toluene (Arvin et al., 1989) and the presence of toluene enhancing benzene and *p*-xylene degradation (Alvarez and Vogel, 1991). The mechanism of the presence of a substrate enhancing the degradation of a second substrate could possibly be due to the induction of required catabolic enzymes (Arvin et al., 1991).

An inherent limitation of this overall cometabolism/SKIP model and estimated kinetic parameters lies in the fact that it is consortium specific. If the concentration of BTEX in the aqueous phase fluctuates, which is a possibility in many industrial (Stewart et al., 2004) and remediation (Jutras et al., 1997) scenarios that involve the biodegradation of BTEX components, the consortium may change composition over time. However, due to the convergence of typical metabolic pathways of BTEX components it is possible that the current model may be applicable to a change within the bacterial population. The

Table 3-3: Kinetic Parameters Obtained from Degradation of BTEX Components

Compounds	Model type	Parameters	Microorganism	Author
Benzene	Monod	$K_{S,B} = 0.12 \pm 0.02$ mg/L $\mu_{max,B} = 0.73 \pm 0.03$ 1/h $Y_{X/B} = 1.20 \pm 0.05$ g/g	*Pseudomonas putida F1*	Reardon et al., (2000)
Toluene	Monod	$K_{S,T} = 13.8 \pm 0.9$ mg/L $\mu_{max,T} = 0.86 \pm 0.01$ 1/h $Y_{X/T} = 1.28 \pm 0.01$ g/g	*Pseudomonas putida F1*	Reardon et al., (2000)
Toluene	Monod	$K_{S,T} = 12.22$ mg/L $\mu_{max,T} = 0.68$ 1/h $Y_{X/T} = 0.71$ g/g	Consortium	Oh et al., (1994)
BT	SKIP	$I_{T,B} = 5 \pm 0.3$ $I_{B,T} = 0.01 \pm 0.003$	*Pseudomonas putida F1*	Reardon et al., (2000)
BTEX	Competitive inhibition	$K_{S,B} = 0.08 \pm 0.003$ mg/L $K_{S,T} = 0.20 \pm 0.14$ mg/L $K_{S,E} = 0.21 \pm 0.13$ mg/L $K_{S,X} = 0.18 \pm 0.18$ mg/L	*Pseudomonas fragi*	Chang et al., (1993)
BT	Competitive inhibition	$\mu_{max,B} = 0.34 \pm 0.0004$ 1/h $K_{s,B} = 3.17 \pm 0.82$ mg/L $Y_{X/B} = 1.04 \pm 0.09$ g/g $\mu_{max,T} = 0.54 \pm 0.0004$ 1/h $K_{S,T} = 1.96 \pm 0.91$ mg/L $Y_{X/T} = 1.22 \pm 0.1$ g/g $K_{I,B} = 3.10 \pm 0.12$ mg/L $K_{I,T} = 1.71$ mg/L	*Pseudomonas fragi*	Chang et al., (1993)
Tp-X	Cometabolism of p-xylene	$T_T^X = 0.45$ mg/mg	*Pseudomonas fragi*	Chang et al., (1993)
BTEo-X	SKIP, cometabolism	$\mu_{max,B} = 0.44$ 1/h $K_{S,B} = 27.57$ mg/L $Y_{X/B} = 1.35$ g/g $\mu_{max,T} = 0.60$ 1/h $K_{S,T} = 34.12$ mg/L $Y_{X/T} = 1.25$ g/g $\mu_{max,E} = 0.13$ 1/h $K_{S,E} = 0.36$ mg/L $Y_{X/E} = 0.85$ g/g $I_{T,B} = 2$ $I_{B,T} = -0.4$ $I_{E,B} = 4$ $I_{X,B} = -0.7$ $T_B^X = 0.5$, $T_T^X = 0.5$	Consortium	Current Study

applicability of the current model to changes in the enrichment process is a topic needing further investigation. In addition, the model provides more accurate predictions of substrate degradation than it does biomass growth. However, prediction of biomass growth is, overall, quite accurate in comparison to attempts by other authors to model mixed populations using SKIP models (Reardon et al., 2002) and does not require quantification of proportions of pure species that comprise the consortium. Overall, the current study provides a method of obtaining an empirical equation to estimate biomass growth of a bacterial consortium. This method has not been demonstrated to date by other authors using an unquantified mixed population of bacteria.

3.7 Conclusions

This study found that during the degradation of individual BTEX components by a bacterial consortium, benzene, toluene and ethylbenzene could be used as a sole carbon source, whereas *o*-xylene could not. When combinations of BTEX components were present, relative to single substrate degradation, several interactions were identified including enhancement, inhibition and cometabolism. This array of interactions has not been quantified for BTEX components prior to the current study. It was found that the model that provided the most accurate description of the interactions was sum kinetics with interaction parameters (SKIP) model. In addition, the cometabolism of *o*-xylene was modeled mathematically. Finally, the SKIP and cometabolism models were validated by successfully modeling growth of a bacterial consortium and substrate degradation when all four BTEX components were present simultaneously. A method for obtaining an empirical equation to predict biomass growth of an unquantified bacterial consortium has also been provided.

Chapter 4

Response of a Solid-Liquid Two-Phase Partitioning Bioreactor to Transient BTEX Loadings

Jennifer V. Littlejohns, Andrew J. Daugulis

4.1 Preface to Chapter 4

Previous research on treating VOCs using a TPPB has focused on the degradation of single contaminants. However, complex mixtures of contaminants, such as BTEX, are more frequently encountered in industrial scenarios. Therefore, this chapter describes the performance of the SL-TPPB for the treatment of a continuous gas stream contaminated with a mixture of BTEX. System performance during fluctuating inlet loadings is the focus of this study, as loading fluctuations are reflective of industrial conditions. In addition, as such a mixture of components had not been treated in a TPPB prior to this thesis, the stirred tank configuration was used in this investigation to provide a comparison to previous stirred tank TPPB systems for the treatment of single VOCs. The investigation in this chapter finds that the stirred-tank SL-TPPB is very effective at treating BTEX contaminated gases relative to other biotreatment methods, and has the ability to dampen inlet loading fluctuations. This study includes the quantification of BTEX concentrations in gas, aqueous and solid phases during loading fluctuations which demonstrates for the first time that a solid, polymeric second phase has the ability to sequester and release large amounts of VOCs during dynamic periods. The previous investigations in Chapters 2 and 3, which quantified oxygen transfer rates and biodegradation kinetics of the enriched bacterial consortium, provide fundamental explanations for the sufficient oxygen levels and relative rates of biodegradation of BTEX components within the SL-TPPB.

This chapter will provide a benchmark system to compare to the performance of an airlift SL-TPPB, which is a less energy-intensive alternative to the stirred-tank TPPB, described in Chapter 6. In addition, the experimental data obtained in this chapter will provide information for parameter estimation and determination of model accuracy for the stirred-tank SL-TPPB model developed in Chapter 5.

4.2 Abstract

A two-phase partitioning bioscrubber (TPPB) consisting of an aqueous phase containing a bacterial consortium and a polymeric phase of silicone rubber pellets (solid volume fraction 0.1) was used to treat a gaseous waste stream containing benzene, toluene, ethylbenzene and o-xylene (BTEX). The function of the solid polymer phase was to absorb/desorb the gaseous volatile organic compounds providing a buffering effect to protect the cells from high transient loadings and to sequester the BTEX for subsequent degradation. The TPPB was subjected to high and fluctuating inlet loadings of BTEX in the form of 4 h step changes of 2, 4, 6 and 10 times the nominal inlet loading of 60 g m^{-3} h^{-1} total BTEX in approximately equal amounts, and removal efficiencies and elimination capacities were determined. It was found that overall removal efficiencies of greater than 95% can be achieved while obtaining overall elimination capacities of up to 282 g m^{-3} h^{-1} during transient operation and TPPB operation succumbs to toxic substrate levels between step changes of 6 and 10 times the nominal loading value (360–600 g m^{-3} h^{-1}). BTEX concentrations in the aqueous phase and the polymer phase of the TPPB were monitored throughout the imposed step changes to determine the extent to which the sequestering phase can buffer the aqueous phase from BTEX. With the polymer phase comprising only 10% of the total working volume of the reactor, the polymer beads accounted for up to 93%, 91% and 70% of the total BTEX present in the working volume for step changes of 2, 4 and 6 times the nominal loading, respectively.

Keywords: TPPB; VOCs; Bacterial consortium; Transient loading; Biodegradation

4.3 Introduction

Benzene, toluene, ethylbenzene and *o*-xylene, collectively known as BTEX, are volatile compounds that are commonly used in many sectors of the petroleum industry and are often emitted in gaseous waste streams. Traditionally, physical or chemical treatment methods have been used in order to stay within regulation emission guidelines (Khan and Ghoshal, 2000), however, biofilters, which provide a low-cost, energy efficient and effective alternative to the destruction of toxic volatile chemicals (Datta and Allen, 2005), have been shown to be successful in treating low concentrations (less than 5 g m^{-3}) of BTEX components in gaseous waste streams (Oh and Bartha, 1997; Torkian et al., 2003). Although biofilters are effective for the treatment of low concentrations of contaminants, there has been recent interest in biological BTEX treatment beyond the current abilities of biofilters; that is, the biological treatment of high and fluctuating loadings of BTEX (Jutras et al., 1997; Stewart et al., 2001)

Two-phase partitioning bioreactors (TPPBs) have recently been shown to be extremely effective for the treatment of high and fluctuating loadings of contaminants in waste gas streams (Boudreau and Daugulis, 2006; Djeribi et al., 2005; Muñoz et al., 2006; Nielsen et al., 2005a; Van Groenstijn and Lake, 1999). TPPBs consist of an aqueous, cell containing phase and a nontoxic, nonbioavailable second phase that traditionally consists of an immiscible organic solvent. These systems are effective for the treatment of toxic contaminants with relatively low water solubility due to the ability of the target compound to partition into the second phase in much higher concentrations than the cell containing aqueous phase, thus buffering the cells from elevated concentrations. As the target compounds are metabolized in the aqueous phase, they are continuously delivered from the sequestering phase based on the metabolic demand of the organisms and the maintenance of thermodynamic equilibrium between the two phases. Due to the difficulty in identifying an organic liquid solvent that would be nonbioavailable to a wide array of bacteria, the application of TPPBs with an organic solvent second phase has been limited to an individual, or very limited mixtures of, volatile organic compounds (VOC) and pure strains of microorganisms. However, to effectively degrade mixtures of BTEX components a bacterial consortium is needed

(Bielefeldt and Stensel, 1999). Bacterial consortia have been used in TPPBs with a silicone oil second phase (Djeribi et al., 2005; Van Groenestijn and Lake, 1999), as silicone oil is nonbioavailable to a wide range of bacteria. However, organic solvent second phases can be selected based on their affinity to the target contaminant, whereas silicone oil cannot, as its properties are fixed.

A more effective second phase that provides the ability to use a bacterial consortium in a TPPB includes replacing the organic liquid phase with a solid, polymeric phase, as polymers are generally nonbioavailable to a wide range of bacteria. Recent research using solid–liquid TPPBs has shown the effective uptake, release and subsequent degradation of high concentrations of phenol using a bacterial consortium (Prpich and Daugulis, 2005). The use of polymers as a second phase has additional advantages over organic liquids and silicone oil, as they are generally very inexpensive, non-volatile, can be formed into many shapes and sizes, and can be tailored to a particular target molecule through monomer selection, cross-linking, and polymer processing.

In the present work, a solid–liquid TPPB has been used to treat high and fluctuating loadings of a mixture of BTEX simultaneously in a continuous waste gas stream using a bacterial consortium. This is the first report of the use of a solid–liquid TPPB wherein a bacterial consortium aids in providing efficient treatment, as it provides more effective and complete degradation of BTEX mixtures in comparison to pure strains (Alvarez and Vogel, 1991; Attaway and Schmidt, 2002). Bacterial consortia also provide a robustness that is more practical in industrial settings. Moreover, a TPPB has not been used for such a mixture of contaminants to date. Concentrations of BTEX components in the gaseous, aqueous and polymer phases were monitored during imposed inlet concentration step changes in order to quantify the degree to which the polymer phase buffered toxicity in the aqueous phase. Although the ability of TPPBs to outperform bioreactors without a second phase has been previously attributed to the ability of the polymer phase to rapidly sequester large concentrations of target compounds (Boudreau and Daugulis, 2006), it has not been demonstrated to be the case prior to the current study. Finally, this paper also provides results that prompt discussion of current methods for reporting elimination capacity.

4.4 Materials and Methods

4.4.1 Chemicals

All chemicals used in the fermentation medium were obtained from either Sigma Aldrich (Canada) or Fisher Scientific (Canada). Benzene (99% assay) and *o*-xylene (98%, HPLC grade) were obtained from Sigma Aldrich, and toluene and ethylbenzene were obtained from Fisher Scientific. Tryptic Soy Broth (TSB) for inoculum preparation was obtained from DIFCO (Canada).

4.4.2 Polymer Selection

In order to select an appropriate polymer for the uptake and release of BTEX in a TPPB, a variety of polymers with different properties was tested for BTEX polymer/aqueous partitioning, BTEX diffusivity and bioavailability. The methods for these tests are described elsewhere (Amsden et al., 2003; Prpich and Daugulis, 2004). The polymers tested include; nylon 6,6 (Zytel 42-A®, Dupont), ethylene vinyl acetate (ELVAX 360®, Dupont), styrene–butadiene copolymer (Scientific Polymer Products Inc.), silicone rubber (GE-Mastercraft), poly(butylene terephthalate) (Hytrel 8206®, Dupont) and polyurethane elastomer (Desmopan 9370A®, Bayer Materials Science). On the basis of the aforementioned criteria, it was found that silicone rubber was the most favourable polymer for use in the TPPB. For further information on methods and experimental data for partition coefficients and diffusion coefficients, see Appendix A and Appendix B, respectively.

4.4.3 Bacterial Consortium Enrichment

A bacterial consortium to metabolize BTEX components was enriched from petroleum contaminated soil (Sarnia, Ontario) and a commercial mixture of petroleum hydrocarbon metabolizing bacteria composed of strains of *Pseudomonas* (Petrox-1, CL Solutions). The enrichment was completed by adding 0.5 g of both the contaminated soil and the commercial mixture to a 1.5 L bioreactor with a 1 L working volume consisting of medium with the following composition (g L^{-1}); 7 (NH$_4$)$_2$SO$_4$, 0.75

MgSO$_4$ · 7H$_2$O, 6.6 K$_2$HPO$_4$, 8.42 KH$_2$PO$_4$, and 1 mL L^{-1} trace elements. Trace element solution was prepared as follows (g L^{-1}): 16.2 FeCl$_3$ · 6H$_2$O, 9.44 CaHPO$_4$, 0.15 CuSO$_4$ · 5H$_2$O, and 40 citric acid (Davidson and Daugulis, 2003). This medium formulation was used for all experiments in this study.

The bioreactor was maintained at a temperature of 30 °C, pH of 6.9 and agitation of 800 rpm. Gaseous BTEX was continuously fed into the reactor as the sole carbon source at a rate of 50 g m^{-3} h^{-1} with approximately equal amounts of each component along with air at a flow rate of 1 L min^{-1}. The continuous addition and removal of medium was undertaken to achieve an aqueous dilution rate of 0.1 h^{-1} in order to effectively washout the bacteria that were not metabolizing the BTEX. This enrichment was conducted for 12 d, and the resulting culture was stored for long-term maintenance in 12% dimethyl-sulfoxide at −70 °C in 1.5 mL vials.

A denatured gradient gel electrophoresis was completed by Microbial Insights (TN, USA) using 16S rRNA to determine the dominant members of the microbial population. It was found that the bacterial consortium used in this study was composed of seven unique species of *Pseudomonas*, 5 with an excellent similarity index and 2 with a good similarity index.

4.4.4 Experimental Setup

The TPPB setup for experimentation performed in this study is shown in Figure 4-1. The bioreactor used was a 6.5 L New Brunswick BioFlo III with a working volume of 3 L. 10% of this working volume consisted of silicone rubber polymer beads with a diameter of 2.2 mm and density of 1150 g L^{-1} and the other 90% consisted of aqueous medium. This polymer volume was found to be the largest fraction possible while avoiding operational difficulties such as clogging in the bioreactor. The bioreactor was automatically maintained throughout all experimentation at a temperature of 30 °C, an agitation of 800 rpm to disperse the polymer beads in the aqueous phase and a pH of 6.9 (by the addition of 6 M KOH). Dissolved oxygen was continuously monitored using a polarographic-membrane electrode (Broadley and James Corp.) and automatically recorded. All tubing used to deliver BTEX into the
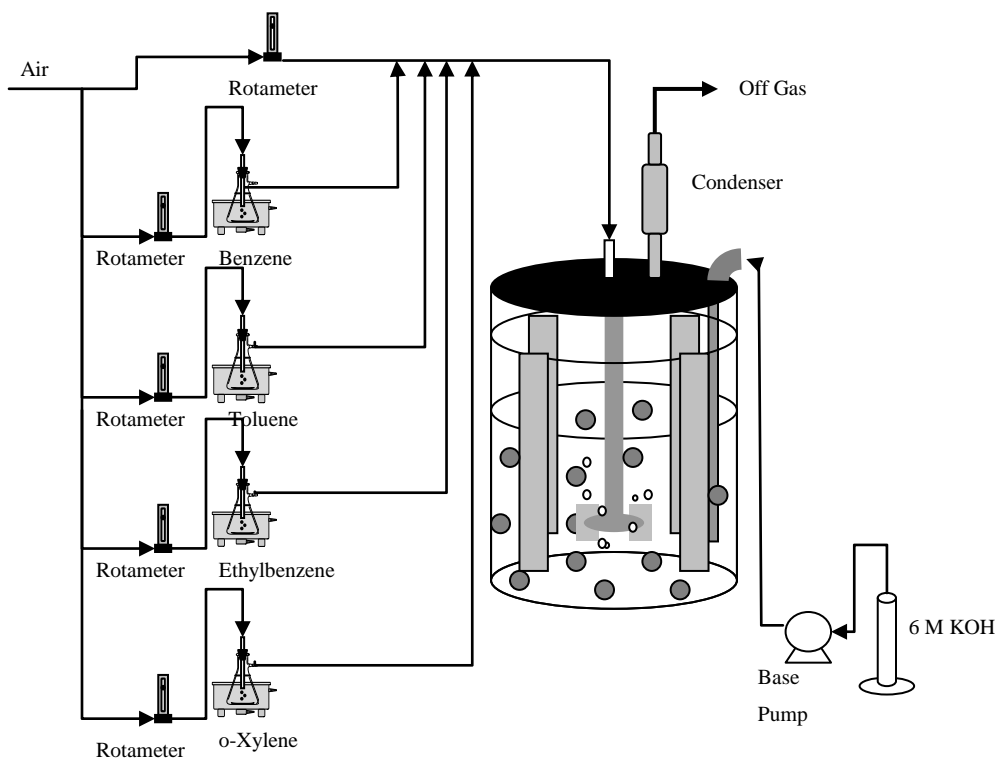
Figure 4-1: TPPB setup for BTEX treatment

bioscrubber, and bioscrubber seals, were composed of Teflon, which is resistent to BTEX permeation. The nominal operating point from which step changes were imposed was a loading of approximately $60 \text{ g m}^{-3} \text{ h}^{-1}$ which consisted of a total gas flow rate of 0.55 L min^{-1} (enriched BTEX gas flow and makeup aeration) and an approximate average concentration of 5.5 g m^{-3} total BTEX in approximately equal parts. Empty bed residence time (EBRT) for all experimentation was 5.5 min. The inoculum for the TPPB was prepared by adding 1 mL of the culture stored for long-term maintenance to 100 mL of sterile TSB medium and incubating the mixture for 24 h at 180 rpm and 30 °C. The resulting culture was then centrifuged, resuspended in medium and added in an appropriate volume to the TPPB to obtain an initial cell concentration of 0.5 g L^{-1}.

4.4.5 Step Changes

After approximately 200 h of TPPB operation at the nominal loading, the system reached a characteristic quasi-steady state biomass concentration that arises in response to the carbon source being directed towards maintenance energy as described by Nielsen et al., (2005c). At this point, 4 h step changes were imposed on the system in order to simulate fluctuations of high BTEX loadings in the inlet gas stream. Step changes were performed at approximately 2, 4, 6 and 10 times the nominal loading ($2\times$, $4\times$, $6\times$ and $10\times$, respectively). During step changes, the total gas flow rate was kept constant at approximately 0.55 L min^{-1} and only the BTEX concentration was increased in order to increase loading. Prior to the system reaching quasi-steady state and during all step changes, BTEX components in the inlet gas stream were maintained at approximately equal concentrations.

4.4.6 Sampling Procedure

Prior to achieving quasi-steady state operation, inlet gas samples were taken periodically (12–24 h) and analyzed by GC/FID using the method described in Section 3.5.4. Even minor fluctuations in rotameter settings were found to result in significant fluctuations in inlet concentrations. Aqueous phase samples from the reactor were also taken periodically in order to determine biomass concentration and identify when the system had reached quasi-steady state. Biomass concentration was determined by optical density measurements with a Biochrom Ultrospec 3000 UV/vis spectrophotometer (Biochrom, Ltd., UK) at 600 nm. During the imposed step changes, inlet and outlet BTEX concentrations and biomass measurements were taken approximately every 13 min. In addition, polymer phase BTEX concentrations for step changes of $2\times$, $4\times$ and $6\times$ and liquid phase BTEX concentrations for step changes of $2\times$, $4\times$, $6\times$ and $10\times$ were determined approximately every 30–50 min. Polymer phase concentrations throughout the step change of $10\times$ were regrettably not measured as the system was clearly failing and the information was deemed unnecessary as the biological component of the TPPB was not functioning. Only a polymer concentration for the $10\times$ loading at $t = 182$ min is reported in this study.

To determine aqueous phase and polymer phase BTEX concentrations, two samples were taken simultaneously from the bioreactor; an aqueous sample consisting of 10 mL of the aqueous phase and an aqueous/polymer sample consisting of 10 mL of combined polymer and aqueous phases. Aqueous phase samples and aqueous/polymer samples were withdrawn from a port in the bioreactor using a 10 mL pipette with a narrow inlet hole and a 10 mL pipette with an enlarged inlet hole, respectively, in order to disallow/allow entry of the polymers into the sample. After the sample was withdrawn from the bioreactor it was rapidly delivered into an airtight 125 mL amber bottle containing approximately 5 drops of phosphoric acid to immediately kill all biomass and capped with Teflon lined, silicone rubber septum. Both the aqueous samples and polymer/aqueous samples in the amber bottles were permitted to equilibrate for 24 h at 30 °C and the headspace from each bottle was sampled and measured using GC/FID. Concentrations of BTEX in the aqueous phase of the bioreactor were determined using Equation 4-1.

$$C_{i,l} = \frac{\left(C_{i,g,aq} \; V_{g,aq} \right) + \left(\dfrac{C_{i,g,aq}}{H_i} \; V_{l,aq} \right)}{V_{l,aq}} \qquad \textbf{4-1}$$

where $C_{i,l}$ is the concentration of species i (one of benzene, toluene, ethylbenzene or o-xylene) in the aqueous phase of the bioreactor (g m^{-3}), $C_{i,g,aq}$ is the concentration of species i in the gas phase at equilibrium in the glass bottle containing the aqueous phase sample (g m^{-3}), H_i is the Henry's constant for species i (mg L^{-1} gas phase L mg^{-1} liquid phase), $V_{g,aq}$ is the volume of headspace in the glass bottle containing the aqueous phase sample (m^3), and $V_{l,aq}$ is the volume of the aqueous phase sample extracted from the bioreactor (m^3).

Concentrations of BTEX in the polymer phase were determined using Equation 4-2.

$$C_{i,p} = \frac{\left(C_{i,g,poly} \ V_{g,poly} \right) + \left(\dfrac{C_{i,g,poly}}{H_i} \ V_{l,poly} \right) + \left(\dfrac{C_{i,g,poly}}{H_i} \ K_i \ V_{p,poly} \right) - \left(C_{i,l} \ V_{l,poly} \right)}{V_{p,poly}} \qquad \textbf{4-2}$$

where $C_{i,p}$ is the concentration of species i in the polymer phase of the bioreactor (g m^{-3}), $C_{i,g,poly}$ is the concentration of species i in the gas phase at equilibrium in the glass bottle containing the aqueous/polymer phase sample (g m^{-3}), K_i is the partition coefficient for species i (mg L^{-1} gas phase L mg^{-1} liquid phase), $V_{g,poly}$ is the volume of headspace in the glass bottle containing the aqueous/polymer phase sample (m^3), $V_{l,poly}$ is the volume of the aqueous phase in the glass bottle containing the aqueous/polymer phase sample and $V_{p,poly}$ is the volume of polymer in the aqueous/polymer phase sample (m^3).

Henry's coefficients used in Equations 4-1 and 4-2 were determined by adding a known volume of each BTEX compound into an airtight 125 mL septa bottle containing 50 mL of water. The bottle was then left for 24 h at 30 °C to equilibrate and the headspace concentration was measured allowing for the determination of the aqueous phase concentration. The Henry's constants for B, T, E and X were found to be 0.26, 0.35, 0.43 and 0.25 mg L^{-1} gas phase L mg^{-1} liquid phase, respectively. Partition coefficients used in Equation 4-2 were determined during the polymer selection experiments, and the polymer volume used in Equation 4-2 was estimated by multiplying the number of polymer beads taken in a particular sample by an average bead volume calculated using an average polymer bead diameter ($n = 100$).

4.4.7 Performance Quantification

The performance of VOC treatment systems is often quantified using two instantaneous measurements; removal efficiency (RE) (Equation 4-3) and elimination capacity (EC) (Equation 4-4).

$$RE = \frac{F_{g,in}\left(C_{g,in} - C_{g,out} \right)}{F_{g,in} C_{g,in}} \times 100\% \qquad \textbf{4-3}$$

$$EC = \frac{F_{g,in}\left(C_{g,in} - C_{g,out}\right)}{V_{sys}}$$

4-4

where $F_{g,in}$ is the gas flow rate into the reactor (L h^{-1}), $C_{g,in}$ is the instantaneous concentration of BTEX in the inlet gas (g m^{-3}), $C_{g,out}$ is the instantaneous concentration of BTEX in the outlet gas (g m^{-3}) and V_{sys} is the working volume of the TPPB (L). The instantaneous REs and ECs were determined prior to and during each step change. Overall REs and ECs (calculated from the initiation of the transient until the system returning to quasi-steady state) will be discussed in a later section.

4.5 Results and Discussion

4.5.1 TPPB Performance

During quasi-steady state operation of the TPPB prior to the application of step changes, an instantaneous maximum RE of 99% and instantaneous minimum RE of 95% were obtained during all four experimental runs. During BTEX concentrations step changes of 2× and 4×, maximum ECs of 157 and 285 g m^{-3} h^{-1} were achieved with the RE remaining above 95% (Figure 4-2a and b). However, when a step change of 6× was imposed on the system, the RE ranged from a maximum value of 95% to a minimum value of 68% (Figure 4-2c). Furthermore, following the step change, the RE fell to a minimum of −10% but recovered to original levels in less than 60 min after the loading was returned to nominal levels. Although the performance decreased relative to the step changes of 2× and 4×, the TPPB system was able to eventually recover to performance levels that were obtained before the introduction of the step change.

Shown in Figure 4-2d are the instantaneous ECs and REs for a step change of 10×. The RE and EC drop rapidly after the imposition of the step change and do not recover after step change completion. Samples taken 24 h after the completion of the step change (data not shown) confirm that the system did not recover as the EC was <10 g m^{-3} h^{-1} for nominal loadings. Figure 4-2 reveals that the maximum step change loading after which the TPPB could subsequently recover to original RE levels lies between 360

72
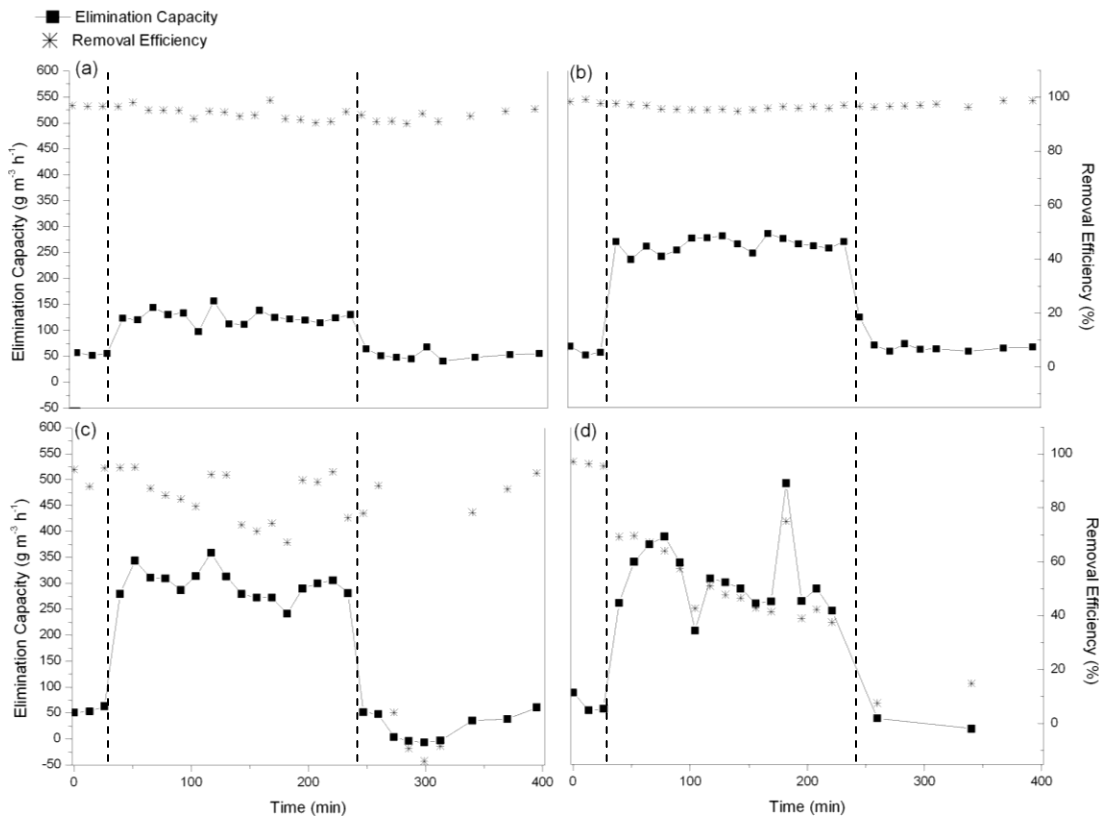
Figure 4-2: Total BTEX elimination capacities and removal efficiencies for a) 2X step change b) 4X step change c) 6X step change and d) 10X step change. Vertical dashed lines indicate step change time period.

and 600 g m^{-3} h^{-1}. The step change of 6× does not appear to be mass transfer limited (gas to liquid), as large removal efficiencies are shown at the beginning of the step change; however, the step change of 10× does appear to be mass transfer limited (gas to liquid) as removal efficiencies drop immediately after step change initiation.

During all nominal loadings and step change conditions, the RE for individual BTEX compounds was in the order benzene > toluene > ethylbenzene > o-xylene (data not shown). This was an expected result, as the degradation kinetics for this particular bacterial consortium have been previously characterized in Chapter 3, and degradation rates were found to be in an identical order to those found in

the current study for benzene, toluene and ethylbenzene. It was also previously determined that *o*-xylene is cometabolized in the presence of both benzene and toluene and, therefore, *o*-xylene degradation rates are expectedly lower than those for benzene and toluene. Dissolved oxygen was measured and was found to remain above 80% during each step change of 2×, 4×, 6× and 10× (data not shown). This reveals that oxygen was not limited during step change experimentation, which may be partially due to the addition of silicone rubber pellets as it was shown in Chapter 2 that the addition of silicone rubber pellets increases the oxygen transfer rate into the working volume of a TPPB system during dynamic operation.

4.5.2 Overall Elimination Capacities and Removal Efficiencies

Figure 4-2c shows that subsequent to the 6 times step change, a negative EC was calculated for a short period of time (<60 min). However, the capacity of a bioreactor to eliminate compounds entering the inlet stream should intuitively be greater than or equal to 0. The operating conditions reflected in the data of Figure 4-2c reveal a situation in which current reporting methods for EC are somewhat ambiguous. For dynamic situations during which a bioreactor system sequesters high concentrations of target compounds, as is particularly the case for TPPBs, reporting ECs on an instantaneous basis may not be reflecting the true permanent removal of compounds from the waste gas stream. During a step change imposed on a solid–liquid TPPB system a concentration driving force exists in the direction of the polymer. Subsequent to the step change, elevated concentrations can remain in the TPPB working volume and the same compounds that were removed earlier from the waste gas stream can be stripped and detected in the outlet gas stream, reducing instantaneous ECs. In order to account for this situation, we propose that an overall EC be reported during periods of operation starting from the beginning of the imposed dynamic until the system has returned to original quasi-steady state values. In order to approximate the overall elimination capacity (EC$_{overall}$), Equation 4-5 can be used.

$$EC_{overall} = \frac{F_{g,in}}{V_{sys} \; t_{overall}} \sum_{i=1}^{n} \left(C_{g,in,i} - C_{g,out,i} \right) \; t_{i,i+1} \qquad\qquad \textbf{4-5}$$

Table 4-1: Overall Performance of TPPB

Step Change	Time Period of Dynamic Operation (min)	Average Biomass (g L^{-1})	$EC_{overall}$ (g m^{-3} h^{-1})	$RE_{overall}$ (%)	Normalized $EC_{overall}$ (g m^{-3} h^{-1} g^{-1} biomass)
2X	39-249	5.9	134	94	23
4X	39-249	8.2	282	96	34
6X	39-313	6.8	230	81	34

where i is the sample number, n is the total number of samples taken during the overall period, $t_{overall}$ is the time of the overall period (min) and $t_{i,i+1}$ is the time between sample i and the next proceeding sample (min). $EC_{overall}$ for step changes of 2×, 4× and 6× can be seen in Table 4-1.

In addition to the current study, several authors have observed lower than expected REs subsequent to step changes in inlet loading (Boudreau and Daugulis, 2006; Marek et al., 2000). An overall RE ($RE_{overall}$) can be approximated using Equation 4-6.

$$RE_{overall} = \frac{F_{g,in} \sum_{i=1}^{n} \left(C_{g,in,i} - C_{g,out,i} \right)}{F_{g,in} \sum_{i=1}^{n} \left(C_{g,in,i} \right)} \times 100\% \qquad \textbf{4-6}$$

$RE_{overall}$ values for the present system can also be seen in Table 4-1.

Slightly different average quasi-steady state values for biomass concentration were obtained for each run which is shown in Table 4-1. Therefore, $EC_{overall}$ values were normalized with respect to biomass concentration and are also reported in Table 4-1. These normalized $EC_{overall}$ values consistently reveal that during the imposition of larger step changes (4× and 6×) each gram of cells is able to eliminate approximately 34 g L^{-1} h^{-1}, which suggests that this is the maximum utilization rate for the bacterial consortium in this TPPB system.

4.5.3 Aqueous Phase and Polymer Phase Concentrations

Aqueous phase concentrations for individual BTEX components for all step change conditions can be seen in Figure 4-3. Data from the smallest step change of 2× (approximately 120 g m^{-3} h^{-1}), seen in Figure 4-3a, show that during the step change (time 39–249 min), concentrations of all BTEX components increase slightly relative to concentrations before the step change, however, remain at <2 mg L^{-1} in all cases. Following the step change, aqueous concentrations gradually drop back to levels similar to those before the imposition of the step change due to a combination of physical desorption of BTEX from the polymer to the aqueous phase and microbial degradation. Figure 4-3a also reveals that
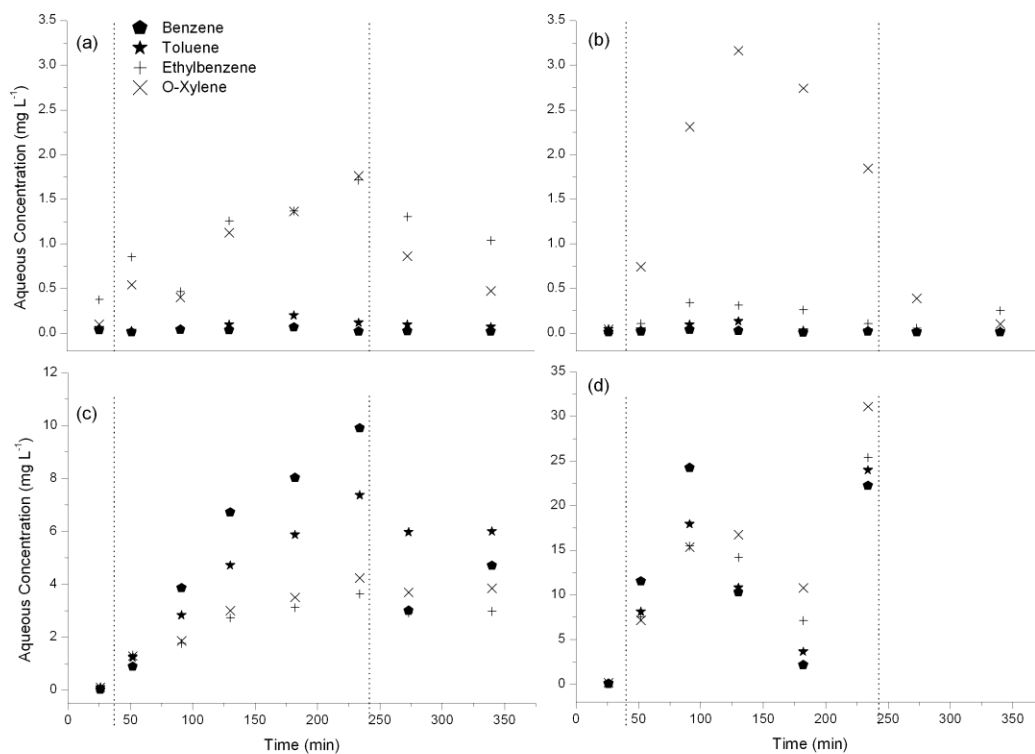
Figure 4-3: Aqueous phase BTEX concentrations for a) 2X step change b) 4X step change c) 6X step change d) 10X step change. Vertical dashed lines indicate step change time period.

benzene and toluene are present in much lower concentrations in the aqueous phase than ethylbenzene and *o*-xylene.

Figure 4-3b shows aqueous phase BTEX concentrations during a step change of 4× (approximately 240 g m^{-3} h^{-1}). Again, concentrations of BTEX components increase during the step change period relative to before the step change is applied, but stay below 3.5 mg L^{-1}. Also, concentrations gradually decrease to original levels after the step change is completed.

Aqueous phase BTEX concentrations during a step change of 6× are shown in Figure 4-3c. Again, concentrations of all BTEX components in the aqueous phase increase during the step change, but remain below 10.5 mg L^{-1}, and decrease after the completion of the step change. However, the order of individual BTEX concentrations in the aqueous phase in Figure 4-3c does not follow the expected trend that was observed during 2× and 4× step changes wherein the magnitude of individual BTEX concentrations was inversely proportional to individual degradation rates found for this particular consortium in Chapter 3. In contrast, the order of aqueous phase individual BTEX concentrations observed during the step change of 6× is benzene > toluene > *o*-xylene > ethylbenzene. It should be noted that this order follows what would be expected for an abiotic system, as the compounds with the highest aqueous phase concentration would be those with the highest water solubility; benzene (1780 mg L^{-1}) > toluene (515 mg L^{-1}) > *o*-xylene (198 mg L^{-1}) > ethylbenzene (152 mg L^{-1}) (Kuo, 1999). This observation can be attributed to the bacterial consortium not effectively degrading the influx of BTEX compounds caused by the step change, which is confirmed in Figure 4-2c as the RE decreases significantly during the step change period. Figure 4-3d shows BTEX concentrations in the aqueous phase during a step change of 10×. It can be seen that BTEX concentrations accumulate to high levels even after the completion of the step change when the BTEX loading is reduced back to nominal levels (total BTEX is 162.5 mg L^{-1} at $t = 340$ min), indicating that biological activity has ceased, possibly due to inhibitory aqueous phase concentrations. Although different bacterial strains have different inhibitory aqueous phase concentrations, it has been found that for *Pseudomonas putida* F1, substrate inhibition

(decline of specific growth rate) occurs for benzene concentrations >20 mg L^{-1} and toluene concentrations >30 mg L^{-1} (Abuhamed et al., 2004).

BTEX concentrations in the polymer phase for step changes of 2×, 4× and 6× are shown in Figure 4-4. An entire set of data for BTEX concentrations in the polymer phase for the step change of 10× was not obtained, as explained previously, but polymer concentrations at $t = 182$ min were determined to be 5367, 5154, 4854 and 5581 mg L^{-1} for benzene, toluene, ethylbenzene and o-xylene, respectively. Figure 4-4 shows that concentrations in the polymer phase are much higher than the aqueous phase concentrations, as expected. For all step changes, the trends for individual BTEX components in the
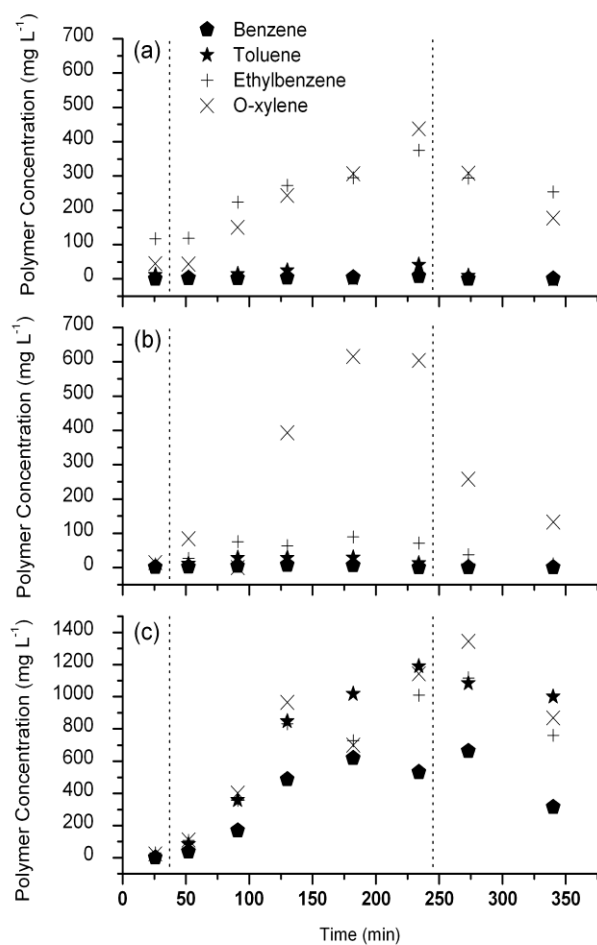
Figure 4-4: Polymer phase BTEX concentrations for (a) 2× step change, (b) 4× step change, (c) 6× step change. Vertical dashed lines indicate step change time period.

78

polymer phase are similar to those observed in the aqueous phase. An exception to this can be seen for the step change of 6×, wherein benzene has the lowest polymer phase concentration (Figure 4-4c), but the highest aqueous phase concentration (Figure 4-3c). This, however, is expected, as partition coefficients that were measured during the polymer phase selection process for silicone rubber revealed that BTEX components have partition coefficients (mg L^{-1} gas phase L mg^{-1} liquid phase) in the following order: ethylbenzene (593 ± 5) > o-xylene (414 ± 2) > toluene (200 ± 4) > benzene (62 ± 2) and thus, as benzene concentrations in the aqueous phase are not exceptionally higher than the other BTEX compounds, benzene concentrations in the polymer phase are expected to be lower than the other BTEX compounds.

An important point shown by Figure 4-4 is that polymers appear to effectively buffer large concentrations of BTEX compounds in a SL-TPPB. This is the first study to monitor polymer phase concentrations during transient loadings applied to a TPPB to reveal conclusively that uptake by polymers is responsible for the increased performance of a SL-TPPB relative to a single phase reactor. With the polymer phase composing only 10% of the total working volume of the reactor, the polymer beads accounted for 93%, 91% and 70% of the total BTEX present in the working volume for step changes of 2×, 4× and 6×, respectively (at $t = 237$ min).

4.5.4 System Comparison and Limitations

There is difficulty in comparing the system in the present work (well mixed) to biofiltration methods (plug flow) as the responsiveness of these systems are dissimilar and the step changes tested on biofilters are typically longer. However, there have been several studies that investigated the performance of biofilters during step changes in inlet concentrations of less than 5 h (Deshusses et al., 1996; Marek et al., 2000), although step changes typically tested for biofilters generally used much higher gas flow rates with lower concentrations than the system in question and render system comparisons difficult.

Technologies that can be compared to the solid–liquid TPPB include liquid–liquid TPPBs, single liquid phase bioreactors and extractive membrane bioreactors. Nielsen et al., (2005a) examined the

treatment of high and fluctuating loadings of benzene in a waste gas stream using a liquid–liquid TPPB containing 33% *n*-hexadecane and a pure strain of *Achromobacter xylosoxidans* Y234 (Nielsen et al., 2005a). During 4 h loading step changes of up to 650 g m^{-3} h^{-1}, REs of greater than 99% were maintained (Empty bed residence time (EBRT) of 3 min). The REs during these step changes are higher than those obtained in the current study, possibly due to the combined effect of organic solvents being more rapid in the uptake of contaminants in comparison to polymer beads and the difficulty in treating a multi-component waste gas (this study) as opposed to treating a single contaminant (the work by Nielsen et al., 2005a).

Jianping et al., (2006) investigated step changes of toluene using a gas–liquid–solid airlift loop bioreactor wherein the intention of the solid (activated charcoal) was to immobilize cells, not to sequester contaminants. During 24 step changes of up to 3 times the nominal concentrations (1.5 g m^{-3}) in the inlet gas stream, an RE of greater than 80% was maintained with a maximum instantaneous EC of approximately 168 g m^{-3} h^{-1} (EBRT of 0.66 min). This performance is comparable to our system, however, the gas–liquid–solid airlift treated a single contaminant, toluene, which is notably less difficult than treating all four BTEX compounds, particularly *o*-xylene which is notoriously more recalcitrant than the other three compounds (Attaway and Schmidt, 2002). Neal and Loehr, (2000) compared single liquid phase bioreactors to biofilters for the degradation of toluene containing waste gas streams for different loadings at steady state operation. The single liquid phase bioreactor obtained extremely high REs (96–99.7%) for mass loadings ranging from 5 to 30 g m^{-3} h^{-1} at low gas flow rates from 0.071 to 0.13 L min^{-1} (EBRT of 13.3 min). The RE achieved was similar for the biofilter that was operated at similar loadings with higher gas flow rates (EBRT of 1–2 min). These REs achieved are higher than the current study, but at much lower ECs.

Little investigation has been made on the response of membrane bioreactors to transient loadings in waste gas streams, and much more research is necessary to understand these systems better (Kumar et al., 2008b). It is known that membrane bioreactors are limited by the surface area of the membrane

(Wilderer, 1995) and are extremely sensitive to biofilm thickness (Dubus, 1995). These limitations are addressed by the use of a solid–liquid TPPBs as polymer beads provide a much larger surface area for absorption and biofilms do not form on the polymer surface (Amsden et al., 2003).

Experimental testing in this study has utilized lower waste gas flow rates than is typically used for conventional biotreatment systems in order to be able to simulate a high concentration waste gas stream while maintaining a reasonable loading for the bioreactor. Therefore, the TPPB in the current study may be limited by size constraints in the treatment of higher gas flow rates. In addition, the energy intensive stirred tank configuration used in this study may not be practical upon scale up and research entailing replacement of the stirred tank with an airlift bioreactor is currently underway in our laboratory. Also, the dynamic periods investigated were of relatively short duration and longer perturbations may lead to different system responses. Moreover, it is important to note that the effect of cycling step changes will likely affect microbial culture evolution and future work characterizing the solid–liquid TPPB during long-term operation would be beneficial. From the results of this study, it is also of intent to recognize that many of the VOC treatment devices mentioned here, such as biofilters, may also benefit from the addition of solid polymer beads into the system as a suspended or packing medium, and further work in this area is suggested.

Chapter 5

Model for a Solid-Liquid Stirred Tank Two-Phase Partitioning Bioreactor for the Treatment of BTEX

Jennifer V. Littlejohns, Kim B. McAuley, Andrew J. Daugulis

5.1 Preface to Chapter

The previous chapters in this thesis investigated the performance of the stirred-tank SL-TPPB for the treatment of a gas stream containing BTEX, and provided detailed characterization of oxygen transfer and biodegradation rates within such a system. These investigations provided insight into the mechanisms involved during operation of the stirred-tank SL-TPPB to treat BTEX, and the next logical step is to develop a mathematical model of this system. Mathematical models are useful tools that can increase understanding of phenomena occurring within an SL-TPPB system, as well as predict performance under various operating conditions. Therefore, in order to fully characterize the stirred-tank SL-TPPB for the treatment of BTEX, the investigation in this chapter develops and applies a dynamic mathematical model to predict system performance. The model incorporates parameter estimates of mass transfer and biodegradation kinetics from Chapters 2 and 3, kinetic model structure from Chapter 3, and experimental data for parameter estimation and determination of model accuracy from Chapter 4. The mathematical model that is developed can be used to predict the performance of a stirred-tank SL-TPPB for the treatment of gaseous BTEX over dynamic inlet loadings with reasonable accuracy.

As the experimental operation of the stirred-tank SL-TPPB provides a foundation from with which to compare performance of the airlift SL-TPPB for the treatment of BTEX, so does the model in this chapter provide a framework for the development of a model for the airlift SL-TPPB. The stirred tank model developed here will provide the structure and a number of parameter estimates for the tanks-in-series model that will be used to describe the airlift SL-TPPB in Chapter 8.

5.2 Abstract

A dynamic mathematical model has been developed to predict the performance of a stirred tank, solid-liquid two-phase partitioning bioreactor (SL-TPPB) for the treatment of benzene, toluene, ethylbenzene and o-xylene (BTEX) contaminated gases. The SL-TPPB system consists of an aqueous phase containing a bacterial consortium and a solid phase of silicone rubber beads (10% v/v) with a high affinity for BTEX compounds. The silicone rubber beads serve to sequester and release BTEX according to thermodynamic equilibrium, which increases mass transfer from the gas phase and reduces aqueous phase concentrations of these toxic compounds during fluctuating inlet loadings. The model was developed from mass balances on BTEX components in the gas, aqueous and polymer phases, and biomass in the aqueous phase. Dynamic experimental data from this system were used to fit model parameters and to assess the accuracy of the model. An estimability analysis of model parameters and initial conditions was completed to determine the parameters to which model output are most sensitive, and to identify the parameters and initial conditions that should be targeted for estimation. It was found that the developed model, with estimated parameters and initial conditions, has the ability to predict experimental off-gas BTEX concentrations with reasonable accuracy, which are the outputs of greatest importance.

84

5.3 Introduction

Mathematical models for biodegradation systems used in the treatment of waste gas streams serve two purposes: 1) to explain the phenomena that are occurring within the bioreactor to achieve decontamination of the waste gas stream and 2) to predict the performance of the system under various operating conditions. Recently, models have been developed and validated, with the objective of predicting performance under various operating conditions, for several novel biotreatment systems of waste gases including foamed emulsion bioreactors for the treatment of toluene (Kan and Deshusses, 2008), dual liquid-phase biofilters for hydrophobic pollutants (Fazaelipoor, 2008), hybrid bioreactors composed of a bubble column bioreactor and biofilter compartments for the treatment of benzene (Yeom, 2007), and membrane bioreactors for the treatment of toluene (England et al., 2005).

A novel biotreatment system that has been shown to be very promising for the treatment of gases contaminated by benzene, toluene, ethylbenzene and o-xylene (BTEX) is the stirred tank solid-liquid two-phase partitioning bioscrubber (SL-TPPB), which has been experimentally investigated in Chapter 4. This system consists of an aqueous phase containing a bacterial consortium with the ability to degrade BTEX and a second nonbioavailable, immiscible and biocompatible phase of silicone rubber beads to uptake and release BTEX during dynamic operation. This uptake and release of BTEX by the polymer beads reduces toxic substrate levels in the aqueous phase during periods of high loading and increases mass transfer of BTEX out of the gas phase. Although models for liquid-liquid TPPBs for the treatment of waste gases, which have an organic solvent sequestering phase, have been developed and validated (Fazaelipoor, 2007; Koutinas et al., 2007; Neilsen et al., 2007a; Neilsen et al., 2007b), no models exist for suspended growth SL-TPPBs, despite several benefits of using polymers as a sequestering phase over organic solvents (Amsden et al., 2003). This study discusses the development and application of such a model to predict outlet gas concentrations in a 3 L stirred tank solid-liquid TPPB for the treatment of a continuous gas stream containing BTEX. The model, which describes the experimental system studied in Chapter 4, enables improved understanding of the phenomena occurring within the system and predicts

performance under various inlet loading fluctuations. Values for model parameters are initially obtained from independent experiments, empirical correlations and literature values, and then the dynamic experimental data, shown as Figure 4-2, Figure 4-3 and Figure 4-4 in Chapter 4, are used to fit model parameters and initial conditions, and to assess the accuracy of the model. Parameter estimability analysis is used to determine which model parameters and initial conditions should be estimated from the data, and which should be left at initial values. Based on this analysis, experimental data are used to estimate influential parameters and initial conditions to improve predictions of SL-TPPB behaviour.

5.4 Model Development

A schematic of the solid-liquid stirred tank TPPB used in Chapter 4 can be seen in Figure 5-1. In this system, BTEX is delivered into a well-mixed bioreactor via a continuous gas stream. The gas bubbles are dispersed throughout the bioreactor due to the agitation, and BTEX is transferred from the gas phase to the aqueous phase containing the bacterial consortium. If a build-up of BTEX occurs in the
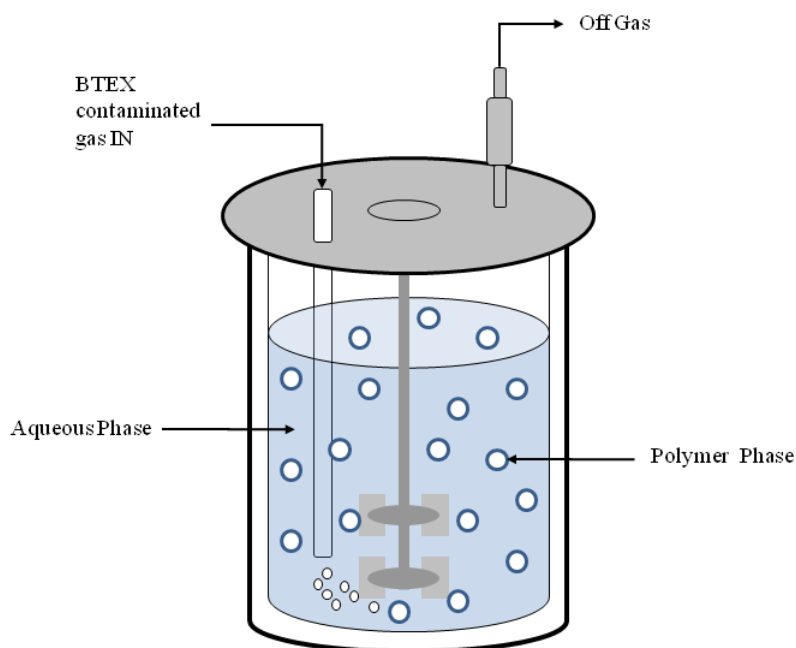
Figure 5-1: Schematic of the 3L stirred-tank SL-TPPB containing silicone rubber beads (10% v/v) and a BTEX degrading bacterial consortium.

aqueous phase, for example, during feed fluctuations, BTEX partitions from the aqueous phase to the polymer beads due to thermodynamic driving forces. Alternatively, as the cells metabolize BTEX in the aqueous phase, BTEX transfers out of the polymer phase to the aqueous phase for subsequent degradation.

` The model for the SL-TPPB was developed using the following key assumptions:

1. The contents of each phase in the reactor (gas, liquid and polymer) are of uniform BTEX concentration and composition.

2. BTEX is transferred from the gas phase to the aqueous phase, and from the aqueous phase to the polymer phase (Kars et al., 1997). Direct transfer between the gas-phase and the polymer is neglected.

3. The biomass is distributed throughout the liquid and consumes BTEX only from the aqueous phase.

4. All polymer beads are spherical and are the same size.

5. The diffusion coefficients of BTEX in the polymer are constant.

6. Constant partition coefficients describe equilibrium between the liquid and polymer phases. Henry's law describes equilibrium between the gas and liquid phases.

7. Substrate toxicity can be described using the model by Luong, (1987).

8. Substrate interactions can be described using the model developed in Chapter 3.

9. Oxygen levels are sufficiently high so that biological reactions are not oxygen limited.

10. A lumped overall mass-transfer coefficient can describe BTEX mass transfer from the liquid to polymer phases.

11. The resistance to BTEX mass transfer in the gas phase and microbial cell walls is negligible.

12. Mass transfer of BTEX to/from the headspace to/from the liquid is negligible.

13. Temperature and pH are constant.

Table 5-1: List of Equations for the Stirred-Tank SL-TPPB Model

Gas-Phase Balances

$$\frac{dC_{i,g}}{dt} = F_g \frac{C_{i,in}}{V_g} - E_P k_L a_i \left(C_{i,gl}^* - C_{i,l}\right)\frac{V_l}{V_g} - F_g \frac{C_{i,g}}{V_g}$$

5-1

Liquid-Phase Balances

$$\frac{dC_{i,l}}{dt} = E_{P,i} k_L a_i \left(C_{i,gl}^* - C_{i,l}\right) - \frac{3k_{O,i}}{R_p}\left(C_{i,l} - C_{i,lp}^*\right) - r_i$$

5-2

$$\frac{dX}{dt} = r_B Y_{X/B} + r_T Y_{X/T} + r_E Y_{X/E} - k_d X$$

5-3

Polymer-Phase Balances

$$\frac{dC_{i,p}}{dt} = \frac{3k_{O,i}}{R_p}\left(C_{i,l} - C_{i,lp}^*\right)\frac{V_l}{V_p}$$

5-4

Headspace Predictions for Liquid Samples

$$C_{i,aq,HS} = \frac{C_{i,l} \times V_{l,aq}}{V_{g,aq} + \dfrac{V_{l,aq}}{H_i}}$$

5-5

Headspace Predictions for Liquid and Polymer Samples

$$C_{i,poly,HS} = C_{i,l} \times V_{l,poly} + \frac{C_{i,p} \times V_{p,poly}}{\dfrac{V_{l,poly}}{H_i} + \dfrac{K_i V_{l,poly}}{H_i} + V_{g,poly}}$$

5-6

Table 5-1 contains the set of equations used to model the system. Mass balances on BTEX components in each phase were used to develop ordinary differential equations to describe BTEX concentrations in the gaseous, liquid and polymer phase, which are listed in Table 5-1 as Equations 5-1, 5-2, and 5-4, respectively. The outlet gas BTEX concentrations determine the performance of the SL-TPPB (as the objective of the system is the treatment of contaminated gases) and were the primary interest in the current study. The concentration of biomass in the aqueous phase is represented in Table

5-1 by Equation 5-3. During the dynamic experiments, aqueous samples and aqueous + polymer samples were removed from the reactor and were allowed to reach phase equilibrium, to provide information about BTEX concentrations in the aqueous and polymer phases, as described in Section 4.4.6. Equations 5-5 and 5-6 are included in the model so that these head-space measurements can be used to obtain information about the model parameters.

Table 5-2 contains thermodynamic and kinetic expressions that were substituted into the primary equations listed in Table 5-1. The thermodynamic expressions that are used to determine concentrations

Table 5-2: Thermodynamic and Kinetic Expressions for use in the Stirred-Tank SL-TPPB Model

Aqueous Phase in Equilibrium	
$C_{i,gl}^{*} = C_{i,g} \big/ H_{lg}$	**5-9**
$C_{i,lp}^{*} = C_{i,p} \big/ K_{lp}$	**5-10**
Microbial Kinetics	
$r_B = \dfrac{\dfrac{\mu_{max,B} C_B}{\left(K_{s,B} + C_B\right) + I_{T,B} C_T + I_{X,B} C_X} \left(1 - \dfrac{C_{B,l}}{C_{B,INH}}\right) X}{Y_{X/B}}$	**5-11**
$r_T = \dfrac{\dfrac{\mu_{max,T} C_T}{\left(K_{s,T} + C_T\right) + I_{B,T} C_T} \left(1 - \dfrac{C_{T,l}}{C_{T,INH}}\right) X}{Y_{X/T}}$	**5-12**
$r_E = \dfrac{\dfrac{\mu_{max,E} C_E}{\left(K_{s,E} + C_E\right)} \left(1 - \dfrac{C_{E,l}}{C_{E,INH}}\right) X}{Y_{X/E}}$	**5-13**
$r_X = \left(\begin{array}{l} \left(T_B^X \left(\dfrac{dC_B}{dt}\left(\dfrac{1}{X}\right)\right)\right)\left(\dfrac{C_X}{K_{s,X} + C_X}\right) X \\ + \left(T_T^X \left(\dfrac{dC_T}{dt}\left(\dfrac{1}{X}\right)\right)\right)\left(\dfrac{C_X}{K_{s,X} + C_X}\right) X \end{array} \right)\left(1 - \dfrac{C_{X,l}}{C_{X,INH}}\right)$	**5-14**

in the aqueous phase in equilibrium with the gas phase and the polymer phase are listed as Equations 5-9 and 5-10, respectively, in Table 5-2. Kinetic expressions that were developed previously in Chapter 3, in combination with the model by Luong, (1987) to account for substrate toxicity are shown in Table 5-2 as Equations 5-11, 5-12, 5-13 and 5-14 for benzene, toluene, ethylbenzene and o-xylene, respectively.

5.5 Parameter Values

Parameter values were obtained from independent experiments, empirical correlations, and/or literature values, and are listed in Table 5-3. The following section outlines how the parameters listed as "Shown in Current Study" were obtained from experiments and correlations.

5.5.1 Experiments for Parameter Values

The experiments that were performed in this study allowed for the determination of diffusivity of BTEX components into the polymer ($D_{p,B}$, $D_{p,T}$, $D_{p,E}$, $D_{p,X}$) and the specific rate of consumption for maintenance (k_m) and were used in correlations to obtain model parameter values.

5.5.1.1 Materials

Benzene and toluene were obtained from Sigma-Aldrich (Oakville, Canada) and ethylbenzene and o-xylene were obtained from Fisher Scientific (Nepean, Canada). Silicone rubber, primarily composed of polydimethylsiloxane, was obtained from GE (Huntersville, North Carolina) in the form of 100% silicone rubber caulking which was dried to spherical beads of density 1.15 g L^{-1} and diameter 2.2 mm. BTEX compounds were used during the determination of $D_{p,B}$, $D_{p,T}$, $D_{p,E}$ and $D_{p,X}$ as described in Section 5.5.1.4.1. These diffusivities were used in the determination of overall mass transfer coefficients for BTEX between aqueous and polymer phases ($k_{o,B}$, $k_{o,T}$, $k_{o,E,}$, $k_{o,X}$) as described in Section 5.5.2.2. BTEX compounds and silicone rubber beads were used in the determination of k_m, as described in Section 5.5.1.4.2, which was used in the determination of the endogenous respiration coefficient (k_d) as described in Section 5.5.2.4.

Table 5-3: Initial Parameter Values for the Stirred-Tank SL-TPPB

Parameter	Value	Unit	S_θ	Method of Determination
E_P	2	-	0.2	Chapter 2
$k_L a_B$	0.0189	s^{-1}	0.00264	Shown in Current Chapter
$k_L a_T$	0.0166	s^{-1}	0.00232	Shown in Current Chapter
$k_L a_E$	0.0155	s^{-1}	0.00216	Shown in Current Chapter
$k_L a_X$	0.0155	s^{-1}	0.00216	Shown in Current Chapter
K_B	62	mg L^{-1} solid L mg^{-1} aqueous	2.88	Chapter 4
K_T	200	mg L^{-1} solid L mg^{-1} aqueous	19.5	Chapter 4
K_E	414	mg L^{-1} solid L mg^{-1} aqueous	153.08	Chapter 4
K_X	593	mg L^{-1} gas L mg^{-1} aqueous	86.4	Chapter 4
H_B	0.26	mg L^{-1} gas L mg^{-1} aqueous	0.04	Chapter 4
H_T	0.35	mg L^{-1} gas L mg^{-1} aqueous	0.02	Chapter 4
H_E	0.43	mg L^{-1} gas L mg^{-1} aqueous	0.02	Chapter 4
H_X	0.25	mg L^{-1} gas L mg^{-1} aqueous	0.03	Chapter 4
$K_{o,B}$	1.05 E-8	m s^{-1}	1.8375E-06	Shown in Current Chapter
$K_{o,T}$	9.3 E-9	m s^{-1}	1.63625E-06	Shown in Current Chapter
$K_{o,E}$	8.5 E-9	m s^{-1}	1.48225E-06	Shown in Current Chapter
$K_{o,X}$	8.5 E-9	m s^{-1}	1.48225E-06	Shown in Current Chapter
ε	0.09	-	0.02	Calderbank, 1958
$\mu_{max,B}$	0.00012	s^{-1}	0.0018	Chapter 3
$\mu_{max,T}$	0.00017	s^{-1}	0.0023	Chapter 3
$\mu_{max,E}$	0.000036	s^{-1}	0.006	Chapter 3
$K_{s,B}$	27.57	mg L^{-1}	11.01	Chapter 3
$K_{s,T}$	34.12	mg L^{-1}	12.12	Chapter 3
$K_{s,E}$	0.36	mg L^{-1}	1.76	Chapter 3
$K_{s,X}$	0.1	mg L^{-1}	10	Chapter 3
$I_{T,B}$	2	-	0.5	Chapter 3
$I_{X,B}$	-0.7	-	0.5	Chapter 3
$I_{B,T}$	-0.4	-	0.5	Chapter 3
$I_{E,B}$	4	-	0.5	Chapter 3
$C_{B,INH}$	20	mg L^{-1}	15	Abuhamed et al., 2004
$C_{T,INH}$	20	mg L^{-1}	15	Abuhamed et al., 2004
$C_{E,INH}$	35	mg L^{-1}	15	Estimated from Abuhamed et al., 2004
$C_{X,INH}$	35	mg L^{-1}	15	Estimated from Abuhamed et al., 2004
$Y_{X/B}$	1.35	mg mg^{-1}	0.27	Chapter 3
$Y_{X/T}$	1.25	mg mg^{-1}	0.25	Chapter 3
$Y_{X/E}$	0.85	mg mg^{-1}	0.17	Chapter 3
T_B^X	0.5	-	0.1	Chapter 3
T_T^X	0.5	-	0.1	Chapter 3
k_d	2.5E-6	s^{-1}	0.000001	Shown in Current Chapter

5.5.1.2 Equipment

To determine k_m, as described in Section 5.5.1.4.2, the bioreactor used was a New Brunswick Bioflo III with a 3 L working volume of aqueous media of composition described in Section 3.5.1. Air was diffused through flasks containing BTEX components, which were combined with makeup air to create a gaseous stream containing BTEX. The bioreactor was operated at identical conditions to the TPPB being modeled in the current study, and was therefore automatically maintained at a temperature of 30 ℃, a pH of 6.9 and agitated at 800 rpm.

5.5.1.3 Experimental Procedure

5.5.1.3.1 Diffusion Coefficients of BTEX in Silicone Rubber, $D_{p,B}, D_{p,T}, D_{p,E}, D_{p,X}$

The diffusion coefficients for BTEX species in silicone rubber were determined experimentally by adding 3 g silicone rubber into a sealed 125 ml amber bottle filled to the top with aqueous medium. 5 ul of each BTEX component was injected into the aqueous medium, and the amber bottles were maintained at 30 ℃ and agitated at 180 rpm. Periodic 1 ml measurements of the aqueous phase were taken using a gas-tight syringe, through self-sealing septa at the top of the bottle, which were injected into 2 ml gas tight containers. These containers were left to equilibrate for one hour, at which time the gas phase concentrations in the 2ml containers were measured using GC/FID. The method for GC/FID is explained in Section 3.5.4. The concentration of BTEX absorbed into the polymer at the time the sample was taken from the amber bottle was then calculated using Henry's constants. Diffusion coefficients were then determined using the method described by Amsden et al., (2003), and were used in Section 5.5.2.2, in order to determine $k_{o,B}$, $k_{o,T}$, $k_{o,E}$ and $k_{o,X}$.

5.5.1.3.2 Specific Rate of Consumption for Maintenance, k_m

To determine k_m, BTEX was delivered to the single-phase bioscrubber via a continuous gas stream containing BTEX at a loading of 60 mg L^{-1} h^{-1} with approximately equal amounts of each compound until the system reached steady-state (>200 hours). Gas samples of the inlet and outlet gas

streams, along with biomass samples were taken approximately every 12 hours. Gas samples were analyzed using GC/FID and biomass concentrations were analyzed using optical density measurements using methods described in Section 3.5.4. Once the system had reached steady state, Equation 5-15 was applied (Nielsen et al., 2005c).

$$k_m = \frac{LR - SR}{X \cdot V_l}$$ **5-15**

This value was used in Section 5.5.2.4, to determine k_d.

5.5.2 Correlations for Parameter Estimates

The correlations used in this study utilized experimental values determined in the current study, along with literature values, and allowed for the determination of volumetric mass transfer coefficients for BTEX (k_La_B, k_La_T, k_La_E, k_La_X), overall mass transfer coefficients for BTEX between aqueous and polymer phases ($k_{o,B}$, $k_{o,T}$, $k_{o,E}$, $k_{o,X}$), entrained gas volume (ε) and the endogenous respiration coefficient (k_d).

5.5.2.1 Volumetric Mass Transfer Coefficients, k_La_B, k_La_T, k_La_E, k_La_X

The experimental methodology used for determining physical enhancement coefficients and volumetric oxygen mass transfer coefficients in a stirred tank reactor are described in Chapter 2. These volumetric oxygen mass transfer coefficients were used to determine volumetric BTEX mass transfer coefficients using the correlation shown in Equation 5-16 (Metcalf and Eddy, 1991).

$$k_La_i = \psi \cdot k_La_O$$ **5-16**

The parameter ψ was estimated using Equation 5-17 (Nielsen and Villadsen, 1994).

$$\psi = \frac{D_i}{D_O}$$ **5-17**

Diffusion coefficients used in Equation 5-17 for oxygen and BTEX in water at 30 °C are $3.51 \cdot 10^{-5}$, 1.17×10^{-5}, 1.03×10^{-5}, 9.33×10^{-6} and 9.33×10^{-6} cm^2 s^{-1}, respectively (EPA, 2006e).

5.5.2.2 Overall Mass Transfer Coefficients for BTEX between Aqueous and Polymer Phases, $k_{o,B}$, $k_{o,T}$, $k_{o,E}$, $k_{o,X}$

The overall mass transfer coefficient for BTEX between aqueous and polymer phases must consider both aqueous and polymer resistances to mass transfer. The overall mass transfer coefficient was calculated using Equation 5-18 (Ma et al., 2002).

$$\frac{1}{k_{O,i}} = \frac{1}{K_i k_{p,i}} + \frac{1}{k_{l,i}}$$

5-18

In order to determine mass transfer coefficients on the liquid and polymer sides, semi-empirical equations can be used which are shown as Equation 5-19 (Ma et al., 2002) and Equation 5-20, respectively (Yao et al., 2003).

$$k_{l,i} = \frac{D_{i,l}}{R_p}$$

5-19

$$k_{p,i} = \frac{D_{i,p}\pi^2}{2R}$$

5-20

5.5.2.3 Entrained Gas Volume, ε

Gas holdup in the reactor was estimated using the correlation seen in Equation 5-21 (Calderbank, 1958), which was used to determine the entrained gas volume in the system;

$$\varepsilon = 1.8 * Pm^{0.14} \upsilon_s^{0.5}$$

5-21

where $P_m = P_g/\rho V_l$ and $\varepsilon = V_g/V_g+V_l$.

5.5.2.4 Endogenous Respiration Coefficient, k_d

The maintenance requirements for the system were modeled using the specific endogenous respiration coefficient, as it provides more realistic predictions compared to the specific rate of substrate consumption for maintenance (Roels, 1983). However, both approaches account for the same

macroscopic observation and are related by Equation 5-22, which was used to determine the parameter value of k_d.

$$k_d = Y_{X/i} k_m \qquad \text{5-22}$$

5.6 Modeling

5.6.1 Stirred-Tank SL-TPPB Data

The experimental data for pseudo steady-state and dynamic operation of the solid-liquid TPPB that are modeled in the current study were obtained previously as described in Chapter 4. The experimental data for the dynamic conditions modeled were obtained after operation of the SL-TPPB until pseudo steady-state biomass concentrations were reached (>200 hours). The approximate operating conditions that were used to obtain the modeled experimental data are listed in Table 5-4 for step changes of 2, 4, 6 and 10 times nominal BTEX loadings. The data being modeled consist of operation at a nominal BTEX loading during pseudo-steady state for approximately 30 minutes, followed by a dynamic loading step change for approximately 230 min, followed by a return to nominal loading for approximately 150 min. Inlet concentrations fluctuated considerably during data collection due to minor increases or decreases in the rotameter settings.

Table 5-4: Experimental Conditions Modeled for the Stirred-Tank SL-TPPB

Operational conditions	Total BTEX Loading rate (mg L^{-1} h^{-1})	Inlet Concentration (mg L^{-1}) of total BTEX*	Flow rate (L h^{-1})
Nominal	60	5.36	33.6
Two times Nominal	120	10.72	33.6
Four times Nominal	240	21.44	33.6
Six times Nominal	360	32.16	33.6
Ten times Nominal	600	53.6	33.6

*All BTEX components are present in approximately equal concentrations

5.6.2 Numerical Methods

Matlab^{TM} was used to generate model predictions by numerical integration of the differential Equations 5-1, 5-2 and 5-4 for each BTEX compound and Equation 5-3 for biomass, using the solver ode23s. The period of operation that was modeled includes steady-state operation at nominal loading, followed by a dynamic step change, followed by a return to nominal loading at conditions described in Section 5.6.1. The model was solved for step changes of 2, 4, 6 and 10 times the nominal loading. The initial conditions for each equation that were input into the ODE solver were determined by experimental measurements at steady-state operation prior to each step change. However, as there is experimental error present in the measured initial condition values, these initial conditions were also treated as parameters during estimability analysis and parameter estimation.

As stated previously, inlet concentrations fluctuated during experimental operation due to minor increases or decreases in the rotameters. Therefore, to model these fluctuations, BTEX inlet concentration used in the model were approximated using measured experimental data and by interpolating between the each sequential inlet sample concentration to model periods between samples. As little experimental data exist beyond t=150 min for the step change to 10 times the nominal loading, predictions beyond this point were not determined and used for parameter estimation.

Parameter and initial condition estimates, as described in the following section, were determined by finding the parameter values that minimize the objective function which was the weighted sum of squared errors between the model predictions and the experimental measurements for BTEX concentrations in the outlet gas, headspace in the aqueous phase samples, headspace in the aqueous + polymer phase samples, and biomass concentrations using the "lsqnonlin" Matlab^{TM} routine.

5.6.3 Estimability Analysis and Parameter Estimation

An estimability analysis of the 43 parameters in the model and 52 initial condition inputs was completed to determine which parameters and initial conditions had the largest impact on model predictions. This was followed by estimation of the most sensitive parameters (and initial conditions)

within realistic upper and lower bounds to obtain more precise values than provided by the initial parameter values and experimental measurements of initial conditions, and to improve the accuracy of the model predictions. The estimability analysis ranked the parameters and initial conditions according to their influence on model outputs, correlation with other model parameters and uncertainty in initial values using the method described by Kou et al., (2005). Prior to estimability analysis, the sensitivity coefficients were scaled using uncertainties, S_θ, in the initial parameter values divided by the uncertainties in the measured outputs (Thompson et al., 2009). The scaling factors S_θ for the initial parameter guesses are shown in Table 5-3. Ranking of parameters and initial conditions was completed until the sum of squares residuals for each column in the residual matrix was less than of 10×10^{-7}.

The parameters and initial conditions that were ranked the highest are those that are most estimable from the available data, because these parameters have large influences on model predictions and have little correlation with the effects of other parameters that rank higher on the list. The high ranking parameters and initial conditions were, therefore, the targets for estimation using experimental data from the SL-TPPB runs. The parameter values in Table 5-3 and measured initial conditions were used as the initial guesses for estimation, and the model predictions were fit to the experimental data by minimizing an objective function that consisted of the sum of squared errors weighted by uncertainties in the different types of experimental measurements. Upper and lower bounds (see Table 5-5) on the estimated parameters and initial conditions were used to ensure that the estimated values remained physically realistic. A series of parameter-estimation calculations was performed, beginning with the most estimable parameter, ($K_{s,X}$, by itself) followed by the two most estimable parameters ($K_{s,X}$, and $\mu_{max,E}$) then the three and so on. Parameter estimation stopped when including additional parameters did not cause a noticeable decrease in the objective function for parameter estimation.

5.7 Results and Discussion

5.7.1 Estimability Analysis and Parameter Estimation

The parameters and initial conditions that were identified to have the largest impact on model output were identified by the estimability analysis and are ranked in Table 5-5. From the information provided by experimental step change SL-TPPB runs, it was determined that at least 20 parameters or initial conditions could be estimated. It can be seen that the most influential parameters are those that govern the rate of biological degradation, which might be expected, as biological uptake is the only true

Table 5-5: Parameter Ranking and Estimates for the Stirred-Tank SL-TPPB

Estimability Rank	Parameter/Initial Condition	Upper/Lower Bounds	Estimated Value
1	$K_{s,X}$	1/0.001	0.005375
2	$\mu_{max,E}$	0.00036/0.0000036	3.641E-6
3	$\mu_{max,B}$	0.0012/0.000012	6.103E-5
4	$C_{E,in,2}$	0.5/0.01	0.02
5	$C_{E,in,4}$	0.5/0.01	0.02
6	$C_{E,in,10}$	0.5/0.01	0.16
7	$\mu_{max,T}$	0.0017/0.000017	3.209E-05
8	$C_{E,in,6}$	0.5/0.01	0.05
9	$K_{o,X}$	6.5 E-10/5.5 E-6	1.408E-7
10	$k_L a_B$	0.00189/0.189	0.0789
11	$k_L a_T$	0.00166/0.166	0.0766
12	$k_L a_X$	0.00155/0.155	0.0355
13	H_T	0.45/0.20	0.22
14	$C_{Bio,in,4}$	7000/9000	8500.53
15	$C_{Bio,in,6}$	6000/8000	7451
16	$C_{Bio,in,10}$	7000/9000	7200
17	$C_{Bio,in,2}$	5000/7000	6568.53
18	$I_{T,B}$	-	-
19	$C_{E,INH}$	-	-
20	$I_{E,B}$	-	-

sink for BTEX components in the system and its rate can govern the driving force between phases. The initial conditions for ethylbenzene concentration in the gas phase are also shown to be influential to the model predictions. This could be due to the fact that ethylbenzene has a relatively large interaction with benzene degradation (see $I_{E,B}$ in Table 5-3) and all other species interact with benzene. Other model parameters and initial conditions that are highly estimable include gas-liquid mass transfer coefficients and initial biomass concentrations. Gas-liquid mass transfer is relatively rapid in comparison to other system dynamics, which accounts for these parameters being highly ranked. Biomass concentrations are slow to respond to step changes, which explains why initial conditions of biomass concentration would be influential to the model predictions.

In order to determine the optimal number of parameters and initial conditions to estimate, the estimation routine was completed for an incrementing number of parameters and initial conditions in the order of rank shown in Table 5-5. The weighted sum of squared errors between the experimental data and model predictions as a function of the number of parameters estimated can be seen plotted in Figure 5-2.
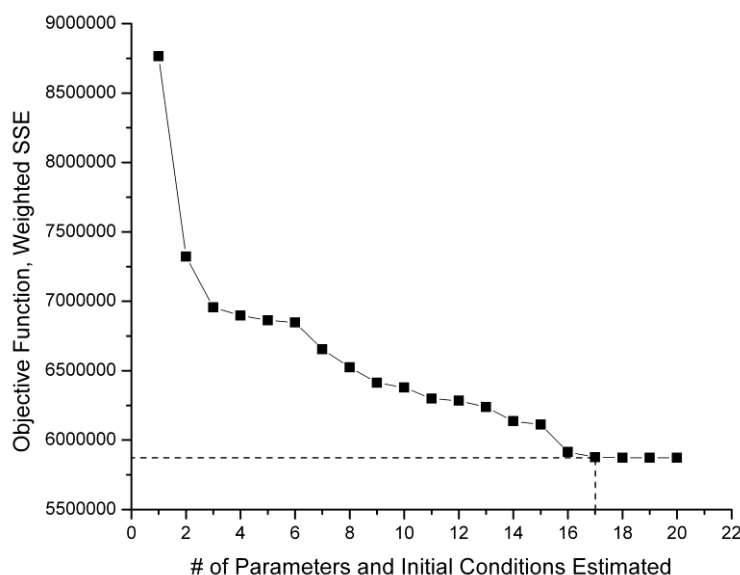
Figure 5-2: Objective function for increasing number of parameters and initial conditions estimated

This shows that after the prediction of the parameter/initial conditions in rank 17, the model predictions do not improve noticeably. Therefore, 17 parameters and initial conditions were estimated, whose values can be seen in Table 5-5. One of the important observations is that the maximum specific growth rates that were estimated are an order of magnitude lower than the original values. This may be possibly attributed to a change in the population distribution and kinetics of the microbial consortium from the time these kinetic values were initially determined in Chapter 3 until the experimental step changes were performed in Chapter 4, as it is known that microbial consortia populations can change during the length of time of biodegradation experiments (Baptista et al., 2008). Also, biological activity from short shake flask experiments may not reflect biological activity during lengthy bioreactor runs.

5.7.2 Model Predictions

The model predictions for the outlet gas concentration were of primary interest in this study, as reduction of outlet BTEX concentrations is the objective of the treatment system. Figure 5-3 to Figure 5-6 show the inlet concentrations (inputs into the model) and the experimental and predicted outlet gas concentrations for benzene, toluene, ethylbenzene and o-xylene, respectively, for nominal loadings at steady state, followed by 4 hour step changes of 2X, 4X, 6X and 10X the nominal loadings, with a subsequent return to nominal loadings. It can be seen that the model predictions are successful in accurately predicting the off-gas behavior during these dynamic periods for all compounds. However, for benzene and toluene during the 4X step change, the off-gas concentration was slightly over-predicted. In addition, for benzene, toluene and ethylbenzene during the 6X step change, the model predicts that the system returns to nominal off-gas concentrations upon completion of the step change slightly faster than the experimental data. Overall, the model has the ability to predict that substrate toxicity occurs during the 10X step change, as outlet concentrations increase significantly, however, xylene concentrations in the outlet gas were slightly over-predicted.
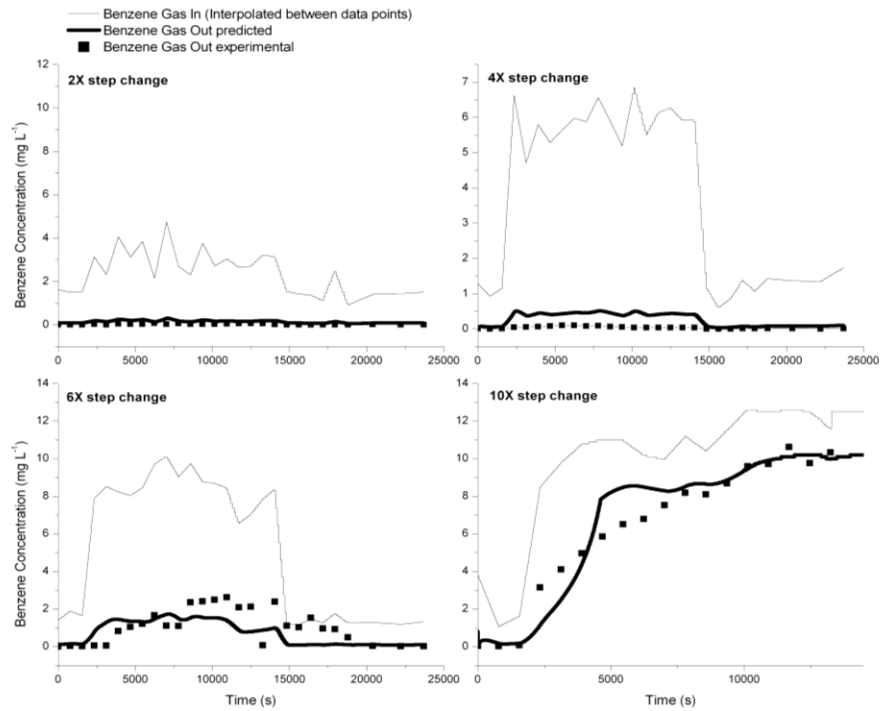
Figure 5-3: Predicted and experimental benzene concentrations in gas streams over a range of step change conditions
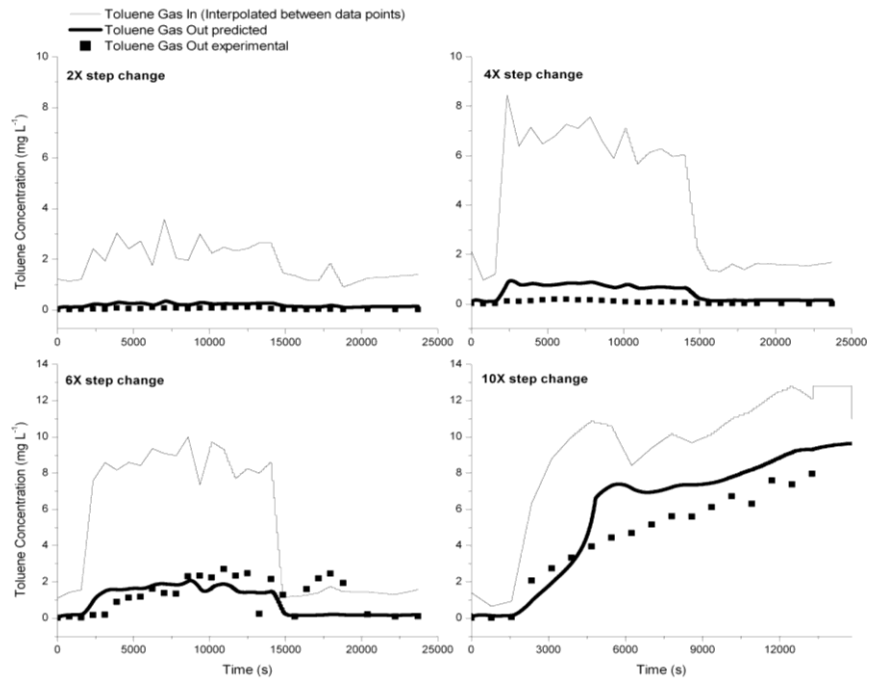
Figure 5-4: Predicted and experimental toluene concentrations in gas streams over a range of step change conditions
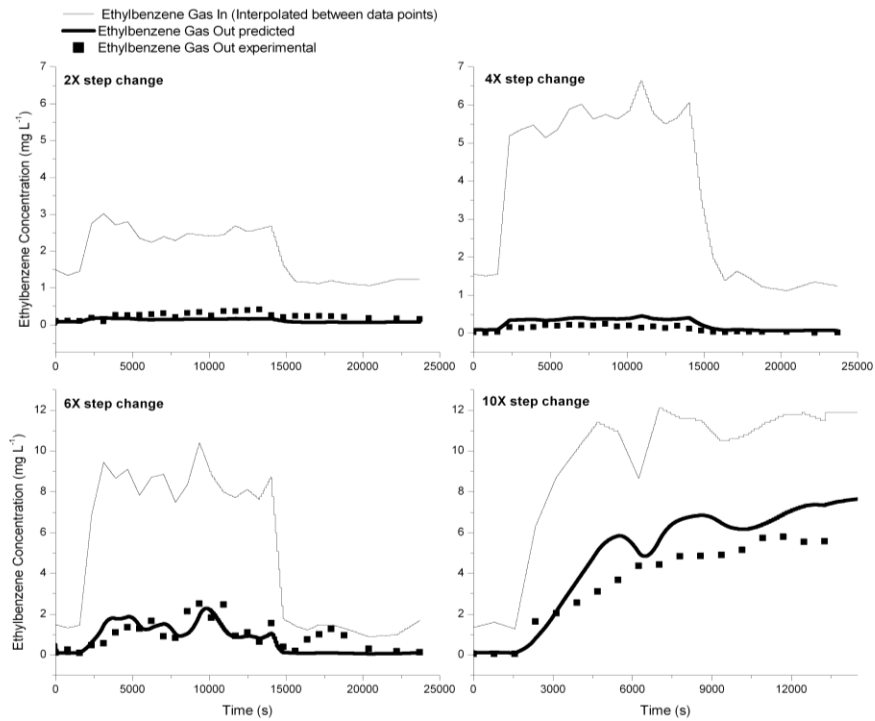
Figure 5-5: Predicted and experimental ethylbenzene concentrations in gas streams over a range of step change conditions
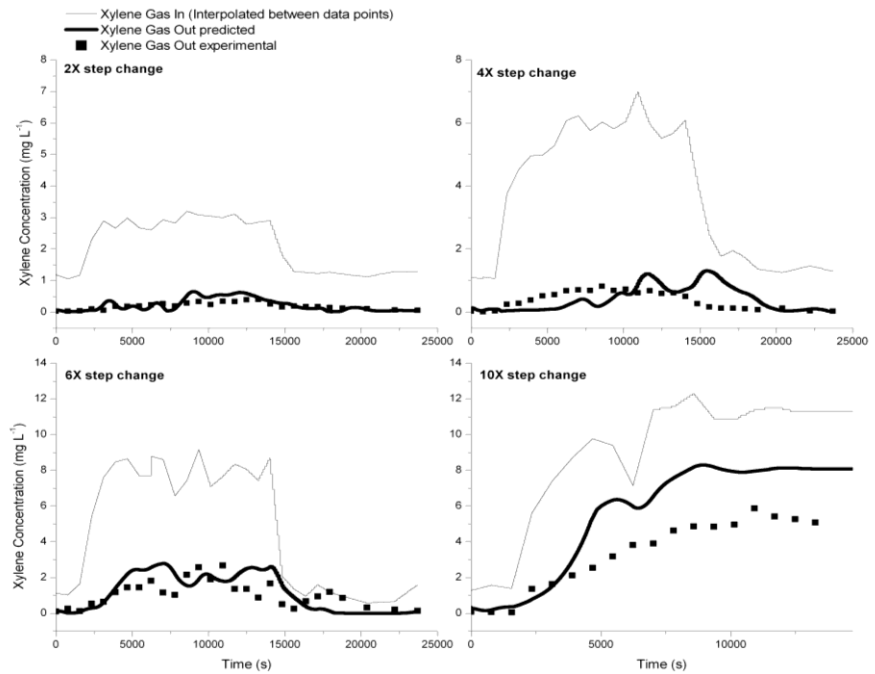
Figure 5-6: Predicted and experimental xylene concentrations in gas streams over a range of step change conditions

The predictions and experimental data for biomass concentrations over all step changes are shown in Figure 5-7. It can be seen that the biomass concentrations are accurately predicted for step changes of 2X and 4X. For the 6X step change, biomass is slightly over-predicted, particularly near the end of the step change. Possibly this may account for the under-predicting of benzene, toluene and ethylbenzene gas concentrations after the completion of the 6X step change, as seen in Figure 5-3, Figure 5-4 and Figure 5-5, respectively. The biomass concentration was under-predicted during the 10X run, as the biomass was predicted to decline during the step change, however, as the technique used to measure biomass concentrations does not distinguish between viable and non-viable cells, the experimental biomass concentrations appeared to stay relatively constant.
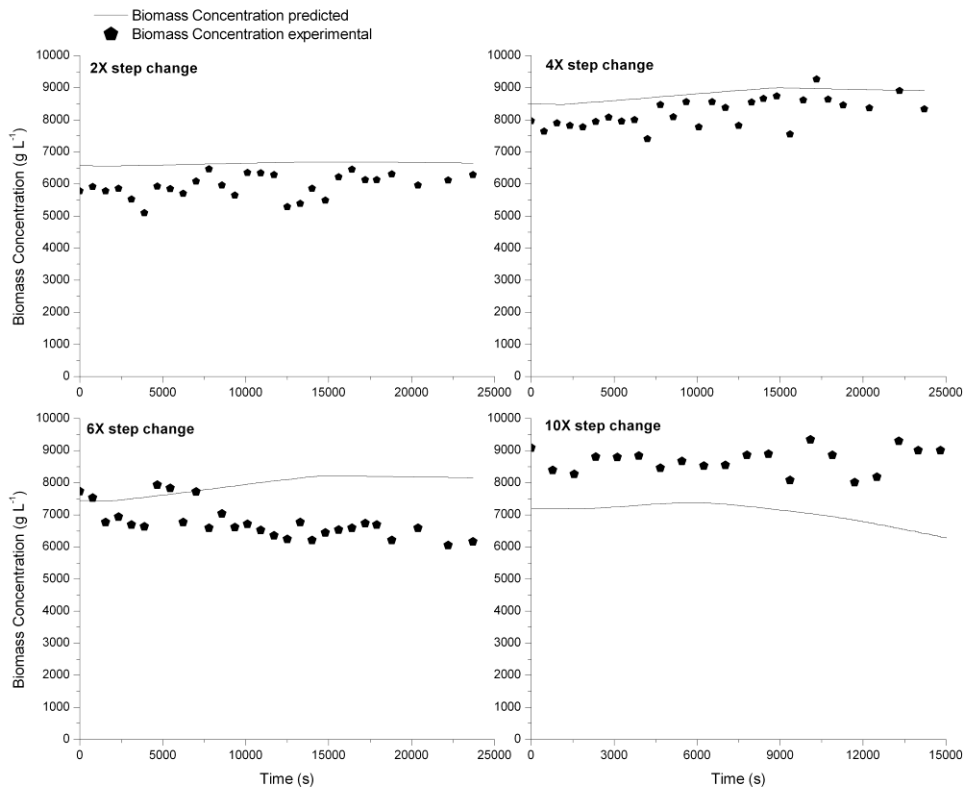
Figure 5-7: Predicted and experimental biomass concentrations over a range of step change conditions

The developed model has been shown to predict dynamic experimental data that range from the system completely damping out step change loading fluctuations to the system succumbing to substrate toxicity, with reasonable accuracy. Future work in this area should be focused on validating this model under varying inlet flow rates and polymer volume fractions. In addition, this well-mixed model provides a framework and select parameter estimates for models of more complex SL-TPPBs that cannot be assumed to be well-mixed, such as airlift reactors.

5.8 Conclusions

A mechanistic model of a stirred-tank SL-TPPB for the treatment of gaseous BTEX has been presented with the primary objective of predicting outlet gas concentrations. Experimental data obtained from operation of this system over dynamic step change conditions were used to estimate parameters and assess model accuracy. As estimability analysis of the model parameters and initial conditions allowed for the identification of those values that have the most significant impact on model output, which were found to be those that influenced biological activity. After the estimation of the identified model parameters and initial conditions, the model was able to predict dynamic experimental data with reasonable accuracy. The model is capable of predicting a range of responses from the SL-TPPB including completely damping out inlet fluctuations during smaller inlet loading step changes, to the system succumbing to toxic aqueous concentrations during larger inlet loading step changes.

Chapter 6

A Two-Phase Partitioning Airlift Bioreactor for the Treatment of BTEX Contaminated Gases

Jennifer V. Littlejohns, Andrew J. Daugulis

6.1 Preface to Chapter 6

The previous chapters described the detailed characterization of the stirred-tank SL-TPPB for the treatment of gas streams containing BTEX, which expanded the application of TPPBs beyond the treatment of single VOC to an industrially common mixture of contaminants. In addition, the research in this thesis considered other aspects that pertain to the application of this system to industrial implementation, including utilizing a bacterial consortium which reduces contamination concerns and performance during transient BTEX loadings. However, a major concern for industrial implementation of any technology, and particularly for an environmental technology, is energy intensity. Although the stirred tank provided an adequate configuration for initial investigation of BTEX treatment by TPPBs, maintaining similar gas-liquid mass transfer rates during scale-up of the stirred-tank SL-TPPB would require immense energy inputs. Therefore, this chapter investigates the application of the TPPB technology in a pneumatically agitated airlift bioreactor system for the treatment of BTEX, which requires significantly less energy inputs relative to the stirred tank configuration.

The stirred-tank SL-TPPB for the treatment of BTEX studied in the previous chapters provides a benchmark comparison to the airlift SL-TPPB that is investigated in this chapter. The results of the present chapter show that the airlift SL-TPPB is an effective, energy efficient alternative to the stirred-tank SL-TPPB for the treatment of BTEX contaminated gas streams over a specific region of operating conditions. This chapter also shows that the airlift SL-TPPB has the ability to buffer dynamic inlet loadings relative to a single phase airlift operated under identical operating conditions in a similar manner to the stirred-tank SL-TPPB described in Chapter 4. However, the airlift SL-TPPB can encounter mass transfer limitations at both high and low inlet gas flow rates wherein either sufficient BTEX is not transferred out of the gas phase or oxygen limitations occur. This prompted a study of oxygen mass transfer and hydrodynamics in the airlift SL-TPPB which will be addressed in Chapter 7. Finally, the data obtained for the airlift SL-TPPB at steady state over various operating conditions will be used to

determine model accuracy and estimate parameters for the mathematical model of the airlift SL-TPPB that will be investigated in Chapter 8.

6.2 Abstract

This investigation characterizes a novel 11 L airlift two-phase partitioning bioreactor (TPPB) for the treatment of gases contaminated with a mixture of benzene, toluene, ethylbenzene and o-xylene (BTEX). The application of the TPPB technology in an airlift bioreactor configuration provides a novel technology that reduces energy intensity relative to traditional stirred tank TPPB configurations. The addition of a solid second phase of silicone rubber beads (10% v/v) or of a liquid second phase of silicone oil (10% v/v) resulted in enhanced performance of the airlift bioreactor relative to the single phase case, with 20% more BTEX being removed from the gas phase during an imposed transient loading. During a 4 hour loading step change of three times the nominal loading (60 g m^{-3} h^{-1}), overall removal efficiencies for the airlift TPPBs containing a liquid or solid phase remained above 75%, whereas the single phase airlift had an overall removal efficiency of 47.1%. The airlift TPPB containing a silicone rubber second phase was further characterized by testing performance during steady state operation over a range of loadings and inlet gas flow rates in the form of a 3^2 factorial experimental design. Optimal operating conditions that avoid oxygen limitations and that still have a slow enough gas flow rate for sufficient BTEX transfer from the gas phase to the working volume are identified. The novel solid-liquid airlift TPPB reduces energy inputs relative to stirred tank designs while being able to eliminate large amounts of BTEX during both steady state and fluctuating loading conditions.

Keywords: Airlift; Biodegradation; BTEX; Microbial consortium; Partitioning bioreactor

6.3 Introduction

Printing facilities (Thanacharoenchanaphas et al., 2007), petroleum refineries (Stewart et al., 2001) and contaminated sites undergoing remediation (Liang et al., 2009) are all sources of gaseous emissions of benzene, toluene, ethylbenzene and o-xylene (BTEX). Due to the toxicity of BTEX components, treatment of these waste gas streams is needed in order to meet regulatory emission standards. Biological treatment methods, such as biofilters, can provide a low-cost, energy efficient and effective solution for the degradation of BTEX. However, biofilters can have limitations such as bed drying, biomass clogging and the inability to effectively handle fluctuations in loading (Khan and Ghoshal, 2000). Therefore, there has been recent interest in the design and improvement of novel biological BTEX treatment systems that have the ability to operate beyond the current abilities of biofilters (Studer and von Rohr, 2008; Kan and Deshusses, 2005). However, design of novel biological treatment systems can often involve stirred tank reactors, which are energy intensive and defy the energy benefits that are typically associated with biological treatment methods. A solution to this is the implementation of airlift bioreactors, which can provide a low energy alternative to traditional stirred tanks.

An example of such a novel biological treatment method that has been researched to date primarily in stirred tank vessels is the two-phase partitioning bioreactor (TPPB), which is gaining popularity for the destruction of toxic compounds in waste gases (Aldric and Thonart, 2008; Arriaga et al., 2006; Bailon et al., 2009; Muñoz et al., 2008). TPPBs consist of a cell containing aqueous phase and a nontoxic, non-bioavailable second phase that can sequester high and fluctuating concentrations of toxic substrates and release them to the aqueous phase for subsequent degradation based on microbial metabolic demand. This provides the ability to treat fluctuating concentrations of toxic compounds with low water solubility by alleviating toxic levels in the aqueous phase and improving mass transfer out of the gas phase. Silicone oil has been traditionally used as the immiscible phase in a TPPB and is nonbioavailable to microbial consortia, however, because of its fixed chemical structure, silicone oil

cannot be modified for optimal uptake and release of target molecules. Although other organic solvents can be selected for treatment of a particular contaminant based on pairing with the target molecule, they are typically limited to systems that treat single VOCs and the use of pure strains of microorganisms due to the potential bioavailability of the organic solvent. This limits the use of other organic solvent second phases for BTEX mixtures, as treatment of waste gases containing BTEX requires the use of a bacterial consortium, since there is no known pure strain of bacteria with the ability to effectively degrade all BTEX components (Bielefeldt and Stensel, 1999). An alternative to a second liquid phase in a TPPB is solid polymers, as they can be selected based on pairing the polymer with the contaminant molecule and they are typically nonbioavailable to bacteria. In Chapter 4, solid silicone rubber polymer beads were utilized as the second phase in a 3 L stirred tank TPPB containing a microbial consortium to treat transient loadings of BTEX.

The objective of most research to date on suspended cell TPPBs has been directed towards characterizing the abilities and performance of these systems for different applications and under a variety of operating conditions (Malinowski, 2001) and, therefore, as mentioned previously, traditional stirred tanks have been used. Although stirred tanks provide a convenient configuration for preliminary investigation, scale up of mechanically agitated TPPBs is constrained by their energy intensity. Airlift bioreactors require less energy, and therefore, facilitate design scale up, providing a potential practical replacement for traditional mechanically agitated configurations. This research is the first investigation of a TPPB in an airlift configuration with the objective of providing an enhanced biotreatment option with reasonable energy inputs for industrial use.

There were three main objectives in the investigation of this novel TPPB system: 1) To perform an initial scoping investigation of the airlift TPPB by operating with a second phase of silicone rubber beads (solid-liquid airlift TPPB) and a single phase airlift (control airlift) for the treatment of a continuous gas stream contaminated with BTEX. This initial scoping consisted of operation of both systems until steady state biomass concentration was reached at a nominal loading of 20 g m^{-3} h^{-1}, followed by a four

hour BTEX step change of two times that nominal loading (2X). The performance of the solid-liquid airlift TPPB was also compared to the performance of the solid-liquid mechanically agitated TPPB investigated in Chapter 4. 2) To subject both airlift systems described in the scoping study to an increased step change loading of 3 times the nominal loading (3X) in order to approach limits of system operation. In addition, an airlift containing a second phase of silicone oil (liquid-liquid airlift TPPB) was tested at these conditions in order to provide the solid-liquid airlift TPPB a comparison to a more conventional second phase found in TPPB literature. 3) To identify optimal steady-state operating regions for the solid-liquid airlift TPPB over a range of gas flow rates and BTEX loadings.

6.4 Materials and Methods

6.4.1 Chemicals

Benzene and o-xylene were obtained from Sigma Aldrich (Oakville, Canada), and toluene and ethylbenzene were obtained from Fisher Scientific (Nepean, Canada). All chemicals used for the fermentation medium were obtained from either Sigma Aldrich (Oakville, Canada) or Fisher Scientific (Nepean, Canada).

6.4.2 Selection of Partitioning Phases

Silicone rubber, primarily composed of polydimethylsiloxane, was obtained from GE (Huntersville, USA) in the form of 100% silicone rubber caulking. The caulking was dried to approximately spherical shaped beads of density 1.15 g L^{-1} and diameter 2.2 mm. The rationale for selecting silicone rubber as the partitioning phase was based on consideration of BTEX partitioning between the liquid and polymer phases, diffusivity though the polymer, and polymer bioavailability, is described in Section 4.4.2. An additional polymer selection criterion for an airlift TPPB is that the polymer must be suspended throughout the airlift bioreactor by liquid velocities induced by gas flow rates within the typical airlift operating range, due to the airlift bioreactor not being mechanically agitated. A range of polymers (those tested in Section 4.4.2) were examined for suspension under a range of flow

rates from 1 to 12 L min^{-1} and it was determined that silicone rubber was the easiest to suspend due to its density (1150 g L^{-1}) being only slightly higher than that of water. See Appendix C for results on the ability to suspend various polymers over a range of inlet flow rates.

Silicone oil with viscosity 5 cSt, obtained from Sigma Aldrich (Oakville, Canada), was the liquid partitioning phase that was selected for comparison, as it is nonbioavailable to microorganisms and can therefore be used with the BTEX degrading bacterial consortium. In addition, it is used as the sequestering phase in TPPBs by a number of other authors (Aldric and Thonart, 2008; Gardin et al., 1999; Muñoz et al., 2007).

6.4.3 Microorganisms

The bacterial consortium used in all experimentation was enriched from petroleum contaminated soil as previously described in Section 3.5.2. A denaturing gradient gel electrophoresis was performed by Microbial Insights (Rockford, USA) which revealed that the consortium used in all experimentation in the current study consists of seven different species of *Pseudomonas*.

6.4.4 Experimental Setup

The experimental setup for the solid-liquid airlift TPPB is shown in Figure 6-1. The bioreactor used was a 13 L Chemap AG Series 3000 Fermentor (Männedorf, Switzerland) with dimensions listed in Table 6-1. The airlift had a total working volume of 11 L with either 10% silicone rubber polymer beads, 10% silicone oil, or without a second phase. The aqueous phase had the following composition (g L^{-1}); 7 $(NH_4)_2SO_4$, 0.75 $MgSO_4 \cdot 7H_2O$, 6.6 K_2HPO_4, 8.42 KH_2PO_4, and 1 ml L^{-1} trace elements. The trace element solution consisted of (g L^{-1}); 16.2 $FeCl_3 \cdot 6H_2O$, 9.44 $CaHPO_4$, 0.15 $CuSO_4 \cdot 5H_2O$, and 40 citric acid. Each bioreactor run was inoculated at an initial biomass concentration of 0.5 g L^{-1}. Throughout experimental runs, the temperature was maintained at 30° C and the pH was maintained at 6.9 by the addition of 6M KOH. The dissolved oxygen (DO) concentration was monitored continuously during all experimentation using an Ingold (Mississauga, Canada) polarographic probe. All tubing used to deliver
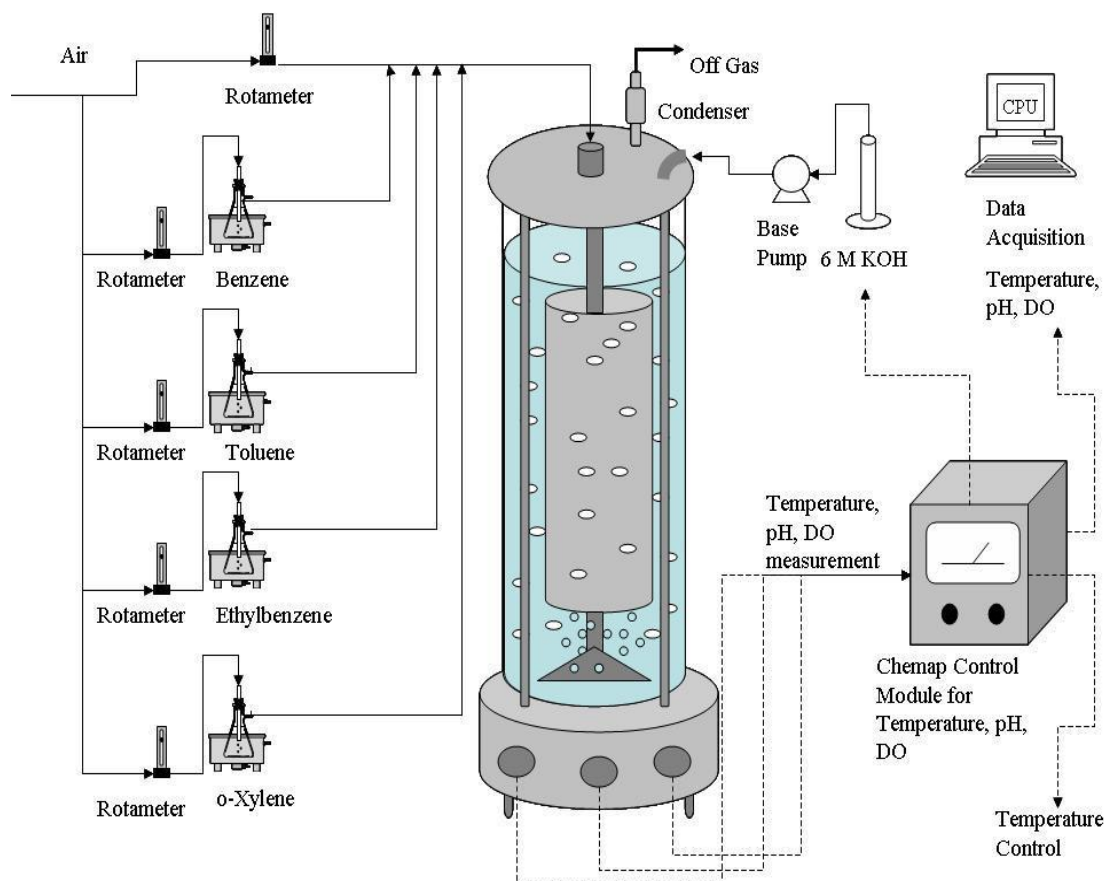
Figure 6-1: Experimental setup for a solid-liquid airlift TPPB for the treatment of BTEX

Table 6-1: Geometry of Airlift Bioreactor

D_T (m) tank diameter	D_R (m) riser diameter	h_T (m) tank height	h_R (m) riser height	A_d/A_r downcomer cross-sectional area/ riser cross-sectional area	V_r (L) riser volume	V_d (L) downcomer volume	V_T (L) total volume
0.14	0.1	0.76	0.53	1.96	4.16	4.43	11

BTEX into the bioscrubber, and bioscrubber seals, were composed of teflon, which is resistant to BTEX permeation.

6.4.5 Experimental Conditions

Before step change operation, each airlift bioreactor system was operated under nominal conditions until steady state biomass concentrations were achieved (> 150 hours). Biomass concentrations reach a steady state, even with the continued addition and consumption of substrate, due to the substrate being directed towards maintenance purposes rather than cell growth (Nielsen et al., 2005). Under nominal conditions before and after step changes, the gas stream had a flow rate of 3 L min^{-1} (Empty bed residence time (EBRT) of 3.7 min) and a BTEX concentration which corresponds to a loading of 20 g m^{-3} h^{-1}. The inlet gas phase for all experimentation contained approximately equal proportions of benzene, toluene, ethylbenzene and o-xylene. During step changes of 2X and 3X (40 and 60 g m^{-3} h^{-1}, respectively), the concentration in the inlet gas was increased and the gas flow rate remained constant.

During steady state investigation of the solid-liquid airlift TPPB, 9 conditions were tested in a 3^2 factorial experimental design for gas flow rates of 2, 3 and 4 L min^{-1} (EBRT of 5.5, 3.7 and 2.75 min, respectively) and BTEX loadings of 20, 60 and 100 g m^{-3} h^{-1}.

6.4.6 Sampling Procedure

Samples of the gaseous stream at the entry and exit of the bioreactor were taken approximately every 12 hours during operation leading to steady state and during steady state operation, and every 13 minutes during imposed BTEX step changes. Even minor changes in rotameters resulted in significant fluctuations in inlet concentrations. Gas phase samples were analyzed by GC/FID using the method described in Section 3.5.4. Aqueous phase samples from the bioreactor were also taken at the time of gas sampling in order to monitor biomass concentrations which were determined by optical density

measurements at 600 nm with a Biochrom Ultrospec 3000 UV/vis spectrophotometer (Cambridge, UK) and compared to a calibration curve relating optical density to cell dry weight.

Samples of the aqueous and polymer phases in the solid-liquid airlift TPPB during step change transients were taken approximately every 40 minutes and concentrations in both phases were determined as described previously in Section 4.4.6 using partition coefficients for BTEX in polymer which were previously determined to be 62 ± 2, 200 ± 4, 593 ± 5 and 414 ± 2 mg L^{-1} gas phase L mg^{-1} liquid phase for benzene, toluene, ethylbenzene and o-xylene, respectively. Concentrations in the aqueous phase for the control airlift were determined by taking a 10 ml sample of the reactor and quickly injecting it into an air-tight 125 ml glass bottle containing 10 drops of pure phosphoric acid to immediately kill bacteria in the sample. The bottles were left to equilibrate over 12 hours and then headspace concentrations were determined using GC/FID. Using Henry`s constants of 0.26, 0.35, 0.43 and 0.25 mg L^{-1} gas phase mg^{-1} L aqueous phase for benzene, toluene, ethylbenzene and o-xylene, respectively, as determined in Section 4.4.6, concentrations in the original aqueous phase sample were then estimated. Concentrations in the aqueous and silicone oil phases in the liquid-liquid airlift TPPB were determined by taking a 10 ml sample of the mixed reactor contents and quickly injecting it into an air-tight 125 ml glass bottle containing 10 drops of pure phosphoric acid. Again, the bottles were left to equilibrate over 12 hours and then headspace concentrations were determined. By assuming that the silicone oil and aqueous phase were in equilibrium in the bioreactor, and by using Henry`s constants and partition coefficients for BTEX components between aqueous and oil phases, the concentrations in the aqueous and oil phases in the original sample were determined. Partition coefficients between aqueous and silicone oil phases were previously determined by adding a known amount of each BTEX component into an airtight bottle containing 10 ml silicone oil, 40 ml aqueous phase and 75 ml headspace. By measuring headspace concentrations and using Henry's constants, partition coefficients for benzene, toluene, ethylbenzene and o-xylene were determined to be 103, 312, 909 and 666 mg L^{-1} oil phase mg^{-1} L aqueous phase.

6.4.7 Performance Indicators

Instantaneous performance indicators for VOC gas treatment systems include removal efficiency (RE) and elimination capacity (EC) which are shown as Equations 6-1 and 6-2, respectively;

$$RE = \frac{\left(C_{g,in} - C_{g,out}\right)}{C_{g,in}} \times 100\%$$

6-1

$$EC = \frac{F_g\left(C_{g,in} - C_{g,out}\right)}{V_{sys}}$$

6-2

Where F_g is the gas flow rate (L h^{-1}), $C_{g,in}$ is the instantaneous concentration of BTEX in the inlet gas (g L^{-1}), $C_{g,out}$ is the instantaneous concentration of BTEX in the outlet gas (g L^{-1}) and V_{sys} is the working volume of the TPPB (m^{-3}).

During transient periods, overall RE and EC, or cumulative RE and EC, are also useful performance indicators that account for stripping from the working volume after the completion of a step change. The period during which these performance indicators are determined is from the initiation of the transient period until performance has stabilized to nominal output conditions after the step change completion. Overall RE and EC are shown as Equation 6-3 and 6-4, respectively;

$$RE_{overall} = \frac{\sum_{i=1}^{n}\left(C_{g,in,i} - C_{g,out,i}\right)}{\sum_{i=1}^{n}\left(C_{g,in,i}\right)} \times 100\%$$

6-3

$$EC_{overall} = \frac{F_g}{V_{sys}t_{overall}} \sum_{i=1}^{n}\left(C_{g,in,i} - C_{g,out,i}\right)t_{i,i+1}$$

6-4

Where i is the sample number, n is the total number of samples taking during the overall period of transient performance due to the step change, $t_{overall}$ is the time of the overall transient performance due to the step change (min) and $t_{i,i+1}$ is the time between sample i and the next proceeding sample (min).

6.5 Results and Discussion

6.5.1 Initial Scoping Investigation

The initial experiments, which consisted of BTEX step changes of 2X, were performed to obtain an indication of how well the solid-liquid airlift TPPB would perform relative to both a control airlift and a solid-liquid stirred tank TPPB described in Chapter 4. Both airlift bioreactor systems were operated at the nominal loading of 20 g m^{-3} h^{-1} for at least 150 hours until steady state biomass concentrations were reached, at which time the four hour transients of 2X were introduced (Figure 6-2a). At the nominal loadings, prior to step changes, performances of systems were similar, as average REs of 75.8% and ECs
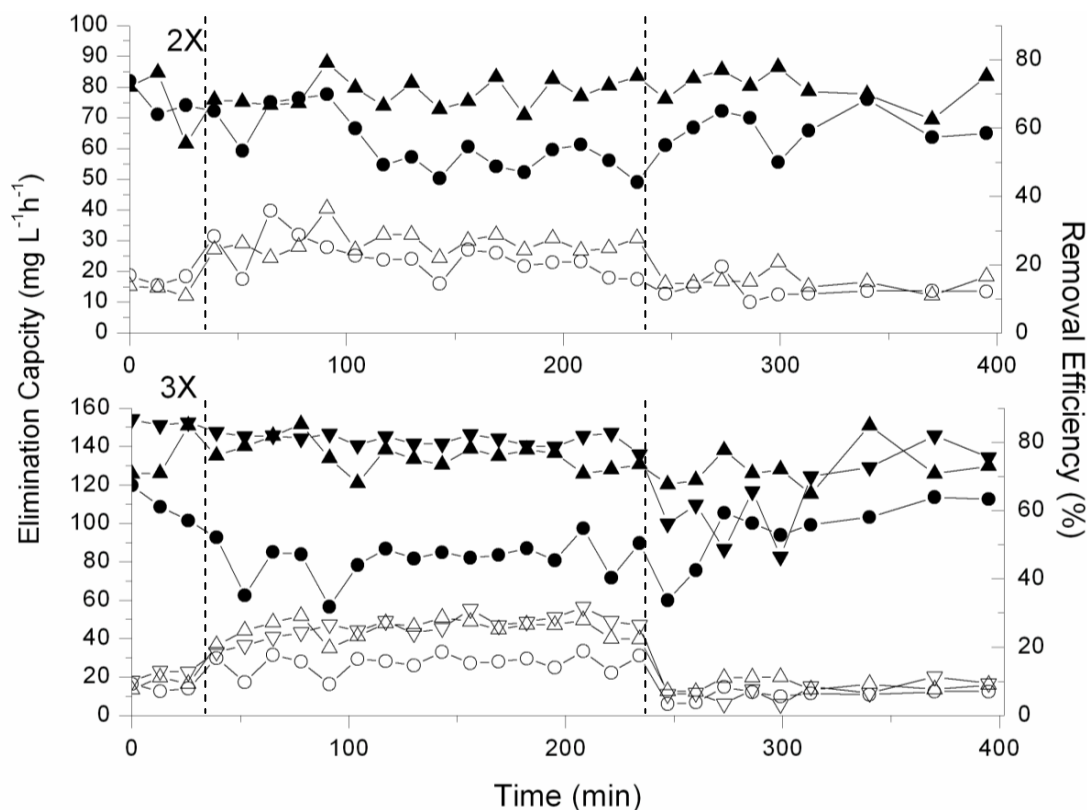
Figure 6-2: a: Step change of 2X for solid-liquid airlift TPPB (triangles) and control airlift (circles), RE – solid shapes, EC – hollow shapes. b: Step change of 3X for solid-liquid airlift TPPB (triangles), liquid-liquid airlift TPPB (inverted triangles), and control airlift (circles), RE – solid shapes, EC – hollow shapes. Dotted lines represent the start and end of the step change.

of 18.7 g m^{-3} h^{-1} were achieved for the solid-liquid airlift TPPB and average REs of 72.3% and ECs of 17.9 g m^{-3} h^{-1} were achieved for the control airlift. In general, during both nominal loadings, as well as step changes, there was a trend of removal being highest for toluene > benzene > ethylbenzene > o-xylene.

During the BTEX step changes (Figure 6-2a), the overall RE and EC were 73.8% and 27.3 g m^{-3} h^{-1}, respectively, for the system with polymers and 53.2% and 21.5 g m^{-3} h^{-1} respectively, for the system without polymers. During the 2X step change, biodegradation of specific compounds was of the order toluene (60.8%), ethylbenzene (57.9%), benzene (55.2%), and o-xylene (46.1%), for the airlift without polymers, and toluene (82.6%), ethylbenzene (74.8%), benzene (71.2%) and o-xylene (63.5%), for the airlift containing polymers. Therefore, the benefits of a sequestering phase become most obvious during transient periods, which is a result that has also been observed for stirred tank TPPBs (Daugulis and Boudreau, 2008). It should be noted that, due to fluctuations in rotameter settings during step changes, there are instances where both systems have similar ECs with different REs, which can be seen, for example, at t=100, 155, 210 in Figure 6-2a. Comparison between the solid-liquid stirred tank TPPB at a nominal loading of 60 g m^{-3} h^{-1} in Chapter 4, and the solid-liquid airlift TPPB at a nominal loading of 20 g m^{-3} h^{-1} reveals that the latter removes 20% less from the gas stream during steady state and transient periods. This suggests that BTEX mass transfer limitations may be a concern for the airlift. However, the airlift system still has the ability to reduce off gas concentrations significantly. In addition, the initial scoping experiments demonstrated the ability of the solid-liquid airlift TPPB to buffer fluctuations in inlet loading relative to a single phase airlift, which is a very useful characteristic in industrial settings, as feed fluctuations commonly occur (Stewart et al., 2001).

The DO traces for both airlift systems for the 2X transient are shown in Figure 6-3. It can be seen that the DO decreased for both systems upon the initiation of the increased BTEX loading followed by an increase back to nominal levels after the completion of the step change. However, it took the airlift
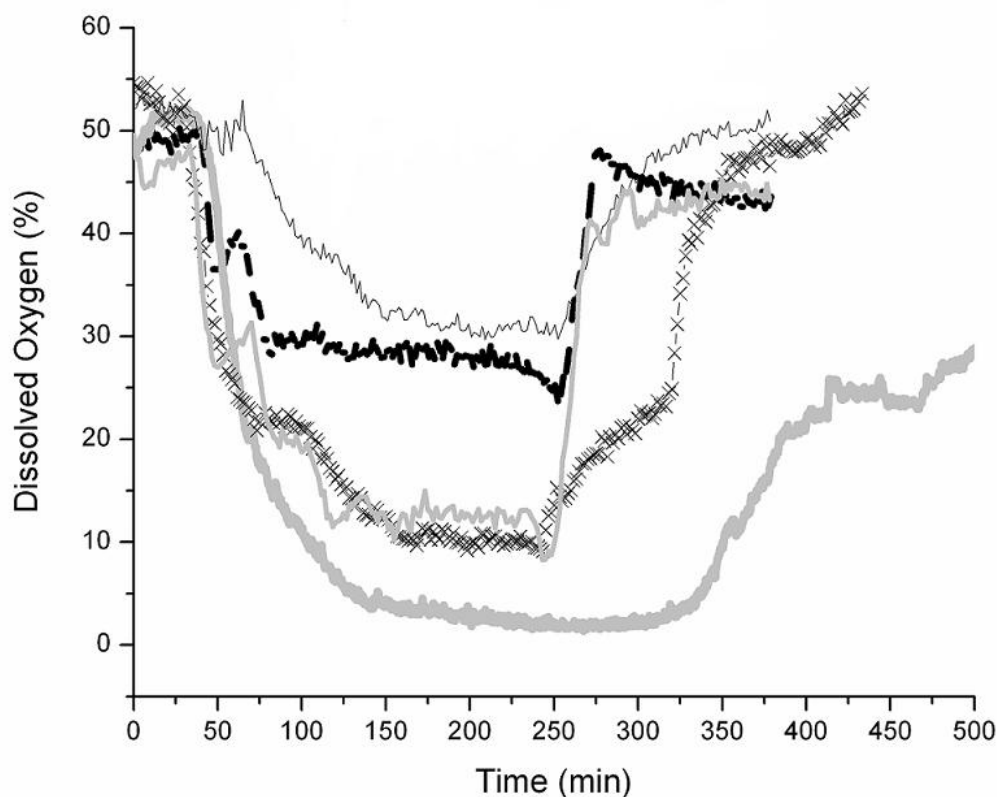
Figure 6-3: Dissolved oxygen traces for step changes of 2X for solid-liquid airlift TPPB and control airlift and 3X for solid-liquid airlift TPPB, liquid-liquid airlift TPPB, and control airlift.

——— 2X step no second phase	——— 3X step no second phase
——— 2X step with polymers	—×— 3X step with polymers
	——— 3X step silicone oil

SL-TPPB longer to reach original DO levels compared to the control airlift after the completion of the transient. This has been observed in previous TPPB literature (Boudreau and Daugulis, 2006) and has been attributed to the additional oxygen requirements needed to degrade the substrate sequestered by the polymer during the transient that is partitioned back to the aqueous phase upon completion of the step change.

In order to confirm that the polymer beads were sequestering BTEX from the aqueous phase during the step change and releasing the BTEX after the loading was returned to nominal levels, BTEX

119
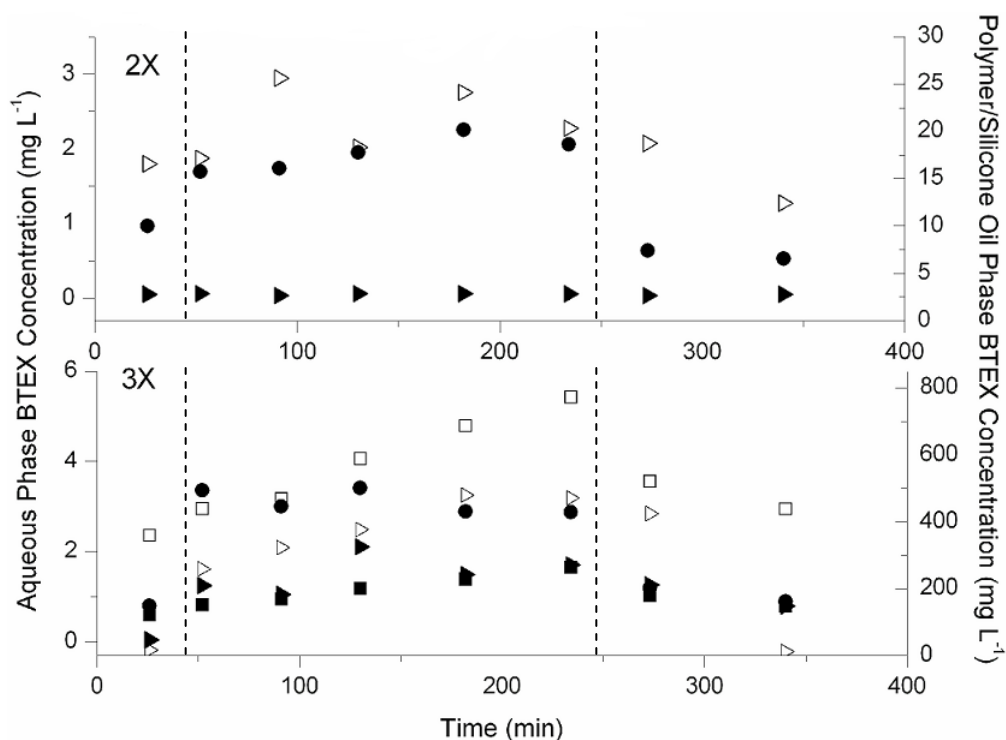
Figure 6-4: a) During a step change of 2X; concentrations in a solid liquid airlift TPPB in the aqueous phase (solid triangle) and polymer phase (hollow triangle) and concentrations in the control airlift aqueous phase (solid circle) b) During a step change of 3X; concentrations in a solid liquid airlift TPPB in the aqueous phase (solid triangle) and polymer phase (hollow triangle), concentrations in the liquid-liquid airlift TPPB in the aqueous phase (solid square) and silicone oil phase (hollow square) and concentrations in the control airlift aqueous phase (solid circle). Dotted lines represent the start and end of the step change.

concentrations in the aqueous and silicone rubber phases were determined and are shown in Figure 6-4a. As can be seen, aqueous phase BTEX concentrations are much lower in the solid-liquid airlift TPPB compared to the control airlift (0.06 mg L^{-1} vs. 2.25 mg L^{-1}), suggesting that the polymer beads buffer the aqueous BTEX concentrations during inlet fluctuations. This may account for the superior performance of BTEX removal by the airlift containing polymers, as the driving force for BTEX transfer from the gas phase into the liquid phase is increased. It can also be seen that much higher concentrations of BTEX are present in the polymer beads relative to the aqueous phase in the solid-liquid airlift TPPB (approximately 400 times), again indicating that the second phase serves to buffer aqueous phase concentrations. At time = 234 min, the polymer beads contained 97% of the total BTEX present in the airlift TPPB. These results

are comparable to those for a stirred tank TPPB in Chapter 4, wherein 93% of the total BTEX present in the bioreactor was in the polymer phase during a step change of 2X.

6.5.2 Increased Step Change Loading of 3X

To further explore the operation of the airlift system under transient loading, step changes of 3X were undertaken for the solid-liquid airlift TPPB, the control airlift, and also for the liquid-liquid airlift TPPB with a silicone oil sequestering phase. Silicone oil was tested to give a direct comparison between a second phase of polymer beads and traditional silicone oil in an airlift TPPB, as silicone oil is a common material used in liquid-liquid TPPBs (Aldric and Thonart, 2008; Gardin et al., 1999; Muñoz et al., 2006). Table 6-2 displays the performance of all three airlift systems during steady state operation before the introduction of the step changes, and shows comparable performance by the three systems. This result is in agreement with Nielsen et al., (2007b) who showed that the addition of an n-hexadecane phase into a bioreactor only slightly increases steady state performance for the treatment of a benzene contaminated gas stream, while Bailon et al., (2009) have shown that the addition of a silicone oil phase significantly increased performance at steady state for the treatment of a dichloromethane contaminated gas stream. This discrepancy may be due to the water solubility of benzene being significantly larger than that of dichloromethane. Benzene has a high gas-liquid mass transfer rate, irrespective of the presence of the second phase, however, dichloromethane gas-liquid mass transfer was increased due to the presence of silicone oil. The higher biomass concentration for the liquid-liquid airlift TPPB and the solid-liquid TPPB seen in Table 6-2 may be attributed to the buffering of substrates during the dynamic period of bioreactor start-up, allowing biomass to reach higher steady state levels. The higher biomass concentrations in the silicone oil system relative to the polymer-containing system may be due to the uptake and release of substrates by silicone oil being instantaneous, whereas the uptake and release of silicone rubber is much slower.

121

Table 6-2: Performance for Airlift Systems at Steady-State at a Loading of 20 mg L^{-1} h^{-1}

System	Duration of operation before reaching SS (h)	EC (mg L^{-1} h^{-1})	RE (%)	Biomass (g L^{-1})	DO (%)
Control (no second phase)	177	18.3 ± 4.3	72.3 ± 11.3	1.10	47
With polymers	165	18.5 ± 4.9	75. 3 ± 8.1	1.42	53
With Oil	189	19.0 ± 3.8	78.6 ± 5.2	2.09	50

Results of the step change of 3X nominal loading for all airlift systems are shown in Figure 6-2b, which further demonstrates the buffering abilities of the TPPB airlift systems during dynamic loadings. The RE for the control airlift dropped to an average of 45% during the transient, whereas the REs for both TPPBs remained above 75%. The performance for both the TPPB systems were quite similar during the transient period, as the overall RE and EC for the solid-liquid airlift TPPB was 75.4% and 38.6 g m^{-3} h^{-1}, respectively, and the overall RE and EC for the liquid-liquid airlift TPPB was 75.0% and 37.2 g m^{-3} h^{-1}, respectively. The control airlift had much lower performance, with an overall RE and EC of 47.1% and 21.7 g m^{-3} h^{-1}, respectively. During the 3X step change, biodegradation of specific compounds was of the order toluene (58.9%), ethylbenzene (57.8%), benzene (48.3%), and o-xylene (25.5%), for the single phase airlift, toluene (81.2%), ethylbenzene (79.8%), benzene (71.4%) and o-xylene (65.6%), for the airlift containing polymers, and toluene (87.2%), benzene (78.7%), ethylbenzene (71.1%) and o-xylene (65.9%), for the airlift containing silicone oil. DO traces for all three systems for the 3X step change can be seen in Figure 6-3. Although DO levels decreased during the step change in all cases, the DO in the airlift TPPBs took much longer to recover with the liquid-liquid airlift TPPB taking the longest. Figure 6-3 shows that during the step change of 3X, oxygen limiting conditions were likely being approached.

Concentrations in the aqueous, silicone rubber and silicone oil phases were also determined during the 3X transients and are reported in Figure 6-4b. Aqueous phase BTEX concentrations are lower in the liquid-liquid TPPB (< 1.8 mg L^{-1}) and the solid-liquid TPPB (< 2.1 mg L^{-1}) in comparison to the control airlift (< 3.5 mg L^{-1}), showing sequestration of BTEX from the liquid phase during inlet fluctuations. This sequestration is further demonstrated by the fact that at time = 234 min, the polymer

beads contained 96% and the silicone oil contained 98% of the total BTEX present in the airlift bioreactors. These results are comparable to those for a stirred tank configuration in Chapter 4, wherein 91% of the total BTEX present in the bioreactor was in the polymer beads during a step change of 4X the nominal loading. This suggests that, the use of a second phase to sequester VOCs during fluctuating inlet loadings is beneficial to a biotreatment system, regardless of whether the bioreactor is in airlift or stirred tank configuration.

Although the current results show that the liquid-liquid airlift TPPB and the solid-liquid airlift TPPB have similar performance during fluctuating inlet loadings, there are numerous benefits to using a polymer phase in comparison to an immiscible liquid, including the fact that polymers are generally much less expensive, are non-volatile, can be formed into many shapes and sizes, and are generally non-hazardous environmentally and for operators. From transient loading investigations, however, it has become apparent that both oxygen and BTEX mass transfer limitations are concerns during airlift operation. Therefore, in order to further characterize the impact that potential mass transfer limitations may have on solid-liquid TPPB performance, the effect of loading and inlet gas flow rate during steady state operation was determined.

6.5.3 Identification of Optimal Steady-State Regions for SL-TPPB

Inlet gas flow rates and loadings were varied in the form of a 3^2 factorial experimental design, and the solid-liquid airlift TPPB was operated under each set of conditions until steady state biomass concentrations were reached (>150 hours for each condition). The average RE and EC and the respective standard errors can be seen for each set of operating conditions in Figure 6-5. This plot shows a similar decrease in RE as loading is increased from 60 to 120 g m^{-3} h^{-1} for all flow rates. However, at the lowest loading condition of 20 g m^{-3} h^{-1}, there are differences in performance for different inlet gas flow rates, with flow rate of 3 L min^{-1} achieving the maximum RE. This may be explained in part by consideration of Figure 6-6a. It can be seen that at a flow rate of 2 L min^{-1}, the system appears to be oxygen limited
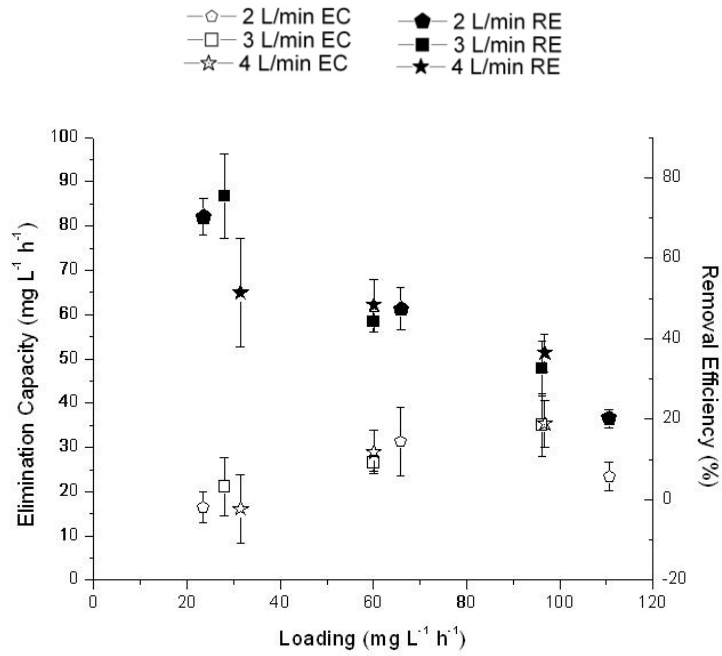
Figure 6-5: Steady-state ECs and REs for airlift SL-TPPB under varying flow rates and loadings
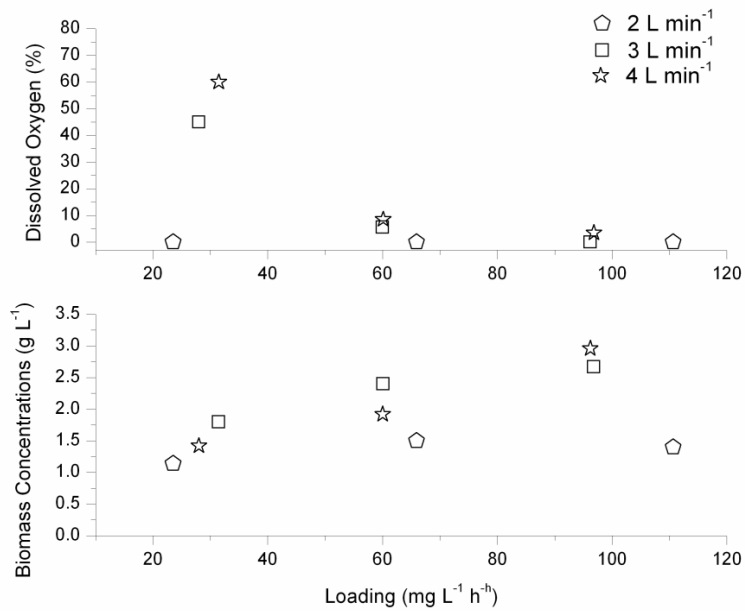
Figure 6-6: a) Steady-state DO concentrations for airlift SL-TPPB under varying gas flow rates and loadings. b) Steady-state biomass concentrations for airlift SL-TPPB under varying gas flow rates and loadings.

under all loadings tested. At flow rates of 3 and 4 L min^{-1} the system is not oxygen limited, however, at a flow rate of 4 L min^{-1} the EBRT is too small for effective BTEX mass transfer from the gas phase to the liquid phase. VOC mass transfer limitations during high inlet flow rates in airlift bioreactors that result in decreases in system performance have been observed by other authors including Vergara-Fernandez et al., (2008) who used an internal loop airlift bioreactor to treat toluene, and Harding et al., (2003) who used an external loop airlift bioreactor with a spinning sparger for the treatment of toluene. Therefore, there exist optimal operating regions for the airlift bioreactor that avoid oxygen limiting conditions while having a high enough EBRT for contaminants to transfer out of the gas phase. Figure 6-6a and Figure 6-6b also demonstrate the impact that DO levels can have on steady state biomass concentrations. Since airlift TPPB operation at a flow rate of 2 L min^{-1} is oxygen limited under all loadings (Figure 6-6a), the biomass concentrations at 2 L min^{-1} remain constant despite an increase in loading (Figure 6-6b). Operation at flow rates of 3 and 4 L min^{-1} has a DO of greater than 0% for all loadings, and it can be seen that biomass levels steadily increase as loading is increased. In comparison to the mechanically agitated solid-liquid TPPB investigated in Chapter 4, steady state biomass concentrations are much lower in the current study likely due to the lower loadings and lower REs achieved. However, Figure 6-7 shows a linear correlation between the average EC of the airlift TPPB and steady state biomass concentrations. Therefore, despite oxygen limitations, the BTEX removed from the gas corresponds to the biomass growth in the reactor.

In comparison to traditional biotreatment methods, the airlift TPPB provides comparable performance at steady state. For example, Zilli et al., (2004) investigated the removal of benzene using traditional biofiltration and received maximum ECs of 3.2, 6.4 and 26 g m^{-3} h^{-1} with REs of 52, 53 and 84%, for packing materials of raw sugarcane, sieved sugarcane and peat, respectively.   In addition, Kamarthi and Willingham, (1994) determined ECs of 20-30 g m^{-3} h^{-1} for REs of 70-90% for a biofilter containing compost media treating BTEX. As previously stated, there has been recent interest in developing biotreatment biotreatment strategies to outperform conventional biotreatment methods. Such strategies
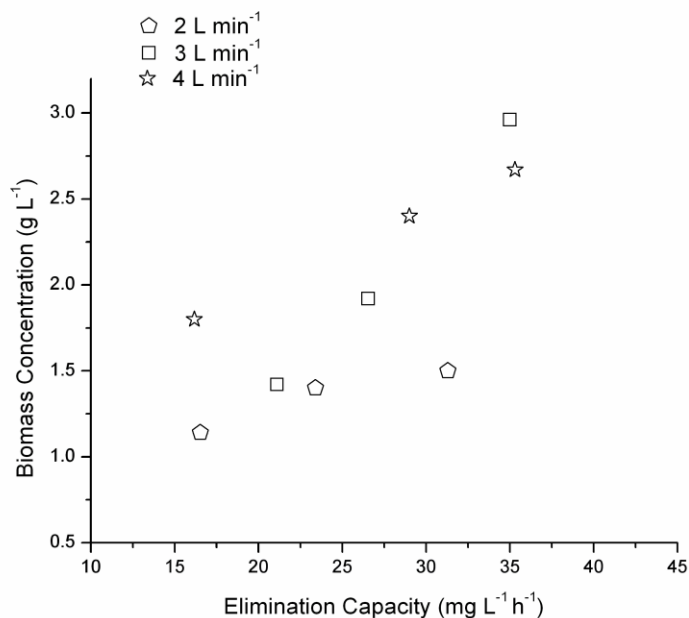
Figure 6-7: Steady-state biomass concentrations as a function of average EC for the solid-liquid airlift TPPB for varying gas flow rates and loadings.

to outperform conventional biotreatment methods. Such strategies include the addition of activated carbon into biofiltration units which can receive a maximum EC of 83.65 g m^{-3} h^{-1} with a RE of 67% for the treatment of BTEX using a mixture of sugar cane bagasse, compost and granulated activated carbon as media (Mathur et al., 2007). In addition, Mohammad et al., (2007) have reported excellent performance for BTEX treatment in mesophilic and thermophilic bioreactors, with a maximum EC of 188 g m^{-3} h^{-1} at a RE of 62% for the mesophilic unit and a maximum EC of 218 g m^{-3} h^{-1} at a RE of 85% for the thermophilic unit. The performance of these treatment methods are significantly larger than those obtained in the current study at steady-state, but characterization of these techniques to buffer inlet fluctuations is needed. The steady state performances of the solid-liquid airlift TPPB at loadings of 60 g m^{-3} h^{-1} are more than 40% lower than the performance of the stirred tank solid-liquid TPPB in Chapter 4 at the same loading. The performance of an airlift TPPB will also likely be lower than other research for stirred tank TPPBs for compounds such as dichloromethane (Bailon et al., 2009), hexane (Arriaga et al.,

2006), toluene (Daugulis and Boudreau, 2008) and benzene (Nielsen et al., 2005a), as these systems were not oxygen or VOC mass transfer limited, and approached 100% RE even at high loadings. However, the solid-liquid airlift TPPB still has the ability to buffer loading fluctuations in the same manner as the stirred tank configurations, and, under optimal operating conditions, has the ability to reduce BTEX concentrations in the off gas significantly. Despite reduced performance at elevated VOC loadings, airlift systems will have a critical advantage over mechanically agitated devices in terms of reduced energy requirement. A preliminary estimate of the energy requirement for the airlift can be made using Equation 6-5 (Chisti, 1989).

$$\frac{P_g}{V_{sys}} = \frac{\rho_l g \upsilon_{S,r}}{1 + \frac{A_d}{A_r}}$$

6-5

Where P_g is the power input (kW), ρ_l is the liquid density (g L^{-1}), g is acceleration due to gravity (m s^{-2}) and $\upsilon_{S,r}$ is the superficial gas velocity in the riser (m s^{-1}). $\upsilon_{S,r}$ was determined to be 0.006 m s^{-1}.

A preliminary estimate of the energy requirement for the stirred tank can be made by using Rushton curves that relate the Reynolds number to the Power number for a flat blade turbine (Rushton et al., 1950) and correcting the power for aeration (Ohyama et al., 1955). The conditions used for the calculation of the power input for the stirred tank investigated in Chapter 4 are an agitation speed of 800 rpm, impeller diameter of 8 cm and a volumetric gas flow rate of 0.56 L min^{-1}.

Power inputs per unit volume for the airlift and stirred tank are therefore estimated to be 0.019 and 14.7 W L^{-1}, respectively, and thus the energy saved by using the airlift may greatly outweigh a 20% decrease in performance relative to a stirred tank reactor.

6.6 Conclusion

During transient operation at a loading of 60 g m^{-3} h^{-1}, the polymer-containing airlift TPPB has been shown to have superior performance to a single phase airlift and comparable performance to the liquid-liquid airlift TPPB with silicone oil as the partitioning phase. It was found that for a loading of 20

g m^{-3} h^{-1} there is an optimal performance at a flow rate of 3 L min^{-1} which has a large enough EBRT for sufficient BTEX to transfer out of the gas phase and also a large enough gas flow rate to avoid oxygen limiting conditions. Although performance of the airlift TPPB is lower than the performance of a stirred tank TPPB due largely to mass transfer, the energy input is much larger for the stirred tank, giving the airlift an important advantage.

ACKNOWLEDGEMENTS

Chapter 7

Oxygen Mass Transfer and Hydrodynamics in a Multi-Phase Airlift Bioscrubber System

Jennifer V. Littlejohns, Andrew J. Daugulis

7.1 Preface to Chapter 7

It was shown in Chapter 2 that the addition of polymer beads in a stirred-tank SL-TPPB increased the OTR and it was observed in Chapter 4 that during operation of the stirred-tank SL-TPPB, oxygen limiting conditions did not occur. However, in Chapter 6 during investigation of the airlift SL-TPPB for BTEX treatment, although it was shown that the system had the ability to effectively treat BTEX contaminated gases under specific operating conditions, gas flow rates that resulted in oxygen limiting conditions and insufficient BTEX mass transfer were identified. Not surprisingly, these oxygen limitations reduced the performance of the airlift SL-TPPB in comparison to the stirred-tank SL-TPPB. These results prompted the investigation in this chapter of oxygen mass transfer and hydrodynamics in the airlift SL-TPPB.

The results of this chapter provide a possible explanation to the mass transfer limitations encountered during operation of the airlift SL-TPPB by showing that the polymers do not cause physical enhancement of volumetric mass transfer coefficients ($k_L a$) and the magnitude of $k_L a$s are lower relative to those obtained in Chapter 2 for the stirred tank SL-TPPB. However, the implications of this chapter are that the addition of polymers with a high affinity for oxygen into an airlift can increase the OTR during dynamic periods. An RTD analysis on the airlift SL-TPPB is also described in this chapter, which shows that the addition of silicone rubber polymer beads increases aqueous phase mixing. The investigation in this chapter not only provides a possible explanation for the observed performance of the airlift SL-TPPB in terms of oxygen limitations, but also provides a number of parameter estimates that will be used in the mathematical model of the airlift SL-TPPB in Chapter 8.

7.2 Abstract

The addition of select polymer beads to stirred tank bioscrubber systems has been shown to greatly enhance the removal and treatment of toxic VOCs via the capture and sequestration of poorly soluble compounds such as benzene, and the release of these materials, based on equilibrium partitioning, to microorganisms in the aqueous phase. In this study, oxygen volumetric mass transfer coefficients were determined for an 11 L airlift vessel containing tap water alone, tap water with nylon 6,6 polymer beads (10% v/v), and tap water with silicone rubber beads (10% v/v), over various inlet gas flow rates, with the aim of initially characterizing a low-energy pneumatically agitated reactor (concentric tube airlift). In addition, oxygen transfer rates into the airlift with and without polymers with high oxygen affinity were determined. To further characterize this reactor system, a residence time distribution analysis was completed to determine hydrodynamic parameters including the Peclet number (Pe), circulation time (t_c) and mixing time (t_m) over various gas flow rates for the airlift containing tap water with and without silicone rubber. It was found that the addition of silicone rubber beads, which has a high affinity for oxygen, reduced the measured volumetric mass transfer coefficient relative to a system without polymers due to oxygen sorption during the dynamic period of testing, but increased the overall amount of oxygen that was transferred to the system during the dynamic period. The addition of nylon 6,6, which has very low oxygen uptake, allowed for estimation of the physical effect of solids addition on gas-liquid mass transfer and it was found that there was no effect on the measured volumetric mass transfer coefficient relative to a system without polymers. However, hydrodynamic parameters revealed that the addition of silicone rubber into an airlift vessel improves liquid phase mixing. This investigation has defined key operational features of a low-energy three-phase airlift bioscrubber system for the treatment of toxic VOC substrates.

Keywords: Mass Transfer; Mixing; Multiphase Reactors; Hydrodynamics; Airlift; Bioreactor

7.3 Introduction

Airlift vessels are a useful reactor design due to their simple construction, low energy requirements and low shear environment (Chisti, 1989). In Chapter 6 the performance of a novel airlift solid-liquid two-phase partitioning bioreactor (TPPB) for the treatment of a gaseous mixture of benzene, toluene, ethylbenzene and o-xylene (BTEX) was examined. The addition of a solid phase, composed of silicone rubber beads, to an airlift bioreactor was shown to increase performance during fluctuating inlet BTEX loadings relative to an airlift without silicone rubber. This was due to silicone rubber absorbing/desorbing BTEX according to achieving equilibrium conditions while meeting metabolic demand, which increased substrate gas-liquid mass transfer and maintained BTEX aqueous phase concentrations at sub-inhibitory levels. However, during this investigation it was found that oxygen mass transfer from the gas to the aqueous phase was the rate limiting step for biodegradation, as dissolved oxygen (DO) reached 0% at average elimination capacities of 31.2 g m^{-3} h^{-1} and removal efficiencies of 49.8% during steady state loadings of 60 g m^{-3} h^{-1}. In addition, overall system performance of the airlift TPPB was lower in comparison to the stirred tank TPPB investigated in Chapter 4, whose DO remained over 80% while achieving elimination capacities of 58.5 g m^{-3} h^{-1} and removal efficiencies of 97.1% at a steady-state loading of 60 g m^{-3} h^{-1}.

Characterization of oxygen mass transfer within the airlift TPPB is of interest, as past research has determined that the presence of an immiscible sequestering phase in a mechanically agitated TPPB enhances the oxygen transfer rate (OTR) to the system relative to single phase systems. This has been shown to be the case for a TPPB using the organic solvent, n-hexadecane, which has a high affinity for oxygen, as oxygen transfers in parallel from the gas phase to the aqueous/solvent phases which have a higher combined DO saturation concentration (Nielsen et al., 2005b). The presence of silicone rubber beads, which also have a high affinity for oxygen, have also provided an increase in OTR in a stirred tank TPPB (Chapter 2) due to mass transfer in series from the gas phase to the aqueous phase, then subsequently from the aqueous phase to the polymer phase. In such arrangements, uptake by the polymer

increases the gas-aqueous driving force over dynamic periods. This transport in series model is commonly used for gas-aqueous-solid systems in which the suspended solids are larger than the liquid film thickness between the gas and liquid phases (Alper et al., 1980). In addition, it was also demonstrated in Chapter 2 that the addition of polymers in a stirred tank has a physical enhancement effect on oxygen mass transfer. Physical enhancement of gas-liquid mass transfer in three phase systems has been observed in several studies (Zhang et al., 2006; Ruthiya et al., 2003; Tinge and Drinkenburg, 1995) and is caused by enhanced boundary layer mixing due to turbulence at the gas-liquid interface (Zhang et al., 2006; Ruthiya et al., 2003), resulting in a larger refreshment rate of liquid in the boundary layer by mixing with the bulk fluid. In addition, physical enhancement may involve changes in the gas-liquid interfacial area by coalescence inhibition caused by particles being present at the gas-liquid interface (Ruthiya et al., 2003).

In addition to oxygen mass transfer, hydrodynamic characterization of airlift bioreactors provides important information necessary to describe system performance and facilitate mathematical modeling. In contrast to stirred tank vessels that are assumed to be well-mixed, airlift bioreactors can often have an axial variation of composition, particularly in the downcomer (Chisti, 1989). Hydrodynamic studies have shown that the presence of solids in three phase systems can have a neutral (Sánchez et al., 2005; Lindert et al., 1992) and positive (Comte et al., 1997; Lu et al., 1994) impact on mixing depending on the reactor geometry, solid size, solid density and solid loading.

Despite the numerous studies on oxygen mass transfer and mixing in three phase airlift bioreactors, the airlift partitioning bioreactor has not been characterized to date due to the unique physical properties of the solid phase. The purpose of this study was to determine the impact of silicone rubber beads in an airlift reactor on the measured effective volumetric mass transfer coefficient (k_La_{eff}) over a range of air flow rates relative to the k_La_{eff} in an airlift containing solids with low oxygen affinity (nylon 6,6) and to the volumetric mass transfer coefficient in airlift without solids (k_La). Results were compared to the volumetric mass transfer coefficient of a stirred tank containing silicone rubber, nylon 6,6 and

without solids. The OTR was then determined in the airlift with and without silicone beads to show the true amount of oxygen entering each system. In addition, hydrodynamic characterization was completed for an airlift with and without silicone rubber beads by quantifying Peclet number (Pe), circulation time (t_c) and mixing time (t_m). This work has provided insight into the observed performance of an airlift TPPB for treatment of BTEX contaminated gases in Chapter 6. In addition this work has determined the impact of the addition solids with high oxygen affinity on mass transfer and hydrodynamics in an airlift, which had not been undertaken to date.

7.4 Materials and Methods

7.4.1 Equipment

The reactor used was a 13 L Chemap AG Series 3000 concentric tube airlift fermentor (Männedorf, Switzerland) with dimensions listed in Table 6-1. All experiments were conducted at 30 ± 0.1 °C and DO and pH were monitored continuously by probes located at the bottom of the vessel using a Measurement Computing TracerDAQ data acquisition system.   Throughout all experimentation, the working volume of the reactor was 11 L with either no solid phase or with 10% v/v polymer beads. The polymer used with a high affinity for oxygen (O_2 diffusivity = 3.4 x 10^{-5} cm^2 s^{-1} (Merkel et al., 2000), O_2 solubility = 0.18 cm^3(STP)/cm$^3 \cdot$ atm (Merkel et al., 2000)) was silicone rubber that was obtained from GE-Mastercraft ® in the form of 100% silicone rubber caulking dried to spherically shaped beads (diameter = 2.5 mm). The polymer used with a low affinity for oxygen (O_2 diffusivity = 1.6 x 10^{-9} cm^2 s^{-1} (Jarus et al., 2002), O_2 solubility = 0.035 cm^3(STP)/cm$^3 \cdot$ atm (Weinkauf et al., 1992)) was Nylon 6,6, which was obtained from Dupont Canada (diameter = 2.59 mm). The stirred tank used was described previously in Section 2.4.1.

7.4.2 Oxygen Mass Transfer Coefficients

$k_L a$ for the airlift reactor containing solely tap water was determined for flow rates of 0.09, 0.18, 0.27, 0.36, 0.45 and 0.54 vvm while $k_L a_{eff}$ for the airlift containing tap water and 10% v/v silicone rubber

beads was determined for flow rates of 0.09, 0.18, 0.27 and 0.361 vvm and k_La_{eff} for the airlift containing

tap water and 10% v/v Nylon 6,6 beads was determined for flow rates of 0.27, 0.36, 0.45 and 0.54 vvm.

The reason for k_La_{eff} to be not determined over all flow rates is due to the difficulty of fluidizing Nylon

6,6 at low flow rates arising from its slightly higher density than water. Silicone rubber was studied at

lower flow rates due to its hydrophobicity and tendency to stay at the gas-liquid interface. The k_La_{eff} and

k_La for the stirred tank system were determined at 800 rpm at 0.17, 0.25 and 0.33 vvm in all cases.

To determine k_La and k_La_{eff}, the unsteady-state method was used as described by Shuler and

Kargi, (2002). The vessel was first sparged with nitrogen gas in order to remove all oxygen from the

system then air was delivered from a 3 - hole sparger located at the bottom of the riser column. For

consistency, data between 10% and 80% of DO saturation were used for the determination of k_La and

k_La_{eff}, according to Equation 7-1,

$$OTR = \frac{dC_l}{dt} = k_La\left(C_l^* - C_l\right) \quad \textbf{or} \quad \frac{dC_l}{dt} = k_La_{eff}\left(C_l^* - C_l\right) \qquad \textbf{7-1}$$

where C_l is the DO concentration in the liquid phase (mg L^{-1}) and C_l* is the saturation concentration of

oxygen in the liquid phase (mg L^{-1}). Surface aeration effects were found to be negligible by determining

that k_La and k_La_{eff} were much larger when using sparging than without (data not shown).   Probe response

times were also found to have a negligible effect on k_La and k_La_{eff} over the flow rates used in this study,

using the method described in Section 2.4.1 wherein the probe response time constant was found to be

13.5 s.

Since airlift bioreactors have a concentration profile that is axially distributed, it must be

determined if Equation 7-1, which assumes the vessel to be well mixed, is accurate to describe k_La and

k_La_{eff} throughout an airlift vessel. Andre et al., (1983) determined k_La using a tanks-in-series model to

account for axial distribution and compared it to the k_La obtained using Equation 7-1 with a single probe

located at the bottom of the airlift vessel. It was found that if Equation 7-2 holds true, than Equation 7-1 provides an accurate estimate of the $k_L a$ determined using the tanks-in-series model,

$$k_L a \times t_c \leq 2 \quad \textbf{or} \quad k_L a_{eff} \times t_c \leq 2 \qquad \textbf{7-2}$$

where t_c is the circulation time in the airlift (s). Determination of this hydrodynamic parameter will be described in the following section. It was found that the data obtained in this study satisfied Equation 7-2, and therefore it is valid to use Equation 7-1 to determine $k_L a$ and $k_L a_{eff}$ in the airlift reactor. This assumption is consistent with other authors who have used a well-mixed model (Equation 7-1) to determine $k_L a$ in airlift vessels larger than the one in the current study (Lindert et al., 1992; Freitas and Teixeira, 2001; Guo et al., 1997).

OTR for the airlift with a single aqueous phase only was determined using Equation 7-1. For the airlift containing silicone rubber, OTR was determined based on the approach described in Section 2.4.3, which results in Equation 7-3,

$$OTR = k_L a \left(\frac{V_l}{V_p + V_l} \right) \left(C_l^* - C_l \right) \qquad \textbf{7-3}$$

where V_l is the liquid volume (L) and V_p is the polymer volume (L). For consistency in OTR determination for all runs, data between 10% and 80% of DO saturation was used. The amount of oxygen transferred to the system with and without polymers was then determined by fitting a polynomial to the OTR curve using MATLAB ®, then integrating the polynomial and multiplying the result by the working volume of the reactor.

7.4.3 Residence Time Distribution

The Residence Time Distribution (RTD) was investigated in an airlift containing tap water alone and an airlift containing tap water with 10 % v/v silicone rubber beads over inlet air flow rates of 0.09, 0.18, 0.27 and 0.36 vvm. Due to this system not being continuous inlet and outlet flow, the present analysis should more appropriately be called a circulation time distribution, however the term RTD will

be used for the remainder of the manuscript due to wide-spread use of this term. RTD experiments were undertaken using tracer experiments consisting of a 5 ml pulse injection of 99.7% pure acetic acid from Fisher Scientific (Nepean, Canada) 10 cm from the top surface of the working volume and subsequent measurement of the tracer until uniformity within the reactor was reached. Acetic acid was selected as the tracer based on tracer criteria outlined by Swaine and Daugulis, (1988). Equation 7-4 can be used to describe the RTD for a pulse injection when injection and detection are at different points in a loop reactor (Takao et al., 1982) and can be fit to the experimental tracer response curve by estimating the Peclet number, Pe,

$$\frac{C_t}{C_{t,\infty}} = \frac{1}{2}\sqrt{\frac{Pe}{\pi\theta}} \sum_{j=-\infty}^{\infty} \exp\left(-\frac{Pe(j+z^*-\theta)^2}{4\theta}\right) \qquad \textbf{7-4}$$

where;

$$Pe = \frac{U_c L}{D_{ax}} \qquad \textbf{7-5}$$

C_t is the dynamic measurement of pH, $C_{t,\infty}$ is the final pH at equilibrium, θ is the dimensionless time ($=t/t_c$), z^* is the dimensionless geometrical distance between injection and detection ($=z/L$), U_c is the mean circulation velocity (m s^{-1}), L is the mean reactor length (m), and D_{ax} is the axial dispersion coefficient (m^2 s^{-1}). The experimental data were fit to this model by minimizing the sum of squares error, which provided an estimate of Pe. RTD experimentation also allowed for the estimation of circulation time (t_c) and mixing time (t_m). The circulation time can be estimated by the graphical measurement of the time it takes between two consecutive peaks on the RTD response curve. The mixing time was determined by measuring the time it took the RTD response curve to reach equilibrium. For this study, considering pure error in pH measurement, equilibrium was reached when the normalized tracer curve reached 1 ± 0.05. It should be noted that this approach assumes equal liquid velocities in the riser and downcomer, which is valid as the areas of the riser and downcomer are approximately equal. This approach also assumes

identical dispersion coefficients in each section which may not be exact as it is known that the downcomer is considerably more plug flow than the riser (Chisti, 1989). However, this approach is deemed valid for the purposes of comparison between systems.

7.5 Results and Discussion

7.5.1 Oxygen Volumetric Mass Transfer Coefficients

Figure 7-1 shows k_La for the single phase system and k_La_{eff} for the systems containing Nylon 6,6 and silicone rubber, for both the airlift and stirred tank vessels. For all cases, k_La and k_La_{eff} increased with gas flow rate, which is a trend that has been observed for reactors with and without solids by several other authors (Giovannettone and Gulliver, 2008, Guo et al., 1997; Hwang and Lu, 1997). For both the stirred tank and airlift, relative to the single phase systems, the vessels containing silicone rubber beads had a reduced k_La_{eff} over all measured flow rates. Reduced mass transfer coefficient in stirred tank systems with second phases possessing high oxygen affinities has been observed by several authors for reactors
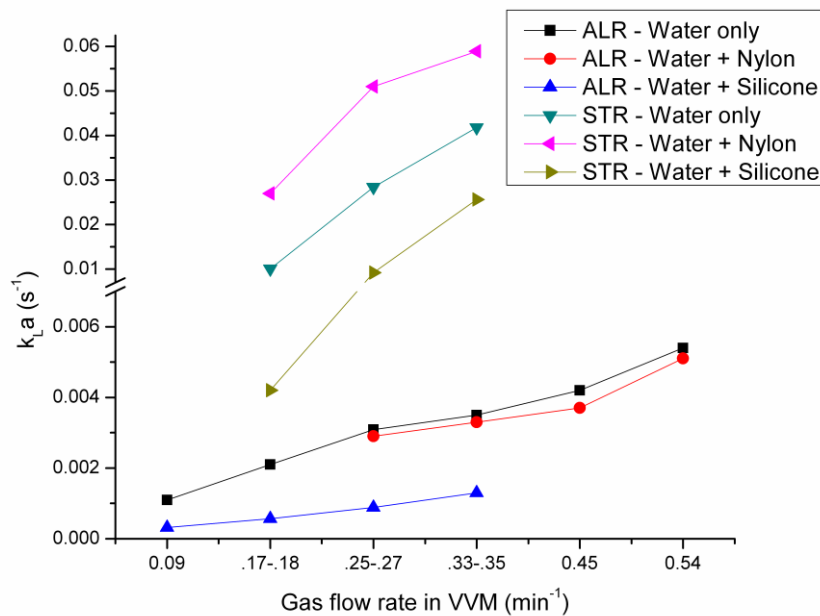
Figure 7-1: k_La and k_La_{eff} for airlift systems for a range of inlet gas flow rates

138

containing liquid phases of n-hexadecane (Nielsen et al., 2005), alkanes n-C_{12-13} (at < 800 rpm) (Clarke et al., 2006), polymer phases of silicone rubber (Chapter 2) and extendosphere particles of 55-60% SiO_2 (Sánchez et al., 2005). The observed decrease in k_La_{eff} can be attributed to the uptake of oxygen by the silicone rubber during the dynamic period of k_La_{eff} measurement. As the oxygen is absorbed by the polymer, the DO within the aqueous phase is reduced, causing the aqueous phase to take longer to reach saturation. In an aqueous-polymer or immiscible aqueous-liquid mixture, a polarographic DO probe measures the partial pressure of oxygen within the aqueous phase, which is the partial pressure of oxygen within the system. As both the aqueous and sorbent phase will have equal partial pressures at equilibrium concentrations that are not equal, the DO measurements, and therefore the k_La_{eff} measurements, will correspond only to aqueous phase concentration and will not account for the increased concentration in the working volume due to the presence of the sorbent. Therefore, a lower k_La_{eff} does not necessarily indicate that the gas-aqueous mass transfer is reduced by the presence of polymers, as the measured DO is the outcome of transfer from aqueous phase to the polymers subtracted from transfer from the gas to aqueous phase.

Figure 7-1 also shows that in the airlift Nylon 6,6 did not have a significant effect on k_La_{eff} relative to the airlift without solids, whereas the addition of Nylon 6,6 into a stirred tank caused an increase of up to 45% relative to the single phase stirred tank system. This is an interesting result, as Nylon 6,6 was previously used in Chapter 2 as an inert control in a mechanically agitated TPPB to demonstrate that the addition of polymers into the bioreactor can result in the physical enhancement of gas-liquid mass transfer by increasing k_La_{eff}. However, the results of the current study are in agreement with Lindert et al., (1992) who determined that the addition of polycarbonate beads of density 1241 kg m^{-3} and diameter 2.7 mm, which have a low affinity for oxygen, to an external loop airlift bioreactor had no significant impact on k_La_{eff} relative to a bioreactor without polymers. It is speculated that this can be attributed to the high shear environment of the stirred tank relative to the airlift, resulting in physical enhancement due to the Nylon 6,6. One mechanism that has been proposed for the physical enhancement

of k_La in bioreactors involves increased turbulence at the gas liquid interface (Zhang et al., 2006; Ruthiya et al., 2003), and turbulence in the airlift is reduced in comparison to the stirred tank at 800 rpm. The magnitude of k_La_{eff} and k_La are larger for the stirred tank compared to the airlift by 16.4, 13.4 and 20.1 times for the systems with Nylon 6,6, silicone rubber and the single phase systems, respectively, at a gas flow rate of 0.33 - 0.35 vvm (in order to be able to compare all systems). The results from Figure 7-1 help to explain the increased performance of the stirred tank TPPB in Chapter 4 compared to the airlift TPPB in Chapter 6 for the treatment of BTEX contaminated gases, as the results of the present study indicate that the polymers within the airlift TPPB did not physically enhance gas-liquid mass transfer as they did in the stirred tank and stirred tank gas-liquid mass transfer is more rapid.

The OTR, which provides a more complete measure of mass transfer from the gas phase to the reactor system by taking into account both k_La and gas-liquid driving force, is shown in Figure 7-2 for the
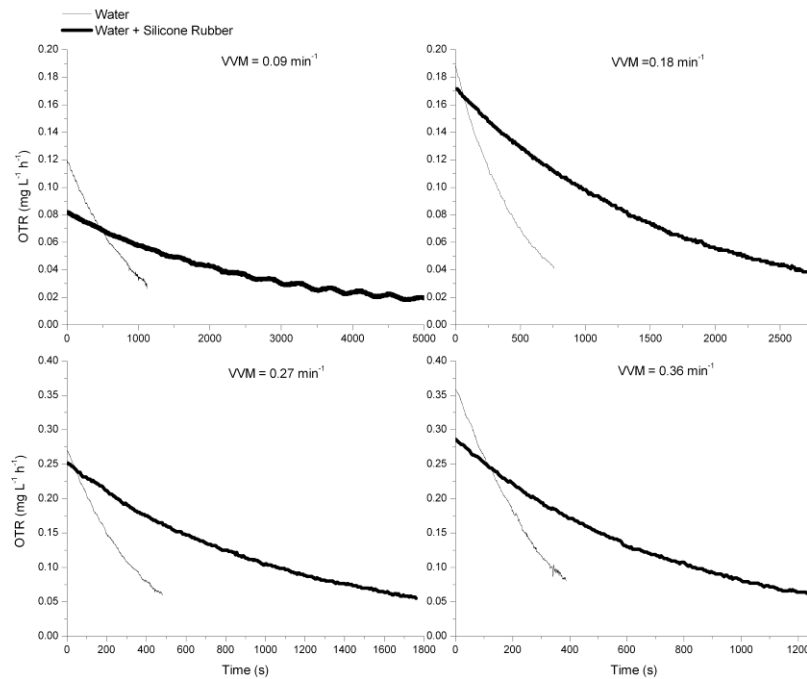
Figure 7-2: OTR for airlift reactors with and without silicone rubber from 10 to 80% DO saturation

single phase airlift case and the airlift with silicone rubber beads between 10 and 80% DO saturation. It

can be seen that the system without polymers has a larger initial instantaneous OTR compared to the

system with silicone rubber (up to 31% at t = 0), however, it takes the airlift containing silicone rubber up

to 4.5 times as long to reach 80% of DO saturation compared to the single phase case. This shows that,

although silicone rubber does not enhance the instantaneous OTR in the airlift, oxygen is being

transferred to the system for a longer period of time due to the high affinity of the silicone rubber for

oxygen. The amount of oxygen transferred to the airlift reactors between 10 and 80% of DO saturation

can be seen plotted in Figure 7-3, which shows that the airlift system with polymers contains up to 226%

more oxygen by the time that 80% DO saturation is reached in the aqueous phase. This increased oxygen

capacity in the airlift containing silicone rubber beads has a benefit for biotic systems, wherein oxygen

can be released to the cells in the aqueous phase during dynamic fluctuations that could otherwise lead to
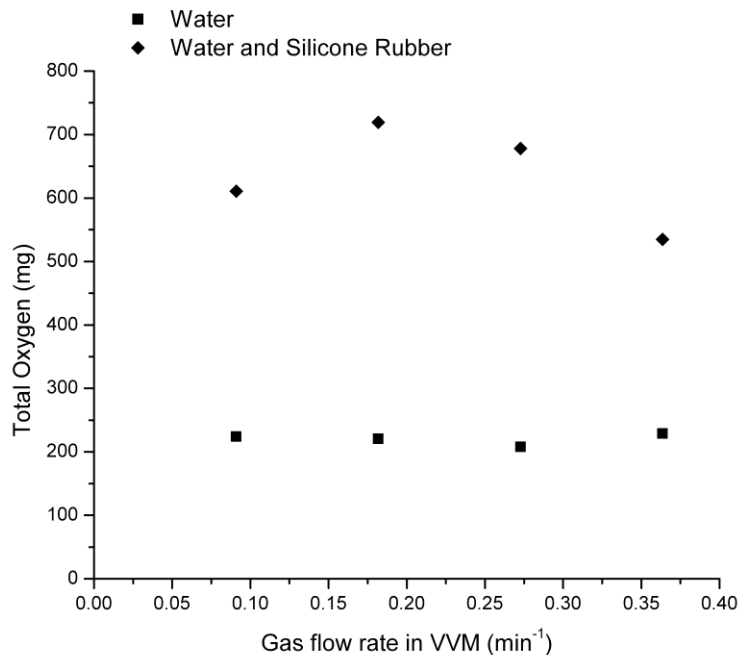
Figure 7-3: Total oxygen transferred to the airlift reactor with and without silicone rubber beads over 10 to 80% DO saturation

oxygen limitations in the system. In addition, this further validates the fact that silicone rubber takes up oxygen from the aqueous phase which reduces k_La_{eff}, as seen in Figure 7-1. It should be noted that the impact of particles on physical enhancement of gas-liquid mass transfer can be affected by particle hydrophobicity (Schumpe et al., 1987); however, in the calculations used for OTR in the current study, it has been assumed that silicone rubber has no physical enhancement effect on gas-liquid mass transfer in a similar manner to Nylon 6,6.

7.5.2 Hydrodynamics

Figure 7-4 shows Equation 7-4 fit to RTD experimental data for a flow rate of 0.09 vvm for an airlift containing a single phase of tap water and an airlift containing tap water with 10% v/v silicone rubber beads, respectively. These predictions, as well as those for all other gas flow rates tested (data not shown), fit well to the RTD experimental data, validating the use of this model to estimate airlift hydrodynamic parameters. In order to fit the experimental data to Equation 7-4, Pe was estimated for an
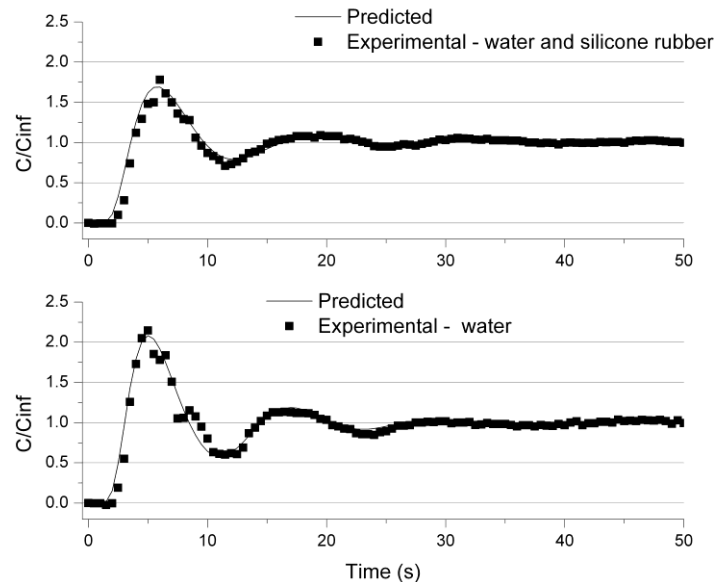
Figure 7-4: Predicted (lines) and experimental (squares) tracer response for an airlift containing tap water and silicone rubber (top) and for an airlift containing tap water (bottom)

142

airlift with and without silicone rubber beads over a range of gas flow rates, and these estimated values are shown in Figure 7-5. *Pe* is the dimensionless number, defined in Equation 7-5, which relates the extent of bulk fluid flow to the extent of dispersion within the airlift vessel. For larger *Pe,* the airlift system becomes closer to plug flow conditions and when *Pe* is smaller it indicates that the system is closer to being well-mixed. Within concentric tube airlift bioreactors, it is often assumed that the downcomer section is plug-flow (Kanai et al., 2000; Znad et al., 2004), with the riser column being more well-mixed in nature. It should be noted that this study provides an overall *Pe* for the airlift vessel, which is commonly reported in studies comparing hydrodynamic parameters in systems under different conditions (Giovannettone and Gulliver, 2008; Merchuk et al., 1998). In Figure 7-5, the *Pe* values trend upwards at higher flow rates and are larger by 60% and 12%, for the system with and without silicone rubber,
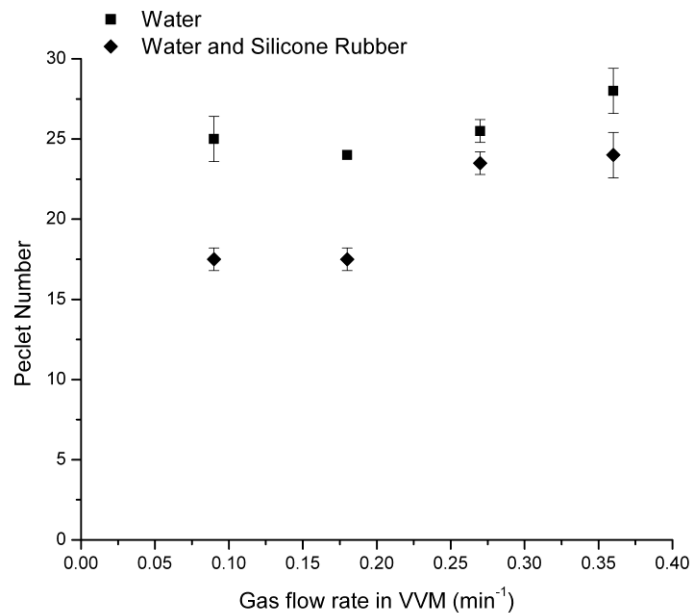
Figure 7-5: Peclet numbers for various inlet gas flow rates in an airlift without silicone rubber (squares) and an airlift containing silicone rubber (diamonds)

respectively, over the range of aeration rates employed. This trend is consistent with the literature, as it has been shown that the liquid velocity (Merchuk and Stein, 1981) as well as the axial dispersion coefficient (Giovannettone and Gulliver, 2008) will increase with increasing gas flow rate. Although these will have counteracting effects on *Pe*, in general, *Pe* increases with gas flow rate (Chisti, 1989; Sikula and Markoš, 2008). An important observation arising from Figure 7-5 is that *Pe* is larger in an airlift without silicone rubber beads than in a system with solids by up to 41%. This indicates that the addition of the polymer beads improves mixing in the airlift, as a lower *Pe* indicates that the system is closer to being well-mixed.

The RTD trace was also used to examine the impact of the addition of silicone rubber on reactor hydrodynamics over various gas flow rates, including on circulation time and mixing time. The circulation time is shown for the airlift system with and without silicone rubber beads in Figure 7-6. It
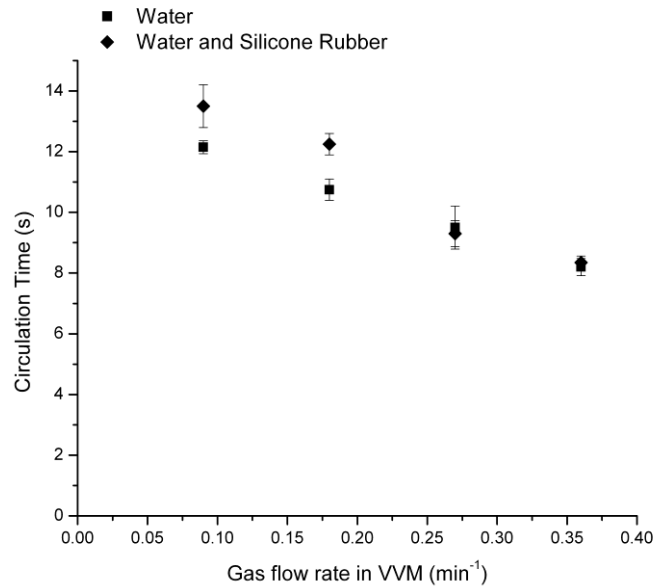
Figure 7-6: Circulation time over various inlet gas flow rates in an airlift without silicone rubber (squares) and an airlift containing silicone rubber (diamonds). Error bars represent one standard deviation.

can be seen that with increased gas flow rate, there is a decrease in circulation time due to the inlet gas inducing a faster liquid velocity for both systems. The airlift containing polymers has slightly higher circulation times (slower liquid velocities) in comparison to the single phase vessel at flow rates of 0.09 and 0.18 vvm by 11.6% and 12%, respectively, but circulation times are similar for both systems at the higher flow rates of 0.27 and 0.36 vvm. The results at lower flow rates are consistent with Guo et al., (1997) who determined that the addition of solids decreased the liquid circulation velocity for external loop airlift bioreactors containing glass beads, polystyrene and Lexan, and Lu et al., (1995), who found the addition of calcium alginate beads reduced liquid circulation velocity in an airlift. This was explained by the solids increasing the drag in the system, particularly for heavier solids. At flow rates of 0.27 and 0.36 vvm the addition of polymers gives no observable effect on circulation time (and therefore liquid velocity), which provides an interesting observation when considered with the finding for Pe for the airlift with and without solids. From Equation 7-4, at higher flow rates when liquid velocities of both systems are similar, it appears that the addition of polymers must increase axial dispersion in order to lower Pe relative to the system without polymers.

Mixing time is another hydrodynamic parameter that can be determined from RTD experimentation. Figure 7-7 displays mixing times over a range of flow rates for an airlift with and without silicone rubber beads. These data show that t_m decreases with increased gas flow rate, which is an observation that has been reported by other authors (Ganzeveld et al., 1995, Freitas and Teixeira, 1998) and is due to increased gas flow rates causing increased turbulence within the reactor. Figure 7-7 also shows that the addition of silicone rubber reduces t_m by up to 33%, and therefore improves mixing efficiency, compared to an airlift without silicone rubber beads. In contrast to the current study, several studies that have observed a decrease in mixing with the addition of solids relative to a system without solids (Sharp et al., 1998, Fretias and Teixeira, 1998), which may be attributed to the difference in solid properties between studies. The oxygen mass transfer and hydrodynamic parameters determined in this study show that the addition of silicone rubber into an airlift vessel does increase mixing of the bulk

145
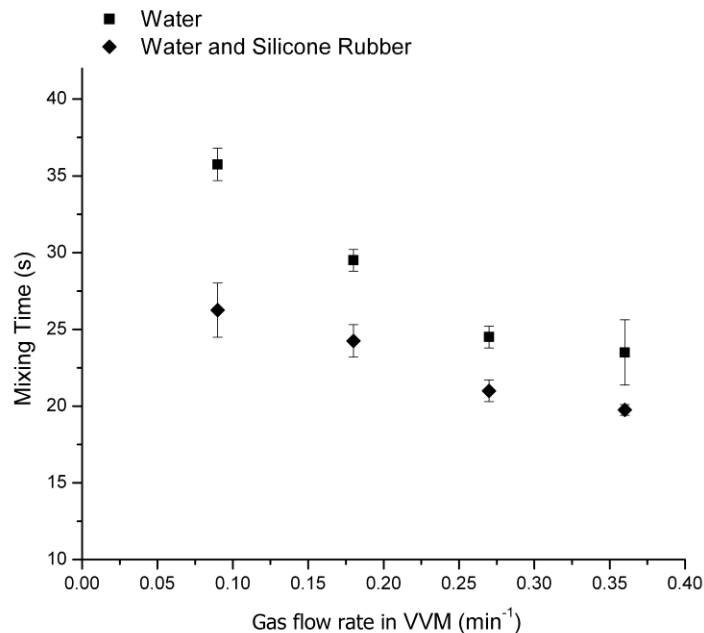
Figure 7-7: Mixing time over various inlet gas flow rates in an airlift without silicone rubber (squares) and an airlift containing silicone rubber (diamonds). Error bars represent one standard deviation.

aqueous phase, but does not provide physical enhancement (interactions with boundary layers or bubble size) of gas-liquid mass transfer. This provides an explanation for previous work that noted reduced performance and oxygen limitations in the airlift TPPB in Chapter 6 relative to the stirred tank TPPB in Chapter 4 for the treatment of a BTEX contaminated gas stream. However, the addition of polymers can help to relieve oxygen limitations in such bioreactors, as oxygen has been shown to be taken up by the silicone rubber during dynamic periods, which can be released back to the aqueous phase. It should be noted that the effectiveness of these polymers to overcome oxygen limitations depends on the timescale of system dynamics, such as microbial demand and feed fluctuations. The mass transfer and hydrodynamic phenomena associated with the airlift TPPB characterized in this study, are currently being used to estimate parameters for modeling the airlift TPPB for the treatment of BTEX contaminated gas streams.

7.6 Conclusions

It was determined in this study that the addition of silicone rubber beads to an airlift vessel reduced the k_La_{eff} relative to a system without polymers due to the uptake of oxygen by the polymers possessing high oxygen affinity during the dynamic period of measurement. Using Nylon 6,6 as an inert control, it was determined that the addition of polymers likely has no physical enhancement on the gas-liquid mass transfer coefficient. OTRs for the airlift with and without silicone rubber showed that, although the airlift without polymers had a larger initial OTR, the system containing silicone rubber had an overall larger mass of oxygen transferred to its working volume. This suggests polymers with a high affinity for oxygen within an airlift bioreactor will deliver oxygen to the aqueous phase during dynamic substrate loadings based on microbial demand. Hydrodynamic parameters from RTD experiments showed that the addition of silicone rubber beads into an airlift vessel enhanced liquid phase mixing, as the Pe, and t_m were lower relative to a system without polymer beads. In addition, t_c was slightly lower for the system containing silicone rubber beads at lower gas flow rates. The data obtained in this study have provided characterization of a unique three-phase airlift system and useful parameters for use in mathematical models currently under development.

Chapter 8

Model for a Solid-Liquid Two-Phase Partitioning Bioscrubber for the Treatment of BTEX

Jennifer V. Littlejohns, Kim B. McAuley, Andrew J. Daugulis

8.1 Preface to Chapter 8

In previous chapters, this thesis has characterized the stirred-tank SL-TPPB via experimentation and mathematical modeling, and the airlift SL-TPPB via experimentation. In this chapter, a steady-state mathematical model for the airlift SL-TPPB is developed to further characterize the system for the treatment of BTEX. It was determined during experimental investigation in Chapter 6 that the airlift SL-TPPB experienced operating regions that resulted in decreased performance for the treatment of BTEX due to oxygen and/or BTEX mass transfer limitations. Therefore, the model developed in this chapter allows for the prediction of performance of the airlift SL-TPPB under steady-state operation over various BTEX loadings and inlet gas flow rates to identify operating conditions that result in the most favorable performance.

As the concentration profile of BTEX components in each phase in an airlift vessel is axially distributed, a tanks-in-series model is used to describe the level of mixing in the airlift SL-TPPB, and the model framework for each well-mixed tank is obtained from the stirred-tank SL-TPPB model developed in Chapter 5. In addition, many of the parameter values and estimates for the stirred tank model in Chapter 5 are used in the airlift model in this chapter, including kinetic parameters and liquid-polymer mass transfer coefficients. Several of the parameter values used in this model are also obtained from Chapter 7, including the appropriate number of tanks-in-series that describes the level of mixing in the airlift SL-TPPB. The implications of this chapter are that the developed airlift SL-TPPB model can predict performance under operating regions that result in improved BTEX and oxygen mass transfer, as well as oxygen and BTEX mass transfer limitations, with reasonable accuracy.

8.2 Abstract

A steady-state mathematical model was developed to predict performance of an airlift solid-liquid two-phase partitioning bioreactor (SL-TPPB) for the treatment of a gas stream containing benzene, toluene, ethylbenzene and o-xylene (BTEX). The airlift SL-TPPB is a low-energy input system that utilizes a sequestering phase of solid silicone rubber beads (10%v/v) that will uptake and release large amounts of BTEX according to maintaining equilibrium conditions. This increases mass transfer out of the gas phase during dynamic loading periods and improves system performance. The model was developed from mass balances on gas, aqueous and polymer phases for each BTEX component and oxygen, and consisted of a tanks-in-series model, to represent the axial distribution in concentration profiles. An estimability analysis was performed on the model parameters and those that were found to be most influential on model predictions were estimated using experimental airlift SL-TPPB data. The developed tanks-in-series model was able to predict the removal efficiency (RE) and elimination capacity (EC) of BTEX components and dissolved oxygen concentrations over various inlet loadings (20, 60 and 100 mg L^{-1} h^{-1}) and gas flow rates (2, 3 and 4 L min^{-1}) that resulted in a range of system performance from effective BTEX treatment to oxygen limiting conditions. It was also predicted that the riser section removed the largest percent fraction of total BTEX within the airlift.

Keywords: Airlift; BTEX; Bioreactor; Tanks-in-series Model; Parameter Estimation

8.3 Introduction

Airlift bioscrubbers provide an energy efficient alternative to stirred tank bioscrubbers for the treatment of VOC laden gas streams. However, sufficient mass transfer from the gas phase is a concern for both tank configurations due to low solubility of oxygen and potential low solubility of VOCs in water. In particular, oxygen mass transfer of airlift reactors is often slower than in stirred tanks agitated above 400 rpm (Fontana et al., 2009; Chapter 7). Chapter 6 investigated an airlift system for the treatment of benzene, toluene, ethylbenzene and o-xylene (BTEX) that contained a second suspended phase of solid silicone rubber beads (10% v/v) with a high affinity for BTEX, called the airlift solid-liquid two-phase partitioning bioreactor (SL-TPPB). The silicone rubber beads served to uptake excess BTEX from the cell containing aqueous phase during increased loading fluctuations which was released back to the aqueous phase according to metabolic demand and maintaining equilibrium conditions. This effectively dampened inlet loading fluctuations by increasing mass transfer from the gas phase, and therefore improved performance, relative to an airlift without a silicone rubber phase. However, it was observed that during operation of the airlift SL-TPPB, oxygen and/or BTEX mass transfer was rate limiting. This prompted investigation of the steady state performance of the airlift SL-TPPB under various operating conditions (inlet loadings and gas flow rates) in the form of a 3^2 factorial experimental design to identify regions of operating conditions that resulted in increased performance of the system. Using the data provided by the steady-state experimental investigation of the airlift SL-TPPB, the current study describes the development and application of a steady-state mathematical model for the airlift SL-TPPB in order to quantify the observed phenomena and provide a tool to predict performance under various operating conditions.

To model airlift systems, wherein the flow regime lies between the two extremes of perfectly mixed and plug flow (Swaine and Daugulis, 1988) causing concentration profiles to vary axially, there are two modeling techniques that are commonly used. The first is the axial dispersion model (Jia et al., 2006; Nikakhtari and Hill, 2006; Sikula and Markoš, 2008) that is based on a one dimensional Fick's Law type

of equation that was developed to describe mixing that slightly deviates from plug flow (Turner and Mills, 1990). The second, more commonly used model, is the tanks-in-series model wherein the number of well-mixed tanks-in-series used to model the system, *N*, describes the level of mixing in the vessel; a higher number of tanks being closer to plug flow and a lower number of tanks in series being closer to well-mixed conditions (Kanai et al., 2000; Sikula et al., 2006; Znad et al., 2004). Tanks-in-series mixing has been shown to provide more accurate predictions in comparison to axial dispersion model when system hydrodynamics are closer to perfectly well-mixed and is easier to numerically compute (Abu-Reesh and Abu-Sharkh, 2003; Turner and Mills, 1990) and was therefore be the modeling strategy used in this study. Furthermore, as a well-mixed stirred tank SL-TPPB has previously been modeled for the treatment of BTEX in Chapter 5, the framework for each tank-in-series and preliminary parameter estimation have been completed.

This study describes the development of a steady-state model for an 11 L airlift SL-TPPB for the treatment of BTEX that was experimentally investigated by in Chapter 6. Performance indicators (removal efficiency and elimination capacity) were predicted over various loadings and inlet gas flow rates. An estimability analysis of model parameters was completed in order to identify the parameters to which output is most sensitive. Experimental data was used to assess model accuracy and to estimate the parameters that were most sensitive in order to improve model predictions.

8.4 System Description

A schematic of the airlift SL-TPPB used in Chapter 6, which is modeled in the current study, can be seen in Figure 8-1. In this system, the gas stream containing BTEX is delivered into the vessel below the riser column. The gas bubbles travel up the riser column, transferring BTEX to the liquid phase containing the bacterial consortium. BTEX from the liquid also partitions into the polymer phase. The mixture of the aqueous phase and polymer particles moves downwards in the downcomer column.
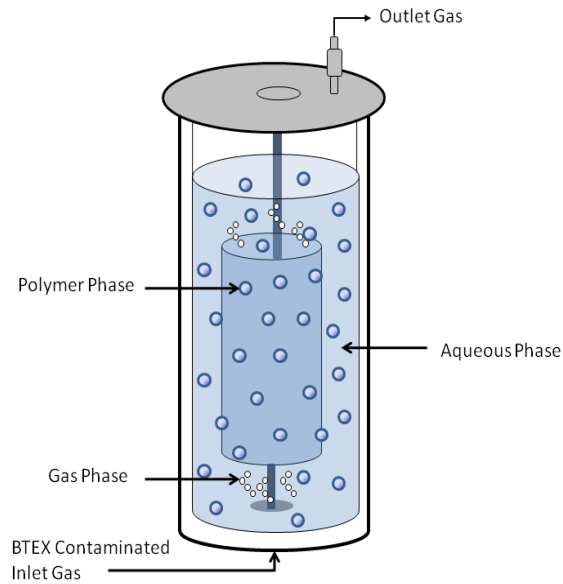
Figure 8-1: Schematic of the 11 L airlift two-phase partitioning bioscrubber containing silicone rubber polymers (10% v/v) and BTEX degrading bacterial consortium

8.5 Airlift Conceptualization

Previous hydrodynamic characterization of the airlift SL-TPPB using a residence time distribution analysis determined the Peclet numbers (*Pe*) over a range of inlet gas flow rates, which were used to determine the number of tanks-in-series, *N*, from the following correlation (Swaine and Daugulis, 1988; Znad et al., 2004);

$$N = \frac{Pe}{2}$$

8-1

This correlation provides an estimate of the number of tanks-in-series that represent mixing with an inlet flow rate of 2, 3 and 4 L min^{-1} to be 9, 11 and 11, respectively. However, it is known that the downcomer section in airlift systems is nearly plug flow relative to the riser, and has been represented as 10 tanks-in-series by other authors in studies of airlifts of similar size as that used in the current study (Kanai et al., 2000; Znad et al., 2004). It has been stated that the number of tanks-series does not have a strong effect on simulation results (Sikula et al., 2006), and therefore, the number of tanks-in-series used to represent
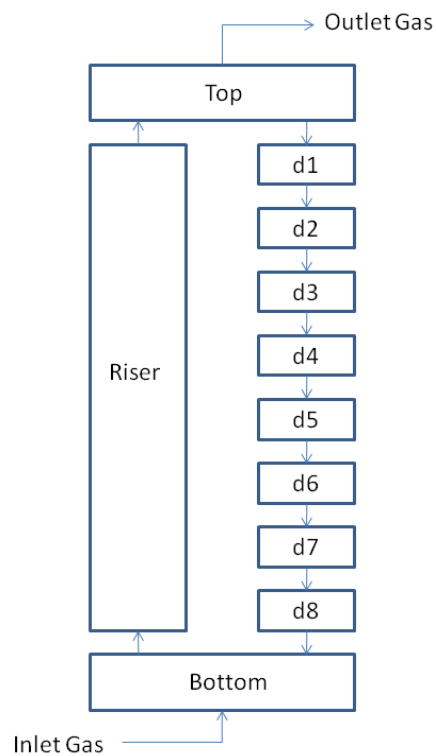
Figure 8-2: Representation of the 11 L SL-TPPB using tanks-in-series to describe mixing for model development

all flow rates was selected to be 11. These 11 well-mixed tanks were distributed as shown in Figure 8-2: one as the bottom, one as the riser, one as the top and the remaining eight to represent plug flow in the downcomer section.

8.6 Model Development

The model for the airlift SL-TPPB was developed using the following key assumptions;

1. Mixing within the airlift in each phase can be described using tanks-in-series model

2. BTEX is transferred from the gas phase to the aqueous phase, and from the aqueous phase to the polymer phase (Kars et al., 1997). Direct transfer between the gas-phase and the polymer is neglected.

3. The biomass is distributed throughout the liquid, is constant throughout the reactor and consumes BTEX only from the aqueous phase.

4. All polymer beads are spherical and are the same size.

5. Diffusion coefficients of BTEX in polymer are constant.

6. Constant partition coefficients describe equilibrium between the liquid and polymer phases. Henry's law describes equilibrium between the gas and liquid phases.

7. Substrate toxicity can be described using the model by Luong, (1987).

8. Substrate interactions can be described using the model developed in Chapter 3.

9. The specific growth rate has a dependence on oxygen concentrations according to the model by Bailey and Ollis, (1986).

10. A lumped overall mass-transfer coefficient can describe mass transfer from liquid to polymer phases.

11. The resistance to mass transfer in the gas phase and microbial cell walls is negligible.

12. Mass transfer of BTEX to/from the headspace to/from the liquid is negligible.

13. Temperature and pH are constant.

14. Polymers have the same circulation velocity as the liquid phase.

15. Polymers do not affect gas-hold up in the reactor.

16. Liquid flow rate is constant in each section of the airlift.

Table 8-1 lists the steady-state equations developed from mass balances that are used to describe the concentrations of BTEX components and oxygen in the gas (Equations 8-2 to 8-6), aqueous (Equations 8-7 to 8-11) and polymer (Equations 8-12 to 8-16) phases in each CSTR within the airlift SL-TPPB. Biomass concentrations were treated as a model input in order to simplify the system. Although aqueous phase and polymer phase equations were developed to complete the set of equations, these were not used in the objective function or to estimate parameters, as aqueous and polymer phase concentrations were not measured experimentally.

Table 8-1: List of Equations for Airlift SL-TPPB Model

Gas-Phase Balances

Bottom section

$$F_{g,in}\frac{C_{i,in}}{V_{b,g}} + F_{g,d}\frac{C_{i,d8,g}}{V_{b,g}} - k_L a_i\left(C^*_{i,in,gl} - C_{i,b,l}\right)\frac{V_{b,l}}{V_{b,g}} - k_L a_i\left(C^*_{i,d8,gl} - C_{i,b,l}\right)\frac{V_{b,l}}{V_{b,g}} - F_{g,r}\frac{C_{i,b,g}}{V_{b,g}} = 0$$

8-2

Top section

$$F_{g,r}\frac{C_{i,r,g}}{V_{t,g}} - k_L a_i\left(C^*_{i,r,gl} - C_{i,t,l}\right)\frac{V_{t,l}}{V_{t,g}} - F_{g,d}\frac{C_{t,g}}{V_{t,g}} - \left(F_{g,r} - F_{g,d}\right)\frac{C_{i,t,g}}{V_{t,g}} = 0$$

8-3

Riser section

$$F_{g,r}\frac{C_{i,b,g}}{V_{r,g}} - k_L a_i\left(C^*_{i,b,gl} - C_{i,r,l}\right)\frac{V_{r,l}}{V_{r,g}} - F_{g,r}\frac{C_{i,r,g}}{V_{r,g}} = 0$$

8-4

Downcomer section #1

$$F_{g,d}\frac{C_{i,t,g}}{V_{d1,g}} - k_L a_i\left(C^*_{i,t,gl} - C_{i,d1,l}\right)\frac{V_{d1,l}}{V_{d1,g}} - F_{g,d}\frac{C_{i,d1,g}}{V_{d1,g}} = 0$$

8-5

Downcomer section z
Z = 2 to 8

$$F_{g,d}\frac{C_{i,d_{Z-1},g}}{V_{d1,g}} - k_L a_i\left(C^*_{i,dz-1,gl} - C_{i,dz,l}\right)\frac{V_{d1,l}}{V_{d1,g}} - F_{g,d}\frac{C_{i,d_Z,g}}{V_{d1,g}} = 0$$

8-6

Liquid-Phase Balances

Bottom section

$$k_L a_i\left(C^*_{i,in,gl} - C_{i,b,l}\right) + k_L a_i\left(C^*_{i,d8,gl} - C_{i,b,l}\right) + F_l\frac{C_{i,d8,l}}{V_{b,l}} - F_l\frac{C_{i,b,l}}{V_{b,l}} - \frac{3k_{O,i}}{R_p}\left(C_{i,b,l} - C^*_{i,b,lp}\right) - r_i = 0$$

8-7

Top section

$$F_l\frac{C_{i,r,l}}{V_{t,l}} - F_l\frac{C_{i,t,l}}{V_{t,l}} + k_L a_i\left(C^*_{i,r,gl} - C_{i,t,l}\right)\frac{1}{V_{t,l}} - \frac{3k_{O,i}}{R_p}\left(C_{i,t,l} - C^*_{i,t,lp}\right) - r_i = 0$$

8-8

Riser section

$$F_l\frac{C_{i,b,l}}{V_{r,l}} - F_l\frac{C_{i,r,l}}{V_{r,l}} + k_L a_i\left(C^*_{i,b,gl} - C_{i,r,l}\right) - \frac{3k_{O,i}}{R_p}\left(C_{i,r,l} - C^*_{i,r,lp}\right) - r_i = 0$$

8-9

Downcomer section #1

$$F_l\frac{C_{i,t,l}}{V_{d1,l}} - F_l\frac{C_{i,d1,l}}{V_{d1,l}} + k_L a_i\left(C^*_{i,t,gl} - C_{i,d1,l}\right) - \frac{3k_{O,i}}{R_p}\left(C_{i,d1,l} - C^*_{i,d1,lp}\right) - r_i = 0$$

8-10

Downcomer section z
Z = 2 to 8

$$F_l\frac{C_{i,dz-1,l}}{V_{d1,l}} - F_l\frac{C_{i,dz,l}}{V_{d1,l}} + k_L a_i\left(C^*_{i,dz-1,gl} - C_{i,dz,l}\right) - \frac{3k_{O,i}}{R_p}\left(C_{i,dz,l} - C^*_{i,dz,lp}\right) - r_i = 0$$

8-11

Polymer-Phase Balances

Bottom section

$$F_p\frac{C_{i,d8,p}}{V_{b,p}} - F_p\frac{C_{i,b,p}}{V_{b,p}} + \frac{3k_{O,i}}{R_p}\left(C_{i,b,l} - C^*_{i,b,lp}\right)\frac{V_{b,l}}{V_{b,p}} = 0$$

8-12

Top section

$$F_p\frac{C_{i,r,p}}{V_{t,p}} - F_p\frac{C_{i,t,p}}{V_{t,p}} + \frac{3k_{O,i}}{R_p}\left(C_{i,t,l} - C^*_{i,t,lp}\right)\frac{V_{t,l}}{V_{t,p}} = 0$$

8-13

Riser section

$$F_p\frac{C_{i,b,p}}{V_{r,p}} - F_p\frac{C_{i,r,p}}{V_{r,p}} + \frac{3k_{O,i}}{R_p}\left(C_{i,r,l} - C^*_{i,r,lp}\right)\frac{V_{r,l}}{V_{r,p}} = 0$$

8-14

Downcomer section #1

$$F_p\frac{C_{i,t,p}}{V_{d1,p}} - F_p\frac{C_{i,d1,p}}{V_{d1,p}} + \frac{3k_{O,i}}{R_p}\left(C_{i,d1,l} - C^*_{i,d1,lp}\right)\frac{V_{d1,l}}{V_{d1,p}} = 0$$

8-15

Downcomer section Z
Z = 2 to 8

$$F_p\frac{C_{i,d_{z-1},p}}{V_{d_1,p}} - F_p\frac{C_{i,d_Z,p}}{V_{d_1,p}} + \frac{3k_{O,i}}{R_p}\left(C_{i,d_z,l} - C^*_{i,d_z,lp}\right)\frac{V_{d_1,l}}{V_{d_1,p}} = 0$$

8-16

Table 8-2 contains thermodynamic and kinetic expressions that were substituted into the primary equations listed in Table 8-1. The thermodynamic expressions that are used to determine concentrations in the aqueous phase in equilibrium with the gas phase and the polymer phase are listed as Equations 8-17 and 8-18, respectively, in Table 8-2. Kinetic expressions that were developed in Chapter 3 were combined with models to account for substrate toxicity (Luong, 1987) and oxygen limitations (Bailey and Ollis, 1997), and are shown in Table 8-2 as Equations 8-19, 8-20, 8-21 and 8-22 for benzene, toluene, ethylbenzene and o-xylene, respectively. In addition, an expression for oxygen consumption by biomass is shown as Equation 8-23. Performance indicators, which are the focus of this study, include elimination capacity (Equation 8-24) and removal efficiency (Equation 8-25) and are shown in Table 8-2, which are functions of the predicted BTEX concentrations in the outlet gas, and were the outputs modeled in this work.

8.7 Parameter Values and Model Inputs

Parameters values and model inputs were obtained directly from literature values and from empirical correlations that utilize literature values and/or physical dimensions of the system components. Those parameter values and model inputs that were obtained from correlations will be described in more detail below. A list of all parameter values and their origin can be seen in Table 8-3, and a list of all model input values, all of which were a function of gas flow rate, can be seen in Table 8-4.

8.7.1 Correlations for Parameter Values

The correlations used in this study to determine parameter values utilized estimates from literature and/or dimensions of system components, and allowed for the determination of volumetric mass transfer coefficients for BTEX over various inlet gas flow rates ($k_L a_{B,FR\#}$, $k_L a_{T,FR\#}$, $k_L a_{E,FR\#}$, $k_L a_{X,FR\#}$), the overall mass transfer coefficient for oxygen, $k_{o,O}$ and the oxygen growth yield, $Y_{X/O}$.

Table 8-2: Thermodynamic and Kinetic Expressions

Equilibrium Expressions

$$C^*_{i,\sec,gl} = \frac{C_{i,\sec,g}}{H_{lg}}$$

8-17

$$C^*_{i,\sec,lp} = \frac{C_{i,\sec,p}}{K_{lp}}$$

8-18

Kinetic Expressions

$$r_{B,\sec} = \frac{\dfrac{\mu_{\max,B} C_{B,\sec c,l}}{\left(K_{s,B} + C_{B,\sec,l}\right) + I_{T,B} C_{T,\sec,l} + I_{X,B} C_{X,\sec,l}} \left(1 - \dfrac{C_{B,\sec,l}}{C_{B,INH}}\right) X_{\sec}}{Y_{X/B}} \left(\frac{C_{O,\sec,l}}{K_{c,B} + C_{O,\sec,l}}\right)$$

8-19

$$r_{T,\sec} = \frac{\dfrac{\mu_{\max,T} C_{T,\sec,l}}{\left(K_{s,T} + C_{T,\sec,l}\right) + I_{B,T} C_{T,\sec,l}} \left(1 - \dfrac{C_{T,\sec,l}}{C_{T,INH}}\right) X_{\sec}}{Y_{X/T}} \left(\frac{C_{O,\sec,l}}{K_{c,T} + C_{O,\sec,l}}\right)$$

8-20

$$r_{E,\sec} = \frac{\dfrac{\mu_{\max,E} C_{E,\sec,l}}{\left(K_{s,E} + C_{E,\sec,l}\right)} \left(1 - \dfrac{C_{E,\sec,l}}{C_{E,INH}}\right) X_{\sec}}{Y_{X/E}} \left(\frac{C_{O,\sec,l}}{K_{c,E} + C_{O,\sec,l}}\right)$$

8-21

$$r_{X,\sec} = \left(T_B^X\left(\frac{dC_{B,\sec,l}}{dt}\left(\frac{1}{X_{\sec}}\right)\right)\right)\left(\frac{C_{X,\sec,l}}{K_{s,X} + C_{X,\sec,l}}\right) X_{\sec}$$
$$+ \left(T_T^X\left(\frac{dC_{T,\sec,l}}{dt}\left(\frac{1}{X_{\sec}}\right)\right)\right)\left(\frac{C_{X,\sec,l}}{K_{s,X} + C_{X,\sec,l}}\right) X_{\sec}$$

8-22

$$r_{O,\sec} = \frac{\left(r_{B,\sec} Y_{X/B} + r_{T,\sec} Y_{X/T} + r_{E,\sec} Y_{X/E}\right)}{Y_{X/O}}$$

8-23

Key Performance Indicators

$$EC = \frac{F_g\left(C_{i,in} - C_{i,t,g}\right)}{V_{total}}$$

8-24

$$RE = \frac{\left(C_{i,in} - C_{i,t,g}\right)}{C_{i,in}} \times 100\%$$

8-25

Table 8-3: Initial Parameter Values for Airlift SL-TPPB Model

Parameter	Values			Unit	S_Θ	Method of Determination
	Flow 1	Flow 2	Flow 3			
$k_L a_B$	0.00069	0.001	0.0013	s^{-1}	0.00264	Shown in Current Chapter
$k_L a_T$	0.00061	0.00089	0.0012	s^{-1}	0.00232	Shown in Current Chapter
$k_L a_E$	0.00057	0.00083	0.0011	s^{-1}	0.00216	Shown in Current Chapter
$k_L a_X$	0.00057	0.00083	0.0011	s^{-1}	0.00216	Shown in Current Chapter
$k_L a_O$	0.002	0.003	0.004	s^{-1}	0.0005	Chapter 7
K_B	62			mg L^{-1} solid L mg^{-1} aqueous	2.88	Chapter 4
K_T	200			mg L^{-1} solid L mg^{-1} aqueous	19.5	Chapter 4
K_E	414			mg L^{-1} solid L mg^{-1} aqueous	153.08	Chapter 4
K_X	593			mg L^{-1} solid L mg^{-1} aqueous	86.4	Chapter 4
K_O	10			mg L^{-1} solid L mg^{-1} aqueous	2	Shiku et al., 2006
H_B	0.26			mg L^{-1} gas L mg^{-1} aqueous	0.04	Chapter 4
H_T	0.22			mg L^{-1} gas L mg^{-1} aqueous	0.02	Chapter 5
H_E	0.43			mg L^{-1} gas L mg^{-1} aqueous	0.02	Chapter 4
H_X	0.25			mg L^{-1} gas L mg^{-1} aqueous	0.03	Chapter 4
H_O	34.17			mg L^{-1} gas L mg^{-1} aqueous	2	Sandler, 1999
$K_{o,B}$	1.05 E-8			$m\ s^{-1}$	1.837E-06	Chapter 5
$K_{o,T}$	9.3 E-9			$m\ s^{-1}$	1.6362E-06	Chapter 5
$K_{o,E}$	8.5 E-9			$m\ s^{-1}$	1.4822E-06	Chapter 5
$K_{o,X}$	1.4 E-7			$m\ s^{-1}$	1.4822E-06	Chapter 5
$K_{o,O}$	3.06 E-8			$m\ s^{-1}$	3.06E-6	Shown in Current Chapter
$\mu_{max,B}$	0.000061			s^{-1}	0.0018	Chapter 5
$\mu_{max,T}$	0.000032			s^{-1}	0.0023	Chapter 5
$\mu_{max,E}$	0.0000036			s^{-1}	0.006	Chapter 5
$K_{s,B}$	27.57			mg L^{-1}	11.01	Chapter 3
$K_{s,T}$	34.12			mg L^{-1}	12.12	Chapter 3
$K_{s,E}$	0.36			mg L^{-1}	1.76	Chapter 3
$K_{s,X}$	0.0054			mg L^{-1}	10	Chapter 5
$I_{T,B}$	2			-	0.5	Chapter 3
$I_{X,B}$	-0.7			-	0.5	Chapter 3
$I_{B,T}$	-0.4			-	0.5	Chapter 3
$I_{E,B}$	4			-	0.5	Chapter 3
$C_{B,INH}$	20			mg L^{-1}	15	Abuhamed et al., 2004
$C_{T,INH}$	20			mg L^{-1}	15	Abuhamed et al., 2004
$C_{E,INH}$	35			mg L^{-1}	15	Estimated from Abuhamed et al., 2004
$C_{X,INH}$	35			mg L^{-1}	15	Estimated from Abuhamed et al., 2004
$Y_{X/B}$	1.35			mg mg^{-1}	0.27	Chapter 3

$Y_{X/T}$	1.25	mg mg^{-1}		0.25	Chapter 3
$Y_{X/E}$	0.85	mg mg^{-1}		0.17	Chapter 3
$Y_{X/O}$	0.94	mg mg^{-1}		0.2	Shown in Current Chapter
T_B^X	0.5	-		0.1	Chapter 3
T_T^X	0.5	-		0.1	Chapter 3
k_d	2.5E-6	s^{-1}		0.000001	Chapter 5
$K_{C,B}$	0.5	mg L^{-1}		0.2	Bailey and Ollis, 1997
$K_{C,T}$	0.5	mg L^{-1}		0.2	Bailey and Ollis, 1997
$K_{C,X}$	0.5	mg L^{-1}		0.2	Bailey and Ollis, 1997

Table 8-4: Input Values for Airlift SL-TPPB Model

Input	Value			Unit	Method of Estimation
	Flow 1	Flow 2	Flow 3		
$C_{in,i,L20}$	0.46	0.31	0.23	mg L^{-1}	Measured
$C_{in,i,L60}$	1.37	0.92	0.69	mg L^{-1}	Measured
$C_{in,i,L100}$	2.29	1.52	1.15	mg L^{-1}	Measured
X_{L20}	1140	1420	1800	mg L^{-1}	Measured
X_{L60}	1500	1920	2400	mg L^{-1}	Measured
X_{L100}	1600	2960	2670	mg L^{-1}	Measured
F_l	0.368	0.482	0.535	L s^{-1}	Current Study
F_p	0.042	0.055	0.061	Ls^{-1}	Current Study
$F_{g,in}$	0.0333	0.05	0.0667	L s^{-1}	Measured
$F_{g,r}$	0.04	0.061	0.081	L s^{-1}	Current Study
$F_{g,d}$ *(for d1 to d8)*	0.0071	0.011	0.015	L s^{-1}	Current Study
$V_{l,b}$	0.573	0.571	0.569	L	Current Study
$V_{l,t}$	1.84	1.88	1.91	L	Current Study
$V_{l,r}$	3.67	3.65	3.64	L	Current Study
$V_{p,d}$	0.0544	0.0542	0.054	L	Current Study
$V_{g,b}$	0.0129	0.0158	0.0183	L	Current Study
$V_{g,t}$	0.0417	0.0425	0.0432	L	Current Study
$V_{g,r}$	0.08	0.10	0.12	L	Current Study
$V_{g,d}$	0.0098	0.012	0.014	L	Current Study

8.7.1.1 Volumetric Mass Transfer Coefficients for BTEX over Various Inlet Gas Flow Rates, $k_L a_{B,FR\#}$, $k_L a_{T,FR\#}$, $k_L a_{E,FR\#}$, $k_L a_{X,FR\#}$

      Volumetric mass transfer coefficients are a function of inlet gas flow rate, which is an operating condition that is varied in this study. Therefore, volumetric mass transfer coefficients for BTEX were determined for each flow rate used. To determine volumetric mass transfer coefficients for BTEX in the airlift reactor, volumetric mass transfer coefficients for oxygen over flow rates of 2, 3 and 4 L min^{-1} previously determined in Chapter 7 in an airlift SL-TPPB were utilized in Equation 8-26 (Metcalf and Eddy, 1991).

$$k_L a_{i,FR\#} = \psi \cdot k_L a_{O,FR\#} \qquad\qquad \textbf{8-26}$$

The parameter ψ was estimated using Equation 8-27 (Nielsen and Villadsen, 1994).

$$\psi = {D_i}/{D_O} \qquad\qquad \textbf{8-27}$$

Diffusion coefficients used in Equation 8-27 for oxygen and BTEX in water at 30 °C are $3.51 \cdot 10^{-5}$, 1.17×10^{-5}, 1.03×10^{-5}, 9.33×10^{-6} and 9.33×10^{-6} cm^2 s^{-1}, respectively (EPA, 2006e).

8.7.1.2 Overall Oxygen Mass Transfer Coefficient, $k_{o,O}$

      The overall mass transfer coefficient for BTEX between aqueous and polymer phases must consider both aqueous and polymer resistances to mass transfer. The overall mass transfer coefficient was calculated using Equation 8-28 (Ma et al., 2002).

$$\frac{1}{k_{O,i}} = \frac{1}{K_i k_{p,i}} + \frac{1}{k_{l,i}} \qquad\qquad \textbf{8-28}$$

In order to determine mass transfer coefficients on the liquid and polymer sides, semi-empirical equations can be used which are shown as Equation 8-29 (Ma et al., 2002) and Equation 8-30, respectively (Yao et al., 2003).

$$k_{l,i} = \frac{D_{O,l}}{R_p} \qquad\qquad \text{8-29}$$

$$k_{p,i} = \frac{D_{O,p}\pi^2}{2R} \qquad\qquad \text{8-30}$$

The diffusivity of oxygen in silicone rubber is 3.4×10^{-5} cm^2 s^{-1} (Merkel et al., 2000).

8.7.1.3 Oxygen Growth Yield, $Y_{X/O}$

The oxygen growth yield can be estimated using the correlation developed by Mateles, (1971), shown as Equation 8-31.

$$Y_{X/O} = \left[16\left(\frac{2Q_C + Q_H/2 - Q_O}{Y_{X/i} \cdot M} + \frac{Q_O'}{1600} - \frac{Q_C'}{600} + \frac{Q_{Nit}'}{933} - \frac{Q_H'}{200} \right) \right]^{-1} \qquad \text{8-31}$$

The composition of the bacterial consortium used in this study, which is composed of bacteria of the genus *Pseudomonas*, was approximated using the composition of *Escherichia coli*, as they are both gram negative rods (Buchanan and Gibbons, 1974). The composition of *Escherichia coli* is typically reported as 50 wt% carbon, 8 wt% hydrogen, 20 wt% oxygen and 14 wt% nitrogen (Nicholson, 2005; Todar, 2000). $Y_{X/O}$ was approximated for the BTEX mixture by using the average composition of each BTEX component.

8.7.2 Correlations and Equations for Model Inputs

The correlations and equations used in this study to determine model inputs, which are functions of inlet flow rate, utilized literature values and dimensions of system components, and allowed for the

determination of gas, liquid and polymer volumes in each section ($V_{g,sec,FR\#}$, $V_{l,sec,FR\#}$, $V_{p,sec,FR\#}$), gas flow rates ($F_{g,d,FR\#}$, $F_{g,r,FR\#}$), and liquid and polymer flow rates ($F_{l,FR\#}$, $F_{p,FR\#}$).

8.7.2.1 Volumes of Gas, Liquid and Polymer in Each Airlift Section, $V_{g,sec,FR\#}$, $V_{l,sec,FR\#}$, $V_{p,sec,FR\#}$

The gas volumes in the riser, downcomer, top and bottom sections in the airlift SL-TPPB are a function of inlet gas flow rate and can be approximated using Equations 8-32, 8-33, 8-34 and 8-35, respectively, under the assumption that $\varepsilon_r = \varepsilon_t = \varepsilon_b$ (Znad et al., 2004).

$$V_{g,r,FR\#} = V_r \varepsilon_{r,FR\#} \qquad \text{8-32}$$

$$V_{g,d,FR\#} = V_d \varepsilon_{d,FR\#} \qquad \text{8-33}$$

$$V_{g,t,FR\#} = V_t \varepsilon_{r,FR\#} \qquad \text{8-34}$$

$$V_{g,b,FR\#} = V_b \varepsilon_{r,FR\#} \qquad \text{8-35}$$

Gas hold up in the airlift was estimated using Equation 8-36 (Chisti, 1989), which can be used to determine the hold-up in the riser and downcomer sections in Equation 8-37 and Equation 8-38 (Chisti, 1989), respectively.

$$\varepsilon_{g,FR\#} = 4.334 \times 10^{-3} \left(\frac{P_g}{V_l} \right)_{FR\#}^{0.499} \qquad \text{8-36}$$

$$\varepsilon_{g,FR\#} = 0.89 \varepsilon_{g,r,FR\#} \qquad \text{8-37}$$

$$\varepsilon_{g,FR\#} = \frac{A_r \varepsilon_{g,r,FR\#} + A_d \varepsilon_{g,d,FR\#}}{A_r + A_d} \qquad \text{8-38}$$

A preliminary estimate of the energy requirements for the airlift for use in Equation 8-36 can be made using Equation 8-39 (Chisti, 1989).

$$\left(\frac{P_g}{V_l}\right)_{FR\#} = \frac{\rho_L g \upsilon_{S,r,FR\#}}{1+\dfrac{A_d}{A_r}}$$

8-39

Where $\upsilon_{S,r}$ was found to be 0.004, 0.006 and 0.008 m s^{-1} for inlet flow rates of 2, 3 and 4 L min^{-1}.

The volumes of liquid and polymer in each section were then determined by subtracting the volume of gas in a section from the total volume of the section; the remaining volume consisted of 10% polymers and 90% aqueous phase. The total volume for the top section was determined by subtracting the aqueous volume of the other airlift sections from the total liquid volume of 11 L, and then accounting for 10% polymers and the gas hold-up in the top section.

8.7.2.2 Gas Flow in Riser and Downcomer

The gas flow rate in the downcomer and riser were determined for the inlet gas flow rates used in this study using Equation 8-40 and 8-41, respectively.

$$F_{g,d,FR\#} = \varepsilon_{d,FR\#} A_d \overline{U}_{l,FR\#}$$

8-40

$$F_{g,r,FR\#} = F_{in,FR\#} + F_{g,d,FR\#}$$

8-41

In order to evaluate $F_{g,d,FR\#}$ from Equation 8-40, $\bar{U}_l$ must also be determined for various inlet air flow rates, which can be estimated using Equation 8-42 (Chisti, 1989).

$$\overline{U}_{l,FR\#} = \frac{x_c}{t_{c,FR\#}(1000)}$$

8-42

In order to determine the circulation time, $t_{c,FR\#}$, the data obtained from the tracer experiment for various inlet air flow rates described in Section 7.4.3 were used.

8.7.2.3 Liquid and Polymer Flow Rates, $F_{l,FR\#}, F_{p,FR\#}$

The liquid and polymer flow rate in the airlift SL-TPPB can be calculated using Equation 8-43 and 8-44, respectively, over various flow rates.

$$F_{l,FR\#} = \overline{U}_{FR\#} A_r \left(1 - \varepsilon_{r,FR\#}\right)(1 - 0.1) \qquad \textbf{8-43}$$

$$F_{p,FR\#} = \overline{U}_{l,FR\#} A_r (0.1) \qquad \textbf{8-44}$$

8.8 Modeling

8.8.1 Solid-Liquid TPPB Data

The experimental data modeled in this study were obtained from Chapter 6, which consisted of 9 runs at various operating conditions in an airlift SL-TPPB. A continuous gas stream containing BTEX was delivered into the system, and measurements were obtained until steady-state biomass concentrations were reached (> 200 hours). Various operating conditions were tested using a 3^2 factorial design at inlet loadings of 20, 60 and 100 mg L^{-1} h^{-1} and inlet gas flow rates of 2, 3 and 4 L min^{-1}. During these runs, inlet and outlet gas-phase concentrations of BTEX components and DO concentrations were measured. Rotameter settings fluctuated considerably, causing fluctuations in inlet and outlet BTEX concentrations during experimental runs. Average performance indicators were reported and used to estimate model parameters and assess model accuracy.

8.8.2 Numerical Methods

Matlab$^{\text{TM}}$ was used to generate model predictions by solving the non-linear set of Equations shown in Table 8-1 for each BTEX component and oxygen using the solver fsolve. As stated previously, inlet concentrations fluctuated during experimental operation due to minor increases or decreases in the rotameters. Therefore, individual BTEX inlet gas phase concentrations were approximated by taking the average measured inlet total BTEX concentrations and assuming each component was delivered into the system in equal amounts, as these proportions remained relatively constant throughout experimentation. The inlet BTEX gas-phase concentrations, along with experimentally measured biomass concentrations, which were used as a model input, are listed in Table 8-4.

Parameter estimates, as described in the following section, were determined by finding the parameter values that minimize the objective function, which was a weighted sum of squared errors

between the model predictions and the experimental performance indicators for BTEX components and DO concentrations. The "lsqnonlin" Matlab^{TM} routine was used to obtain the parameter estimates.

8.8.3 Estimability Analysis and Parameter Estimation

The estimability analysis and parameter estimation were completed using methods similar to those used for a stirred-tank SL-TPPB model in Chapter 5. An estimability analysis of the 55 parameters in the model was completed to determine which parameters and had the largest impact on model predictions, while taking into account correlated effects of parameters and uncertainty in initial parameter values. This estimability analysis was followed by estimation of the most important parameters, within realistic upper and lower bounds, to obtain improved parameter values that fit the SL-TPPB data better than the initial parameter values listed in Table 8-3. The estimability analysis ranked the parameters according to their influence on model outputs, correlation with other model parameters and uncertainty in initial values using the method described by Kou et al., (2005). The parametric sensitivity coefficients were scaled appropriately using uncertainties in the initial parameter values and in the measured responses (Thompson et al., 2009). The uncertainty scaling factors S_θ for the initial parameter guesses are shown in Table 8-3.

The parameters that were ranked highest using the estimability analysis are those that are most estimable, because these parameters have large influences on model predictions and have little correlation with the effects of other parameters that rank higher on the list. The high ranking parameters were, therefore, the targets for estimation using experimental data from the nine steady-state airlift SL-TPPB runs. The model predictions were fit to the experimental data by minimizing an objective function that consisted of the sum of squared errors weighted by uncertainties in measured BTEX performance indicators (RE and EC) and DO concentrations. The standard deviations used as weighting factors in the objective function and during estimability analysis were 1.3% for RE, 0.7 mg L^{-1} h^{-1} for EC and 0.5% for DO, respectively. Upper and lower bounds (see Table 8-5) on the estimated parameters were used to

ensure that the estimated values remained physically realistic. A series of parameter-estimation calculations was performed, beginning with the most estimable parameter, ($\mu_{max,E}$, by itself) followed by the two most estimable parameters ($\mu_{max,E}$ and $K_{s,X}$) then the three and so on. Parameter estimation stopped when including additional parameters did not cause a noticeable decrease in the objective function for parameter estimation.

8.9 Results and Discussion

8.9.1 Estimability Analysis and Parameter Estimation

The estimability analysis and parameter estimation was completed to identify and estimate parameters to improve model predictions. The ranked list of parameters (from most estimable to least estimable) is shown in Table 8-5. Using the experimental data from the nine runs completed in the airlift SL-TPPB, it was determined that over 27 parameters could be estimated. The parameters that ranked the highest were those that govern the rate of biological degradation. These ranking results are similar to that found for the model for the stirred-tank SL-TPPB in Chapter 5, on which the stirred tank model structure in this current study was based. Other parameters that were ranked highly are gas-liquid volumetric mass-transfer coefficients for BTEX and oxygen, particularly at an inlet gas flow rate of 2 L min^{-1}. This high ranking can be attributed to the fact that the experimental data indicate that the system was oxygen limited at an inlet gas flow rate of 2 L min^{-1}. In addition, the system is sensitive to volumetric mass-transfer coefficients because, if the rate of gas-liquid mass transfer is not rapid, mass transfer will limit the rates of biodegradation and uptake by polymers.

The appropriate number of parameters to estimate in this model was evaluated by increasing the number of parameters estimated, in the order of their rank listed in Table 8-5, and determining when the objective function no longer reduced appreciably. A plot of the objective function for parameter estimation, as a function of the number of parameters estimated, is shown in Figure 8-3. This figure indicates that little improvement to the model fit can be obtained by estimating more than 25 parameters.

Estimates for the 25 top-ranked parameters are shown in Table 8-5. The remaining 30 parameters were held at their initial values because these parameters had little influence on the model predictions or were already well-known (small uncertainties S_θ). One interesting observation is that specific growth rates

Table 8-5: Ranking and Parameter Estimates for Airlift SL-TPPB Model

Estimability Rank	Parameter	Upper/Lower Bounds	Estimated Value
1	$\mu_{max,E}$	0.00057/0.000017	0.00011
2	$K_{S,X}$	1.5/0.001	0.54
3	$\mu_{max,T}$	0.0026/0.000086	0.00053
4	$\mu_{max,B}$	0.0022/0.000092	0.00062
5	$I_{E,B}$	1/-1	0.0014
6	$I_{X,B}$	1/-1	-0.0056
7	$k_L a_{E,FR2}$	0.0097/0.00087	0.0019
8	$k_L a_{B,FR2}$	0.0056/0.00066	0.00082
9	$k_L a_{O,FR3}$	0.0051/0.00041	0.00083
10	$k_L a_{O,FR2}$	0.0051/0.00041	0.00087
11	$k_L a_{O,FR3}$	0.0071/0.00071	0.001
12	$k_L a_{E,FR3}$	0.0081/0.00091	0.0031
13	$k_L a_{B,FR3}$	0.0095/0.00085	0.0016
14	$k_L a_{T,FR2}$	0.0009/0.0001	0.0006
15	$k_L a_{T,FR3}$	0.0072/0.00092	0.0022
16	$k_L a_{B,FR4}$	0.0079/0.00082	0.0019
17	$k_L a_{T,FR4}$	0.0071/0.0009	0.0021
18	$I_{T,B}$	3/-3	2
19	$I_{B,T}$	2.2/-2.4	-0.4
20	$Y_{X/O}$	1.04/0.34	.93
21	$k_L a_{X,FR2}$	0.0027/0.00017	.00056
22	$k_L a_{E,FR4}$	0.011/0.0011	0.005
23	$k_{o,B}$	0.00000088/0.0000000088	0.0000000913
24	$k_L a_{X,FR3}$	0.0033/0.00013	0.00083
25	$K_{S,E}$	7.12/0.0002	2.12
26	$k_{o,X}$	-	-
27	$Y_{X/B}$	-	-
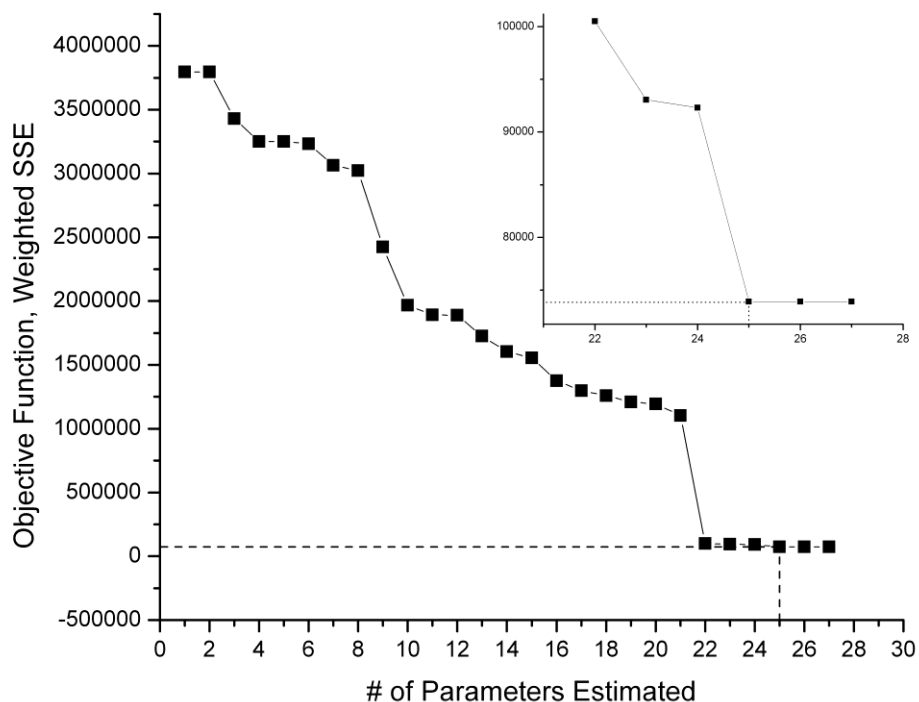
Figure 8-3: Objective function with increasing number of estimated parameters. Dotted line represents the plateau in objective function and the corresponding number of estimated parameters. Inset displays objective function over limited range to display plateau at 25 estimated parameters.

were predicted to be an order of magnitude faster than the initial parameter values, which were estimated in Chapter 5 to fit to experimental stirred-tank SL-TPPB. This may be due to the fact that the airlift SL-TPPB is gas-liquid mass transfer limited, whereas the smaller stirred-tank SL-TPPB was kinetically limited. Furthermore, in the current study the oxygen volumetric mass-transfer coefficients were consistently estimated to be significantly lower than their initial values. The mass-transfer coefficients estimated in the current study indicate that oxygen mass-transfer limitations influence the performance of the SL-TPPB.

8.9.2 Model Predictions

Predictions of the performance indicators are plotted, along with experimental data, for benzene, toluene, ethylbenzene and *o*-xylene in Figure 8-4, Figure 8-5, Figure 8-6 and Figure 8-7, respectively. It can be seen that the predicted performance indicators fit the experiment data quite well, particularly at an inlet gas flow rate of 2 L min^{-1} and the lowest loading of 20 mg L^{-1} h^{-1} total BTEX. The predictions for ethylbenzene RE and EC at a loading of 60 mg L^{-1} h^{-1} total BTEX appear to deviate the most from the experimental data, however, only by approximately 15%. The results show that the model can predict the trend of decreasing REs with increasing loadings for all compounds. The model predictions at a loading of 20 mg L^{-1} h^{-1} total BTEX and an inlet gas flow rate of 3 L min^{-1} are consistently lower than the experimental performance indicators (e.g., by 13% for xylene RE). The model predicts that these are the

Figure 8-4: Removal efficiencies and elimination capacities for benzene during steady-state operation over a range of loadings. Inlet gas flow rates of 2 L min^{-1} (squares), 3 L min^{-1} (triangles), and 4 L min^{-1} (pentagons) are shown for experimental data (solid) and model predictions (hollow).

Figure 8-5: Removal efficiencies and elimination capacities for toluene during steady-state operation over a range of loadings. Inlet gas flow rates of 2 L min^{-1} (squares), 3 L min^{-1} (triangles), and 4 L min^{-1} (pentagons) are shown for experimental data (solid) and model predictions (hollow).

Figure 8-6: Removal efficiencies and elimination capacities for ethylbenzene during steady-state operation over a range of loadings. Inlet gas flow rates of 2 L min^{-1} (squares), 2 L min^{-1} (triangles), and 2 L min^{-1} (pentagons) are shown for experimental data (solid) and model predictions (hollow).
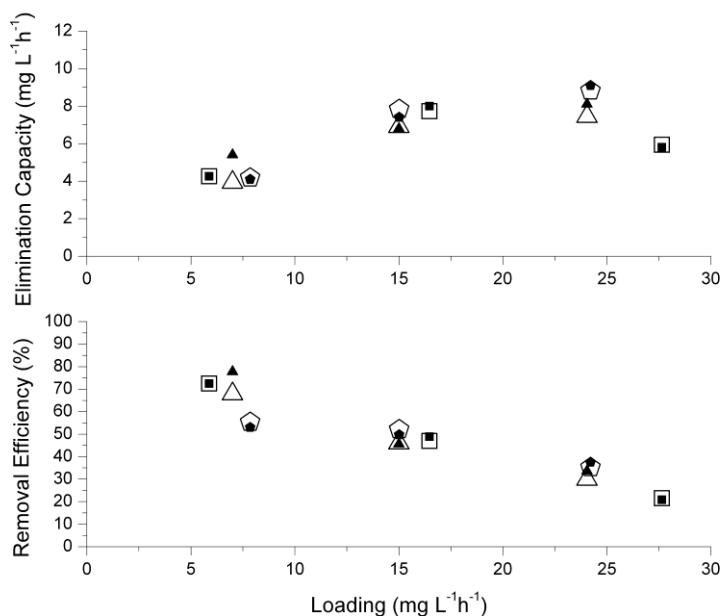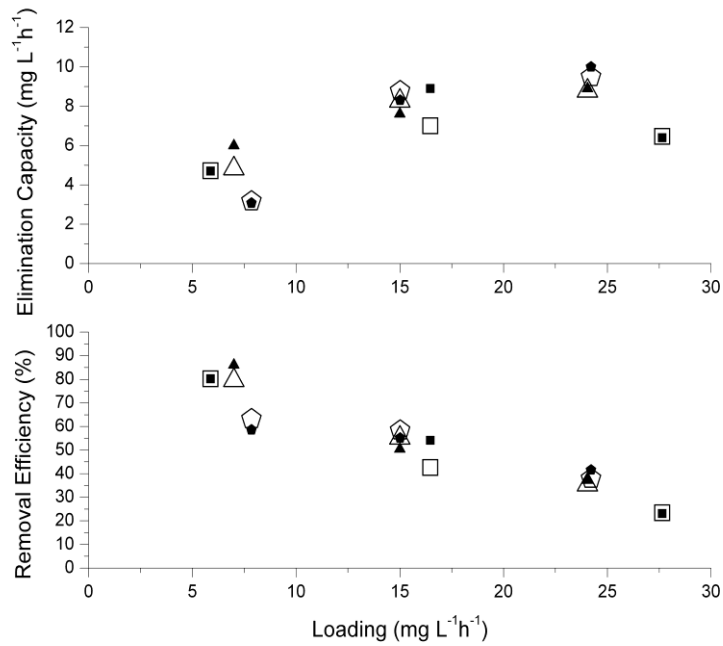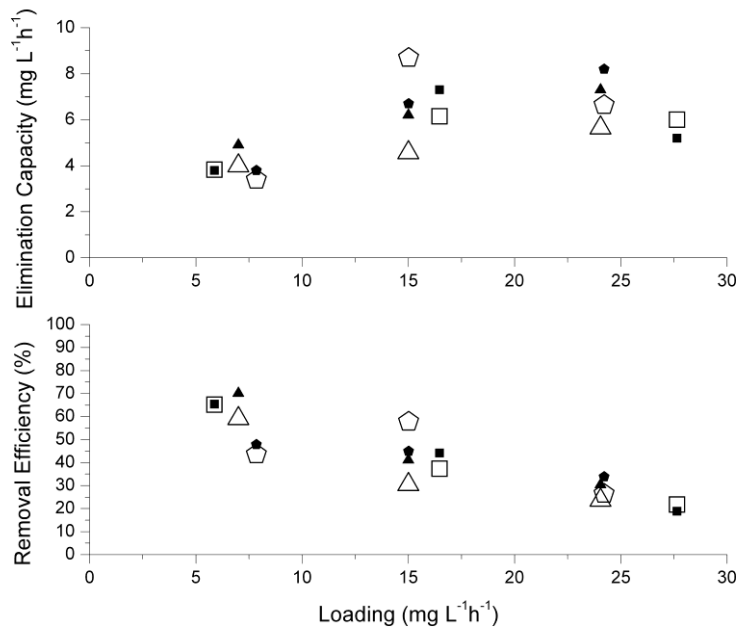
171
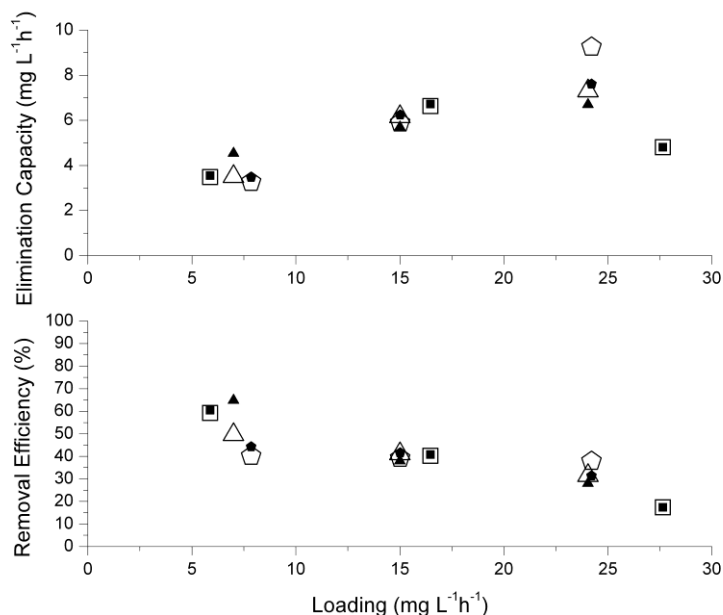
Figure 8-7: Removal efficiencies and elimination capacities for *o*-xylene during steady-state operation over a range of loadings. Inlet gas flow rates of 2 L min^{-1} (squares), 3 L min^{-1} (triangles), and 4 L min^{-1} (pentagons) are shown for experimental data (solid) and model predictions (hollow).

best operating conditions (from the nine different runs) as the performance indicators are the highest at these conditions. Note that the performance at the lower loading of 20 mg L^{-1} h^{-1} total BTEX and 2 L min^{-1} is predicted to have similar performance.

Figure 8-8 shows the predicted and experimental DO concentrations for each set of operating conditions. The model has the capability to predict that the system is oxygen limited at the inlet gas flow rate of 2 L min^{-1} for all loadings, which is reflected in the ECs in Figure 8-4, Figure 8-5, Figure 8-6 and Figure 8-7. In these figures, the values for both the predictions and experimental data plateau at a total BTEX loading of 60 mg L^{-1} h^{-1}. The model also successfully predicts that at the flow rates of 3 and 4 L min^{-1} and a loading of 20 mg L^{-1} h^{-1}, there is ample DO within the system, which is an important system characteristic for enabling effective BTEX removal.
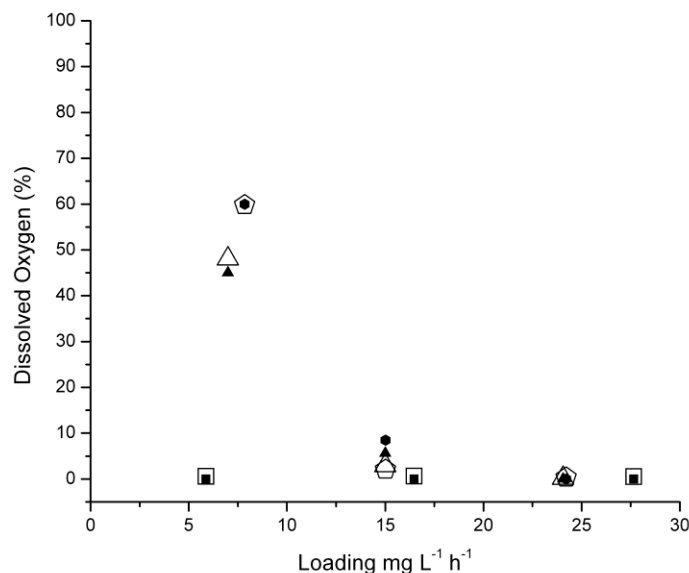
Figure 8-8: Dissolved oxygen concentrations during steady-state operation over a range of loadings. Inlet gas flow rates of 2 L min^{-1} (squares), 3 L min^{-1} (triangles), and 4 L min^{-1} (pentagons) are shown for experimental data (solid) and model predictions (hollow).

The predicted concentration profile in the sections of the airlift shown in Figure 8-2 for each BTEX compound can be seen in Figure 8-9 for a loading of 20 mg L^{-1} h^{-1} and an inlet gas flow rate of 3 L min^{-1}. It can be seen that the concentrations of benzene, toluene and ethylbenzene in the gas phase decrease significantly in the bottom, riser and top stages of the airlift and subsequently plateau in the downcomer sections. Note that the decrease in gas-phase xylene concentrations in the bottom, riser and top sections is less pronounced. The fraction (in each section) of the total amount of each compound degraded is represented by the size of the bubbles in Figure 8-9. The fraction degraded is largest in the riser section for benzene, toluene and ethylbenzene, but is largest in the bottom section for xylene. A total of 57, 75 and 59% of the benzene, toluene and ethylbenzene, respectively, is removed in the bottom, riser and top sections. However, only 32% of the xylene is removed in these three initial stages. Toluene and xylene, in particular, have very distinct removal profiles in the airlift which may be due to the

173
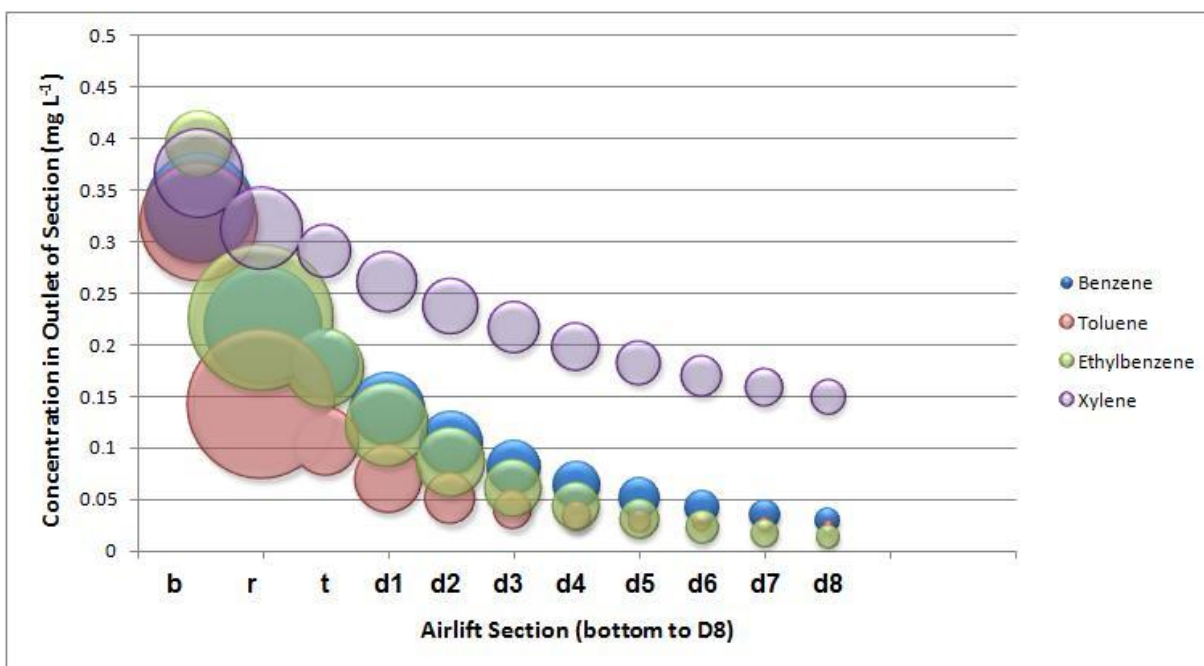
Figure 8-9: Gas Phase Concentration distribution in Airlift for Gas Flow Rate = 3 L min^{-1} and Loading Rate = 20 mg L^{-1} h^{-1}. Center of bubble corresponding to Y-axis represents concentration in outlet of airlift section, size of bubble corresponds to percent fraction of total compound degraded in airlift section.

volumetric mass-transfer coefficients for xylene being lower than those for toluene at a flow rate of 3 L min^{-1} (by 38%), causing the removal from the gas phase to be initially much more rapid for toluene in comparison to xylene.

8.10 Conclusions

A steady-state tanks-in-series model has been developed to model removal efficiency, elimination capacity and dissolved oxygen concentrations in an airlift SL-TPPB for the treatment of gas streams containing BTEX. An estimability analysis on model parameters revealed that the microbial kinetic parameters have the largest influence on model predictions. Experimental data from the operation of the airlift SL-TPPB at steady-state over a range of loadings and inlet gas flow rates was used to estimate parameters and assess model accuracy. BTEX volumetric mass-transfer coefficients were estimated to be smaller in comparison with values obtained for a stirred-tank SL-TPPB, indicating that mass-transfer

limitations are more important in the airlift system than the smaller well-mixed system. The model is capable of predicting performance indicators and dissolved oxygen concentrations in the airlift SL-TPPB over a range of loadings (20 to 100 mg $L^{-1} h^{-1}$) and inlet gas flow rates (2 to 4 L min^{-1}). In addition, the model predicts that the riser section removes the largest fraction of BTEX within the airlift and that a smaller fraction is removed in the downcomer sections.

ACKNOWLEDGEMENTS

Chapter 9
Summary and Conclusions

It was the objective of this thesis to thoroughly investigate the use and limitations of the SL-TPPB for the degradation of BTEX contaminated gas streams. Stirred-tank and airlift configurations were considered throughout this work and were characterized both experimentally and through mathematical modeling. It was found that the stirred tank configuration provided overall superior performance to the airlift configuration. However, both configurations were shown to have the ability to dampen inlet loading fluctuations, which provides an advantage over other biotreatment options. In addition, the airlift configuration provided adequate treatment of a gas streams containing BTEX under certain regions of operating conditions. Due to the lower energy inputs of the airlift (0.019 W L^{-1}) relative to the stirred-tank (14.7 W L^{-1}), the airlift SL-TPPB is the preferable option for industrial use for gas streams that fit into the acceptable region of operating conditions.

The first significant contribution derived from this thesis was the development of a method to determine physical enhancement of k_La in the stirred tank SL-TPPB wherein the sequestering phase has a high affinity for oxygen. Using the static gassing out method, k_Las in a stirred-tank reactor containing polymers with a high oxygen affinity (silicone rubber) were determined and comparing to k_Las obtained in a stirred-tank reactor containing polymers with similar density and size to silicone rubber, but low oxygen affinity (Nylon 6,6). This allowed for the impact of silicone rubber on physical enhancement of k_La to be isolated from the impact of oxygen absorption on k_La. In addition, this contribution showed that silicone rubber increased the OTR during dynamic periods, which provided an explanation for previous research that found SL-TPPBs to have increased DO levels during dynamic substrate loading fluctuations relative to single phase systems. These findings not only allowed for the characterization of the oxygen mass transfer phenomena that occur in SL-TPPB, but are useful for any aerobic system that may encounter oxygen limitations.

In the next investigation, a bacterial consortium was enriched from petroleum contaminated soil that had the ability to degrade a BTEX mixture. This investigation also characterized the substrate interactions that occurred during the biodegradation of BTEX by the developed bacterial consortium. It was found that the presence of certain BTEX component resulted in the inhibition, enhancement and cometabolism of other BTEX components. A SKIP and cometabolism model to describe these interactions and a method to quantify the growth of the bacterial consortium was developed. These findings contribute to the quantification of a range of substrate interactions that were not previously observed to occur among BTEX components.

Experimental operation of the stirred-tank SL-TPPB was the next investigation completed. It was found that the system was capable of removing >95% of the BTEX in a continuous gas stream during nominal steady-state loadings of 60 mg L^{-1} h^{-1}. In addition, the system was capable of maintaining REs of >95% during dynamic 4 h step changes of 2 and 4 times the nominal steady-state loading. It was shown that the RE decreased significantly during a step change of 6 times the nominal loading, however, the RE recovered to >95% after the completion of the step change. Finally, the system capability limits were identified during a step change of 10 times the nominal loading, wherein the biomass succumbed to substrate toxicity and did not recover subsequent to the step change. In addition, polymer and aqueous phase concentrations were monitored during step change operation and it was shown that during step changes of 2 and 4 times the nominal loading, >90% of the total BTEX in the working volume was present in the polymer near the end of the transient. These findings show that the polymers are effective at sequestering large concentrations of BTEX during dynamic periods, confirming that uptake by polymers is the mechanism for improved performance of TPPBs relative to single phase systems for the treatment of contaminated gas streams.

A mathematical model of the stirred-tank SL-TPPB was the next significant contribution in this thesis. The stirred-tank SL-TPPB model was developed from mass balances on the BTEX components and biomass to describe the dynamic performance of the system. Initial values for model parameters

177

were obtained from the literature, or correlations that utilized values obtained from independent experiments and/or literature. This study included an estimability analysis of the model parameters which identified that the values with the largest influence on model output were kinetic parameters. Experimental steady-state and dynamic data for the stirred-tank SL-TPPB were utilized to assess model accuracy and to estimate the parameters that were highly ranked according to the estimability analysis to improve model predictions. It was shown that the developed model had the ability to predict a range of stirred-tank SL-TPPB performance including the complete damping of small inlet step change loadings and the failure of the system due to build up of toxic BTEX levels in the aqueous phase.

Following the characterization of the stirred-tank SL-TPPB, experimental operation of the airlift SL-TPPB was undertaken as an option for BTEX treatment that requires low energy inputs. It was found that the airlift SL-TPPB had the ability to remove >20% more BTEX during step change inlet loadings of 2 and 3 times the nominal loading of 20 mg L^{-1} h^{-1}, relative to a single phase airlift system operated under similar conditions. In addition, similar performance to the airlift SL-TPPB was observed during operation of an airlift liquid-liquid TPPB with a liquid sequestering phase of silicone oil, which showed that solid polymers can be as effective as organic solvents at increasing BTEX mass transfer from the gas phase during dynamic operation. However, during the imposed step changes, oxygen limitations were approached in all systems. Therefore, steady-state operation of the SL-TPPB under various inlet gas flow rates and BTEX loadings was completed in the form of a 3^2 experimental design to identify favourable operating regions for the system. It was found that at low inlet gas flow rates and high BTEX loadings the system was oxygen limited and at high inlet gas flow rates mass transfer of BTEX out of the gas phase was limited. Operating conditions of an inlet gas flow rate of 3 L min^{-1} and a BTEX loading of 20 mg L^{-1} h^{-1} were identified to not be oxygen limited and allow for sufficient BTEX to be transferred from the gas phase, which resulted in an RE of >75%. Although favourable operating conditions for the airlift SL-TPPB were identified, overall it was found that the performance of the airlift SL-TPPB is significantly lower than that of the stirred-tank SL-TPPB due to mass transfer limitations.

Due to the oxygen limitations observed during the experimental investigation of the airlift SL-TPPB, a study of oxygen mass transfer and hydrodynamics in the airlift SL-TPPB was completed next. The method developed during the study of oxygen mass transfer in the stirred-tank SL-TPPB was used to determine the physical enhancement of k_La due to the presence of silicone rubber in an airlift system. It was found that the presence of silicone rubber in the airlift did not cause a physical enhancement of gas-liquid mass transfer in the same manner that was observed in the stirred-tank reactor. In addition, the k_Las determined in the airlift were lower than those observed in the stirred tank which may provide an explanation for the oxygen limitations observed in the airlift SL-TPPB during BTEX treatment. However, it was shown that, due to the oxygen absorption by the silicone rubber, there are larger amounts of oxygen transferred into the system during dynamic periods in comparison to a single phase airlift. These findings reveal that the addition of polymers may circumvent potential oxygen limitations in comparison to a single phase system by absorbing and desorbing oxygen according to metabolic demand in a similar manner to BTEX. The hydrodynamic investigation, which consisted of an RTD analysis showed that the addition of silicone rubber beads into an airlift increased overall mixing relative to a single phase airlift. Therefore, although polymers did not physically enhance k_La in the airlift SL-TPPB, they caused an increase in overall liquid phase mixing in comparison to single phase airlifts.

The final contribution in this thesis was the development and application of a steady-state mathematical model of the airlift SL-TPPB for the treatment of BTEX. This model consisted of mass balances on BTEX components and oxygen in a series of cascading continuously stirred tank reactors to represent the extent of mixing in the airlift. The number of tanks-in-series to describe mixing was determined to be 11 using information provided from the hydrodynamic study on the airlift SL-TPPB. An estimability analysis was completed on model parameters which identified that, similar to the stirred-tank model, biological kinetics to have the largest influence on model predictions. k_Las for BTEX components and oxygen were also ranked highly, as appropriate estimates for these parameters enabled the prediction of experimentally observed mass transfer limitations. Experimental steady-state data for

the airlift SL-TPPB were utilized to assess model accuracy and to estimate the highly ranked parameters to improve model predictions. It was shown that the tanks-in-series model for the SL-TPPB had the ability to predict performance under favourable operating conditions, as well as under operating conditions that resulted in oxygen limitations.

In summary, the major contributions in this thesis have been; 1) The development of a method to determine the physical enhancement of k_La in systems containing polymers with a high affinity for oxygen, 2) Observation of a range of interactions between BTEX compounds during biodegradation that were not quantified prior to this thesis, 3) The development of a model to describe the growth of a bacterial consortium of unquantified composition, 4) The first experimental investigation of a SL-TPPB for the treatment of more than one contaminant, 5) The development and analysis of the first model of a SL-TPPB for both stirred tank and airlift configuration, 6) The first experimental investigation of an airlift TPPB and 7) The first study of oxygen mass transfer and hydrodynamics in a gas-liquid-solid airlift reactor wherein the solid phase had a high affinity for oxygen.

9.1 Future Work

The results presented in this thesis indicated that the SL-TPPB in both the stirred-tank configuration and the less energy intense airlift configuration is a possible treatment option for gas streams containing BTEX. Future work in this area would be to determine the performance of the system to treat a gas stream containing fluctuating relative proportions of BTEX components, as gas streams containing equal proportions of BTEX components are rarely found in industrial scenarios. Mixtures of polymers matched to the array of contaminants present in the gas stream may improve system performance. In addition, investigation of SL-TPPBs for the treatment of contaminated gas streams has been limited to the treatment of BTEX compounds. As BTEX has relatively moderate water solubility, in most cases it can be effectively transferred from the gas phase to the aqueous phase where it is subsequently degraded by the microbial population or absorbed by the polymer phase. The application of

180

such as system for treatment of gas streams containing compounds with lower solubility (e.g. hexane) or compounds with higher water solubility (e.g. phenol) would be valuable to determine the range of solubility of target compounds to which the SL-TPPB can be applied.

Future work for modeling the airlift SL-TPPBs includes the investigation of a dynamic mathematical model to predict step change operation, which would further characterize the airlift SL-TPPB system. In addition, the validation of both the stirred-tank and airlift SL-TPPB models using experimental data obtained under operating conditions not utilized for parameter estimation would help to identify operating ranges to which the developed models are applicable.

As the airlift configuration reduces energy intensity and is therefore the preferable SL-TPPB design, scale-up of the airlift SL-TPPB would be required to apply this technology in the field. In addition, optimization of the physical design of the airlift system, including investigating the impact on the height to diameter ratio and area of downcomer to riser ratio, to improve mixing and polymer flow may improve system performance and ease scale-up. In order to move the airlift SL-TPPB towards commercial implementation, gas-liquid mass transfer needs to be improved. Future work investigating the use of a spinning sparger (Meng et al., 2002) in the airlift SL-TPPB is recommended to possibly increase k_La at low energy input.

Future work using silicone rubber containing Iron will increase the density of the solids which may allow for suspension of smaller beads. The use of smaller beads increases the rate of uptake and release of BTEX, which may increase the driving force for BTEX from the gas phase. Another option to apply this concept in industry includes the use of silicone rubber polymers within the packing material in biofilters. Although there are many limitations associated with biofilters, as described in Section 1.1.4, they are the most widely used industrial biodegradation systems and the addition of polymers that are customized for uptake of target compounds would likely greatly improve performance, particularly during loading fluctuations.

References

Abu-Reesh IM, Abu-Sharkh BF. 2003. Comparison of Axial Dispersion and Tanks-in-Series Models for Simulating the Performance of Enzyme Reactors. Ind Eng Chem Res 42:5495-5505.

Abuhamed T, Bayraktar E, Mehmetoglu T, Mehmetoglu Ü. 2004. Kinetics model for growth of *Pseudomonas putida* F1 during benzene, toluene and phenol biodegradation. Process Biochem 39**:**983–988.

Alagappan G, Cowan RM. 2003. Substrate inhibition kinetics for toluene and benzene degrading pure cultures and a method for collection and analysis of respirometric data for strongly inhibited cultures. Biotechnol Bioeng 83:798-809.

Aldric J, Thonart P. 2008. Performance evaluation of a water/silicone oil two-phase partitioning bioreactor using *Rhodococcus erythropolis* T902.1 to remove volatile organic compounds from gaseous effluents. J Chem Technol Biot 83:1401-1408.

Aldric J-M, Lecomte J-P, Thonart P. 2009. Study on Mass Transfer of Isoproylbenzene and Oxygen in a Two-Phase Partitioning Bioreactor in the Presence of Silicone Oil. Appl Biochem Biotechnol 153:67-79.

Alper E, Wichtendahl B, Deckwer W-D. 1980. Gas absorption mechanism in catalytic slurry reactors. Chem Eng Sci 35:217-222.

Alvarez PJ, Vogel TM. 1991. Substrate interactions of benzene, toluene, and para-xylene during microbial degradation by pure cultures and mixed culture aquifer slurries. Appl Environ Microbiol **57**:2981–2985.

Amsden BG, Bochanysz J, Daugulis AJ. 2003. Degradation of xenobiotics in a partitioning bioreactor in which the partitioning phase is a polymer. Biotechnol Bioeng 84:399-405.

Andre G, Robinson CW, Moo-Young M. 1983. New Criteria for Application of the Well-Mixed Model to Gas-Liquid Mass Transfer Studies. Chem Eng Sci 38:1845-1854.

Andrews JF. 1968. A mathematical model for the continuous culture of microorganisms utilizing inhibitory substrates. Biotechnol Bioeng 10:707-723.

Arriaga S, Muñoz R, Sergio H, Benoit G, Revah S. 2006. Gaseous hexane biodegradation by *Fusarium solani* in two liquid phase packed-bed and stirred-tank bioreactors. Environ Sci Technol 40:2390-2395.

Arvin E, Jensen BK, Gundersen AT. 1989. Substrate interactions during aerobic biodegradation of benzene. Appl Environ Microbiol **55**:3221–3225.

Attaway HH, Schmidt MG. 2002. Tandem Biodegradation of BTEX Components by Two *Pseudomonas sp*. Curr Microbiol 45:0030-0036.

Bailey J, Ollis D. 1986. Biochemical Engineering Fundamentals 2nd ed. New York: McGraw Hill Book Company.

Bailon L, Nikolausz M, Kastner M, Veiga MC, Kennes C. 2009. Removal of dichloromethane from waste gases in one- and two- liquid –phase stirred tank bioreactors and biotrickling filters. Water Res 43:11-20.

Baptista IIR, Zhou NY, Emanuelsson EAC, Peeva LG, Leak DJ, Mantalaris A, Livingston AG. 2008. Evidence of Species Succession During Chlorobenzene Biodegradation. Biotechnol Bioeng 99:68-74.

Beenackers AACM, Van Swaaij WPM. 1993. Mass transfer in Gas-Liquid Slurry Reactors. Chem Eng Sci 48: 3109-3139.

Bielefeldt AR, Stensel HD. 1999. Modeling competitive inhibition effects during biodegradation of BTEX mixtures. Water Res 33:707-714.

Boudreau NG, Daugulis AJ. 2006. Transient performance of two-phase partitioning bioreactors treating a toluene contaminated gas stream. Biotechnol Bioeng 94:448-457.

Bowen HJM. 1970. Absorption by Polyurethane Foams; New Method of Separation. J Chem Soc (A) 9:1082-1085.

Broadley James Cooperation. 2000. Broadley and James model D100 series OxyProbe instruction manual.

Brown WA. 2001. Developing the best correlation for estimating the transfer of oxygen from air to water. Chem Eng Educ 35:134-147.

Bruce LJ, Daugulis AJ. 1991. Solvent Selection Strategies for Extractive Biocatalysis. Biotechnol Prog. 7:116-124.

Buchanan RE, Gibbons NE. 1974. Bergey's Manual of Determinative Bacteriology. Baltimore:Waverly Press, Inc.

Calderbank PH. 1958. Physical rate processes in industrial fermentation – Part I: The interfacial area in gas-liquid contacting with mechanical agitation. Chem Eng Res Des 36:443-463.

Chang MK, Voice TC, Criddle CS. 1993. Kinetics of competitive inhibition and cometabolism in the biodegradation of benzene, toluene, and *p*-Xylene by two *Pseudomonas* Isolates. Biotechnol Bioeng 41:1057–1065.

Chisti MY. 1989. Airlift Bioreactors. Essex, England:Elsevier.

Clarke KG, Williams PC, Smit MS, Harrison STL. 2006. Enhancement and repression of the volumetric oxygen transfer coefficient through hydrocarbon addition and its influence on oxygen transfer rate in stirred tank bioreactors. Biochem Eng J 28:237-242.

Clean Air Act Amendments. 1990. Title III, Section 112.

Collins LD, Daugulis AJ. 1999. Simultaneous Biodegradation of Benzene, Toluene, and p-Xylene in a Two-Phase Partitioning Bioreactor: Concept Demonstration and Practical Application. Biotechnol Prog 15:74-80.

Comte MP, Bastoul D, Hébrard, Roustan M, Lazarova. 1997. Hydrodynamics of a three-phase fluidized bed the inverse turbulent bed. Chem Eng Sci 52:3971-3977.

Datta I, Allen D. 2005. Biofilter technology. In: Shareefdeen Z, and Singh A, Editors, Biotechnology for Odor and Air Pollution Control. Berlin: Springer. pp. 125-145.

Daugulis AJ, Boudreau NG. 2008. Solid-liquid two-phase partitioning bioreactors for the treatment of gas-phase volatile organic carbons (VOCs) by a microbial consortium. Biotechnol Lett 30:1583-1587.

Davidson CT. 2002. Novel use of a two-phase partitioning bioreactor for the removal and destruction of benzene and toluene in a gas stream. Ph.D. thesis. Canada:Queen's University.

Davidson CT, Daugulis AJ. 2003. The treatment of gaseous benzene by two-phase partitioning bioreactors: a high performance alternative to the use of biofilters. Appl Microbiol Biotechnol. 62: 297-301.

Debus O. 1995. Transport and reaction of aromatics, O_2 and CO_2 within a membrane bound biofilm in competition with suspended biomass. Water Sci Technol 31:129-141.

Deeb RA, Alvarez-Cohen L. 1999. Temperature Effects and Substrate Interactions During the Aerobic Biotransformation of BTEX Mixtures by Toluene-Enriched Consortia and *Rhodococcus rhodochrous*. Biotechnol Bioeng 62:526-533.

Deshusses M, Hamer G, Dunn I. 1996. Transient-state behavior of a biofilter removing mixtures of vapours of MEK and MIBK from air. Biotechnol Bioeng 49:587-598.

Dimitriou-Christidis P, Autenrieth RL. 2006. Kinetics of biodegradation of binary and ternary mixtures of PAHs. Biotechnol Bioeng 97:788–800.

Djeribi R, Dezenclos T, Pauss A, Lebeault J-M. 2005. Removal of Styrene from Waste Gas Using a Biological Trickling Filter. Eng Life Sci 5:450-457.

Dos Santos LMF, Livingston AG. 1995. Novel membrane bioreactor for detoxification of VOC wastewaters: biodegradation of 1,2-dichloroethane. Water Res 29:179-194.

Dubus O. 1995. Transport and reaction of aromatics, O_2 and CO_2 within a membrane bound biofilm in competition with suspended biomass. Water Sci Technol 31:129-141.

Edwards FG, Nirmalakhandan N. 1999. Modeling and Airlift Bioscrubber for Removal of Airphase BTEX. J Environ Eng 125:1062-1070.

England E, Fitch MW, Mormile M, Roberts M. 2005. Toluene removal in membrane bioreactors under recirculating and non-recirculating liquid conditions. Clean Techn Environ Policy 7:259-269.

EPA (U.S. Environmental Protection Agency). 2006a. Modeling Subsurface Petroleum Hydrocarbon Transport. EPA On-line Tools for Site Assessment Calculation: Henry's Law Constants. 2009.

EPA (U.S. Environmental Protection Agency). 2006a. Benzene Hazard Summary. 2009.

EPA (U.S. Environmental Protection Agency). 2006b. Toluene Hazard Summary. 2009.

EPA (U.S. Environmental Protection Agency). 2006c. Ethylbenzene Hazard Summary. 2009.

EPA (U.S. Environmental Protection Agency). 2006d. o-Xylene, m-Xylene, p-Xylene Hazard Summary. 2009.

EPA (U.S. Environmental Protection Agency). 2006e. Diffusion Coefficient Estimation - Extended Input Range. 2007.

England E, Fitch MW, Mormile M, Robert M. 2005. Toluene removal in membrane bioreactors under recirculating and non-recirculating liquid conditions. Clean Technol Environ Policy 7:259-269.

Fazaelipoor MH. 2007. A model for treating polluted air streams in a continuous two-liquid phase stirred tank bioreactor. J Hazard Mater 148:453-458.

Ferreira Jorge RM, Livingston AG. 2000. Biological treatment of an alternating source of organic compounds in a single tube extractive membrane bioreactor. J Chem Technol Biotechnol 75:1174-1182.

Fontana RC, Polidoro TA, da Silveira MM. 2009. Comparison of stirred tank and airlift bioreactors in the production of polygalacturonases by *Aspergillus oryzae.* Bioresource Technol 100:4493-4498.

Freitas C, Teixeira JA. 1998. Hydrodynamic studies in an airlift reactor with an enlarged degassing zone. Bioproc Eng 18:267-279.

Freitas C, Teixeira JA. 2001. Oxygen mass transfer in a high solids loading three-phase internal-loop airlift reactor. Chem Eng J 84:57-61.

Ganzeveld KJ, Chisti Y, Moo-Young M. 1995. Hydrodynamic behavior of animal cell microcarrier suspensions in split-cylinder airlift bioreactors. Bioproc Eng 12:239-247.

Gardin H, Lebeault JM, Pauss A. 1999. Biodegradation of xylene and butyl acetate using an aqueous -silicon oil two-phase system. Biodegradation 10:193-200.

Giovannettone JP, Gulliver JS. 2008. Gas Transfer and Liquid Dispersion Inside a Deep Airlift Reactor. AIChE J 54:850-861.

Gogoi NC, Dutta NN. 1996. Empirical approach to solid-liquid mass transfer in a three-phase sparged reactor. Fuel Process Technol 48: 145-157.

Gomes N, Aguedo M, Teixeira J, Belo I. 2007. Oxygen mass transfer in a biphasic medium: Influence on the biotransformation of methyl ricinoleate into γ-decalactone by the yeast Yarrowia lipolytica. Biochem Eng J 35:380-386.

Grady CPL, Smets BF, Barbeau DS. 1996. Variability in kinetic parameter estimates: a review of possible causes and a proposed terminology. Water Res 30:742-748.

Guo YX, Rathor MN, Ti HC. 1997. Hydrodynamics and mass transfer studies in a novel external-loop airlift reactor. Chem Eng J 67:205-214.

Harding RC, Hill GA, Lin Y-H. 2003. Bioremediation of toluene-contaminated air using an external loop airlift bioreactor. J Chem Technol Biot 78:406-411.

Hecht V, Brebbermann D, Bremer P, Deckwer WD. 1995. Cometabolic degradation of trichloroethylene in a bubble column bioscrubber. Biotechnol Bioeng 47:461-469.

Ho CS, Ju LK, Baddour RF. 1990. Enhancing penicillin fermentations by increased oxygen solubility through the addition of n-hexadecane. Biotechnol Bioeng 36:1110-1118.

Hwang, S.-J., Lu, W.-J., 1997. Gas-liquid mass transfer in an internal loop airlift reactor with low density particles. Chem Eng Sci 52:853-857.

Jarus D, Hiltner A, Baer E. 2002. Barrier properties of polypropylene/polyamide blends produced by microlayer coextrusion. Polymer 43:2401-2408.

Jia X, Wen J, Jiang Y, Liu X, Feng W. 2006. Modeling of batch phenol biodegradation in internal loop airlift bioreactor with gas recirculation by Candida tropicalis. Chem Eng Sci 61:3463-3475.

Jia X, Wen J, Wang X, Feng W, Jiang Y. 2009. CFD Modeling of Immobilized Phenol Biodegradation in three-phase Airlift Loop Reactor. Ind Eng Chem Res. 48:4514-4529.

Jianping W, Yu C, Xiaoqiang J, Guozhu M. 2006. Removal of toluene from air streams using a gas-liquid-solid three-phase airlift loop bioreactor containing immobilized cells. J Chem Technol Biotechnol 81:17-22.

Johnson T, Thomas S. 1999. Nitrogen/oxygen permeabilty of natural rubber/epoxidised natural rubber and natural rubber/epoxidised natural rubber blends. Polymer 40:3223-3228.

Johnson T, Woolhouse KJ, Prommer H, Barry DA, Christofi N. 2003. Contribution of anaerobic microbial activity to natural attenuation of benzene in groundwater. Eng Geol 70:343-349.

Jutras EM, Smart CM, Rupert R, Pepper IL, Miller RM. 1997. Field-scale biofiltration of gasoline vapors extracted from beneath a leaking underground storage tank. Biodegradation 8:31-42.

Kalen JD, Boyce RS, Cawley JD. 1991. Oxygen tracer diffusion in vitreous silica. J Am Ceram Soc 74:203-209.

Kamarthi R, Willingham RT. 1994. Bench-scale evaluation of air pollution control technology based on a biological treatment process. In: Proceedings of the 87th Annual Meeting of the Air and Waste Management Association, Cincinnati, OH.

Kan E, Deshusses MA. 2005. Continuous Operation of Foamed Emulsion Bioreactors Treating Toluene Vapors Biotechnol Bioeng 92:364-371.

Kan E, Deshusses MA. 2008. Modeling of a Foamed Emulsion Bioreactor: I. Model Development and Experimental Validation. Biotechnol Bioeng. 99:1096-1106.

Kanai T, Ichikawa J, Yoshikawa H, Kawase Y. 2000. Dynamic modeling and simulation of continuous airlift bioreactors. Bioprocess Eng 23:213-220.

Kars RL, Best RJ, Drinkenburg AAH. 1997. The sorption of propane in slurries of active carbon in water. Chem Eng J 17:201-210.

Kennes C, Thalasso F. 1998. Review: waste gas biotreatment technology. J Chem Technol Biotechnol 72:303-319.

Khan FI, Kr. Ghoshal A. 2000. Removal of Volatile Organic Compounds from polluted air. J Loss Prevent Proc 13:527-545.

Kim D, Kim YS, Kim SK, Kim SW, Zylstra GJ, Kim YM, Kim E. 2002. Monocyclic Aromatic Hydrocarbon Degradation by *Rhodococcus sp.* Strain DK17. Appl Environ Microbiol 68:3270-3278.

Kluytmans JHJ, van Wachem BGM, Kuster BFM. 2003. Mass transfer in sparged and stirred reactors: influence of carbon particles and electrolyte. Chem Eng Sci 58:4719-4728.

Kou, B., McAuley, K.B., Hsu, C.C., Hsu, C.C., Bacon, D.W., Yao, K.Z. 2005. Mathematical Model and Parameter Estimation for Gas-Phase Ethylene Homopolymerization with Supported Metallocene Catalyst. Ind. Eng. Chem. Res. 44:2428-2442.

Koutinas M, Baptista IIR, Meniconi, A, Peeva LG, Mantalaris A, Castro PML, Livingston AG. 2007. The use of an oil-absorber-bioscrubber system during biodegradation of sequentially alternating loadings of 1,2-dichloroethane and fluorobenzene in a waste gas. Chem Eng Sci 62:5989-6001.

Kumar A, Dewulf J, Luvsanjamba M, Van Langenhove H. 2008a. Continuous operation of membrane bioreactor treating toluene vapors by *Burkholderia vietnamiensis* G4 Chem Eng J 140:193-200.

Kumar A, Dewulf J, Van Langenhove H. 2008b. Membrane-based biological waste gas treatment. Chem Eng J 136:82-91.

Kuo J. 1999. Practical Design Calculations for Groundwater and Soil Remediation. New York:Lewis Publishers.

Langwaldt JH, Puhakka JA. 2000. On-site biological remediation of contaminated groundwater: a review. Environ Pollut 107:187-197.

Liang C, Chen Y, Chang K. 2009. Evaluation of persulfate oxidative wet scrubber for removing BTEX gases. J Hazard Mater doi:10.1016/j.hazmat.2008.08.056.

Lindert M, Kochbeck B, Prüss J, Warnecke H-J, Hempel DC. 1992. Scale-up of Airlift-loop Bioreactors based on Modeling the Oxygen Mass Transfer. Chem Eng Sci 47:2281-2286.

Littlejohns JV, Daugulis AJ. 2007. Oxygen transfer in a gas-liquid system containing solids of varying oxygen affinity. Chem Eng J 129:67-74.

Littlejohns JV, Daugulis AJ. 2008. Kinetics and interactions of BTEX compounds during degradation by a bacterial consortium. Process Biochem 43:1068-1076.

Littlejohns JV, Daugulis AJ. 2009a. Response of a Solid-Liquid Two-Phase Partitioning Biroeactor to Transient BTEX Loadings. Chemosphere 73:1453-1460.

Littlejohns JV, Daugulis AJ. 2009b. A Two-Phase Partitioning Airlift Bioreactor for the Treatment of BTEX Contaminated Gases. Biotechnol Bioeng doi:10.1002/bit.22343

Littlejohns JV, Daugulis AJ. 2009c. Oxygen Mass Transfer and Hydrodynamics in a Multi-Phase Airlift Bioscrubber System. Chem Eng Sci (Accepted)

Livingston AG, Chase HA. 1989. Modeling phenol degradation in a fluidized bed bioreactor. AIChE J 35:1980-1991.

Livingston AG, 1991. Biodegradation of 3,4-dichloroaniline in a fluidized bed bioreactor and a steady-state biofilm kinetic model. Biotechnol Bioeng 38:260-272.

Lo C-S, Hwang S-J. 2004. Dynamic behavior of an internal-loop airlift bioreactor for degradation of waste gas containing toluene. Chem Eng Sci 59:4517-4530.

Lu WJ, Hwang SJ, Chang CM. 1994. Liquid Mixing in Internal Loop Airlift Reactors. Ind Eng Chem Res 33:2180-2186.

Lu WJ, Hwang SJ, Chang CM. 1995. Liquid velocity and gas holdup in three-phase internal loop airlift reactors with low-density particles. Chem Eng Sci 50:1301-1310.

Luong JHT. 1987. Generalization of Monod Kinetics for Analysis of Growth Data with Substrate Inhibition. Biotechnol Bioeng 29:242-248.

Ma JW, Cunningham MF, McAuley KB, Keoshkerian B, Georges MK. 2002. Interfacial Mass Transfer in Nitroxide-Mediated Miniemulsion Polymerization. Macromol Theory Simul 11:953-960.

Malinowski JJ. 2001. Two-phase partitioning bioreactors in fermentation technology. Biotechnol Adv 19:525-538.

Marek J, Paca J, Gerrard A. 2000. Dynamic responses of biofilters to changes in the operating conditions in the process of removing toluene and xylene from air. Acta Biotechnol 20:17-29.

Mason CA, Ward G, Abu-Salah K, Keren O, Dosoretz CG. 2000. Biodegradation of BTEX by bacteria on powdered activated carbon. Bioprocess Eng 23:331-336.

Mateles RI. 1971. Calculation of the Oxygen Requriment for Cell Production. Biotechnol Bioeng 13:581-582.

Mathur AK, Majumder CB, Chatterjee S. 2007. Combined removal of BTEX in air stream by using mixture of sugar cane bagasse, compost and GAC as biofilter media. J Hazard Mater 148:64-74.

Meng AX, Hill GA, Dalai AK. 2002. Hydrodynamic Characteristics in an External Loop Airlift Bioreactor Containing a Spinning Sparger. Ind Eng Chem Res 41:2124-2128.

Merchuk JC, Contreras A, Garcia F, Molina E. 1998. Studies of mixing in a concentric tube airlift bioreactor with different spargers. Chem Eng Sci 53:709-719.

Merchuk JC, Stein Y. 1981. Local Hold-up and Liquid Velocity in Air-Lift Reactors. AIChE J 27:377-388.

Merkel TC, Bondar VI, Nagai K, Freeman BD, Pinnau I. 2000. Gas Sorption, Diffusion, and Permeation in poly(dimethylsiloxane). J Polym Sci Part B:Polym Phys 38:415-434.

Metcalf and Eddy Inc. 1991. Wastewater Engineering: Treatment, Disposal, Reuse. New York:McGraw-Hill.

Mohammad BT, Veiga MC, Kennes C. 2007. Mesophilic and thermophilic biotreatment of BTEX-polluted air in reactors. Biotechnol Bioeng 97:1423-1438.

Muñoz R, Arriaga S, Hernández S, Guieysse B, Revah S. 2006. Enhanced hexane biodegradation in a two phase partitioning bioreactor: Overcoming pollutant transport limitations. Process Biochem 41:1614-1619.

Muñoz R, Villaverde S, Guieysse B, Revah S. 2007. Two-phase partitioning bioreactors for treatment of volatile organic compounds. Biotechnol Adv 25:410-422.

Muñoz R, Chambaud M, Bordel S, Villaverde S. 2008. A systematic selection of the non-aqueous phase in a bacterial two liquid phase bioreactor treating α-pinene. Appl Microbiol Biotechnol 79:33-41.

Neal A, Loehr R. 2000. Use of biofilters and suspended-growth reactors to treat VOCs. Waste Mange 20:59-68.

Newman LM, Wackett LP. 1995. Purification and characterization of toluene 2-mono-oxygenase from *Burkholderia cepacia* G4. Biochemistry 34:14066-14076.

Nicholson W. 2005. Department of Veterinary Science and Microbiology, Microbiology Physiology Course, University of Arizona. 2007. Available: http://www.microvet.arizona.edu/Courses/MIC328/mic328index.html

Nielsen DR, Daugulis AJ, McLellan PJ. 2003. A Novel Method of Simulating Oxygen Mass Transfer in Two-Phase Partitioning Bioreactors. Biotechnol Bioeng 83: 735-742.

Nielsen DR, Daugulis AJ, McLellan PJ. 2005a. Transient Performance of a Two-Phase Partitioning Bioscrubber Treating a Benzene-Contaminated Gas Stream. Environ Sci Technol 39:8971-8977.

Nielsen DR, Daugulis AJ, McLellan PJ. 2005b. A restructured framework for modeling oxygen transfer in two-phase partitioning bioreactors. Biotechnol Bioeng 91:773-777.

Nielsen DR, Daugulis AJ, McLellan PJ. 2005c. Quantifying maintenance requirements from the steady-state operation of a two-phase partitioning bioscrubber. Biotechnol Bioeng 90:248-258.

Nielsen DR, Daugulis AJ, McLellan PJ. 2007a. Dynamic simulation of benzene vapor treatment by a two-phase partitioning bioscrubber: Part I: Model Development, Parameter Estimation, and Parametric Sensitivity. Biochem Eng J 36:239-249.

Nielsen DR, Daugulis AJ, McLellan PJ. 2007b. Dynamic Simulation of Benzene Vapor Treatment by a Two-Phase Partitioning Bioscrubber. Part II: Model Calibration, Validation, and Predictions. Biochem Eng J. 36:250-261.

Nielsen J, Villadsen J. 1994. Bioreaction Engineering Principles. New York:Plenum Publishing.

Nikakhtari H, Hill GA. 2005. Hydrodynamic and oxygen mass transfer in an external loop airlift bioreactor with a packed bed. Biochem Eng J 27: 138-145.

Nikakhtari H, Hill GA. 2006. Continuous bioremediation of phenol-polluted air in an external loop airlift bioreactor with a packed bed. J Chem Technol Biotechnol 81:1029-1038.

Oh Y-, Bartha R. 1997. Construction of a bacterial consortium for the biofiltration of benzene, toluene and xylene emissions. World J Microbiol Biotechnol 13:627-632.

Oh Y-, Choi SC, Kim YK. 1998. Degradation of Gaseous BTX by Biofiltration with *Phanerochaete chrysosporium*. J Microbiol 36:34-38.

Oh YS, Shareefdeen Z, Baltzis BC, Bartha R. 1994. Interaction between benzene, toluene, and *p*-Xylene (BTX) during their biodegradation. Biotechnol Bioeng 44:533–538.

Ohyama Y, Endoh K. 1955. Power characteristics of a gas-liquid contacting mixtures. J Chem Eng Jpn 19:2-11.

Okpokwasili GC, Nweke CO. 2006. Microbial growth and substrate utilization kinetics. Afr J Biotechnol. 5:305-317.

Olsen RH, Kudor JJ, Kaphammer B. 1994. A novel toluene-3-monooxygenase pathway cloned from *Pseudomonas pickettii* PKO1. J Bacteriol 176:3749-3756.

Özbek B, Gayik S. 2001. The studies on the oxygen mass transfer coefficient in a bioreactor. Process Biochem 36:729-741.

Ozkan O, Calimli A, Berber R, Oguz H. 2000. Effect of inert solid particles at low concentrations on gas-liquid mass transfer in mechanically agitated reactors. Chem Eng Sci 55: 2737-2740.

Öztürk SS, Schumpe A. 1987. The influence of suspended solids on oxygen transfer to organic liquids in a bubble column. Chem Eng Sci 42: 1781-1785.

Perry RH, Green DW. 1997. Perry's Chemical Engineers' Handbook, 7th Ed. New York:McGraw-Hill.

Prpich GP, Daugulis AJ. 2004. Polymer development for enhanced delivery of phenol in a solid-liquid Two-Phase Partitioning Bioreactor. Biotechnol Progr 20:1725.

Prpich GP, Daugulis AJ. 2005. Enhanced biodegradation of phenol by a microbial consortium in a solid-liquid two-phase partitioning bioreactor. Biodegradation 16:329-339.

Reardon KF, Mosteller DC, Rogers JB. 2000. Biodegradation kinetics of benzene, toluene, and phenol as single and mixed substrates for *Pseudomonas putida* F1. Biotechnol Bioeng 69:385–400.

Reardon KF, Mosteller DC, Rogers JB, DuTeau NM, Kim K-H. 2002. Biodegradation kinetics of aromatic hydrocarbon mixtures by pure and mixed bacterial cultures. Environ Health Perspect 110:1005–1011.

Rehmann L, Daugulis AJ. 2006. Biphenyl degradation kinetics by Burkholderia xenovorans LB400 in two-phase partitioning bioreactors. Chemosphere 63:972-979.

Roels JA. 1983. Energetics and Kinetics in Biotechnology. New York, USA:Elsevier Biomedical Press.

Roff WJ, Scott JR, Pacitti J. 1971. A Handbook of Common Polymers, 1st ed. London:Butterworths.

Roman RV, Tudose RZ. 1997. Studies on transfer processes in mixing vessels: effect of particles on gas-liquid mass transfer using modified Rushton turbine agitators. Bioprocess Eng 17: 361-365.

Rushton JH, Costich EW, Everett HJ. 1950. Power characteristics of mixing impellers. Chem Eng Progr 46:467-479.

Ruthiya KC, van der Schaaf J, Kuster BFM, Schouten JC. 2003. Mechanisms of physical and reaction enhancement of mass transfer in a gas inducing stirred slurry reactor. Chem Eng J 96:55-69.

Sànchez O, Michaud S, Escudié R, Delgenès JP, Bernet N. 2005. Liquid mixing and gas-liquid mass transfer in a three-phase inverse turbulent bed reactor. Chem Eng J 114:1-7.

Sander R. 1999. Compilation of Henry's Law Constants for Inorganic and Organic Species of Potential Importance in Environmental Chemistry (Version 3): http://www.henrys-law.org

Schumpe A, Saxena AK, Nigam KDP. 1987. Gas/Liquid Mass Transfer in a Bubble Column with Suspended Nonwettable Solids. AIChE J 33:1916-1920.

Segel IH. 1975. Enzyme Kinetics. New York:John Wiley & Sons.

Sharp NA, Daugulis AJ, Goosen MFA. 1998. Hydrodynamic and mass transfer studies in an external-loop air-lift bioreactor for immobilized animal cell culture. Appl Biochem Biotechnol 73:59-77.

Shiku H, Saito T, Wu C-C, Yasukawa T, Yokoo M, Abe H, Matsue T, Yamada H. 2006. Oxygen permeability of surface modified poly(dimethylsiloxane) characterized by scanning electrochemical microscopy. Chem Letters 35:234-235.

Shuler ML, Kargi F. 2002. Bioprocess Engineering: Basic Concepts. Englewood Cliffs:Prentice Hall.

Sikula I, Markoš J. 2008. Modeling of enzymatic reaction in an airlift reactor using an axial dispersion model. Chem Papers 62:10-17.

Sikula I, Jurascik M, Markoš J. 2006. Modelling of Enzymatic Reaction in an Internal Loop Airlift Reactor. Chem Pap 60:446-453.

Stewart WC, Barton TA, Thom RR. 2001. High VOC loadings in multiple bed biofilters: Petroleum and industrial applications. Environ Prog 20:207-211.

Studer M, Rudolf von Rohr P. 2008. Novel Membrane Bioreactor: Able to Cope with Fluctuating Loads, Poorly Water Soluble VOCs, and Biomass Accumulation. Biotechnol Bioeng 99:38-48.

Swaine DE, Daugulis AJ. 1988. Review of Liquid Mixing in Packed Bed Biological Reactors. Biotechnol Prog 4:134-148.

Takao M, Ono S, Hirose T, Murakami Y. 1982. A mathematical solution for response of tracer pulse in a loop reactor with open boundary and recycle. Chem Eng Sci 37:796-798.

Thanacharoenchanaphas K, Changsuphan A, Nimnual R, Thongsri T, Phetkasem S, Lertkanawanitchakul C. 2007. Investigation of BTEX and ozone concentrations in a printing facility in Bangkok, Thailand. Int J Appl Environ Sci 2:31-39.

Thompson, DE, McAuley KB, McLellan PJ. 2009. Parameter Estimation in a Simplified MWD Model for HDPE Produced by a Ziegler-Natta Catalyst. Macromol. React. Eng., 3: 160–177

Tinge JT, Drinkenburg AAH. 1995. The enhancement of the physical absorption of gases in aqueous activated carbon slurries. Chem Eng Sci 50: 937-942.

Todar K. 2000. Microbiology Webbed Out Online textbook. 2007 Available: http://www.bact.wisc.edu/Microtextbook

Torkian A, Dehghanzadeh R, Hakimjavadi M. 2003. Biodegradation of aromatic hydrocarbons in a compost biofilter. J Chem Technol Biotechnol 78:795-801.

Toumi LB, Fedailaine M, Allia K. 2008. Modelling Three-Phase Fluidized Bed Bioreactor for Wastewater Treatment. Int J Chem React Eng 6:1-16.

Turner JR, Mills PL. 1990. Comparison of axial dispersion and mixing cell models for design and simulation of fischer-tropsch slurry bubble column reactors. Chem Eng Sci 45:2317-2324.

Vergara-Fernández AO, Quiroz EF, Aroca GE, Alarcón, Pulido NA. 2008. Biological treatment of contaminated air with toluene in an airlift reactor. Electron J Biotechnol [online]. 15 October 2008, 11. [cited 25 January 2009] Available from: http://www.ejbiotechnology.info/content/vol11/issue4/full/10/index.html. ISSN: 0717-3458.

Van Groenestijn JW, Lake ME. 1999. Elimination of alkanes from off-gases using biotrickling filters containing two liquid phases. Environ Prog 18:151-155.

Weinkauf, D.H., Kim, H.D., Paul, D.R., 1992. Gas Transport Properties of Liquid Crystalline Poly(p-

phenyleneterephthalamide). Macromolecules 25 (2)788-796.

Wilderer PA. 1995. Technology of membrane biofilm reactors operated under periodically changing process conditions. Water Sci Technol 31:173-183.

Williams PA, Murray K. 1974. Metabolism of benzoate and the methylbenzoates by *Pseudomonas putida (arvilla)* mt-2: Evidence for the existence of a TOL plasmid. J Bacteriol 120:416-423.

Yao KZ, McAuley KB, Marchildon EK. 2003. Simulation of continuous solid-phase polymerization of nylon 6,6. III. Simplified model. J Appl Polym Sci 89:3701-3712.

Yen KM, Karl MR, Blatt LM, Simon MJ, Winter RB, Fausset PR, Lu HS, Harcourt AA, Chen KK. 1991. Cloning and characterization of a *Pseudomonas mendocina* KR1 gene cluster encoding toluene-4-monooxygenase. J Bacteriol 173:5315-5327.

Yeom SH. 2007. A simplified steady-state model of a hybrid bioreactor composed of a bubble column bioreactor and biofilter compartments. Proc Biochem 42:554-560.

Yeom SH, Daugulis AJ. 2001. A two-phase partitioning bioreactor system for treating benzene-contaminated soil. Biotechnol Lett 23:467-473.

Yeom S-, Yoo Y. 2002. Analysis of microbial adaptation at enzyme level for enhancing biodegradation rate of BTX. Korean J Chem Eng 19:780–782.

Yoon H, Klingzing G, Blanch HW. 1997. Competition for the mixed substrates by microbial populations. Biotechnol Bioeng 19:1193-1210.

Yu H, Kim BJ, Rittmann BE. 2001. The roles of intermediates in biodegradation of benzene, toluene, and p-xylene by *Pseudomonas putida* F1. Biodegradation 12:455-463.

Zappi ME, Rogers CL, Teeter D. 1996. Bioslurry treatment of a soil contaminated with low concentrations of total petroleum hydrocarbons. J Hazard Mater 46:1-12.

Zhang GD, Cai WF, Xu CJ, Zhou M. 2006. A general enhancement factor model of the physical absorption of gases in multiphase systems. Chem Eng Sci 61: 558-568.

Zilli M, Daffonchio D, Di Felice R, Giordani M, Convert A. 2004. Treatment of benzene contaminated airstreams in laboratory-scale biofilters packed with raw and sieved sugarcane bagasse and with peat. Biodegradation 15:87-96.

Ziomek E, Kirkpatrick N, Reid ID. 1991. Effect of polydimethylsiloxane oxygen carriers on the biological bleaching of hardwood kraft pulp by *Trametes versicolor*. Appl Microbiol Biotechnol 35: 669-673.

Znad H, Bales V, Kawase Y. 2004. Modeling and scale up of airlift bioreactor. Comput Chem Eng 28:2765-2777.

Zylstra GJ, Gibson DT. 1989. Toluene degradation by *Pseudomonas putida* F1: nucleotide sequence of the *todC1C2BADE* genes and their expression in *Escherichia coli*. J Biol Chem 264:14940-14946.

Appendix A: Polymer Partitioning

This section contains methods for determining partition coefficients for BTEX between aqueous and polymer phases and the resulting data that were used for polymer selection.

To determine partition coefficients of BTEX between aqueous and polymer phases, air-tight 125ml bottles containing 60ml of the media described in Section 3.5.1 and 1 or 2g of polymer were used. 1.5 ul, 1 ul, or 0.5 ul of each BTEX component was injected into each bottle which was subsequently agitated at 180 rpm for approximately 24 hours at 30°C in order for the BTEX components to reach equilibrium between the headspace, liquid and polymer phases. BTEX concentrations in the gas phase were then measured using GC/FID, as described in Section 3.5.4. The relationship of BTEX between the gas and liquid phase was determined using the Henry's constants determined in Section 4.4.6, permitting the calculation of BTEX in the polymer phase. The partition coefficients were then calculated using Equation 1-1.
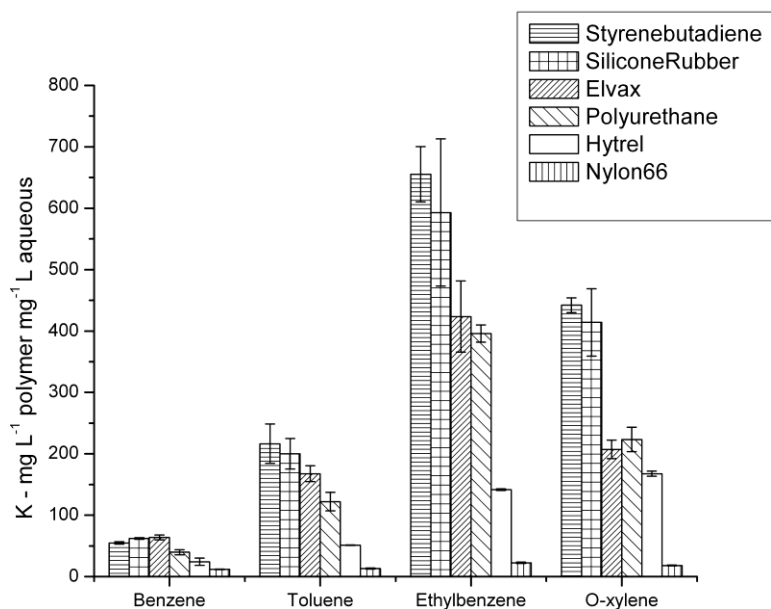

Figure A-1: Partition coefficients for BTEX compounds between various polymers and an aqueous phase

Appendix B: Polymer Diffusivity

This section contains the diffusion coefficients for BTEX into polymers that were used for polymer selection. The method of determining diffusion coefficients of BTEX compounds into polymers is described in Section 5.5.1.3.1.
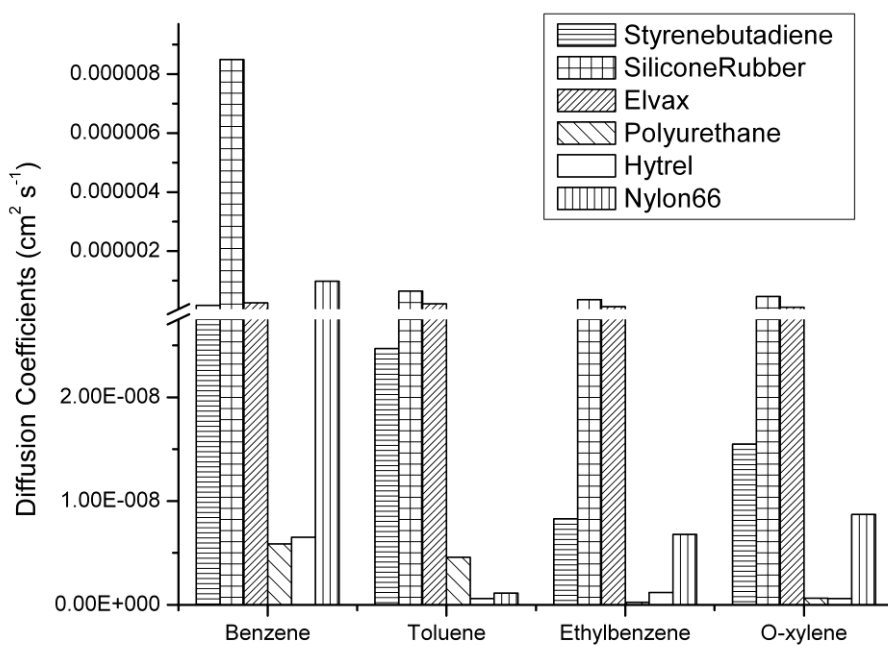

Figure B-1: Diffusion coefficients for BTEX compounds between various polymers and an aqueous phase

Appendix C: Polymer Suspension in Airlift

This section contains data on the inlet gas flow rates that have the ability to evenly disperse a solid polymer phase throughout the airlift vessel, which was a consideration for polymer selection in the airlift SL-TPPB.
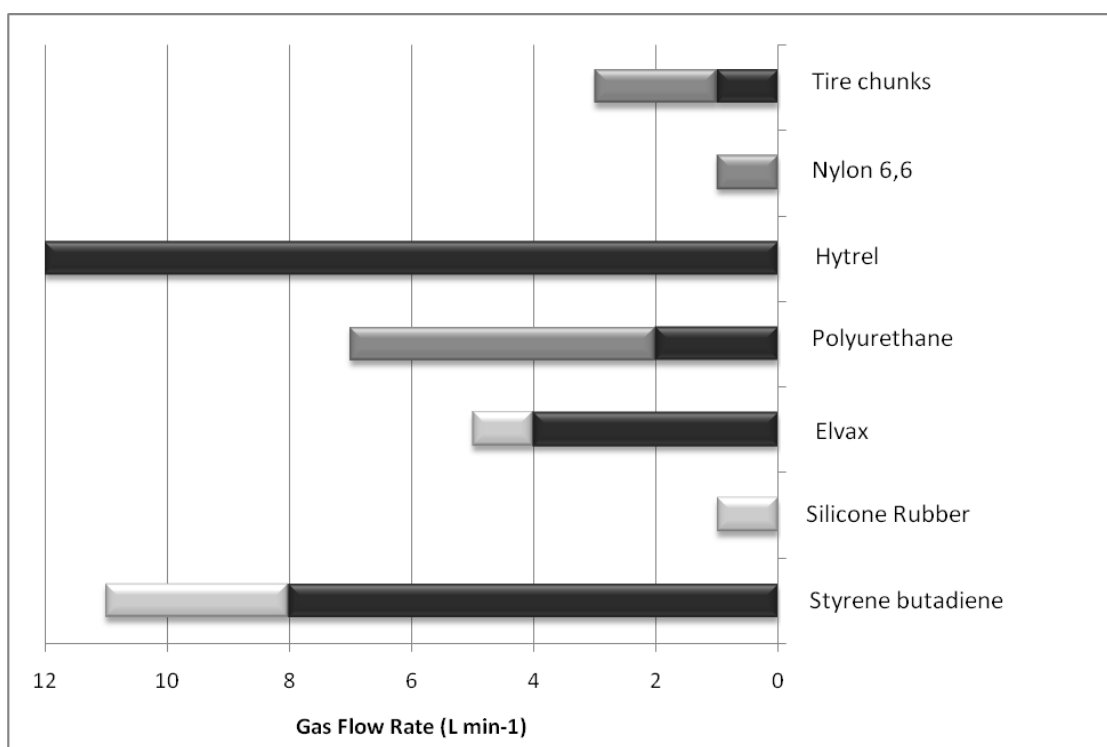

Figure C-1: Inlet gas flow rate at which polymer can be suspended in the 11 L airlift bioreactor. Black bars represent range of no suspension, dark grey bars represent range of suspension with larger distribution of polymer beads at the bottom of the airlift vessel and light grey bars represent range of suspension with larger distribution of polymer beads floating at the top of the airlift vessel.